

COA/N-86

NOTE 86



ST. NO.	1416
U.D.C.	
AUTH.	

THE COLLEGE OF AERONAUTICS
CRANFIELD

THE MEASUREMENT OF AIR TEMPERATURE IN
HIGH SPEED FLIGHT

by

J. M. GEORGE

1958

R 18,134



3 8006 10057 6803



THE COLLEGE OF AERONAUTICS
CRANFIELD

THE MEASUREMENT OF AIR TEMPERATURE IN
HIGH SPEED FLIGHT

by

J. M. GEORGE

Acknowledgements

The author wishes to express his most sincere thanks and appreciation to the following people, this list being in chronological order.

To Messrs. G.M. Lilley and M.C. Wilson, his supervisors, for the valuable guidance and assistance during the compilation of this thesis;

To Mr. T.H. Kerr of the Aero Flight Department at the R.A.E. Bedford, for his willing co-operation in all matters, and not least for arranging for a Hawker Hunter F Mk II aircraft to be at the author's disposal for about nine weeks;

To Mr. J.R.C. Fearon of the Flight Test Department of Rolls Royce at Hucknall for his most generous offer of the use of the I.B.M. Computer at Derby for the analysis of the flight records;

To Mr. P. Adkins of Standard Telephones and Cables Ltd. for arranging for the modification at very short notice of a special type of thermistor suitable for the experimental part of this thesis

To Mr. Goody of the Instrument Department of the A. & A.E.E. at Boscombe Down for providing drawings of one of the test instruments used in the flight tests;

To Sqn. Ldr. I.A. Robertson of the Department of Flight for his assistance in the construction of some of the test equipment;

To Mr. M.A. Perry of the Department of Flight for his advice on the electrical circuitry in the wind tunnel and in the aircraft;

To Messrs. E. Harwood and C. Martin of the Department of Flight for their advice on the design of the temperature probes, and their skill and patience in making these delicate instruments;

To Mr. S.H. Lilley of the Department of Aerodynamics for modifying the wind tunnel in which the initial testing was carried out;

To Mr. O.P. Nicholas of the Aero Flight Department, Bedford, for his invaluable advice and assistance in the choice and installation of the recording apparatus and his willing readiness to be of help at all times;

To Mr. H. Armstrong, foreman in charge of the Aero Flight hangar, and his team who strove so gallantly to keep the aircraft serviceable in the face of many difficulties;

To Mr. G.S. Smith of the R.A.F. station at Cardington for his co-operation in hoisting a barrage balloon and measuring the air temperature at regular intervals for the purpose of the flight tests;

And finally but by no means least to all the pilots of the Aero Flight Department, Bedford, who flew the test sorties for these results with such patience and precision. Particular mention must be made of Flt. Lt. M.S. Goodfellow and Lt. Cdr. J. Humphreys who between them flew about 80% of the sorties, the nature of which must have been extremely exasperating under certain conditions.

List of Symbols

a	Speed of sound.
c_f, C_F	Skin friction coeffs.
C_p, C_v	Specific heats.
E	Internal energy.
H	Ratio of boundary layer thicknesses.
i	Enthalpy, current.
k	Coeff. of conductivity.
k_H	Stanton heat transfer coeff.
M	Mach number.
p	Pressure.
Q, q.	Quantity of heat.
r	Recovery factor; cylindrical co-ord.
R.	Resistance.
Re	Reynolds no.
S.	Reynolds analogy factor.
S	Area
T, t	Temperature.
U, u	Velocity components.
V, v	Velocity components.
V	Volume.
Z	Impedance.

δ	Boundary layer thickness.
η	A parameter.
μ	Coeff. of viscosity.
ν	Coeff. of kinematic viscosity.
θ	Temperature function, cylindrical co-ord.
Φ	Dissipation function.
ρ	Density.
σ	Prandtl number.

Subscripts

1	Stagnation conditions: displacement b.1. thickness (δ_1)
2.	Momentum b.1. thickness (δ_2)
i	Incompressible; equivalent (air speed).
m	Measured.
p	Probe.
r	Radiation.
rr	Reflected radiation.
s	Static.
t	Thermometer.
w	Wall.
w ₀	Wall with zero heat transfer.
∞	Free stream.

Superscript

x.	Intermediate
----	--------------

Introduction

The knowledge of air temperature has always been an essential part of any flight test records for aircraft and engine performance calculations, and therefore the outside air thermometer is of vital importance.

The majority of engine performance characteristics are presented as a function of the non-dimensional r.p.m. parameter $\frac{N}{\sqrt{T}}$ and as, with the development of more advanced types of engines, the slopes of the characteristic curves are increasing, the accurate knowledge of both N and T , is becoming steadily more important.

This report is confined to the measurement of temperature, and Part I is devoted to some theoretical considerations of the recovery factor on a flat plate and a cylinder with its axis parallel to the airstream. The effect of radiation has been taken into account, and heat transfer expressions have been derived for laminar and turbulent boundary layers. The equilibrium temperature of a flat plate has also been evaluated over a range of airspeeds and altitudes assuming various amounts of radiation, and graphs have been included to show the deviation of the recovery factor with the variation of these two parameters.

Part II contains an account of the preliminary testing of one of the temperature probes in the wind tunnel, and these tests were carried out with two main objects in view. The first was to ascertain the suitability of using thermistors as temperature sensing elements in outside air thermometers, and in particular to investigate their sensitivity and stability over a period of time. The second and prime object was to determine what effect a change of incidence would have on the recovery factor of a ventilated pitot thermometer probe.

Part III contains an account and the results of a detailed investigation of the recovery factor of 5 outside air thermometers in flight. The aircraft which was used for this work was a Hawker Hunter F. Mk II, and it was flown over a wide range of airspeeds and altitudes. The 5 thermometers consisted of 4 ventilated pitot probes and one standard surface temperature probe, and the temperatures which they measured were recorded on paper traces, while the airspeed and altitude were recorded on film in an automatic observer panel. The flights mostly took the form of a series of stabilised levels at a particular altitude and over a wide range of airspeeds, but

some accelerated/decelerated levels were made in order to assess the lag of the various probes. The altitude band which was covered ranged from 4000' to 45,000' and this was repeated four times, first in 5000' increments and thereafter in 10,000' increments. Two sorties at 4000' consisted of series of levels past a barrage balloon in which an accurately calibrated thermocouple and its reference junction was measuring the ambient air temperature. This provided a useful check on the measurements which were made on the aircraft. Two sorties at 35,000' included some dives at transonic speed through the test altitude, and those produced some interesting results. These dives necessitated a high rate of descent in which the temperature was changing quite rapidly, depending on the stability of the Mach number, and for this reason these sorties were confined to the stratosphere in which the ambient temperature is supposed to remain constant. In fact it very rarely was constant, and only the probes which had a small lag gave an accurate measurement of the temperature.

The overall results have been presented on 5 graphs showing the variation of the recovery factor of each probe with altitude over the entire range of altitudes which was covered.

1. Historical Background.

With one or two exceptions it has not been possible to measure the true free air temperature on an aircraft in flight because of the aerodynamic heating which raises the temperature of the air when it is brought to rest at the measuring instrument.

One such exception is the axial flow vortex thermometer which has been under development for a number of years in the U.S.A. and in this instrument the dynamic heating of the air has been compensated for by cooling the air back to the true ambient temperature before measuring it. This cooling is effected in a vortex tube using the Ranque effect whereby the temperature at the centre of a vortex is lower than that at the outside and it is in the centre that the measuring element is placed.

The vortex is produced by a helical spinner vane which is rigidly housed within a tube mounted axially parallel to the airstream, and the measuring element is placed to the rear of this vane. The air enters the tube and is rotated by the vane which has a continually tightening helix, thereby cooling the centre of the vortex. The amount of cooling which is obtained is directly affected by the geometry of the helix and the nose shape of the vane. The length is also an important parameter in the design because it is desirable to keep the surface friction to a minimum but if the helix tightens too abruptly it will tend to cause separation and turbulence particularly on the suction side.

Other parameters which affected the results of this thermometer were the size of the housing and the position of the measuring element and many different combinations were tested before any results were obtained which gave the correct amount of cooling throughout the airspeed range.

The measuring element which was used was a nickel resistance wire coil which was wound onto the central shaft but this type of thermometer could be adapted to use thermocouples, thermistors or any other similar type of temperature sensing elements.

This thermometer has been tested extensively on a whirling arm with reference thermometers placed at intervals around its path and the accuracy which was achieved with such a probe was $\pm 0.3^{\circ}\text{C}$. up to 500 m.p.h., but no flight tests had been undertaken at this stage and the effects of high altitude, high speed and icing conditions were unknown.

The disadvantage of such a probe appears to be the accuracy which is required in the manufacture of the helical spinner vane in order to obtain consistent results from one thermometer to the next.

Other types of thermometer measure an increased temperature due to the aerodynamic heating and it is then necessary to make a correction for it. This increase arises from the change in kinetic energy of the air impinging on, or moving past, the thermometer bulb, and may be illustrated by applying the 1st law of Thermodynamics and Bernoulli's equation to an elementary volume of the airstream and assuming adiabatic and

and frictionless flow.

$$dQ = dE + p dV$$

* This restriction is not necessary

Heat added = Change of internal energy + work due to compression

But as the flow is adiabatic $dQ = 0$ and $dE = m C_v dT$

where m is the mass of the elementary volume

$$m = \rho V$$

$$\therefore m C_v dT + p dV = 0$$

$$\text{But } d(pV) = d(mRT) = V dp + p dV$$

$$\therefore m C_v dT + d(mRT) = V dp$$

$$\rho V (C_v + R) dT = V dp$$

$$\therefore \rho C_p dT = dp$$

Dividing by ρ and integrating from ∞ to 1 the equation becomes

$$C_p (T_1 - T_\infty) = \int_{p_\infty}^{p_1} \frac{dp}{\rho}$$

Bernoulli's equation for compressible flow is

$$\frac{v^2}{2} + \int \frac{dp}{\rho} = \text{constant}$$

and substituting this into the previous expression, the temperature increase becomes

$$(T_1 - T_\infty) = \frac{1}{2 C_p} (V_\infty^2 - V_1^2)$$

In particular on the surface of a body $V_1 = 0$, and therefore the difference between the stagnation temperature and the free stream temperature is

$$(T_1 - T_\infty) = (\Delta T)_{ad} = \frac{V_\infty^2}{2 C_p} \quad (2)$$

$(\Delta T)_{ad}$ is the adiabatic temperature increase and when V_∞ is 100 m.p.h. $(\Delta T)_{ad}$ is approximately 1°C .

$$\therefore T_1 = T_\infty + \left(\frac{V_\infty}{100} \right)^2 \quad V_\infty \text{ in m.p.h.} \quad (3)$$

It is more usual with aircraft to measure V_∞ in knots and using these units, equation (2) becomes

$$T_1 = T_\infty + \left(\frac{V_\infty}{87} \right)^2 \quad (4)$$

However in practice adiabatic flow does not always exist, and the temperature which is measured is somewhere between T_∞ and T_1 . It is therefore usual to introduce a factor r , known as the recovery factor, which indicates the percentage of the total available adiabatic temperature increase which has been realised.

Equation (4) now becomes

$$T_w = T_\infty + r \left(\frac{V_\infty}{87} \right)^2 \quad (5)$$

When a thermometer is fitted on an aircraft, it is unlikely that the velocity of the airstream at the probe will be the same as that of the aircraft, and this will have an effect on the resultant recovery factor if it is less than unity.

In order to illustrate this consider an aircraft with a true airspeed of 500 m.p.h. and having two identical probes located in positions where the true local velocities are 300 and 400 m.p.h. respectively. The flow between the free state and the probes is assumed to be adiabatic and so the respective increases of temperature will be

$$\left(\frac{500}{100} \right)^2 - \left(\frac{300}{100} \right)^2 = 16^\circ\text{C} \quad ; \quad \left(\frac{500}{100} \right)^2 - \left(\frac{400}{100} \right)^2 = 9^\circ\text{C}$$

Assuming recovery factors of unity for each probe, their temperature rises will be 9°C . and 16°C . respectively making a total of 25°C . in each case which is the full adiabatic temperature increase.

If however the recovery factors are 0.5, temperature rises at the probes will be 4.5°C . and 8°C . respectively making totals of 20.5°C . and 17°C ., and the overall values of the recovery factors will be 0.82 and 0.68.

This illustrates the advantage of placing the probe in a low velocity airstream provided that the process of deceleration is adiabatic. This effectively is the principle of the ventilated pitot thermometer which is described later.

In equation (5), V_∞ is the true airspeed and in order to obtain this from the equivalent airspeed V_i , which is obtained from flight measurements, a knowledge of T_∞ is required. However it is possible to express (5) in terms of V_i by the relationship

$$V_i \sqrt{\frac{14.7}{p_0}} = V_\infty \sqrt{\frac{288}{T_\infty}} \quad \begin{matrix} p \text{ in lbs/in}^2 \\ T \text{ in } ^\circ\text{K.} \end{matrix} \quad (6)$$

Substituting (6) into (5), it becomes

$$T_w = T_\infty + r \left(\frac{V_i}{87} \right)^2 \frac{14.7}{P_\infty} \cdot \frac{T_\infty}{288}$$

$$T_w = T_\infty + r \frac{T_\infty}{288} \left[\frac{V_i}{87} \sqrt{\frac{14.7}{P_\infty}} \right]^2 \quad (7)$$

where $\left[\frac{V_i}{87} \sqrt{\frac{14.7}{P_\infty}} \right]$ is called the airspeed parameter.

Thus from a plot of T_w against this parameter squared, the slope of the graph is proportional to r and the intercept of the graph on the temperature axis is the free stream temperature T_∞ . Knowing this value it is possible to calculate the recovery factor, r . Thus it is only necessary to measure the indicated temperature at the surface T_w , the indicated airspeed which is corrected to give the equivalent T_w airspeed, and the pressure altitude.

It may be more desirable to express equation (5) in terms of the free stream Mach No, M_∞ .

viz. :

$$\frac{V^2}{2C_p} = T_\infty \cdot \frac{\gamma-1}{2} M_\infty^2$$

$$T_w = T_\infty \left(1 + r \cdot \frac{\gamma-1}{2} M_\infty^2 \right) \quad (8)$$

2. Theoretical Evaluation of the Recovery Factor.

As stated in section 1, the flow is not usually adiabatic and frictionless and this gives rise to the introduction of the recovery factor when evaluating the percentage of the adiabatic temperature increase which has been realized.

In order to derive an expression for this recovery factor it is necessary to include the effect of friction, and the first case which will be considered will be that of the flat plate thermometer.

2.1 The Flat-plate Thermometer.

This is a thin flat plate which is mounted parallel to the airstream and over which it is assumed that there is no pressure gradient.

Using cartesian co-ords x, y , with the origin at the leading edge and introducing velocity components u and v in the x and y directions, the equation of continuity in 2.D. flow is

$$\frac{\partial (\rho u)}{\partial x} + \frac{\partial (\rho v)}{\partial y} = 0 \quad \text{_____} \quad (1)$$

The equations of motion in the x and y directions are derived from the Navier-Stokes equations which may be written as:

$$\rho \frac{Du}{Dt} = X - \frac{\partial p}{\partial x} + \frac{\partial}{\partial x} \left(\mu \frac{\partial u}{\partial x} \right) + \frac{\partial}{\partial y} \left(\mu \frac{\partial u}{\partial y} \right) \quad (2)$$

$$\rho \frac{Dv}{Dt} = Y - \frac{\partial p}{\partial y} + \frac{\partial}{\partial x} \left(\mu \frac{\partial v}{\partial x} \right) + \frac{\partial}{\partial y} \left(\mu \frac{\partial v}{\partial y} \right) \quad (3)$$

The expansion of the L.H.S. is

$$\rho \left(\frac{du}{dt} + u \frac{\partial u}{\partial x} + v \frac{\partial u}{\partial y} \right), \text{ etc.}$$

and as the case under consideration involves steady flow without any external forces, many of these terms may be removed including $\frac{\partial p}{\partial x}$ which was the initial assumption of zero pressure gradient.

The equations therefore reduce to

$$\rho \left(u \frac{\partial u}{\partial x} + v \frac{\partial u}{\partial y} \right) = \frac{\partial}{\partial x} \left(\mu \frac{\partial u}{\partial x} \right) + \frac{\partial}{\partial y} \left(\mu \frac{\partial u}{\partial y} \right) \quad (2')$$

$$\rho \left(u \frac{\partial v}{\partial x} + v \frac{\partial v}{\partial y} \right) = -\frac{\partial p}{\partial y} + \frac{\partial}{\partial x} \left(\mu \frac{\partial v}{\partial x} \right) + \frac{\partial}{\partial y} \left(\mu \frac{\partial v}{\partial y} \right) \quad (3')$$

Some terms in these two equations are less significant than others and these may be eliminated by the following method of quantitative analysis.

Let δ_u be the thickness of the velocity boundary layer, and $\delta_u \ll x$. The velocity in the boundary layer changes from 0 at $y = 0$ to U_∞ at $y = \delta_u$ and letting U_∞ and x be of unit orders of magnitude.

$$\frac{\partial u}{\partial x} = O(1), \quad \frac{\partial u}{\partial y} = O\left(\frac{1}{\delta_u}\right), \quad \frac{\partial^2 u}{\partial y^2} = O\left(\frac{1}{\delta_u^2}\right) \text{ etc.}$$

The eqn. of continuity may be expanded to give

$$\rho \left[\frac{\partial u}{\partial x} + \frac{\partial v}{\partial y} \right] + u \frac{\partial \rho}{\partial x} + v \frac{\partial \rho}{\partial y} = 0$$

orders of magnitude: $= O(1) + O\left(\frac{1}{\delta_u}\right) + O(1) + O\left(\frac{1}{\delta_u}\right)$

and in order for this to be satisfied, it is apparent that $v = O(\delta_u)$.

$$\therefore \frac{\partial v}{\partial x} = O(\delta_u), \quad \frac{\partial v}{\partial y} = O(1), \quad \frac{\partial^2 v}{\partial x^2} = O(\delta_u), \quad \frac{\partial^2 v}{\partial y^2} = O(\delta_u)^{-1}$$

After expansion and application of this analysis, eqn 2' becomes

$$\rho \left(u \frac{\partial u}{\partial x} + v \frac{\partial u}{\partial y} \right) = \mu \left(\frac{\partial^2 u}{\partial x^2} + \frac{\partial^2 u}{\partial y^2} \right) + \frac{\partial u}{\partial x} \cdot \frac{\partial \mu}{\partial x} + \frac{\partial u}{\partial y} \cdot \frac{\partial \mu}{\partial y}$$

$$O(1)O(1) + O(\delta_u)O(\delta_u)^{-1} = O(1) + O(\delta_u)^{-2} + O(1)O(1) + O(\delta_u)^{-1}O(\mu \delta_u^{-1})$$

and it is apparent that terms of order (1) are negligible compared with those of order (δ_u^{-2}) and may therefore be neglected.

Also since the inertia and viscous terms (and the pressure term had it been retained) must be of the same order of magnitude at high Reynolds Nos, the relation is obtained that

$$\frac{\mu}{\rho} = o(\delta_u^2) \quad (4)$$

Equation 2' has now reduced to

$$\rho \left(u \frac{\partial u}{\partial x} + v \frac{\partial u}{\partial y} \right) = \frac{\partial}{\partial y} \left(\mu \frac{\partial u}{\partial y} \right) \quad (5)$$

which is the 1st equation of motion.

Equation 3' may be treated in an identical manner and on expansion becomes

$$\rho \left(u \frac{\partial v}{\partial x} + v \frac{\partial v}{\partial y} \right) = -\frac{\partial p}{\partial y} + \mu \left(\frac{\partial^2 v}{\partial x^2} + \frac{\partial^2 v}{\partial y^2} \right) + \frac{\partial v}{\partial x} \cdot \frac{\partial \mu}{\partial x} + \frac{\partial v}{\partial y} \cdot \frac{\partial \mu}{\partial y}$$

$$o(\rho) o(\delta_u) + o(\delta_u) o(\rho) = o(\delta_u) + o(\delta_u^2) + o(\delta_u) o(\mu) + o(\rho) o(\mu \delta_u^2)$$

Thus on eliminating terms of order (δ_u) and dividing by ρ , this becomes

$$o(\delta_u) = -\frac{1}{\rho} \frac{\partial p}{\partial y} + \frac{\mu}{\rho} o(\delta_u^2) = -\frac{1}{\rho} \frac{\partial p}{\partial y} + o(\delta_u)$$

∴ in order for the pressure term to be of the same order of magnitude as the inertia and viscous terms, ∂p must be of order (δ_u^2) and it may therefore be neglected.

The energy equation which is the balance of internal energy, conduction of heat, convection of heat with the stream and dissipation of heat through friction may be written in the form

$$\rho \frac{D}{Dt} (C_p T) = \frac{Dp}{Dt} + \left\{ \frac{\partial}{\partial x} \left(k \frac{\partial T}{\partial x} \right) + \frac{\partial}{\partial y} \left(k \frac{\partial T}{\partial y} \right) \right\} + \Phi \quad (6)$$

where Φ is the Dissipation function and

$$\Phi = \mu \left[2 \left\{ \left(\frac{\partial u}{\partial x} \right)^2 + \left(\frac{\partial v}{\partial y} \right)^2 \right\} + \left(\frac{\partial v}{\partial x} + \frac{\partial u}{\partial y} \right)^2 - \frac{2}{3} \left(\frac{\partial u}{\partial x} + \frac{\partial v}{\partial y} \right)^2 \right]$$

Applying the same assumptions as before, eqn. (6) may be reduced to:-

$$\rho C_p \left\{ u \frac{\partial T}{\partial x} + v \frac{\partial T}{\partial y} \right\} = \left\{ \frac{\partial}{\partial x} \left(k \frac{\partial T}{\partial x} \right) + \frac{\partial}{\partial y} \left(k \frac{\partial T}{\partial y} \right) \right\} + \Phi \quad (7)$$

Let δ_T be the thickness of the thermal boundary layer and $\delta_T \ll x$. The temperature in the boundary layer changes from T_w at $y = 0$ to T_∞ at $y = \delta_T$, and by the same reasoning as before

$$\frac{\partial T}{\partial x} = o(1); \quad \frac{\partial T}{\partial y} = o(\delta_T^{-1}); \quad \frac{\partial^2 T}{\partial x^2} = o(1); \quad \frac{\partial^2 T}{\partial y^2} = o(\delta_T^{-2})$$

The dissipation function may be reduced to

$$\Phi = \mu \left(\frac{\partial u}{\partial y} \right)^2$$

since all the other terms are small by comparison with this.

Eqn. (7) therefore becomes

$$\rho C_p \left\{ u \frac{\partial T}{\partial x} + v \frac{\partial T}{\partial y} \right\} = \left\{ \frac{\partial}{\partial x} \left(k \frac{\partial T}{\partial x} \right) + \frac{\partial}{\partial y} \left(k \frac{\partial T}{\partial y} \right) \right\} + \mu \left(\frac{\partial u}{\partial y} \right)^2$$

$$\therefore \rho C_p \left\{ u \frac{\partial T}{\partial x} + v \frac{\partial T}{\partial y} \right\} = k \left\{ \frac{\partial^2 T}{\partial x^2} + \frac{\partial^2 T}{\partial y^2} \right\} + \frac{\partial T}{\partial x} \frac{\partial k}{\partial x} + \frac{\partial T}{\partial y} \frac{\partial k}{\partial y} + \mu \left(\frac{\partial u}{\partial y} \right)^2$$

$$o(1) \cdot o(1) + o(1) \cdot o(\delta_T^{-1}) = o(1) + o(\delta_T^{-2}) \quad o(1) \cdot o(k) \quad o(\delta_T^{-1}) \cdot o(k \delta_T^{-1}) + o(\mu \delta_T^{-2})$$

The terms of order (1) on the R.H.S. are small compared with those of order (δ_T^{-2}) and may be neglected, and in order for the convective and conductive terms to be of the same magnitude.

$$\frac{k}{\rho C_p} = o(\delta_T^2) \quad (8)$$

Combining this with (4), it is seen that

$$\frac{\delta_u}{\delta_T} = o \left[\left(\frac{\mu C_p}{k} \right)^{\frac{1}{2}} \right] = \sigma^{\frac{1}{2}} \quad (9)$$

Thus the thermal and velocity boundary layer thicknesses are similar in air where $\sigma = 0.72$ and the energy equation becomes:-

$$\rho C_p \left\{ u \frac{\partial T}{\partial x} + v \frac{\partial T}{\partial y} \right\} = \frac{\partial}{\partial y} \left(k \frac{\partial T}{\partial y} \right) + \mu \left(\frac{\partial u}{\partial y} \right)^2 \quad \text{----- (10)}$$

The boundary conditions for the flat plate with zero heat transfer are:

$$y=0 ; \quad u=v=0 , \quad \frac{\partial T}{\partial y} = 0 .$$

$$y=\infty ; \quad u=U_\infty , \quad T=T_\infty .$$

Equations (1), (5), (10) are the compressible forms of the equations of continuity, motion and energy for a flat plate, and in the incompressible flow ρ , μ and k may be considered constant and the equations become:-

$$\frac{\partial u}{\partial x} + \frac{\partial v}{\partial y} = 0 \quad \text{----- (11)}$$

$$u \frac{\partial u}{\partial x} + v \frac{\partial u}{\partial y} = \nu \frac{\partial^2 u}{\partial y^2} \quad \text{----- (12)}$$

$$u \frac{\partial T}{\partial x} + v \frac{\partial T}{\partial y} = \frac{k}{\rho C_p} \frac{\partial^2 T}{\partial y^2} + \frac{\mu}{\rho C_p} \left(\frac{\partial u}{\partial y} \right)^2 \quad \text{----- (13)}$$

From inspection of eqns. (11), (12), (13) it is apparent that the velocity field is independent of the temperature field, so that the method of solution of these equations is to solve (11) and (12) for the boundary conditions given, and to obtain u and v as functions of a parameter η involving x and y . Then these functions are substituted into (13) and an expression is derived for T which satisfies the remaining boundary conditions.

A stream function ψ is introduced such that

$$u = \frac{\partial \psi}{\partial y} ; \quad v = - \frac{\partial \psi}{\partial x} \quad \text{(14)}$$

and this satisfies the eqn. of continuity.

Then from the b.c. at $\eta = 0$ that $f = f' = 0$, $A_0 = A_1 = 0$.

Substituting into eqn. (15), it becomes

$$A_3 + A_4 \eta + \frac{\eta^2}{2!} (A_2 - A_5) + \frac{\eta^3}{3!} (2A_2 A_3 + A_6) + \dots = 0$$

and in order for this to be a solution of the differential equation, all the coefficients must vanish identically and therefore

$$A_3 = A_4 = 0; \quad A_5 = -A_2^2; \quad A_6 = 0$$

By continuing this process further it can be shown that only A_2, A_5, A_8, A_{11} etc. have finite values, all the remainder being zero.

Putting $A_2 = \alpha$, the series becomes:

$$f = \frac{\alpha \eta^2}{2!} - \frac{\alpha^2 \eta^5}{5!} + \frac{11}{8} \alpha^3 \eta^8 + \dots$$

The asymptotic expansion is assumed to be of the form

$$f = f_1 + f_2 + \dots$$

with the condition that at high values of η , $f_2 \ll f_1$ etc.

The 1st approximation is

$$f_1 = 2(\eta - \beta) \quad \text{where } \beta \text{ is a const.}$$

but as $f_1'' = 0$, the term $f f_1''$ in (15) is replaced by $f_1 f_2''$ which leads to the 2nd approximation.

$$2(\eta - \beta) f_2'' + f_2''' = 0$$

The solution of this is

$$\log f_2'' = 2\beta\eta - \eta^2 + C$$

Then by putting

$$\eta = \frac{1}{2} \left(\frac{U_\infty}{\nu x} \right)^{\frac{1}{2}} y ; \quad \psi = (\nu U_\infty x)^{\frac{1}{2}} f(\eta)$$

a solution may be found in which f is a function of η alone.

From (14)

$$u = \frac{1}{2} U_\infty f' \quad \text{and} \quad v = \frac{1}{2} \left(\frac{\nu U_\infty}{x} \right)^{\frac{1}{2}} (\eta f' - f)$$

where primes denote differentiation w.r.t. η

Then

$$\frac{\partial u}{\partial x} = -\frac{1}{4} \frac{U_\infty}{x} \eta f'' ; \quad \frac{\partial u}{\partial y} = \frac{U_\infty}{2} \left(\frac{U_\infty}{\nu x} \right)^{\frac{1}{2}} f'' ; \quad \frac{\partial^2 u}{\partial y^2} = \frac{U_\infty}{8} \left(\frac{U_\infty}{\nu x} \right) f''' \quad (14a)$$

and substituting these expressions into (12), it becomes

$$-\frac{U_\infty}{2} \cdot \frac{U_\infty}{4x} \eta f' f'' + \frac{U_\infty^2}{8x} (\eta f' f'' - f f''') = \frac{U_\infty^2}{8x} f'''$$

which reduces to

$$f f'' + f''' = 0 \quad (15)$$

The boundary conditions are now:

$$\begin{aligned} \text{at } \eta = 0 & ; \quad f = f' = 0 \\ \text{at } \eta = \infty & ; \quad f' = 2 \end{aligned}$$

The solution of eqn. (15) is found numerically or by a series expansion, and it is this latter method, which was used by H. Blasius², which is described here. Blasius obtained the solution in two parts - firstly a series expansion about $\eta = 0$ and then an asymptotic expansion for higher values of η and the two solutions were joined together at a point $\eta = \eta_1$, at which each solution was still applicable.

The power series was assumed to be of the form

$$\begin{aligned} f(\eta) &= A_0 + A_1 \eta + \frac{A_2}{2!} \eta^2 + \frac{A_3}{3!} \eta^3 + \dots \\ f'(\eta) &= A_1 + A_2 \eta + \frac{A_3}{2!} \eta^2 + \frac{A_4}{3!} \eta^3 + \dots \end{aligned}$$

Assume the constant c to be of the form $c = -\beta^2 + \log \gamma$ where γ is a new constant and then

$$f_2'' = \gamma e^{-(\eta-\beta)^2}$$

which on integrating becomes:

$$f_2' = \gamma \int_{\eta=\infty}^{\eta} e^{-(\eta-\beta)^2} d\eta$$

This satisfies the condition $f_2'(\infty) = 0$, and as $f_1'(\infty) = 2$, the solution

$$f' = f_1' + f_2'$$

satisfies the condition $f'(\infty) = 2$.

Upon further integration

$$f = 2(\eta-\beta) + \gamma \int_{\infty}^{\eta} d\eta \int_{\infty}^{\eta} e^{-(\eta-\beta)^2} d\eta$$

The three unknown constants α, β, γ are used to join the two solutions together at $\eta = \eta_1$, and so form one function $f(\eta)$.

Blasius² determined numerical values for α, β, γ as follows:-

$$\alpha = 1.328, \quad \beta = 0.865, \quad \gamma = 0.231$$

Tables have been compiled by a number of authors tabulating values of f, f' and f'' for a range of values of η and therefore the values of u and v are known for any η . Having obtained these values for u and v , it is now possible to substitute them into eqn. (13) which will be satisfied if the temperature is a function of η only.

$$\text{Let } T_w = T_{\infty} + \frac{1}{8} \cdot \frac{u_{\infty}^2}{J C_p} \cdot \theta(\eta) \quad (16)$$

Then

$$\frac{\partial T}{\partial x} = -\frac{u_{\infty}^2}{8 J C_p} \cdot \theta' \cdot \frac{\eta}{2x}; \quad \frac{\partial T}{\partial y} = \frac{u_{\infty}^2}{8 J C_p} \cdot \frac{\theta'}{2} \cdot \left(\frac{u_{\infty}}{\sqrt{x}}\right)^{\frac{1}{2}}; \quad \frac{\partial^2 T}{\partial y^2} = \frac{u_{\infty}^2}{8 J C_p} \left(\frac{u_{\infty}}{\sqrt{x}}\right) \frac{\theta''}{4}$$

Substituting these expressions into (13) it becomes:

$$\frac{u_{\infty}^3}{32 J C_p} \cdot \frac{\eta}{x} \cdot f' \theta' + \frac{u_{\infty}^3}{32 J C_p} \cdot \frac{\theta'}{x} (\eta f' - f) = \frac{k}{\rho J C_p} \cdot \frac{u_{\infty}^3}{32 J C_p} \frac{\theta''}{\sqrt{x}} + \frac{\mu}{\rho J C_p} \frac{u_{\infty}^3}{16 \sqrt{x}} f''^2$$

which reduces to

$$\theta'' + \sigma f \theta' + 2\sigma f''^2 = 0. \quad (17)$$

The boundary conditions are:

$$\begin{aligned} \eta = 0 & : \theta' = 0 \\ \eta = \infty & : \theta = 0 \end{aligned}$$

The solution of (17) satisfying these conditions has been obtained by E. Pohlhausen³ and is:-

$$\theta(\eta) = 2\sigma \int_{\eta}^{\infty} \exp(-\sigma \int_0^{\eta} f d\eta) \left[\int_0^{\eta} f''^2 \exp(\sigma \int_0^{\eta} f d\eta) d\eta \right] d\eta$$

and if $\theta(0)$ is denoted by $\alpha_2(\sigma)$

$$\alpha_2(\sigma) = 2\sigma \int_0^{\infty} \exp(-\sigma \int_0^{\eta} f d\eta) \left[\int_0^{\eta} f''^2 \exp(\sigma \int_0^{\eta} f d\eta) d\eta \right] d\eta$$

Pohlhausen has tabulated $\alpha_2(\sigma)$ for a range of values of σ and for low values ($\sigma < 2$), $\alpha_2(\sigma)$ approximates to $4\sigma^{\frac{1}{2}}$

∴ the temperature of the flat plate thermometer is given by $\alpha_2(\sigma)$ substituted into equation (16):-

$$T_W = T_{\infty} + \sigma^{\frac{1}{2}} \cdot \frac{U_{\infty}^2}{2Jc_p} \quad (18)$$

This is the expression for the wall temperature with zero heat transfer and it is desirable to rewrite T_W as T_{W_0} in order to distinguish it from the temperature when heat transfer is taking place.

In terms of the recovery factor r ,

$$T_{W_0} = T_{\infty} + r \cdot \frac{U_{\infty}^2}{2Jc_p}$$

and therefore for the flat plate, $r = \sigma^{\frac{1}{2}}$.

In air, $\sigma = 0.72$ and $r = 0.85$.

For laminar flow this is in good agreement with some experimental results obtained by E. Eckert⁴ who measured the temperature of a flat plate at various Reynolds numbers. At the transition point from laminar to turbulent flow the temperature increased, and for fully turbulent flow the recovery factor assumed a value of 0.90. This agrees very closely with a formula suggested by H.B. Squire⁵,

$$\text{viz: } r = \sigma^{\frac{n+1}{n+3}}$$

where n is the index in the power law velocity distribution through the b.l. For the $\frac{1}{7}$ th power law, this results in a value of r of $0.89 \approx \sigma^{\frac{1}{3}}$ i.e. for turbulent flow

$$\underline{T_{w_0} = T_{\infty} + \sigma^{\frac{1}{3}} \cdot \frac{u_{\infty}^2}{2Jc_p}} \quad (19)$$

The above result has been obtained for an incompressible flow but it is also applicable to a compressible one. In a compressible flow, the velocity and temperature boundary layers interact and it is therefore not possible to separate the calculation for the velocity boundary layer from that of the thermal one. However, in the particular case of $\sigma = 1$, there exists a remarkably simple and important relationship that, irrespective of the variation of the viscosity with temperature, T is a function of u only. Using this relationship and substituting it into (10) it is apparent that this will be the solution if simultaneously

$$\frac{\partial^2 T}{\partial x^2} = -\frac{1}{Jc_p}$$

On integration and substitution of the b.c.'s, this becomes

$$\underline{T_{w_0} = T_{\infty} + \frac{u_{\infty}^2}{2Jc_p}} \quad (\sigma = 1)$$

H.W. Emmons and J.G. Brainerd⁶ have shown that for values of σ differing only slightly from unity, the effect of compressibility is small and the incompressible equation holds.

$$\text{viz. } T_{W_0} = T_\infty + \sigma^{\frac{1}{2}} \frac{U_\infty^2}{2J C_p} \quad (18^1)$$

This result has also been shown by H.W. Liepmann⁷ who used a different approach from the one above. He first of all started by considering Couette flow for a compressible fluid, and solved the simplified energy equation (in which the convective heat transfer is zero by virtue of the assumptions that $\frac{\partial T}{\partial x} = v = 0$) and the result which he obtained is that

$$T_{W_0} = T_\infty + \sigma \frac{U_\infty^2}{2J C_p}$$

Then in order to make this result applicable to the case of a flat plate in laminar flow, Liepmann assumed that the walls were no longer parallel, but that one of them diverged at a rate proportional to $x^{\frac{1}{2}}$. This is the same as the rate of growth of a laminar boundary layer on a flat plate and the result which he obtained was

$$T_{W_0} = T_\infty + \sigma^{\frac{1}{2}} \frac{U_\infty^2}{2J C_p} \quad (18^{11})$$

which is the same as for an incompressible flow.

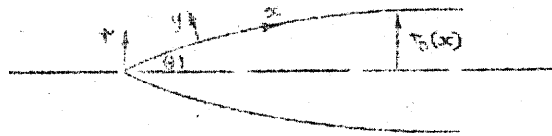
2.2 The Cylinder with its axis parallel to the airstream

Having derived expression (18) for the flat plate thermometer, it is now possible to extend the theory to cover the case of a circular cylinder with its axis parallel to the airstream. This case represents quite closely the standard thermometer probe which is fitted on some aircraft at the present time.

Starting again with the three basic equations, it can be shown³ by using Mangler's transformation that for any axisymmetric body, only the equation of continuity differs from its 2-dimensional counterpart. It now becomes

$$\frac{\partial}{\partial x} (\rho r u) + \frac{\partial}{\partial y} (\rho r v) = 0 \quad (20)$$

2.2.1 Mangler's Transformation



Let L be an arbitrary length and let \bar{x} , \bar{y} etc. represent lengths etc. on the axisymmetric body.

$$\text{Then } \bar{x} = \int_0^x \frac{r_0^2(\xi)}{L^2} d\xi ; \quad \bar{y} = \frac{r_0 y}{L} ; \quad \bar{r}(\bar{x}) = r(x) ; \quad \bar{\rho}(\bar{x}) = \rho(x) ; \quad \bar{u}(\bar{x}, \bar{y}) = u(x, y)$$

$$\text{and } \bar{v}(\bar{x}, \bar{y}) = \frac{L}{r_0(x)} \left[v(x, y) + \frac{r_0'}{r_0} y \cdot u(x, y) \right]$$

Substitution of these into the axisymmetric eqn. of motion gives

$$\bar{\rho} \left(\bar{u} \frac{\partial \bar{u}}{\partial \bar{x}} - \bar{v} \frac{\partial \bar{u}}{\partial \bar{y}} \right) = \frac{\partial}{\partial \bar{y}} \left(\bar{\rho} \frac{\partial \bar{u}}{\partial \bar{y}} \right)$$

which is the equation of motion for a flat plate in 2.D flow.

In the same way the energy equation may be shown to be identical to the 2.D. case.

The equation of continuity (20) may be expanded and simplified after making certain assumptions.

$$\frac{\partial}{\partial x} (\rho r u) + \frac{\partial}{\partial y} (\rho r v) = \frac{\partial}{\partial x} (\rho u) + \frac{\partial}{\partial y} (\rho v) + \frac{\rho u}{r} \frac{\partial r}{\partial x} + \frac{\rho v}{r} \frac{\partial r}{\partial y} = 0$$

v is usually small compared with u and the last term, which is $\frac{r}{r} \cdot \cos \theta$, may be neglected. Then for the particular case of the cylinder in axial flow $\frac{\partial r}{\partial x} = 0$ and so

$$\frac{\partial}{\partial x}(\rho u) + \frac{\partial}{\partial y}(\rho v) = 0$$

Thus for this particular case the equations of continuity, motion and energy are identical to those for the flat plate and therefore all the preceding theory is directly applicable to the cylinder. However near the stagnation point it is likely to be in error because the boundary layer thickness, δ , is not very much less than $r_0(x)$, and this assumption was made in the derivation.

Therefore the recovery factor in laminar flow will be $\sigma^{\frac{1}{2}}$ and the kinetic temperature of the body will be given by the expression as before:

$$T_{w_0} = T_{\infty} + \sigma^{\frac{1}{2}} \cdot \frac{u_{\infty}^2}{2Jc_p} \quad (18)$$

The kinetic temperature rise $(\sigma^{\frac{1}{2}} \frac{u_{\infty}^2}{2Jc_p})$ is that experienced under zero heat transfer conditions as the surface is approached through a boundary layer. So far no account has been taken of any heat transfer either to or from the surface, and this will be considered next.

3. The Equilibrium Temperature

The thermometer probes discussed later in this report have all been insulated from any stray heating from within the aircraft by inserting some insulating material between the probe and the aircraft skin. Thus any heat conduction along the supporting strut has been eliminated.

However radiation effects are always present in the forms of solar radiation to the surface and radiation away from it. The amount of solar radiation which is absorbed by an exposed body is difficult to estimate although various empirical formulae have been suggested. Inevitably any estimations are of an approximate nature and it is better to attempt to eliminate this error than to try to make any quantitative allowance for it.

In the case of the radiation away from the surface it is possible to calculate the amount analytically and draw up a heat balance equating the convective heat input to the radiative heat output.

The equilibrium temperature is that at which the heat input exactly balances the heat output and is obtained as the solution of this equation. It will be lower than the kinetic temperature and consequently the recovery factor will be reduced accordingly.

In this section expressions are derived for the rates of convective and radiative heat transfer in both laminar and turbulent flows.

3.1 Reynolds Analogy

This is a most useful analogy between heat transfer and skin friction which applies in both laminar and turbulent flow and may be expressed as:

$$\frac{k_H}{\frac{\rho}{2} C_f} = S$$

where k_H is the Stanton heat transfer coefficient which is defined as

$$k_H = \frac{q_w}{\rho u_w C_p (T_w - T_\infty)}$$

c_f is the local skin friction coefficient and S is the Reynolds analogy factor.

q_w is the rate of heat transfer and is defined as

$$q_w = -k \frac{\partial T}{\partial y} \quad \text{and} \quad \frac{\partial T}{\partial y} = \frac{\partial T}{\partial \eta} \cdot \frac{\partial \eta}{\partial y}$$

In order to obtain q_w , it is necessary to solve the energy equation (13) for T , and the assumption is made that T can be expressed in the form

$$T = T_w - (T_w - T_\infty) \theta(\eta) \quad (21)$$

The heating due to friction, which is represented in the energy equation by the term $\mu \left(\frac{\partial u}{\partial y} \right)^2$, is small at low Mach numbers, but when considering the case of zero heat transfer, it was necessary to retain it in order to obtain the result derived earlier. However in this case when heat transfer is present, the frictional heating term is small enough to be neglected. M.J. Lighthill⁸ has suggested that when this assumption has been made, the accuracy of the result will be improved by re-defining the Stanton heat transfer coefficient as

$$h_h = \frac{q_w}{\rho_\infty u_\infty c_p (T_w - T_\infty)}$$

It is now proposed to derive a value for S in laminar flow over a flat plate. Substituting for T in terms of η

(by the relationship (21)) into the modified energy equation, it reduces to the functional eqn:

$$\theta'' + \sigma f \theta' = 0 \quad (22)$$

and the boundary conditions are

$$\text{at } \eta = 0 ; \theta = 0$$

$$\eta = \infty ; \theta = 1$$

and the solution was found by Pohlhausen³ to be:

$$\theta(\eta) = \alpha_1(\sigma) \int_0^\eta \left[\frac{f''(\eta)}{f''(0)} \right]^\sigma d\eta$$

$\alpha_1(\sigma)$ has been tabulated for a range of values of σ , and for low values ($\sigma < 2$)

$$\alpha_1(\sigma) \doteq 0.664 \sigma^{\frac{1}{3}}$$

The rate of heat transfer is defined as

$$q = -k \frac{\partial T}{\partial y} = k (T_w - T_\infty) \cdot \frac{1}{2} \sqrt{\frac{u_\infty}{\nu x}} \cdot \theta'(\eta)$$

$$\therefore q_{yw} = 0.332 \sigma^{\frac{1}{3}} (T_w - T_\infty) \left(\frac{u_\infty}{\nu x} \right)^{\frac{1}{2}} \cdot k \quad (23)$$

The skin friction is given by

$$\tau_w = \mu \left(\frac{\partial u}{\partial y} \right)_{y=0}$$

and from (14a)

$$\frac{\partial u}{\partial y} = \frac{u_\infty}{4} \left(\frac{u_\infty}{\nu x} \right)^{\frac{1}{2}} f''(\eta)$$

But $f''(\eta)$ at $\eta = 0 = \alpha = 1.328$.

and therefore

$$\tau_w = \frac{1.328}{4} \mu U_\infty \left(\frac{U_\infty}{\nu x} \right)^{\frac{1}{2}}$$

$$\text{and } c_f = \frac{\tau_w}{\frac{1}{2} \rho_\infty U_\infty^2} = 0.664 \left(\frac{U_\infty x}{\nu} \right)^{-\frac{1}{2}} \quad (24)$$

But from eqns. (23) and (24) and making use of the Stanton heat transfer coefficient:

$$\underline{h_h = \frac{c_f}{2} \sigma^{-\frac{2}{3}}} \quad (25)$$

i.e. for laminar flow, the Reynolds analogy factor $= \sigma^{-\frac{2}{3}}$ and L. Crocco⁴ has demonstrated that this relation is approximately correct in compressible as well as in incompressible flow.

In turbulent flow, the value of this factor which gives the best agreement with experimental results is

$$S = 1.22 \quad (26)$$

Von Karman has estimated a relationship based on the measured structure of the boundary layer which approximates to:

$$\begin{aligned} S &= \sigma^{\frac{1}{3}} & 10^6 < R_e < 10^8 \\ \text{and } S &= 1.17 & \text{at } R_e = 10^5 \end{aligned}$$

However, experimental evidence indicates that these results are low and so the value given in (26) will be used in the derivation of the rate of heat transfer in a turbulent boundary layer (§ 3.4).

3.2. The Intermediate Enthalpy Notation

The enthalpy or heat content of the air in the boundary layer is defined as

$$i = \int_0^T C_p dT \quad (27)$$

and the equation for the zero heat transfer temperature (18) transforms into a zero heat transfer enthalpy eqn.¹⁰

$$i_{w_0} = i_w + \sigma^{\frac{1}{2}} \frac{u_w^2}{2C_p} = i_w \left(1 + \sigma^{\frac{1}{2}} \frac{\gamma-1}{2} M_\infty^2 \right) \quad (28)$$

If the physical properties of air which appear in the incompressible flow equations are evaluated at a temperature corresponding to an intermediate enthalpy, i^* , the resulting heat transfer has been shown by E. Eckert¹¹ to be in good agreement with experimental results for a compressible flow. The significance of this is that an expression may be derived for k_H in an incompressible flow, and then by evaluating the physical properties at this intermediate condition, the expression becomes valid for a compressible flow.

For moderate temperatures, $C_p = \text{constant}$ and $i = C_p T$. This simplifies the problem and it might appear that there is no justification for introducing the enthalpy at all. The reason for doing so is to maintain generality, and the equations which follow are applicable to very high temperatures. They may even be used up to the dissociation temperature where, had T been used as a parameter, they would have been inapplicable.

The expression for i^x which gave the best fit to theoretical results was

$$i^x = i_\infty + 0.5(i_w - i_\infty) + 0.22(i_{w_0} - i_\infty) \quad (29)$$

In this notation

$$k_h = \frac{q_w}{\rho_\infty u_\infty (i_{w_0} - i_w)} \quad (30)$$

For the compressible case

$$k_h^x = \frac{q_w}{\rho^x u_\infty (i_{w_0} - i_w)} = \frac{q_w}{\rho_\infty u_\infty (i_{w_0} - i_w)} \cdot \frac{\rho_\infty}{\rho^x} \quad (31)$$

But from the eqn. of state and making use of the fact that p is constant across the boundary layer,

$$\frac{\rho_\infty}{\rho^x} = \frac{T^x}{T_\infty}$$

and therefore

$$k_h^x = k_h \cdot \frac{T^x}{T_\infty} \quad (32)$$

3.3 Heat Transfer in a Laminar Boundary Layer

Returning to the flat plate, and using the subscript i to denote the incompressible case, it has been shown in para 3.1 that :

$$k_{w_i} = \frac{c_f}{2} \cdot \sigma^{-\frac{2}{3}} = 0.332 (Re_x)^{-\frac{1}{2}} \sigma^{-\frac{2}{3}} \quad (33)$$

Transforming to the intermediate conditions

$$h_u^x = 0.332 \sigma^x \left(Re_x^x \right)^{-\frac{1}{2}} \quad (34)$$

It is assumed that the Prandtl number is independent of temperature, i.e. $\sigma = \sigma^x$

and $Re_x^x = \frac{U_\infty \rho^x x}{\mu^x} = \frac{U_\infty \rho_\infty x}{\mu_\infty} \cdot \frac{\rho^x}{\rho_\infty} \cdot \frac{\mu_\infty}{\mu^x} = Re_x \left[\frac{T_\infty}{T^x} \cdot \frac{\mu_\infty}{\mu^x} \right]$

and therefore substituting this into (34) and invoking eqn. (32),

$$h_u = 0.332 \sigma \left(Re_x \right)^{-\frac{1}{2}} \left[\frac{T_\infty}{T^x} \cdot \frac{\mu_\infty}{\mu^x} \right]^{\frac{1}{2}} \quad (35)$$

At this point it is necessary to assume some variation of μ with T. Two expressions are available:-

1) Sutherlands Law - $\mu = C_1 \left\{ \frac{T^{\frac{3}{2}}}{T + C_2} \right\}$

$$\therefore \frac{\mu^x}{\mu_\infty} = \left(\frac{T^x}{T_\infty} \right)^{\frac{3}{2}} \left[\frac{T_\infty + C_2}{T^x + C_2} \right]$$

2) $\mu = C_3 T^\omega$

$$\therefore \frac{\mu^x}{\mu_\infty} = \left(\frac{T^x}{T_\infty} \right)^\omega \quad (36)$$

Using the second expression,

$$h_u = 0.332 \sigma \left(Re_x \right)^{-\frac{1}{2}} \left(\frac{T_\infty}{T^x} \right)^{\frac{1-\omega}{2}} \quad (37)$$

This is the local heat transfer coefficient and in order to obtain the mean over the length of the plate, it is necessary to integrate k_H , or start with the mean skin friction coefficient, C_F .

This intermediate enthalpy method has only been justified for experiments in air and therefore it is more correct to substitute the value of ω in air into expression (37). The usual value is $\omega = 8/9$.

$$\therefore K_H = k_H \text{ mean} = 0.664 (Re_x)^{-\frac{1}{2}} \sigma^{-\frac{2}{3}} \left(\frac{T_\infty}{T_w}\right)^{\frac{1}{18}} \quad (38)$$

and the mean heat transfer / ft² sec is

$$\underline{Q_{lam} = 0.664 \rho_\infty u_\infty c_p (Re_x)^{-\frac{1}{2}} \sigma^{-\frac{2}{3}} \left(\frac{T_\infty}{T_w}\right)^{\frac{1}{18}} (T_{w_0} - T_w)} \quad (39)$$

3.4 Heat Transfer in a Turbulent Boundary Layer.

3.4.1 Derivation of the Skin Friction Coefficient.

It will be assumed that the boundary layer velocity distribution satisfies the $\frac{1}{7}$ th root law, (and this will be so for Reynolds numbers $< 10^5$). Then

$$\frac{u}{u_{\infty}} = \left(\frac{y}{\delta}\right)^{\frac{1}{7}} \quad (40)$$

It has been shown by H. Blasius that

$$\tau_w = 0.0225 \rho_{\infty} u_{\infty}^2 (Re_{\delta})^{-\frac{1}{4}} \quad (41)$$

The momentum thickness of the boundary layer is defined as

$$\delta_2 = \int_0^{\delta} \frac{u}{u_{\infty}} \left(1 - \frac{u}{u_{\infty}}\right) dy = \frac{7}{72} \delta \quad (42)$$

Then invoking Von Karman's momentum equation

$$\frac{\tau_w}{\rho_{\infty} u_{\infty}^2} = \frac{\partial \delta_2}{\partial x} + \delta_2 (H+2) \frac{\partial u_{\infty}}{\partial x}$$

which reduces to

$$\frac{\tau_w}{\rho_{\infty} u_{\infty}^2} = \frac{\partial \delta_2}{\partial x}$$

for the flat plate since $\frac{\partial u_{\infty}}{\partial x}$ is zero, and substituting for δ_2 from (42) it becomes

$$\frac{\tau_w}{\rho_{\infty} u_{\infty}^2} = \frac{7}{72} \frac{\partial \delta}{\partial x} \quad (43)$$

Comparing (41) and (43)

$$.0225 \rho_{\infty} u_{\infty}^2 (Re_{\delta})^{-1/4} = \frac{7}{72} \rho_{\infty} u_{\infty}^2 \frac{\partial \delta}{\partial x}$$

On integrating

$$.0225 \left(\frac{\nu}{u_{\infty}} \right)^{1/4} x = \frac{7}{72} \cdot \frac{4}{5} \delta^{5/4} + C$$

with the boundary condition that $\delta = 0$ when $x = 0$ i.e. $C = 0$.

$$\therefore \delta = 0.371 x (Re_x)^{-1/5}$$

and $\delta_2 = .036 x (Re_x)^{-1/5}$

$$\therefore c_f = \frac{\tau_w}{\frac{1}{2} \rho_{\infty} u_{\infty}^2} = 2 \frac{\partial \delta_2}{\partial x} = .0576 (Re_x)^{-1/5}$$

and the drag of the plate = $\rho_{\infty} u_{\infty}^2 S \delta_2$ from which the overall skin friction coefficient is

$$C_F = \frac{D}{\frac{1}{2} \rho_{\infty} u_{\infty}^2 S} = .072 (Re_l)^{-1/5} \quad (44)$$

3.4.2. Derivation of the Heat Transfer.

After substituting eqns. (26) and (44) into the Reynolds analogy, it becomes:

$$K_{H_c} = 1.22 x \frac{1}{2} x 0.72 (Re_l)^{-1/5} \quad (45)$$

Then by transforming to the intermediate conditions, the heat transfer coefficient is

$$K_H^x = 1.22 \times .036 (R_{e_t}^x)^{-1/5} = 1.22 \times 0.36 (R_{e_t})^{-1/5} \left[\frac{T_\infty}{T^x} \cdot \frac{\mu_\infty}{\mu^x} \right]^{1/5}$$

and

$$K_H = .0438 (R_{e_t})^{-1/5} \left(\frac{T_\infty}{T^x} \right)^{4/5} \left(\frac{\mu_\infty}{\mu^x} \right)^{-1/5} \quad (46)$$

by virtue of eqn. (32).

Using eqn. (36) for the viscosity variation and giving ω the value $8/9$ as before, eqn. (46) reduces to

$$K_H = 0.0438 (R_{e_t})^{-1/5} \left(\frac{T_\infty}{T^x} \right)^{0.622} \quad (47)$$

and therefore the mean heat transfer / ft² . sec. is

$$Q_{\text{turb}} = 0.0438 \rho_\infty u_\infty c_p (R_{e_t})^{-1/5} \left(\frac{T_\infty}{T^x} \right)^{0.622} (T_{w_0} - T_w) \quad (48)$$

Equation (47) indicates that K_H is proportional to $\left(\frac{T_\infty}{T^x} \right)^{\frac{4-\omega}{5}}$ when the intermediate enthalpy method is used in the derivation, whereas R.J. Monaghan¹³ shows that it is proportional to $\left(\frac{T_\infty}{T_w} \right)^{\frac{3-\omega}{5}}$.

These two solutions are approximately identical since

$$T_\infty < T^x < T_w, \quad \text{and therefore } 1 > \frac{T_\infty}{T^x} > \frac{T_\infty}{T_w}, \quad \text{and} \\ 1 > \frac{4-\omega}{5} > \frac{3-\omega}{5}.$$

By applying either of the expressions (39) or (48) it is possible to calculate the amount of heat transferred to the body by convection. Both expressions are dependent on the Reynolds number and, as the index in the turbulent flow is larger than that in the laminar, it is obvious that the rate of heat transfer is higher in the turbulent boundary layer.

The temperature T_{∞} will be known according to the flight altitude under consideration and thus it only remains to calculate T^X .

This is obtained through the relation, $i = C_p T$ for temperatures at which C_p is constant, and

$$i^X = i_{\infty} + 0.5 (i_w - i_{\infty}) + 0.22 (i_{w_0} - i_{\infty})$$

$$\therefore T^X = T_{\infty} + 0.5 (T_w - T_{\infty}) + 0.22 (T_{w_0} - T_{\infty}) \quad (49)$$

For a 1st approximation, assume that

$$T_{w_0} \approx T_w$$

and substituting this into eqn. (49), it reduces to:-

$$T^X = \underline{.28 T_{\infty} + .72 T_{w_0}} \quad (50)$$

This approximation will be sufficiently accurate for most cases of convective/radiative heat transfer without internal heating or cooling of the body since the difference $(T_{w_0} - T_w)$ is only of the order of a few degrees at $M_{\infty} = 1.0$.

3.5 Heat Transfer by Radiation.

The rate of radiative heat transfer away from the surface of a body is given by the expression

$$Q_r = \epsilon \cdot C_b \cdot (T_w^4 - T_{\infty_r}^4).$$

where ϵ is the emissivity and is dependent on the material and surface finish¹⁴.

C_b is the Stefan-Boltzmann Constant = $2.78 \times 10^{-12} \frac{\text{CHU}}{\text{ft}^2 \text{sec}^{\circ}\text{K}^4}$

$$Q_r = 2.78 \epsilon \cdot \left\{ \left(\frac{T_w}{1000} \right)^4 - \left(\frac{T_{\infty_r}}{1000} \right)^4 \right\} \quad (51)$$

There appears to be some difference of opinion among authors whether the heat is radiated to a surface at the free stream temperature or to one at zero absolute temperature. It would seem to be more logical to accept the former assumption since the heat is absorbed by the surrounding atmosphere which is at the free stream temperature. Only a very small amount will penetrate to infinity but in the calculations which follow both cases will be considered.

In addition to this radiation, the surface will be receiving back heat by radiation from the air and also from the sun.

The amount of the former is given by the expression

$$Q_{rr} = 2.78 \cdot \epsilon \cdot \epsilon_g \cdot \left\{ \left(\frac{T_w}{1000} \right)^4 - \left(\frac{T_{\infty_r}}{1000} \right)^4 \right\}$$

where ϵ_g is the emissivity of the gas.

ϵ_g is usually small and Q_{rr} will be a negligible proportion of the total heat transfer.

The amount of solar radiation, as referred to earlier, will be small if care is taken to shield the surface from direct sunlight. Although various empirical formulae are available for calculating this quantity, it would appear to depend on so many parameters that insufficient is known about it to estimate it with accuracy. It has therefore been omitted from the succeeding calculations and is referred to qualitatively only.

3.6 Calculation of the Equilibrium Temperature

Using the expressions derived in the foregoing paragraphs, some calculations have been made in order to investigate the effect of radiation on a cylindrical body placed with its axis parallel to the airstream. The length of the body has been assumed to be 2" and this case corresponds to that of a standard type of thermometer probe. One of these probes was fitted to the aircraft for the flight tests and the results are included later in this report.

Although some values of the convective heat transfer have been calculated for both laminar and turbulent boundary layers, it has been assumed that the flow is laminar in most cases as the Reynolds number is around 10^5 . Also because the rate of heat transfer is lower through a laminar layer than through a turbulent one, this case gave rise to the largest difference between T_{w_0} and T_w .

Four different cases of radiative heat transfer have been considered using extreme values of ϵ and $T_{\infty r}$.

The equations which have to be solved in order to obtain T_w are:-

1. Laminar.

$$0.664 \rho_{\infty} u_{\infty} C_p (Re_{\ell})^{-\frac{1}{2}} \sigma^{\frac{2}{3}} \left(\frac{T_{\infty}}{T^*} \right)^{\frac{1}{8}} (T_{w_0} - T_w) = 2.78 \epsilon \left\{ \left(\frac{T_w}{1000} \right)^4 - \left(\frac{T_{\infty r}}{1000} \right)^4 \right\} \quad (52a)$$

2. Turbulent

$$0.0438 \rho_{\infty} u_{\infty} C_p (Re_{\ell})^{-\frac{1}{5}} \left(\frac{T_{\infty}}{T^*} \right)^{0.622} (T_{w_0} - T_w) = 2.78 \epsilon \left\{ \left(\frac{T_w}{1000} \right)^4 - \left(\frac{T_{\infty r}}{1000} \right)^4 \right\} \quad (52b)$$

Up to $M = 1.0$, the ratio $\left(\frac{T_\infty}{T^*}\right)^{\frac{1}{8}}$ in (52a) is nearly unity and may be neglected. The L.H.S. of the equations may be written:

$$Q \approx \rho_\infty U_\infty C_p K_H (T_{w_0} - T_w)$$

and $K_{HL} = \frac{0.664 \sigma^{-\frac{2}{3}}}{\sqrt{Re_l}} = \frac{0.825}{\sqrt{Re_l}}$ and $K_{HT} = \frac{.0438 \cdot \left(\frac{T_\infty}{T^*}\right)^{0.622}}{\sqrt[5]{Re_l}}$

The following table has been compiled to assist in the solving of eqns. (52) for numerical cases.

SEA LEVEL

$T_\infty = 288^\circ K$; $l = \frac{1}{6}$ ft.
 $\rho_\infty = .00238 \frac{slugs}{ft^3}$; $\nu = 1.576 \times 10^{-4} \frac{ft^2}{sec}$
 $\tau_{lam} = \sigma^{\frac{1}{2}} = 0.848$; $\tau_{turb.} = 0.89$.

M_∞	U_∞ ft/sec	Re_l $\times 10^{-6}$	$(Re_l)^{-\frac{1}{2}}$ $\times 10^3$	$(Re_l)^{-\frac{1}{5}}$ $\times 10$	T_{w_0L} °K	T_{w_0T} °K	T_T^*	$\left(\frac{T_\infty}{T^*}\right)_T^{0.622}$	K_{HL} $\times 10^3$	K_{HT} $\times 10^3$	$\frac{Q}{T_{w_0} - T_w}$	$\frac{Q}{T_{w_0} - T_w}$
											$\frac{CHU}{ft^2 sec °K}$ $\times 10^3$	$\frac{CHU}{ft^2 sec °K}$ $\times 10^3$
0.2	223	2.371	2.054	.840	289.96	290.05	289.5	.997	1.696	3.68	6.99	15.19
0.4	446	4.723	1.455	.733	295.82	296.0	293.5	.988	1.202	3.17	9.85	26.03
0.6	670	7.092	1.188	.675	305.59	306.5	301.5	.972	0.980	2.88	12.08	35.52
0.8	893	9.454	1.029	.639	319.31	320.9	311.5	.953	0.849	2.66	13.92	43.61
1.0	1117	11.810	0.926	.611	336.92	339.2	323.4	.930	0.765	2.49	15.70	51.10

From the above table it is apparent that the rate of heat transfer in a turbulent layer is from 2 to 3 times greater than in a laminar one and therefore the difference $(T_{w_0} - T_w)$ will be correspondingly smaller for the turbulent case.

Further tables have been compiled for laminar flow at 4 different altitudes up to 45,000' and these are to be found in Appendix I.

The first case which will be considered here in detail is that for a surface with a laminar boundary layer and an emissivity of 0.1. It will also be assumed that the radiation is to a surface at infinity having a temperature of absolute zero, so that in eqn. (51), $T_{\infty r} = 0$.

A specimen set of calculations is shown for the sea level condition:

$$\underline{M = 0.2}$$

$$6.99 \times 10^{-3} (T_{W_0} - T_W) = 0.1 \times 2.78 \times 10^{-12} (T_W)^4$$

$$\text{i.e. } 251.5 (T_{W_0} - T_W) = \left(\frac{T_W}{100}\right)^4$$

$$T_{W_0} = 289.96^\circ \text{ and the 1st approximation is that } T_W = 289.5^\circ.$$

$$\therefore 251.5 \times 0.5 > 70.22.$$

\therefore for a 2nd approximation let $T_W = 289.75$

$$(T_W)^4 = 70.47 \quad \text{and } \therefore (T_{W_0} - T_W) = 0.280^\circ$$

This approximation will be very close because $T_W = 289.68^\circ$ and $(289.68)^4 = 70.44$ which gives $(T_{W_0} - T_W) = 0.279^\circ$

$$T_{W_0} - T_W = 0.279^\circ$$

$$\text{and } T_W = 289.68^\circ \text{ K.}$$

The recovery factor for this wall temperature is

$$r = \frac{T_W - T_{\infty}}{T_{\infty} \sqrt{\frac{\gamma-1}{2} M_\infty^2}} \quad \text{where } T_{\infty} \text{ is the free stream temperature which is } 288^\circ \text{ K.}$$

i.e.

$$\underline{r = 0.729.}$$

$$\underline{M = 0.4.}$$

$$9.85 \times 10^{-3} (T_{w_0} - T_w) = .278 \times 10^{-12} T_w^4$$

$$\text{or } 354.0 (295.82 - T_w) = \left(\frac{T_w}{100}\right)^4$$

$$\therefore (T_{w_0} - T_w) = 0.215^\circ$$

$$\text{and } T_w = 295.58^\circ \text{ K.}$$

$$\therefore \underline{r = 0.823.}$$

$$\underline{M = 0.6.}$$

$$434.4 (305.59 - T_w) = \left(\frac{T_w}{100}\right)^4$$

$$\therefore (T_{w_0} - T_w) = 0.200^\circ$$

$$\text{and } T_w = 305.39^\circ \text{ K}$$

$$\therefore \underline{r = 0.838.}$$

$$\underline{M = 0.8.}$$

$$500.8 (319.31 - T_w) = \left(\frac{T_w}{100}\right)^4$$

$$\therefore (T_{w_0} - T_w) = 0.207^\circ$$

$$\text{and } T_w = 319.09^\circ \text{ K}$$

$$\therefore \underline{r = 0.842.}$$

$$\underline{M = 1.0.}$$

$$565.0 (336.92 - T_w) = \left(\frac{T_w}{100}\right)^4$$

$$\therefore (T_{w_0} - T_w) = 0.226^\circ$$

$$\text{and } T_w = 336.67^\circ \text{ K}$$

$$\therefore \underline{r = 0.845.}$$

From these results it is apparent that the maximum effect of radiation is, as expected, at low Mach numbers where the convective heat transfer is a minimum. The difference $(T_{w_0} - T_w)$ is largest here and the recovery factor differs most from $\sigma^{\frac{1}{2}}$ at these low Mach numbers.

It can also be seen that the recovery factor is not constant with Mach number but it increases and approaches $\sigma^{\frac{1}{2}}$.

If a graph was plotted of T_w against M^2 , a straight line through the various points would intercept the temperature axis at 287.71° K . The recovery factor of the whole set of points based on this free stream temperature

$$\text{is } \underline{r = 0.850.}$$

Thus the assumption that the recovery factor remains constant with Mach number leads to a value which is higher than $\sigma^{\frac{1}{2}}$, and a value of the free stream temperature is obtained which is lower than the true one.

This effect is common to all altitudes and may be summarised in the following tables.

$$\epsilon = 0.1, \quad T_{\infty} = 0^\circ \text{K.}$$

M. N ^o	Alt.		25,000'		36,000'		40,000'		45,000'			
	S.L		T _{W0}	T _W	T _{W0}	T _W	T _{W0}	T _W	T _{W0}	T _W		
0.2			280.96	289.72	240.12	239.93	217.97	217.77	217.97	217.75	217.97	217.72
0.4			295.82	295.58	244.97	244.80	222.38	222.23	222.38	222.21	222.38	222.19
0.6			305.59	305.39	253.08	252.92	229.70	229.56	229.70	229.55	229.70	229.52
0.8			319.31	319.09	264.40	264.23	240.00	239.85	240.00	239.84	240.00	239.82
1.0			336.92	336.67	278.95	278.77	253.21	253.04	253.21	253.02	253.21	253.00

Recovery Factors based on $r = \frac{T_w - T_{\infty}}{T_{\infty} \cdot \frac{\gamma - 1}{2} M_{\infty}^2}$

M _∞	Alt.		25,000'		36,000'		40,000'		45,000'		
	S.L										
0.2			.729		.731		.734		.721		.706
0.4			.823		.825		.826		.825		.820
0.6			.838		.840		.839		.836		.835
0.8			.842		.843		.842		.842		.842
1.0			.845		.846		.843		.843		.843

The overall recovery factors based on the free stream temperatures obtained from plots of $T_w \sim M_\infty^2$ are:-

Altitude	S.L.	25,000'	36,000'	40,000'	45,000'
r overall	0.850	0.8505	0.850	0.8495	0.849.

It is apparent from the above tables that not only does r vary with Mach number but also with altitude. It increases from sea level to the tropopause and then, as might be expected, it decreases with further increase in altitude. This is because, at constant Mach number, the convective heat transfer is proportional to $Q_c \sim M_\infty^2$ and T_{w0} is constant so that T_w must decrease with increase of altitude above the tropopause.

Unfortunately the above results have been derived from very small temperature differences which might be considered negligible. However they do indicate a trend and the next case which is considered is that of the surface having an emissivity of 1.0. This is not likely to be the case in practice but it serves to illustrate the effect of emissivity on $(T_{w0} - T_w)$ and to highlight the trend of the variation of r with M_∞ and altitude.

This case is summarised in the following tables:

$$\epsilon = 1.0. \quad T_{\infty} = 0^\circ K$$

Alt M_∞	S.L.		25,000'		36,000'		40,000'		45,000'	
	T_{w0}	T_w	T_{w0}	T_w	T_{w0}	T_w	T_{w0}	T_w	T_{w0}	T_w
0.2	289.96	287.30	240.12	237.95	217.97	216.05	217.97	215.85	217.97	215.61
0.4	295.82	293.70	244.97	243.29	222.38	220.90	222.38	220.74	222.38	220.55
0.6	305.59	303.64	253.08	251.52	229.70	228.30	229.70	228.16	229.70	227.99
0.8	319.31	317.28	264.40	262.80	240.00	262.80	240.00	238.43	240.00	238.23
1.0	336.92	334.60	278.95	277.17	253.21	251.62	253.21	251.48	253.21	251.27

$$\text{Recovery factors } \sim r = \frac{T_w - T_\infty}{T_\infty + \frac{\gamma-1}{2} M_\infty^2}$$

$M_\infty \backslash \text{Alt.}$	S.L	25,000'	36,000'	40,000'	45,000'
0.2	- .327	- .238	- .026	- .375	- .514
0.4	.619	.628	.635	.612	.585
0.6	.755	.758	.759	.747	.735
0.8	.795	.797	.798	.792	.785
1.0	.810	.811	.812	.809	.805

Overall recovery factors based on the free stream temperatures, T'_∞ , obtained from plots of $T_w \sim M_\infty^2$ are:-

T'_∞	285.10	236.20	214.45	214.25	214.00.
r_{overall}	.868	.867	.866	.868	.871.

From a comparison of the two foregoing cases, it may be seen that the trend of the variation of r with M_∞ and altitude is the same but it is more pronounced in the latter condition. However the trend of the overall recovery factor is reversed in this case, and this is due to the variation of $(T_\infty - T'_\infty)$ with altitude. $(T_\infty - T'_\infty)$ is a maximum at sea level and decreases up to 36,000' at which altitude it begins to increase again. It is approximately proportional to the emissivity, and in the latter case it is about 10 times greater than in the former and therefore T'_∞ has become the dominating factor in lieu of $(T_w - T'_\infty)$ in the expression

$$r_{\text{overall}} = \frac{T_w - T'_\infty}{T'_\infty + \frac{\gamma-1}{2} M_\infty^2}$$

These various effects are illustrated in Figures 1 and 2.

Also further tables are included of the two remaining cases in which it has been assumed that the radiation is to a surface having the free stream temperature T_∞ .

$$\text{i.e. } T_{\infty r} = T_\infty .$$

4. A Ventilated Pitot Tube in a Supersonic Airstream.

If a ventilated pitot tube is placed in a supersonic airstream, a detached shock wave will form in front of the mouth, and it will be very nearly normal over the diameter of the tube. The airflow behind the shock will be subsonic, and the tube will behave as if it were in a subsonic airstream at a higher datum temperature and pressure. The temperature rise which a sensing element placed inside the tube would measure would be a combination of that due to passing through the shock and the normal subsonic recovery of the probe.

An expression is now derived for this:-

Let the total temperature rise be ΔT so that

$$T_{\infty} = T_m - \Delta T.$$

If suffix 2 denotes the flow behind the shock, then

$$\frac{T_2}{T_{\infty}} = \frac{p_2}{p_{\infty}} \cdot \frac{\rho_{\infty}}{\rho_2}$$

and the expressions for the pressure and density ratios across a normal shock are

$$\frac{p_2}{p_{\infty}} = \left\{ \frac{2\gamma}{\gamma+1} M_{\infty}^2 - \frac{\gamma-1}{\gamma+1} \right\}; \quad \frac{\rho_{\infty}}{\rho_2} = \left\{ \frac{2 + (\gamma-1)M_{\infty}^2}{(\gamma+1)M_{\infty}^2} \right\}$$

$$\therefore T_2 = T_{\infty} \left\{ \frac{2\gamma}{\gamma+1} M_{\infty}^2 - \frac{\gamma-1}{\gamma+1} \right\} \left\{ \frac{2 + (\gamma-1)M_{\infty}^2}{(\gamma+1)M_{\infty}^2} \right\}$$

Why not from Mach No ratio?

The air at a temperature, pressure and Mach number of T_2 , p_2 and M_2 respectively is now brought to rest inside the tube and the temperature rise incurred in this process is given by the usual expression

$$T_m = T_2 \left(1 + \frac{\gamma-1}{2} M_2^2 \right)$$

But the ratio of Mach numbers across a shock is

$$M_2^2 = \frac{1 + \frac{\gamma-1}{2} M_\infty^2}{\gamma M_\infty^2 - \frac{\gamma-1}{2}}$$

so that the full expression for T_m in terms of M_∞ is

$$\begin{aligned} T_m &= T_\infty \left\{ \frac{2\gamma}{\gamma+1} M_\infty^2 - \frac{\gamma-1}{\gamma+1} \right\} \left\{ \frac{2 + (\gamma-1) M_\infty^2}{(\gamma+1) M_\infty^2} \right\} \left\{ 1 + r \cdot \frac{\gamma-1}{2} \left[\frac{1 + \frac{\gamma-1}{2} M_\infty^2}{\gamma M_\infty^2 - \frac{\gamma-1}{2}} \right] \right\} \\ &= T_\infty \left\{ 1 + \frac{2\gamma}{\gamma+1} (M_\infty^2 - 1) \right\} \left\{ \frac{1 + \frac{\gamma-1}{2} M_\infty^2}{\frac{\gamma+1}{2} M_\infty^2} \right\} \left\{ 1 + r \cdot \frac{\gamma-1}{2} \left[\frac{1 + \frac{\gamma-1}{2} M_\infty^2}{\gamma M_\infty^2 - \frac{\gamma-1}{2}} \right] \right\} \end{aligned}$$

But $T_\infty = T_m - \Delta T$
 $= T_m \left(1 - \frac{\Delta T}{T_m} \right)$

and $\frac{\Delta T}{T_m} = \frac{T_m - T_\infty}{T_m} = \frac{1}{\left\{ 1 + \frac{2\gamma}{\gamma+1} (M_\infty^2 - 1) \right\} \left\{ \frac{1 + \frac{\gamma-1}{2} M_\infty^2}{\frac{\gamma+1}{2} M_\infty^2} \right\} \left\{ 1 + r \cdot \frac{\gamma-1}{2} \left[\frac{1 + \frac{\gamma-1}{2} M_\infty^2}{\gamma M_\infty^2 - \frac{\gamma-1}{2}} \right] \right\}}$

Thus a graph may be plotted of $\frac{\Delta T}{T_m}$ against M_∞ for various values of the recovery factor, and the ambient temperature may be computed from the relationship

$$T_\infty = T_m \left(1 - \frac{\Delta T}{T_m} \right).$$

The temperature and pressure behind the shock are greater than the free stream values and the probe will behave as if it is at a lower altitude, and it will therefore assume the recovery factor applicable to that altitude. However conditions are not quite the same because the temperature will be greater than the corresponding ambient value for the effective altitude.

As an example consider the tube to be at 40,000' and $M_\infty = 2.0$.

By applying the above ratios for the temperature and pressure across a shock wave, the effective altitude is 5,000' but the static temperature is 366°K as compared with the standard value of 278°K. At this elevated temperature, radiation effects will be considerably more important, and it may be necessary to make some allowance for them unless the tube is well shielded.

If the recovery factor of the tube varied with altitude, there would be an added complication to this approach because the effective altitude is dependent on Mach number, and therefore the recovery factor would be a function of 2 variables.

It is also shown in reference 15 that the effect of the normal shock is to reduce any errors incurred in the assumption of the subsonic recovery factor. As the Mach number is increased, the normal shock strengthens and the Mach number behind it decreases. The temperature which is recovered by the pitot in bringing the air to rest is therefore reduced, and so an error in the recovery factor has a less significant effect on the overall temperature rise.

The example in section 1 illustrates this effect but an adiabatic compression was considered instead of a normal shock wave.

5. Conclusions

The recovery factor of a flat plate, or a cylinder with its axis parallel to the free stream, assumes values which are independent of Mach number and altitude when radiation effects are neglected. These values are $\sigma^{\frac{1}{2}}$ when the flow is laminar, and approximately $\sigma^{\frac{1}{3}}$ when the flow is turbulent. These results have been derived for an incompressible flow, but they are applicable to a compressible one provided that the Prandtl number does not differ greatly from unity.

When radiation effects are taken into account, the recovery factor no longer remains constant, even at normal atmospheric temperatures. It has been shown that it increases with increase of Mach number up to $M = 1.0$, and the effective free stream temperature is reduced. It also no longer remains constant with altitude, and increases or decreases up to the tropopause depending on the emissivity of the surface. Above the tropopause the trend of the recovery factor changes because the temperature of the air is assumed to remain constant, and therefore the radiation effects become increasingly more important when compared with the convection heating which decreases with altitude.

If a ventilated pitot tube is placed in a supersonic airstream, it will effectively be operating at subsonic speed at a lower altitude, owing to the normal shock wave in front of it. It will also be at a higher datum temperature, but as this will be greater than that normally encountered at the effective altitude, radiation effects may become important. For this reason it may not be justifiable to utilise the subsonic recovery factor at this effective altitude for supersonic temperature measurement at the true altitude. This will depend upon the layout of the probe and the effectiveness of the radiation shielding. If the subsonic recovery factor of the tube varies with altitude, then the supersonic value will be dependent on both Mach number and altitude. This will be an added complication to the use of subsonic values for the measurement of temperature at supersonic speeds, but it has been illustrated that any errors incurred in the measurement of the subsonic recovery factor will have a small effect at high supersonic speeds.

List of References

<u>No.</u>	<u>No.</u>	<u>Author</u>	<u>Title</u>	<u>Date</u>
1.	NRL Report 4008	R.E.Ruskin R.M.Schechter J.E.Dinger R.D.Merrill	Development of the NRL Axial-flow Vortex Thermometer.	Sept.1953
2.	NACA T.M.1256	H. Blasius.	The boundary layers in fluids with little friction.	1908.
3.		S. Goldstein.	Modern Developments in Fluid Dynamics	1938.
4.	NACA T.M. 1000	E.R.G.Eckert. W. Weise.	The temperature of unheated bodies in a high speed gas stream.	Dec.1941
5.	RAE Rpt.1783	H.B. Squire.	Heat Transfer Calculations for Aerofoils.	Nov.1942
6.	J.App.Mech.1941 A. 105.	H.W. Emmons J.G.Brainerd.	Temperature effect in a laminar Compressible Fluid boundary layer along a flat plate.	1941.
7.	Douglas Aircraft Co. Rpt. SM.19831	H.W.Liepmann Z.O. Bleviss.	The effects of dissociation and ionization on Compressible Couette flow.	May 1956
8.	Proc. of R. Soc.	M.J.Lighthill.	Theory of heat transfer through a laminar boundary layer.	1950.

<u>No.</u>	<u>No.</u>	<u>Author</u>	<u>Title</u>	<u>Date</u>
9.	RAE Translation 218	L. Crocco	Laminar boundary layers in gases.	Dec.1947.
10.	RAE TN. Aero 2407.	R.J. Monaghan	Formulae and approximations for aerodynamic heating rates in high speed flight.	Oct. 1955
11.	WADC Tech. Rpt. 54-70	E.R.G.Eckert.	Survey on heat transfer at high speeds.	April 1954
12.		H. Schlichting.	Boundary Layer Theory.	1955.
13.	RAE T.N.Aero 2259	R.J. Monaghan.	A survey and correlation of data on heat transfer by forced convection at supersonic speeds.	Sept.1953
14.	RAE T.N.Aero 1834.	T. Nonweiler.	Rate of heat transfer due to aerodynamic heating at high altitudes	Dec. 1946
15.	Rolls Royce Tech. Rpt. PB/JRF I/NAK. (unpub.)	P. Bates	Measurement of free air temperature at supersonic speeds.	Sept.1957

Appendix I

Tables of Heat Transfer Coefficients in Laminar Flow

25,000'

$$T_{\infty} = 238.5^{\circ}$$

$$\rho = .001066 \frac{\text{slugs}}{\text{ft}^3}$$

$$\nu = 3.016 \times 10^{-4} \frac{\text{ft}^2}{\text{sec.}}$$

M_{∞}	U_{∞} ft/sec.	(Re) $\times 10^{-5}$	$(Re)^{-\frac{1}{2}}$ $\times 10^3$	T_{w_0}	K_H $\times 10^3$	$\frac{Q}{(T_{w_0} - T_w)}$ $\frac{\text{CHU}}{\text{ft}^2 \text{ sec}^{\circ}\text{K}} \times 10^3$
0.2	203	1.121	2.987	240.12	2.465	4.11
0.4	407	2.248	2.109	244.97	1.740	5.82
0.6	610	3.370	1.723	253.08	1.421	7.13
0.8	814	4.490	1.491	264.40	1.232	8.25
1.0	1017	5.610	1.335	278.95	1.102	9.21

(Tables Contd.)

36,000'

$$T_{\infty} = 216.5^{\circ} \text{K}$$

$$\rho_{\infty} = .00071 \frac{\text{slugs}}{\text{ft}^3}$$

$$v = 4.181 \times 10^{-4} \frac{\text{ft}^2}{\text{sec}}$$

M_{∞}	U_{∞} ft/sec.	(Re_{∞}) $\times 10^{-5}$	$(Re_{\infty})^{-\frac{1}{2}}$ $\times 10^3$	T_{w_0}	K_H $\times 10^3$	$\frac{Q}{(T_{w_0} - T_w)}$ $\times 10^3$
0.2	194	0.773	3.597	217.97	2.965	3.16
0.4	388	1.545	2.545	222.38	2.100	4.47
0.6	581	2.320	2.076	229.70	1.713	5.45
0.8	775	3.085	1.800	240.00	1.484	6.31
1.0	968	3.862	1.611	253.21	1.330	7.05

(Tables Contd.)

40,000°

$$T_{\infty} = 216.5^{\circ} \text{K}$$

$$\rho_{\infty} = .000587 \frac{\text{slugs}}{\text{ft}^3}$$

$$v = 5.059 \times 10^{-4} \frac{\text{ft}^2}{\text{sec.}}$$

M_{∞}	U_{∞} ft/sec.	(Re_l) $\times 10^{-5}$	$(Re_l)^{-\frac{1}{2}}$ $\times 10^3$	T_{w_0}	K_H $\times 10^3$	$\frac{Q}{(T_{w_0} - T_w)}$ $\times 10^3$
0.2	194	0.640	3.952	217.97	3.260	2.86
0.4	388	1.282	2.807	222.38	2.322	4.07
0.6	581	1.915	2.291	229.70	1.893	4.98
0.8	775	2.550	1.980	240.00	1.635	5.74
1.0	968	3.192	1.775	253.21	1.465	6.41

(Tables Contd.)

45,000'

T_{∞}	= 216.5° K
ρ_{∞}	= .00046 $\frac{\text{slugs}}{\text{ft}^3}$
v	= 6.434 x 10 ⁻⁴ $\frac{\text{ft}^2}{\text{sec.}}$

M_{∞}	U_{∞} ft/sec.	(Re_l) x 10 ⁻⁵	$(Re_l)^{-\frac{1}{2}}$ x 10 ³	T_{w_0}	K_H x 10 ³	$\frac{Q}{(T_{w_0} - T_w)}$ x 10 ³
0.2	194	0.504	4.454	217.97	3.680	2.54
0.4	388	1.005	3.155	222.38	2.600	3.59
0.6	581	1.510	2.573	229.70	2.123	4.39
0.8	775	2.007	2.232	240.00	1.842	5.06
1.0	968	2.512	1.996	253.21	1.654	5.67

Appendix II

Tables of Equilibrium Temperatures and Recovery Factors

Case III. $\epsilon = 0.1$; $T_{cc_r} = T_{cc}$.

Alt M_{∞}	S.L		25,000'		36,000'		40,000'		45,000'	
	T_{W_0}	$T_{W_0} - T_W$	T_{W_0}	$T_{W_0} - T_W$	T_{W_0}	$T_{W_0} - T_W$	T_{W_0}	$T_{W_0} - T_W$	T_{W_0}	$T_{W_0} - T_W$
0.2	289.96	.0067	240.12	.0055	217.97	.0053	217.97	.0058	217.97	.0065
0.6	305.59	.0416	253.08	.0336	229.70	.0291	229.70	.0326	229.70	.0368
1.0	336.92	.105	278.95	.085	253.21	.075	253.21	.0825	253.21	.093

Recovery Factors - $r = \frac{T_W - T_{\infty}}{T_{\infty} \cdot \frac{\gamma-1}{2} M_{\infty}^2}$

Alt M_{∞}	S.L	25,000'	36,000'	40,000'	45,000'
0.2	.845	.845	.846	.845	.845
0.6	.846	.846	.846	.846	.846
1.0	.847	.847	.847	.846	.846

The variation is too small to be significant in this case but it is more apparent in Case IV.

(Tables Contd.)

Case IV. $\epsilon = 1.0$, $T_{w_r} = T_w$.

Alt M_∞	S.L		25,000'		36,000'		40,000'		45,000'	
	T_{w_0}	$T_{w_0} - T_w$	T_{w_0}	$T_{w_0} - T_w$	T_{w_0}	$T_{w_0} - T_w$	T_{w_0}	$T_{w_0} - T_w$	T_{w_0}	$T_{w_0} - T_w$
0.2	289.96	.067	240.12	.0555	217.97	.053	217.97	.058	217.97	.062
0.6	305.59	.405	253.08	0.330	229.70	0.29	229.70	0.316	229.70	0.358
1.0	336.92	1.04	278.95	0.830	253.21	0.738	253.21	0.80	253.21	0.91

$$\text{Recovery Factors : } r = \frac{T_w - T_{\infty}}{T_{\infty} \cdot \frac{\gamma-1}{2} M_\infty^2}$$

Recovery Factor - r.					
Alt M_∞	S.L	25,000'	36,000'	40,000'	45,000'
0.2	.815	.820	.822	.815	.811
0.6	.828	.830	.831	.825	.822
1.0	.831	.831	.832	.830	.829

1. Introduction

The wind tunnel test programme was carried out with two main objects in view.

1. To investigate the possibilities of using thermistors in ventilated pitot thermometer probes on high speed aircraft, and in particular to assess their efficiency, stability and general suitability for this type of work.
2. To investigate the effect on the recovery factor due to variation of the probe incidence to the airstream.

Owing to the limited size of the working section of the wind tunnel which was available for this investigation, the dimensions of the test probes were much smaller than those usually associated with aircraft thermometers. In the design of these probes, it was necessary to compromise between the small frontal area required to attain high subsonic Mach numbers, and the minimum practical size into which a thermistor could be fitted.

Previous experimental results, obtained by research establishments in this country and the U.S.A., have indicated that higher values of the recovery factor have been obtained from a ventilated pitot probe than from a surface temperature probe.

The former type is similar to a total pressure tube which is open to the approaching airstream, and a temperature sensing element is situated inside the tube. The airstream is brought nearly to rest and the consequent temperature increase is very close to the full adiabatic.

However with the surface temperature probe the air is brought to rest through a boundary layer and the resultant temperature rise does not attain the full adiabatic value.

If the pitot tube were not ventilated, the air inside it would be at rest, and any changes in the total temperature of the airstream would take a considerable time to have an effect on the sensing element. For this reason small ventilation holes are drilled in the wall of the tube behind the sensing element so that a low velocity flow of air is continually passing over it. In this way the lag of the instrument is reduced to the time taken for the air to pass down the tube plus the lag of the sensing element itself.

The heat losses are the major problems which have to be overcome in the design of these probes. These losses will arise from conduction through the wall of the probe to the outside surface, which is at a lower temperature due to viscous dissipation in the boundary layer. There will also be conduction through the supporting strut on which the probe is mounted. These will be a loss due to radiation from the outside surface to the surroundings and the magnitude of this has been discussed in Part I. A further possible error is that due to the growth of the internal boundary layer. If this boundary layer thickness approaches the duct radius, the measured temperature of the air will be reduced because the element will be within the thermal boundary layer. However the magnitude of this latter effect should be negligible.

In order to reduce the conduction of heat from the duct to the outside surface, a second stagnation chamber is formed. This is done by fitting a larger tube concentrically around the original one and so forming an annular chamber outside the central duct or inner chamber. Both chambers are independently ventilated to the atmosphere and each is thermally insulated from the other. Thus the sensing element, which is located in the inner chamber, is surrounded by air which is very nearly at the free stream total temperature. The outer chamber also contains air which is nearly at the same temperature and thus there is very little heat lost by conduction through the dividing wall. The temperature of the outside surface, however, is less than the free stream total temperature owing to the viscous dissipation in the boundary layer and therefore heat will be conducted through this wall from the outer chamber. As the two walls are separated by an insulating material, the temperature of the inner chamber is only affected indirectly by the change in the outer wall temperature, and the magnitude of this is very small. The addition of further stagnation chambers will obviously reduce this error still more, although it is hardly warranted because the effect is practically negligible anyway for the double stagnation chamber thermometer.

The reduction of the heat loss through the support may be effected by a strip of thermal insulating material placed between it and the probe. Alternatively the working section of the probe may be insulated internally from the support.

This double stagnation chamber arrangement also provides an effective radiation shield. Any heat transfer through the outer wall as a result of radiation is compensated for by the air flowing through the outer chamber, so that the temperature of the air in the inner chamber is, at the most, only slightly affected.

2. Description of the Apparatus

2.1. The Wind Tunnel

The wind tunnel which was available for this investigation was a supersonic induced flow tunnel having working section dimensions of 2" x 1½". The investigation was confined to subsonic speeds, and two plane liners were fitted to the working section, one of them having a taper to allow for the growth of the boundary layer.

The contraction, which was made of wood, was rectangular in section. It was 4'6" long, and built into it was an electric heater with which the air could be heated before entering the working section. The heating elements were copper wire gauzes through which the air passed, and the amount of heating could be controlled by a 4 position switch which varied a resistance. This heater was not used during the test programme.

The working section was 15" long and had a rectangular section which changed into a circular one at the upstream end of the diffuser. The lower liner was machined aluminium alloy and it contained 17 static pressure tapings. These were located on the centre line and spaced ½" apart. The upper liner was made from mahogany which was machined and polished to give a very true surface. The thermometer probe was mounted from this liner to which it was affixed with two wood screws. The two sidewalls were rectangular blocks of plate glass about ¾" thick and a static pressure tapping was fitted in one of them. This tapping was located half way up the working section (1") and about 10" downstream of the beginning of it.

The pressure leads from the static tapings were connected to a bank of 24 manometer tubes, and these were partially filled with mercury from a resevoir. There was a large clamp between the manometer tubes and the resevoir whereby the levels in all 24 tubes could be maintained after the tunnel was shut down.

Compressed air was supplied to the tunnel from a resevoir which was charged by a compressor. The rate of charging was such that at all subsonic speeds the tunnel could be run continuously although there were slight fluctuations in the supply pressure.

The compressed air entered the tunnel through slots facing in a downstream direction and induced a flow through the working section. These slots were located just downstream of the working section, and just ahead of a conical diffuser through which the air was exhausted to the atmosphere.

2.2 The Design of the Probes

The first aspect of the design which had to be settled was the overall size. This was a compromise between making it small enough to attain high subsonic Mach numbers, and large enough to accommodate the thermistors and still retain thermal efficiency. It was finally decided to make the probe from a $\frac{3}{16}$ " I.D. x 20 S.W.G. brass tube with a 3 mm O.D. stainless steel tube for the inner chamber. This would allow the tunnel to be run up to a Mach number of just under 0.8, the actual value depending on the geometry of the support strut. The two tubes were insulated from each other by tufnol spacers, and the open end was chamfered to enable the air to make a smooth entry, thus preventing separation from the lip when the probe was at an incidence to the airstream. The total included angle of the chamfer was 40° and the effect of varying this has not been investigated.

The next variable parameter in the design was the ratio of the vent area to the inlet area for the two chambers. It was only necessary to provide sufficient ventilation for the inner chamber to ensure that the air within it was not stagnant. Therefore the area ratio was initially fixed at $12\frac{1}{2}\%$ with provision for increasing it if the results were disappointing. In this way the effect of varying this parameter could have been investigated, but the results showed that this was not necessary, although it would have been of interest to have done so, had time permitted. The ventilation for this chamber was provided by two holes, diametrically opposite each other, and inclined rearwards at 30° , and these were located just aft of the thermistor. The outer chamber required a higher air flow in order to compensate for the heat transfer taking place between the air in the chamber and the outside surface. Therefore the area ratio for this was fixed at 50% , and there were 4 ventilation holes drilled normally to the surface and symmetrically placed around it.

The sensing element which was chosen for these probes was a thermistor, which is a thermally sensitive resistor whose temperature coefficient of resistance is negative, and many times greater than that of ordinary metals at room temperature. The

material of which a thermistor is made is a very small bead of a semi-conducting ceramic of a special formula, which is carefully aged in a temperature controlled furnace for a specified length of time. Two very fine platinum wires are moulded into the bead before the ageing process, and these are kept at a calculated distance apart depending on the nominal resistance of the fully aged thermistor. The resistance change of a thermistor is produced by a temperature change in the semi-conductor itself, and this may arise from a change in temperature of the surroundings or internally by heat resulting from power dissipation in the element. This latter cause is because, unlike a thermocouple, a thermistor requires a current to be passed through it in the same way as an ordinary resistor. Thermistors which are heated by the surroundings are called 'directly heated' whereas those which rely on internal power dissipation are known as 'indirectly heated'. It is the former type which was used for this work. A thermistor has a characteristic resistance variation with temperature which obeys the law:

$$R = e^{K/T}$$

so that a graph of $\log_e R$ plotted against $\frac{1}{T^{\circ}K}$. produces a straight line. This is very useful as accurate extrapolation of calibration curves may be made if required.

The standard thermistors which were available were unsuitable for this work as they were enclosed in a protective glass bulb and backed by a copper disc. The overall diameter of these was 4 mm. which precluded their use in these probes, but a special type of thermistor which was under development was found to be suitable. This had a bead which was just over $\frac{1}{4}$ mm. in diameter and which had been coated with a very thin film of glass for protective purposes. However the wires came out from opposite sides of the bead, which meant that each had to be bent through 90° in order to mount them in the probes. A special version of this thermistor was made up for this work, and it had both the wires coming out from the same side of the bead. This avoided the necessity to bend them which was an advantage as they were only .004" dia and were found to be rather brittle.

While awaiting delivery of these modified thermistors, a prototype version of the final probe was assembled with the unmodified thermistor and this was used for some preliminary calibrations and wind tunnel work in order to evolve a technique.

This prototype probe had a fixed support which was swept back at 45° , and the leads from the thermistor were led down the trailing edge to which they were affixed with adhesive.

The mounting of the thermistor in the probe initially presented some difficulties owing to the delicacy of the operation, but subsequently a technique was evolved which was found to be most satisfactory and relatively straightforward. The plug in the inner chamber, through which the wires were to pass, was split and two very shallow scratches were made on one half. The wires were then laid along these and the other half cemented in position. The forward face of the plug was chamfered to form a wedge with a 60° semi-vertex angle, and the thermistor was positioned about .020" forward of this vertex. The reason that it was not placed on the vertex was because this is a stagnation point, and therefore positioning it there would have increased the lag of the instrument. The plug was located inside the inner chamber in such a position that the inclined faces of the wedge lined up with the two vent holes which were drilled at 30° to the normal.

Thicker gauge wires were soldered to the platinum ones at the rear face of the plug, and these were led out through two holes in the tail fairing and along the trailing edge of the support.

When the modified thermistors were available, they were despatched as matched pairs whose resistances were within about 1% of each other at 15°C . A second probe was made using one of such a pair, the other one being used in the settling chamber thermometer which is described elsewhere. This second probe had a variable incidence support which enabled the effect of a change of incidence to be investigated, and the total angular movement which was obtainable was $\pm 12^\circ$. In all other respects, the final version of the probe was identical to the prototype version.

The geometry and detail design of this probe and its support is shown in Figure 1 and plate 1.

2.3 Instrumentation for Temperature Measurement

As a thermistor requires a current to be passed through it, and temperature changes are converted into resistance changes, the most convenient way of measuring the resistance is to balance it against a standard box in a Wheatstone Bridge

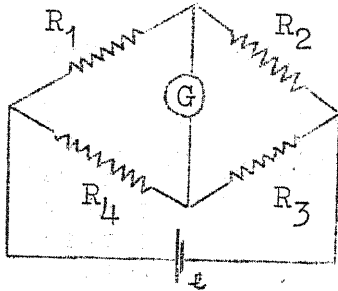
circuit. This was the method which was used, and a few calculations were necessary in order to obtain the optimum working conditions. The resistances of the ratio arms should be equal to attain the maximum sensitivity of the bridge, and it was in fact possible to operate very near to this condition.

Thermistors have a very large negative temperature coefficient of resistance and thus a small temperature change produces a large resistance change. However in the wind tunnel, the air in the settling chamber was virtually at rest at the ambient temperature, and as it entered the working section the velocity increased but the total temperature remained constant. A thermometer, with a recovery factor of unity, placed in the working section would measure this temperature, and therefore regardless of the tunnel speed, the measured temperature would be the ambient value provided that isentropic flow existed between the settling chamber and the working section. Owing to the recovery factor varying from unity small variations of temperature were measured, but the resistance of the thermistor remained approximately constant. This greatly simplified the layout of the bridge circuit, and as the nominal resistance of the thermistor was 2000Ω at 20°C . the two ratio arms were fixed at $2.2 \text{ k}\Omega$ each and the fourth arm was a standard variable resistance box.

Using these values and assuming that the galvanometer resistance was 100Ω and the potential difference applied was 2 volts, the out of balance current per degree temperature rise was calculated to be $10 \mu\text{A}$. The most sensitive galvanometer which was available was a Scalamp with an internal resistance of 90Ω and this was more than adequate.

A very important characteristic of a thermistor is its power sensitivity. This is defined as the rate of change of temperature with power input and is expressed in $^\circ\text{C}/\text{mW}$. Normally this is quite low and no appreciable self heating will occur unless the current is high, but this factor was taken into careful consideration in the layout of the circuit. No value for the power sensitivity had been quoted for this latest type of thermistor but a similar but larger version had a value of $1.6^\circ\text{C}/\text{mW}$.

There were two alternatives in the layout of the bridge and these were:-



1. To have R_2 and R_3 as the matched pair,
2. To have R_4 and R_3 as the matched pair.

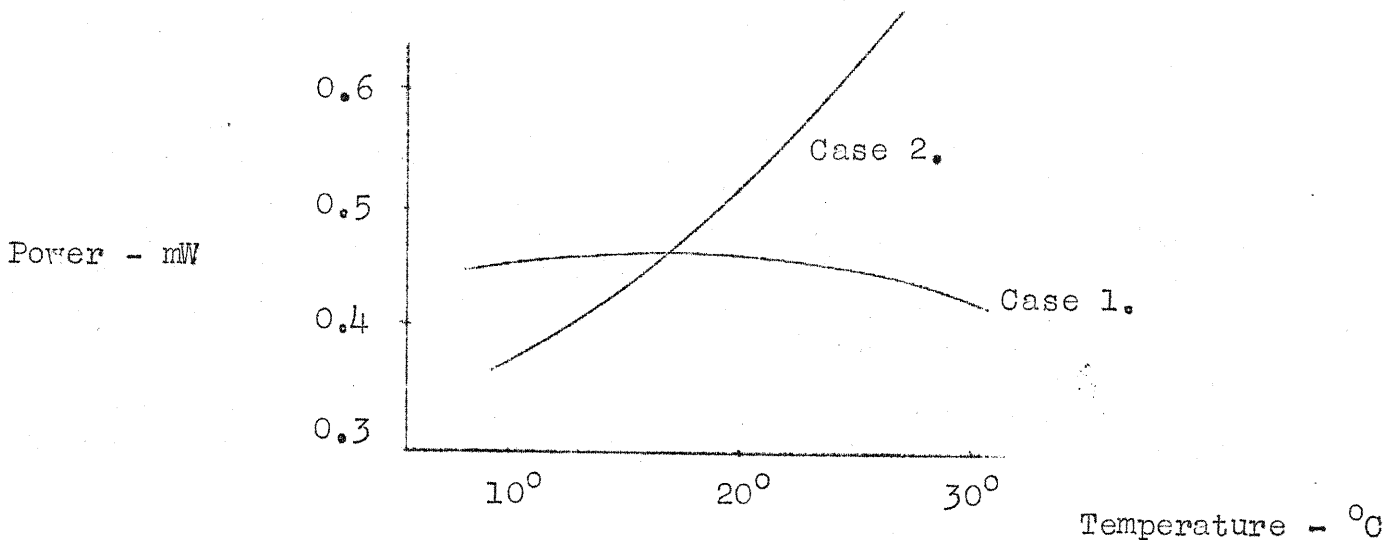
In case 1, the power dissipated in the thermistor

$$= i^2 R = \frac{\epsilon^2}{(R + 2.2 \text{ k}\Omega)^2} \cdot R.$$

whereas in case 2 the expression is

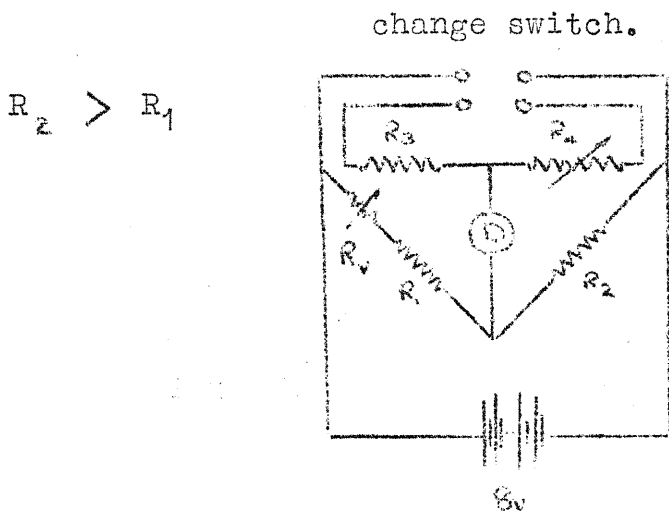
$$i^2 R = \frac{\epsilon^2}{4R}.$$

These two expressions have been plotted below to indicate their various forms over a small range of working temperatures.



It was obviously more advantageous to use case 1 because the power dissipation remained approximately constant with temperature over the working range.

In order to obtain accurate results, it was important that the 2.2 K Ω resistors should be matched very closely. First a selection of wire wound resistors having a nominal resistance of 2.2 k Ω were measured in turn in a bridge network, and two were chosen which differed in resistance by only about 2 Ω . Then these were put into a bridge circuit with a variable resistance box in series with the smaller of the two resistors, and in one of the ratio arms was a standard 1000 Ω resistor whilst in the fourth arm there was another variable resistance box. A reversing switch was used in order to change the positions of the two ratio arms and so compensate for any difference between them. Increased sensitivity was obtained by using 8 volts across the bridge and a Scalamp detector with an internal resistance of 90 Ω . The circuit diagram is shown below:-



R_1 and R_2 are resistors to be matched.

R_3 - standard 1000 Ω .

R_4 - variable resistance box.

R_v - variable resistance box.

D - Scalamp detector.

It was first necessary to match the two ratio arms and this was done by adjusting R_v until there was a large deflection on the Scalamp. Then the ratio arms were reversed and R_v was adjusted until the deflection was of the same magnitude as, but in the opposite direction to, the original one. When this was so, the two ratio arms were exactly equal and the two unbalanced resistors could be matched against them.

This was done by adjusting R_v until there was no current passing through the Scalamp, and then the ratio arms were reversed

and the bridge was again balanced. There was a small difference between the two resistances necessary to balance the bridge, the values being 1.6Ω and 1.4Ω , so a mean value of 1.5Ω was taken and R_1 was replaced by a length of resistance wire. This had a resistance of $2.695\Omega/\text{yard}$ indicating that $20.1''$ would be required, and therefore $24''$ was cut off and one end soldered to R_1 . Using a knife edge to pierce the insulation, the bridge was again balanced twice, and the mean of the two balancing lengths was wound onto a bobbin and finished off with shellac to retain it in position.

For neatness and compactness, the major part of the bridge circuit was built onto a paxolin platform which projected from the end of the variable resistance box. This is illustrated in Plate no.4 and Figure 3.

3. Preliminary Testing.

This preliminary testing with the prototype probe was devoted to overcoming difficulties encountered in the use of thermistors, and it was also useful for evolving techniques for testing in a wind tunnel. The difficulties which were met during this phase have been described here in some detail because thermistors are relatively recent additions to this type of work and little is known of their characteristics.

3.1 Calibration of the Probe.

A small blower tunnel was being constructed for the purpose of calibrating these probes but it was not available at this stage, and so it was decided to use a liquid bath. Oil was rejected as the liquid for this purpose because its viscosity might have prevented it from penetrating along the small diameter duct to the thermistor, and so water was used as the working medium. This appeared to be quite adequate provided that it was left to stand for a sufficiently long time for the temperature to stabilise.

The procedure was to connect the probe into the bridge circuit, and check that it was functioning correctly by blowing warm air through it and noting the deflection of the Scalamp.

When everything had been checked, the probe was wired to a mercury-in-glass thermometer and immersed slowly front first, so as to allow the air to escape through the ventilation holes, into a beaker of water. This was standing in a larger beaker packed with ice and the entire apparatus was lagged with cotton wool. It was then left to stand for an hour, being stirred periodically, by which time the temperature had stabilised and a reading could be taken of the resistance required to balance the bridge.

The temperature of the water was then raised and the procedure was repeated. In this way the probe was calibrated over the range 0° - 45°C and the calibration curve is shown in Figure 4. This has been plotted as resistance against temperature as it is more amenable to accurate interpolation in this form than when plotted on a log scale. However the points obtained from this calibration did obey the characteristic logarithmic law of the thermistor.

3.2 The Initial Runs.

The initial runs were made without the probe in the tunnel in order to investigate the distribution of static pressure along the working section. This was done by increasing the Mach number in the tunnel and observing the mercury levels in the manometer tubes. The variation of static pressure was found to be quite small even at high Mach numbers and it did not affect the experimental results. A small static pressure tube was placed in the position which would be occupied by the probe, and this was in the centre of the working section in a plane with the tapping on the wall. This pressure tapping gave static pressures which corresponded very closely with those in the centre, and so this was used in the tests to obtain the local velocity of the airstream.

The side-wall of the working section was then removed and the probe was screwed into its position on the upper liner. The wires from the thermistor were led out of the tunnel through two small holes and connected into the bridge circuit, and after a continuity check, the tunnel was reassembled.

The temperature of the air in the settling chamber was measured with the mercury-in-glass thermometer against which the probe had been calibrated. This in turn had been calibrated against a standard one and the error was + 0.3°C. A hole was drilled on the centre-line of the upper wall of the settling chamber just upstream of the working section, and the thermometer was lowered through it, until the bulb was in the centre of the chamber. In this way the thermometer was located as near as possible to the same streamline as that passing the probe, and therefore it was measuring the same total temperature.

The tunnel was started by opening the compressed air valve, and the flow was increased until the difference between the static and total pressures, indicated by the manometer tubes, was 0.5" Hg. It was allowed to run for several minutes, after which time the settling chamber thermometer had stabilised, and then the bridge was balanced. Readings were taken of the resistance of the thermistor, and settling chamber temperature and the static and total head pressures.

The speed was then increased until the pressure difference was 1" Hg and the above procedure was repeated. In this way the temperatures were measured over the entire speed range of the tunnel.

Two sets of runs were made and the results of these have been included with the remainder of the results in Appendix III.

3.3 Remarks

The most important finding of the initial runs was that the temperature of the air flowing through the tunnel did not remain constant. The thermometer in the settling chamber showed that the air temperature was varying very slowly by 1 or 2 degrees about a mean value. This was probably because the wind tunnel was in a small room and air was being drawn in from outside to replace that passing through the tunnel.

Also in addition to this gradual change of temperature, there were more rapid fluctuations which the settling chamber thermometer was unable to measure. However the thermistor in the probe with its rapid response easily detected these fluctuations, and caused the Scalamp to deflect and return to zero. On occasions they were so frequent that it took a considerable length of time to balance the bridge accurately, although the magnitude of them was only about $\pm \frac{1}{8} - \frac{1}{4}^{\circ}\text{C}$.

However it was obvious that a more satisfactory method was required to measure the settling chamber temperature in order to avoid the necessity of a long wait for a thermometer to stabilise. The obvious choice was to have another thermistor in the settling chamber, and therefore a thermistor thermometer was designed and built specially for this purpose.

4. Modifications to the Apparatus.

4.1 The Thermistor Thermometer.

This was designed to replace the thermometer in the settling chamber and it consisted of a thermistor suspended exactly in the position which the thermometer bulb had occupied.

The thermistor was one half of a matched pair of the modified type, and the other half was fitted into the second probe which had the variable incidence support and which hereafter is referred to as the No.1 probe.

Using a matched pair in this way proved to be most useful when balancing the bridge because the resistances varied by only about 50Ω . It was therefore possible to switch rapidly from one to the other and balance with the minimum of time spent in varying the resistance. In order to do this, a switch was mounted on the paxolin platform containing the bridge network and the wiring was modified accordingly.

The body of the thermometer was a length of $\frac{1}{4}$ " dural tubing and the thermistor protruded from a tufnol plug in the bottom end. The thermistor was mounted in the usual manner by splitting the plug, making two shallow grooves on one half, and laying the wires along them. The two halves were then cemented together and the completed assembly was fitted into the tube. Inside the tube, thicker gauge wires were soldered to the platinum ones and these were led out through another tufnol plug in the top. This prevented any tension being accidentally applied to the thin thermistor wires.

In order to protect the thermistor from damage, the bottom of the dural tube was threaded to take a hollow brass cap. This cap had 16 small holes drilled in it and these were in 4 columns symmetrically placed around the circumference. The purpose of these was to allow a free flow of air around the thermistor.

A brass collar with a locking screw was provided in order to allow the depth of the thermistor to be varied.

A detailed drawing of the thermometer and a close up view of the element are given in Figure 2 and Plate 2.

4.2 The Blower Tunnel.

It was felt in certain research establishments that it was difficult to obtain a uniform temperature throughout a liquid bath, and that there was a definite need of some instrument or piece of equipment which would be suitable for accurately calibrating temperature measuring devices. The requirement was for a medium which could be maintained at a constant temperature throughout, and that this temperature could be accurately measured.

It was for this reason that a small blower tunnel was built at the A. and A.E.E. at Boscombe Down and another one has been built for this experimental work. Air was the working medium and it was blown round a closed circuit by a centrifugal impeller driven by an electric motor.

One half of the circuit was contained inside a brass tank which was filled with acetone and dry ice for low temperature calibrations, and water for the higher temperature ones. The tank was contained inside a plywood box and it was mounted on blocks which were faced with cork to afford increased insulation.

The circuit itself, which was almost rectangular in shape, was made from $\frac{3}{4}$ " brass tubing which was soldered at the joints. The lower part of the circuit, which was immersed in the working fluid, was divided into 8 segments by brass strips soldered inside the tube. This was to increase the area of metal in contact with the air and so to obtain a more uniform temperature. Vanes were built into the top corner of the circuit just upstream of the working section in order to improve the flow through that section.

The working section of the tunnel was 9" long and it was lagged on the inside with sheet-cork having a thickness of 0.04". The entire length of the circuit from the tank to the impeller, downstream of the working section, was lagged externally with asbestos string and woven asbestos cloth. There was a sliding acetate window in the top of the working section and it covered a 4" rectangular aperture through which the test instruments were admitted for calibration. This window was also used for viewing the thermometer which was housed inside, and which measured the temperature of the air circulating around the tunnel. The thermometer was an accurately calibrated one and it was mounted on corks clear of the walls of the working section.

When a test instrument was in place in the tunnel, the open space around its support strut was sealed with plasticine, or some other suitable material, in order to prevent air being drawn in from the atmosphere. By maintaining good air seals throughout the tunnel the same mass of air was circulated continuously and the temperature became stabilised near to the temperature of the working fluid in the tank. By having as much of the circuit insulated as possible, the heat losses were cut down to a minimum and the temperature inside the circuit remained stabilised for a considerable period of time.

The impeller rotated at about 4,500 R.P.M. and the velocity of the air through the working section was about 20 ft/sec.

The motor which drove the impeller was fitted directly onto the back of the impeller housing but it was separated from it by a thin cork washer. This was to reduce the amount of heat conducted from the motor to the impeller and so into the airstream. The motor was rated at $\frac{1}{20}$ H.P. and it was cooled by a small fan on one end of the main shaft.

The short length of tube from the impeller back into the tank completed the circuit of this tunnel.

The entire unit was portable and it was provided with handles at each end for ease of transportation. A tray was made for it out of Dexion angle brackets and this was fitted with adjustable length legs. This was in order that it might be taken out to an aircraft, on which a test instrument was mounted, and raised into such a position that the calibration could be carried out 'in situ'. This had the advantage that the actual electric circuit of the aircraft was used in the calibration, and thus any errors which might have arisen from an attempt to simulate this in the laboratory were eliminated. It also meant that a check calibration of an instrument could be made without removing it from the aircraft and this saved unnecessary wastage of time.

Plate 5 shows the blower tunnel in its fully insulated form in which it was used for the flight calibrations.

5. The Test Programme.

5.1 Calibrating in the Blower Tunnel.

The instruments which were calibrated in the blower tunnel were the prototype probe, the No.1 probe, and the thermistor thermometer. The prototype probe was recalibrated in order to compare the results with those which were obtained in the water bath. In this way it was hoped to be able to make an estimate of the respective power sensitivities in air and water.

The probes were mounted side by side on a short length of plywood which was just wide enough to span the opening into the working section of the tunnel. The thermistor thermometer was lowered vertically through a hole in this piece of wood, and the element was maintained at the correct depth by setting the brass collar in the requisite position. The holes in the brass cap at the base of the thermometer were lined up with the local airstream, and as the thermistor was insulated thermally from the dural tube, it was assumed that there would not be any errors arising from a temperature difference between the inside and outside of the working section.

The instruments were calibrated against a mercury-in-glass thermometer which had been standardised, and which had a working range of 0 - 50°C, in $\frac{1}{2}^{\circ}$ divisions. The thermometer was mounted horizontally inside the working section, and in view of its length and the restricted view through the window, it was found to be necessary to turn the thermometer round for temperatures above 25°C. In doing this it was noticed that there was a temperature gradient of $\frac{1}{2}^{\circ}$ along the length of the working section and an account was taken of this in the calibrations.

It was also found that the temperature of the air circulating in the tunnel was considerably higher than that of the fluid in the tank. When a mixture of ice and water was used, the temperature of the circulating air was about 10°C. This indicated that there was insufficient lagging around the circuit and that there were probably some small air leaks as well. However as the temperature of the air in the wind tunnel was unlikely to be as low as 10°C, the condition of the blower tunnel was quite adequate for these calibrations. Further modifications were made to it subsequently and these have been described in Part III.

The test instruments were placed in position and the sliding window was then shut as far as possible. It was necessary to seal carefully round the probes and along the edges of the window in order to prevent air from entering the tunnel and this was carried out most effectively with plasticine.

The instruments were connected up into the bridge circuit and each one was checked for continuity. The tank was then filled with a mixture of ice and water, and the motor was started and left to run until the temperature of the air circulating through the working section had stabilised at its equilibrium value. When this temperature had been attained, the resistance of the thermistors was measured in turn in the bridge, and the reading of the mercury thermometer was taken.

A small amount of hot water was then poured into the tank until the temperature had risen by about 3°. The water was stirred well for a few minutes, and the motor was restarted and left as before. The resistances were measured when the temperature had become stabilised, and then more hot water was added and the procedure was repeated.

In this way the instruments were calibrated over a range from 10° - 30°C. and the results were plotted in the form of curves of temperature against resistance. Some actual curves are shown in Figures 4 and 5.

In addition to the results being presented in the form described above, they were also plotted on a logarithmic basis as $\log R \sim 1/T$, in order to compare the slopes of the straight lines with that of the manufacturers characteristic for this type of thermistor.

5.2 Results of the Calibrations

All the calibrations which were carried out in the blower tunnel were consistent with each other, and all had the same characteristic slope when plotted logarithmically. However all the curves were displaced from each other, and this was due to the differences in the nominal resistance of the thermistors.

The most interesting result which arose from the calibrations was the difference between the curves which were obtained for the prototype probe in the blower tunnel and in the water bath. Both results obeyed the logarithmic law but,

for a given resistance, the temperature which was measured in the water bath was higher than that which was measured in the tunnel. The magnitude of this difference was 2.6°C . at $3000\ \Omega$ which corresponded to about 15°C on the blower tunnel calibration.

The reason for this variation was the difference between the power sensitivity for a thermistor in air and water. From the manufacturer's brochure for the standard F.23 element, which was similar in most respects to those used, the power sensitivities in air and water were quoted as $1.6^{\circ}\text{C}/\text{mW}$ and $0.4^{\circ}\text{C}/\text{mW}$ respectively.

At a nominal resistance of $3000\ \Omega$, the current flowing through each arm of the bridge at balance was $0.4\ \text{mA}$, and therefore the power which was dissipated in the thermistor was about $0.5\ \text{mW}$.

The difference between the quoted power sensitivities was $1.2^{\circ}\text{C}/\text{mW}$ and therefore the difference which would have been expected between the two sets of calibrations was 0.6°C .

A temperature of 2.6°C . would indicate a difference of $5.2^{\circ}\text{C}/\text{mW}$ between the power sensitivity in air and water, and assuming that there had been a proportional increase, the absolute values would be of the order of $6.9^{\circ}\text{C}/\text{mW}$ and $1.7^{\circ}\text{C}/\text{mW}$ respectively.

This was conceivable because the power sensitivity was dependent on the mass and thermal capacity of the thermistor. If it had been mounted on a block of copper, for example, the power sensitivity would have been extremely small. The thermistors which were used for this experimental work were stripped of all unnecessary glass bulbs and copper backing discs, and all that remained was a small bead $\frac{1}{4}\ \text{mm}$. in diameter which had been coated with a thin film of glass for protective purposes. The weight of it was fractional compared with the 1.8 grams of the standard F.23 Thermistor, and so it was not altogether unexpected that the power sensitivities should have increased in this way.

In view of this result, a trial run was made in the wind tunnel in order to investigate the effect of flow velocity on this power sensitivity. It was thought that a flow of air past the thermistors would reduce the power sensitivity and so a comprehensive study was made of this under various conditions.

5.3 Investigation of the Power Sensitivity

The No.1 probe was mounted in the working section of the wind tunnel, and both the thermistor thermometer and the mercury thermometer were placed in the centre of the settling chamber as before. This was a safety precaution which was taken in order to keep a check on the readings from the thermistors.

The tunnel was started and the running procedure was the same as for the initial runs with the prototype probe. The supply of air was adjusted until the velocity of flow through the working section was about 500-600 ft/sec, and the tunnel was then left until the conditions had become stabilised. When the temperature was steady, the bridge was balanced in turn for the probe and the thermistor thermometer, and the reading of the mercury thermometer was recorded. The resistances of the elements were converted into temperatures by making use of the calibration curves, and it was at this juncture that the first signs of an inconsistency appeared. The results showed that the temperature indicated by the probe was about 2° lower than that of the mercury thermometer, whilst that indicated by the thermistor thermometer was about $2\frac{1}{4}^{\circ}$ higher. These differences persisted throughout the speed range which was from 100-800 ft/sec, but that of the probe decreased slightly at the lower speeds.

The reason for these differences was the flow of air past the thermistors. In the case of the probe, the velocity of the air flowing through it was greater in the wind tunnel, which had free stream velocities between 100 and 800 ft/sec, than it was in the blower tunnel which operated at a low velocity. This greater mass flow cooled the thermistor and reduced the effect of the self heating caused by the internal power dissipation, so that the temperature measured in the wind tunnel was lower than that measured in the blower tunnel.

In the case of the thermistor thermometer the effect was reversed because the velocity of flow in the settling chamber was very low, and therefore the thermistor was cooled less than it was in the blower tunnel. This accounted for the temperature being elevated.

In order to measure the amount of self heating which was taking place, the tunnel was shut down and the resistance of the thermistor thermometer was balanced against the resistance

box in the usual way. The current was then cut off from this element and it was left to cool down for about $\frac{1}{4}$ minute. Then simultaneously the current was switched on and the key which was in series with the Scalamp was depressed. The light spot on the detector immediately deflected and then slowly returned to its zero position. The extent of the deflection was noted, and then the resistance box was adjusted until the light spot was again deflected by this amount. The amount of resistance taken out of the box to do this was a direct measurement of the change of temperature of the thermistor, and this was found to be equivalent to $2\frac{1}{2}^{\circ}\text{C}$.

When the bridge was first balanced the thermistor was at its equilibrium temperature, and when the current was switched off it cooled back to the ambient condition. Then the moment that the current was switched on and the key was depressed, the element was still at the ambient temperature but the bridge was out of balance and consequently the light spot on the Scalamp was caused to deflect. As the current continued to pass the temperature of the thermistor rose back to its equilibrium value until once again the bridge was balanced and there was no deflection. Therefore this step input technique provided a direct measure of the temperature rise due to self heating, and this was found to be $2\frac{1}{2}^{\circ}\text{C}$. As the power being dissipated in the thermistor was 0.45 mW, the power sensitivity in this zero air flow condition was $5.5^{\circ}\text{C}/\text{mW}$.

It was readily apparent at this stage that these thermistors were extremely sensitive to small changes in temperature, and that the time taken to respond to them was very short indeed. However at the same time they were particularly susceptible to self heating if the internal power dissipation was too large.

In order to reduce this self heating it was necessary to cut down the current flowing through them, but a compromise had to be reached as reducing the current impaired the sensitivity of the instrumentation. With the bridge in its original configuration, it was possible to detect a 1% change in resistance which represented about $\frac{1}{2}^{\circ}\text{C}$. It was felt that it would be quite acceptable to reduce this by a factor of 5 and this would reduce the power dissipation by one of 25 as it is proportional to the square of the current.

When the resistance of the thermistor was 2800 Ω and the bridge was in balance, the circuit was identical to that of two resistors of 5000 Ω in parallel, having a total impedance of 2,500 Ω . In order to reduce the current by a factor of 5, the impedance was increased by the same factor by adding a 10 k Ω wire wound potentiometer in series with the cell. The new

current flowing through the thermistor was 0.08 mA and the power dissipated in it was 0.018 mW.

The probe and the thermistor thermometer were then recalibrated in the blower tunnel in the same manner as before, and the graphs showed that the differences between the two sets of calibrations, with and without the 10k Ω resistor in the circuit, were 2.5 $^{\circ}$ C and 1.2 $^{\circ}$ C at 15 $^{\circ}$ C for the probe and thermometer respectively (Figure 5). The power dissipated in the two cases was 0.018 mW and 0.45 mW, and making the assumption that the power sensitivity varied linearly with the power dissipation, these results yielded values of 5.2 $^{\circ}$ C/mW and 2.8 $^{\circ}$ C/mW respectively for the power sensitivity of the probe and thermometer in the blower tunnel.

But the power sensitivity of the thermometer in the settling chamber was found to be 5.5 $^{\circ}$ C/mW as compared with this value of 2.8 $^{\circ}$ C/mW. This indicated quite conclusively that it did vary with the flow velocity past the element, but it was not possible to deduce in what manner because only two conditions were measured. The value of 5.2 $^{\circ}$ C/mW for the probe in the blower tunnel was consistent with the results for the thermometer, because there was obviously a flow past the thermistor although it was at a very low velocity. Hence the power sensitivity nearly corresponded to the zero flow value for the thermometer in the settling chamber.

In order to determine more exactly what the self heating of the two instruments was with the 10k Ω resistor in the circuit, they were placed in the blower tunnel and the aforementioned step input technique was applied to them with the tunnel both running and static.

The results from these tests have been summarised as follows:-

Temperature Rise due to Self Heating, (10k Ω resistor in)		
Element	Blower Tunnel On	Blower Tunnel Off
No.1 Probe	Negligible	$^{\circ}$ C.
Thermometer	Negligible	$\frac{1}{8}$ $^{\circ}$ C.

From these results it was apparent that even under the worst conditions, the self heating was sufficiently small to be neglected, and the calibrations which were carried out in the blower tunnel with the $10k\Omega$ resistor in the circuit were certainly accurate to $\pm \frac{1}{8}^{\circ}C$.

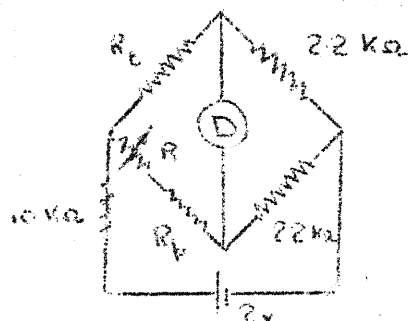
5.4 Final Modifications.

As a result of the incorporation of the thermistor thermometer in the settling chamber, it was found from some trial runs that the two resistances could be measured very accurately. Also the slow variation of temperature which was observed with the mercury thermometer was too slow to cause any error in the measurements with the thermistors because they almost recorded the instantaneous temperature. However, the short period fluctuations were still present, and these caused some inconvenience at the higher speeds because it was necessary to spend a long time balancing carefully in order to ensure an accurate measurement. These fluctuations were picked up by both thermistors and this prompted a further modification.

Instead of measuring the two resistances independently and then evaluating their respective temperatures, it was decided to measure the difference between these resistances. The reason for this was because the recovery factor was dependent on the difference between the two temperatures, and therefore by measuring this, any error incurred in measuring the absolute values and then subtracting them would be eliminated.

In order to do this, the probe was wired up in the circuit in series with the resistance box, and the thermistor thermometer was wired into the opposite arm. The resistance of the probe was less than that of the thermometer for a given temperature, and so resistance had to be added to that arm through the resistance box in order to balance the bridge.

The circuit diagram was:-



When the above modification had been incorporated, it was found that the short period fluctuations had been practically eliminated. The light spot on the detector remained stationary for long periods with just an occasional flicker, the amplitude of which was about $\frac{1}{2}^{\circ}\text{C}$. This greatly simplified the balancing process and led to greater accuracy in the final evaluation of the recovery factor.

The accurate knowledge of the settling chamber temperature was not essential provided that it was known to within $\pm 1^{\circ}\text{C}$., and therefore the use of the mercury thermometer was quite adequate for this purpose. The reason for this was because the slopes of the calibration curves were approximately constant over a small range of temperature, and therefore a difference of resistance would correspond to the same temperature difference anywhere within this region.

In order to interpret the temperature difference more accurately a small portion of the calibration curves was enlarged, and this covered a range of $\pm 2^{\circ}\text{C}$. about the ambient temperature in the settling chamber. This temperature was known from the reading of the mercury thermometer, and hence the resistance of the thermistor thermometer was ascertained from the calibration curve. By subtracting the measured difference from this, the resistance of the probe was found and hence the true temperature difference between them was evaluated.

5.5 Test Runs

Modifications to the instrumentation were now complete and it was in the form which gave the most accurate results. The bridge circuit was arranged so as to measure the difference ($R_t - R_p$), and the actual ambient temperature in the settling chamber was obtained from the mercury thermometer. The $10\text{k}\Omega$ resistor was included in the circuit so that the self heating of the thermistors produced a negligible temperature rise.

It was now possible to commence the test runs and these were made over the full range of incidence of which the probe was capable. This was 12° and it was covered in 2° increments. A scale, which was graduated in 2° divisions, had been scribed on the support strut of the probe and this facilitated the accurate setting of the incidence.

The first run was made at zero incidence, and when the probe had been mounted in the working section, the circuit was

wired up and checked for continuity before reassembling the tunnel. When everything was functioning correctly the tunnel was started, and the flow of air was adjusted until the pressure difference was about 0.2" Hg. on the manometer tubes.

After a short period the bridge was balanced and records were taken of the static and datum pressures, the temperature in the settling chamber and the resistance ($R_t - R_p$).

The airflow was then increased until the pressure difference was about 1" Hg. and the bridge was balanced as before when conditions had become stabilised. This procedure was repeated by increasing the pressure difference by about "2 Hg each time until the tunnel became choked. At this condition further increase in the supply of air from the reservoir caused no increase in the velocity of flow through the working section. The pressure was then reduced through the range and readings were taken at the intermediate values. In this way about 12 speeds were covered at each incidence setting.

When the runs at zero incidence had been completed, the tunnel wall was removed and the incidence was set to 2° . This was done by loosening the locking nut on the support and rotating the probe until the pointer lined up with the 2° division on the scale.

The same procedure as above was used for all the runs, and a specimen set of results is shown below. The remainder of the tables have been included in Appendix III.

6. Analysis and Results

In an airstream in which isentropic flow exists, the total temperature remains constant and may be expressed as:-

$$T_w = t_s \left(1 + \frac{\gamma-1}{2} M^2 \right)$$

In the settling chamber of a wind tunnel, $M = 0$ and $\therefore t_s = T_w$. When a temperature probe is placed in the airstream, it measures a proportion of this total temperature and this may be expressed as:-

$$T_m = t_s \left(1 + r \frac{\gamma-1}{2} M^2 \right) \quad \text{where } T_m \text{ is the measured temp.}$$

From these two equations:-

$$r = \frac{T_m - t_s}{T_w - t_s} = 1 - \frac{T_w - T_m}{T_w - t_s}$$

and $(T_w - T_m)$ is the temperature difference corresponding to the measured resistance $(R_t - R_p)$.

But in a compressible flow, the pressure and temperature ratios may be expressed as:-

$$\frac{p_1}{p_2} \left\{ \frac{1 + \frac{\gamma-1}{2} M_2^2}{1 + \frac{\gamma-1}{2} M_1^2} \right\}^{\frac{\gamma}{\gamma-1}} = \frac{T_1}{T_2} = \left\{ \frac{1 + \frac{\gamma-1}{2} M_2^2}{1 + \frac{\gamma-1}{2} M_1^2} \right\}$$

By considering stagnation conditions in the settling chamber and stream conditions in the working section, these become:-

$$\frac{p_o}{p_s} = \left(\frac{1 + \frac{\gamma-1}{2} M^2}{1} \right)^{\frac{\gamma}{\gamma-1}} ; \quad \frac{T_w}{t_s} = \left(1 + \frac{\gamma-1}{2} M^2 \right)$$

and thus if the pressure ratio is known, the Mach number and temperature ratio can be found.

But $(p_o - p_s)$ has been measured as the difference in levels of two manometer tubes, and p_o has been read from a barometer and hence

$$\frac{p_s}{p_o} = \left(1 - \frac{p_o - p_s}{p_o} \right)$$

This enabled the Mach number and temperature ratio to be evaluated. From the latter, the difference $(T_w - t_s)$ was computed by expressing it as

$$(T_w - t_s) = T_w \left(1 - \frac{t_s}{T_w} \right).$$

and hence the recovery factor was obtained.

The results for the 1st test run of the No.1 Probe at zero incidence have been presented in tabular form below. Although half the runs were made at increasing values of the Mach number, followed by the remainder at the intermediate Mach numbers in descending order, the results have been placed in ascending order for the sake of clarity.

Test Run with the No.1 Probe.

Run No.1

Zero Incidence.

$p_e = 28.80$ "Hg

Manometer tubes										
p_s "Hg	Datum "Hg	$p_e - p_s$ "Hg	$\frac{p_s}{p_e}$	M	$\frac{t_s}{T_M}$	$(R_t - R_p)$ Ω	T_M $^{\circ}C$	$T_M - T_m$ $^{\circ}C$	$T_M - t_s$ $^{\circ}C$	$\gamma = 1 - \frac{T_M - T_m}{T_M - t_s}$
10.15	10.30	0.15	0.994	0.090	0.998	55	18.25	0.00	0.58	1.00
10.60	10.25	0.35	0.986	0.140	0.996	50	18.20	0.05	1.16	0.957
10.85	10.20	0.65	0.975	0.190	0.993	55	18.25	0.00	2.03	1.00
11.50	10.20	1.30	0.954	0.260	0.987	50	18.12	0.07	3.77	0.982
12.50	10.15	2.35	0.916	0.355	0.975	70	17.98	0.08	7.25	0.989
13.40	10.10	3.30	0.885	0.422	0.965	50	17.75	0.15	10.15	0.985
14.10	9.35	4.75	0.833	0.515	0.949	50	17.65	0.15	14.80	0.990
14.60	8.50	6.10	0.787	0.596	0.934	50	17.65	0.15	19.15	0.992
15.10	7.40	7.70	0.733	0.682	0.915	60	17.55	0.05	24.65	0.998
15.30	6.95	8.35	0.711	0.715	0.907	50	17.55	0.15	27.00	0.995
15.55	6.10	9.55	0.670	0.778	0.892	45	17.65	0.20	31.30	0.994
15.65	5.65	10.00	0.654	0.802	0.886	50	17.65	0.15	33.05	0.996

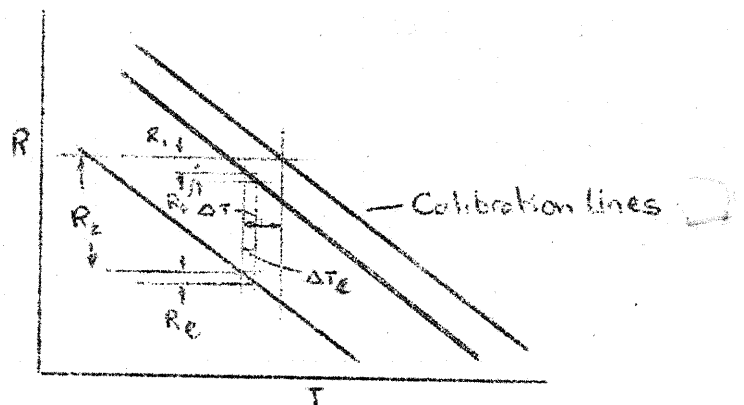
7. Discussion of the Results.

The results from the above table and those from the other test runs have been plotted on a graph of recovery factor against Mach No., and this is included as Figure 6. In order to give some scale to the scatter which is prevalent at low Mach numbers, a boundary of experimental accuracy has been plotted. This boundary layer has been calculated on the assumption of an error of $\frac{1}{8}^{\circ}\text{C}$ in the measurement of $(T_w - T_m)$, and it has further been assumed that the recovery factor would otherwise have been unity.

The accuracy of the final value of the recovery factor is dependent on the accurate measurement of $(T_w - T_m)$, and from the tables of results it is apparent that the equivalent difference of resistance is of the order of 50Ω . It might be pointed out that as this is the small difference between two large quantities it would be better to use two thermistors which had a large difference in their nominal resistances. However, although an error of 5Ω in 50Ω is proportionately larger than one of 5Ω in, say, 500Ω , the error in the temperature difference is exactly the same. This is because regardless of the nominal resistances, the slopes of the calibration curves would be constant over a small temperature range, and therefore the error in temperature resulting from a 5Ω error in resistance would be identical for any spacing of the curves. This is illustrated below where for convenience the calibration curves have been represented as straight lines.

R_1 and R_2 give rise to the same temperature difference ΔT .

The same absolute error, R_e , gives rise to the same error ΔT_e .



This assumed error of $\frac{1}{8}^{\circ}\text{C}$ in $(T_w - T_m)$ for the calculation of the boundary very closely represented the overall limit of accuracy to which this temperature difference could confidently be measured. Although the detector was sensitive to smaller

temperature variations, and the self heating of the thermistors amounted to less than $\frac{1}{8}^{\circ}\text{C}$. in the worst condition, the cumulative effect of these and interpolation from the calibration curves suggested that the overall accuracy was of the order of $\frac{1}{8}^{\circ}\text{C}$. Thus it was purely fortuitous that any points above this boundary should have fallen in line with those on the opposite side. In general the points above this boundary have a large amount of scatter, whilst those beneath it do show quite a reasonable consistency.

From the graph it may be seen that the recovery factor is relatively insensitive to small changes of incidence up to about 6° . However at higher incidences the recovery factor does begin to fall off, although it appears to remain more constant with Mach number.

At low incidences the recovery factor increases with Mach number reaching a peak value of 0.994 at the highest speed, whilst at an incidence of 12° , this peak value has only been reduced to 0.981. Thus variation of the incidence up to quite large amounts does not have a drastic effect on the recovery factor, although it may be dependent in some way on the entrance angle to the probe, which in this case was 40° total included angle.

From this experimental work, it would appear that thermistors are very practical elements for this type of work for the following reasons:-

1. They have an extremely short response time to a change of temperature. Although this was never actually measured, it was apparent from the way in which the rapid fluctuations in temperature in the tunnel were sensed and indicated by the detector. The response time is dependent on the size of the bead and the amount of protective insulation which is surrounding it, and the elements used for this work were stripped to a bare minimum.
2. Their size enables them to be fitted into a very small probe and they are extremely robust provided that reasonable care is taken in handling them.
3. A small temperature change causes a large resistance variation (approx. $80\Omega/^{\circ}\text{C}$. at 15°C . depending on the type), and this is particularly useful when accurate measurements are required.

4. Over the period of these tests, the elements remained perfectly stable and the calibration of the probes had not altered at the end.
5. Unlike a thermocouple, thermistors require no reference element at some known temperature; and as a result they can be wired into a simple series circuit with a galvanometer and a cell and be calibrated to give absolute temperatures.

It was found from these tests that the power sensitivity was dependent on the velocity of flow past these elements, and the self heating would be less if the thermistors were placed in a high velocity flow than if they were in a stagnation region. Also the power sensitivity was greater in air than in water, and for this reason thermistors should be calibrated in the fluid in which they will be used unless the self heating is so small that it is negligible in any medium. Therefore in order to obtain good results from thermistors, it is essential that the internal power dissipation should be kept to the minimum that is necessary to achieve the required accuracy.

The results of the prototype probe have been tabulated in Appendix III, and there is considerable scatter in the recovery factors which were obtained. This was due in part to the inadequacy of the mercury thermometer in the settling chamber, but it was also due to the calibration of the probe having been done in a water bath. The self heating of the element in the probe was very much greater in the wind tunnel than it was in the water bath, and as a consequence a considerable error arose in the measurement of T_m . The combined effect of these two was to produce a set of recovery factors with very little meaning because most of the points lie on the wrong side of the boundary of experimental accuracy.

8. Conclusions.

It was found that thermistors were ideally suited to the measurement of air temperature because of their rapid and positive response to small changes, and also in view of their large resistance change /°C. However it was necessary to ensure that the power dissipated in them was maintained at a sufficiently low level in order to prevent internal self heating.

A ventilated pitot tube fitted with a thermistor was tested at Mach numbers up to 0.8, and at incidences up to 12°. There was a slight increase in the recovery factor with increase of Mach number but this was less pronounced at the higher incidences. Also the recovery factor remained unchanged at incidences up to 6°, but it decreased slightly at the higher values. Up to 6°, the recovery factor attained a maximum value of 0.994 at $M = 0.80$, but at 12°, this figure had decreased to 0.981.

APPENDIX III

Tables of Results

Initial Runs with the Prototype Probe.

Run No.1

$p_c = 29.6$ "Hg.

Manometer tube											
p_s "Hg	Datum "Hg	$p_c - p_s$ "Hg	$\frac{p_s}{p_c}$	M	$\frac{t_s}{T_H}$	T_H °C	R_p	T_m °C	$T_H - T_m$	$T_H - T_s$	T
10.90	10.20	0.70	0.976	0.185	0.993	11.55	3756	10.90	0.65	1.98	0.67
12.45	10.15	2.30	0.924	0.338	0.978	10.05	3840	10.25	0.80	6.25	0.872
13.65	10.05	3.60	0.878	0.435	0.964	10.90	3860	10.05	0.85	10.25	0.917
14.60	9.35	5.25	0.822	0.535	0.945	10.70	3894	9.80	0.90	15.60	0.942
15.75	7.50	8.25	0.721	0.700	0.911	10.55	3910	9.65	0.90	25.25	0.964
15.85	7.40	8.45	0.715	0.710	0.908	10.53	3930	9.45	1.08	26.15	0.959
16.25	6.75	9.50	0.679	0.765	0.895	10.53	3930	9.45	1.08	29.80	0.964
16.95	5.45	11.50	0.612	0.867	0.870	10.25	3970	9.10	1.15	36.9	0.959
16.90	5.05	11.85	0.600	0.886	0.864	10.35	3940	9.35	1.00	38.6	0.974

These results have been based on the calibration of the probe in the water bath.

Tables (Contd.)

Initial Runs with the Prototype Probe

Run No.2

$p_a = 29.9$ "Hg

Manometer tube											
P_s "Hg	Datum "Hg	$P_o - P_s$ "Hg	$\frac{P_s}{P_o}$	M	$\frac{t_s}{T_w}$	T_w	R_p	T_m	$T_w - T_m$	$T_w - t_s$	
11.70	10.15	1.55	0.947	0.280	0.985	12.15	3750	11.00	1.15	4.32	0.734
13.85	10.00	3.70	0.875	0.441	0.963	11.50	3815	10.45	1.05	10.65	0.902
14.50	10.00	4.50	0.850	0.487	0.956	11.15	3840	10.25	0.90	12.65	0.929
15.10	8.80	6.30	0.788	0.594	0.934	11.45	3830	10.30	1.15	19.00	0.939
15.70	7.10	8.60	0.712	0.713	0.908	11.00	3905	9.70	1.30	26.50	0.951
16.15	6.60	9.55	0.680	0.763	0.896	10.65	3935	9.40	1.25	29.95	0.958
16.85	5.25	11.60	0.612	0.867	0.869	11.05	3895	9.75	1.30	37.75	0.966
16.80	4.80	12.00	0.598	0.890	0.863	11.45	3830	10.30	1.15	39.50	0.971

These results have been based on the calibration of the probe in the water bath.

Tables (contd).

Test Runs with the No.1 Probe

Run No.3

4° Incidence.

$p_c = 29.52$ "Hg

Manometer tubes			$\frac{p_s}{p_b}$	M	$\frac{t_s}{T_n}$	$R_c - R_v$	T_n °C	$T_n - T_m$ °C	$T_n - t_s$ °C	$r = 1 - \frac{T_n - T_m}{T_n - t_s}$
ps "Hg	Datum "Hg	$p_c - p_s$ "Hg								
10.40	10.25	0.15	0.995	0.085	0.998	65	16.70	0.00	0.58	1.00
11.00	10.20	0.80	0.974	0.194	0.992	50	16.70	0.20	2.32	0.914
12.50	10.10	2.40	0.920	0.345	0.977	60	16.15	0.10	6.67	0.985
13.45	10.05	3.40	0.885	0.420	0.966	60	16.05	0.10	9.85	0.988
14.00	10.00	4.00	0.865	0.460	0.959	50	15.90	0.20	11.90	0.983
14.60	8.90	5.70	0.807	0.562	0.940	50	15.70	0.20	17.35	0.988
14.80	8.40	6.40	0.784	0.600	0.933	50	15.50	0.18	19.40	0.991
15.40	7.30	8.10	0.725	0.694	0.912	50	15.35	0.20	25.50	0.992
15.80	6.30	9.50	0.678	0.766	0.895	50	15.35	0.20	30.45	0.9935
15.80	5.65	10.15	0.658	0.798	0.887	50	15.25	0.20	32.75	0.994

Tables (contd).

Test Runs with the No.1 Probe

Run No.4

6° Incidence

$p_o = 29.68 \text{ "Hg}$

Manometer tubes		$p_o - p_s$ "Hg	$\frac{p_s}{p_o}$	M	$\frac{t_s}{T_w}$	$R_L - R_P$ Ω	T_w $^{\circ}C$	$T_w - T_m$ $^{\circ}C$	$T_w - t_s$ $^{\circ}C$	$r = 1 - \frac{T_w - T_m}{T_w - t_s}$
p_s "Hg	Datum "Hg									
10.50	10.30	0.20	0.994	0.090	0.998	65	16.50	0.05	0.58	0.915
10.60	10.25	0.35	0.986	0.140	0.996	62	16.00	0.075	1.16	0.935
11.70	10.20	1.50	0.948	0.278	0.985	62	16.60	0.050	4.35	0.988
13.00	10.10	2.90	0.902	0.385	0.971	58	16.40	0.100	8.40	0.988
14.50	9.10	5.40	0.816	0.547	0.944	50	16.20	0.175	16.25	0.989
14.95	8.30	6.65	0.774	0.615	0.930	55	16.30	0.150	20.25	0.993
15.65	6.70	8.95	0.696	0.740	0.901	45	16.30	0.200	28.70	0.993
15.85	5.90	9.95	0.664	0.787	0.890	45	16.40	0.200	31.90	0.994
15.70	5.50	10.20	0.656	0.800	0.887	45	16.50	0.200	32.80	0.994

Tables (contd)

Test Runs with the No.1 Probe.

Run No.5

8° Incidence.

$p_o = 29.71$ "Hg.

Manometer tubes		$p_o - p_s$ "Hg	$\frac{p_s}{p_o}$	M	$\frac{t_s}{T_w}$	$\frac{R_f - R_p}{D}$	T_w °C	$T_w - T_m$ °C	$T_w - t_s$ °C	τ
p_s "Hg	Datum "Hg									
10.80	10.20	0.60	0.980	0.170	0.994	65	16.70	0.025	1.74	0.986
11.50	10.20	1.30	0.956	0.253	0.987	65	16.70	0.025	3.75	0.993
11.95	10.15	1.80	0.940	0.298	0.983	60	16.75	0.075	4.92	0.985
12.60	10.10	2.50	0.915	0.358	0.975	57	17.00	0.075	7.25	0.990
13.40	10.10	3.30	0.889	0.407	0.969	45	16.70	0.190	8.96	0.979
14.00	9.60	4.40	0.852	0.483	0.956	45	16.70	0.190	12.75	0.985
14.40	9.60	4.80	0.838	0.510	0.952	45	16.70	0.190	13.90	0.987
14.55	9.50	5.05	0.828	0.525	0.947	45	16.70	0.190	15.38	0.988
15.15	8.55	6.60	0.778	0.610	0.931	45	16.30	0.190	20.00	0.990
15.30	7.75	7.55	0.745	0.662	0.919	40	16.70	0.250	23.45	0.989
15.75	6.75	9.00	0.696	0.740	0.901	35	16.70	0.300	28.70	0.990
15.90	6.00	9.90	0.667	0.782	0.891	35	16.30	0.300	31.60	0.991

Tables (contd)

Test Runs with No. 1 Probe

Run No.6

10° Incidence

$p_c = 29.76$ "Hg

Manometer tube		$P_c - P_s$ "Hg	$\frac{P_s}{P_c}$	M	$\frac{t_s}{T_H}$	$R_L - R_P$ Ω	T_H °C	$T_H - T_m$ °C	$T_H - t_s$ °C	γ
P_s "Hg	Datum "Hg									
10.60	10.25	0.35	0.986	0.141	0.996	62	17.40	0.010	1.16	0.991
10.80	10.25	0.55	0.980	0.170	0.994	62	17.40	0.010	1.74	0.995
11.40	10.20	1.20	0.960	0.242	0.988	52	17.50	0.100	3.48	0.971
12.55	10.10	2.45	0.916	0.355	0.975	52	17.70	0.100	7.25	0.986
13.35	10.05	3.30	0.890	0.410	0.967	44	17.70	0.180	9.58	0.981
14.30	9.60	4.70	0.840	0.505	0.951	40	17.70	0.220	14.20	0.985
14.55	9.45	5.10	0.830	0.520	0.948	35	17.50	0.250	15.10	0.984
14.75	8.90	5.85	0.805	0.565	0.940	37	17.60	0.240	17.40	0.986
15.15	8.25	6.90	0.769	0.625	0.927	35	17.50	0.250	21.15	0.988
15.30	7.80	7.50	0.749	0.655	0.921	28	17.50	0.340	22.90	0.985
15.60	7.25	8.35	0.719	0.704	0.910	23	17.30	0.390	26.05	0.985
15.80	6.65	9.15	0.691	0.745	0.902	18	17.70	0.450	28.40	0.984
15.85	5.80	10.05	0.662	0.790	0.889	15	17.70	0.470	31.90	0.985

Tables (contd)

Test Runs with the No.1 Probe

Run No.7

12° Incidence

$p_o = 29.76$ "Hg

Manometer tubes			$\frac{p_s}{p_o}$	M	$\frac{t_s}{T_w}$	$R_E - R_F$ Ω	T_w $^{\circ}C$	$T_w - T_m$ $^{\circ}C$	$T_w - t_s$ $^{\circ}C$	τ
p_s "Hg	Datum "Hg	$p_o - p_s$ "Hg								
10.60	10.25	0.35	0.986	0.140	0.996	58	17.80	0.05	1.16	0.957
11.20	10.20	1.00	0.966	0.222	0.990	55	17.70	0.08	2.90	0.972
12.10	10.10	2.00	0.933	0.315	0.980	48	17.70	0.15	5.80	0.974
13.20	10.10	3.10	0.896	0.400	0.969	42	17.70	0.20	9.00	0.978
14.05	10.05	4.00	0.865	0.460	0.961	36	17.90	0.27	11.30	0.976
14.90	10.00	4.90	0.836	0.513	0.949	28	18.00	0.34	14.80	0.977
15.35	9.15	6.20	0.793	0.585	0.936	20	18.00	0.39	18.55	0.979
15.70	8.40	7.30	0.756	0.645	0.923	10	18.10	0.50	22.35	0.978
16.00	7.80	8.20	0.725	0.695	0.912	5	18.20	0.55	25.50	0.979
16.15	7.35	8.80	0.705	0.725	0.905	0	18.10	0.60	27.55	0.970
16.20	6.10	10.10	0.660	0.793	0.888	0	18.20	0.60	34.80	0.983

1. Introduction.

Part III contains an account and the results of a detailed investigation of the recovery factor of 5 outside air thermometers in high speed flight. The aircraft which was used for this work was a Hawker Hunter F. Mk II, and it was flown over a wide range of airspeeds and altitudes. The 5 thermometers consisted of 4 ventilated pitot probes and 1 standard surface temperature probe, and the temperatures which they measured were recorded on paper traces while the airspeed and altitude were recorded on film in an automatic observer panel. It was felt that there was a definite need for a further investigation into this field in view of the uncertain nature of the results which had been previously obtained.

Only a very limited amount of testing has been carried out with ventilated pitot thermometer probes, and this was initiated by the A. & A.E.E. at Boscombe Down and followed up by the Flight Test Department of Rolls Royce at Hucknall using a similar probe. Some results obtained by Rolls Royce from flights with the ventilated pitot have been presented in Reference 1, and these showed a recovery factor in the neighbourhood of 1.00. The aircraft which were used in this case were an English Electric Canberra bomber and 2 Hawker Hunter fighters, and the probe was mounted on the port side of the nose and the starboard side of the belly for the two types respectively. 14 calibrations were obtained of which 12 were between 30,000' and 40,000', and there was a general scatter in the recovery factor between 0.97 and 1.12. The two remaining calibrations at 10,000' and 20,000' yielded recovery factors of 0.96 and 1.02 respectively.

In contrast to the small amount of work carried out on ventilated pitot probes, an extensive programme was undertaken by Rolls Royce using a standard surface temperature probe. Results have been obtained for the recovery factor of such a probe mounted on a variety of aircraft including a Hunter, Sea Hawk, Swift, Canberra and Vulcan, and in each case the recovery factors decreased slightly with increase in altitude and then increased suddenly at some altitude between 20,000' and 40,000'. For the majority of these cases this critical altitude was about 30,000', and in the case of the Canberra, the recovery factor reached a peak value of 1.055 at 35,000' and then fell off sharply to 0.80 at 48,000'.

Following this an extensive investigation was made into the accuracy with which an air thermometer could be calibrated, and for this purpose a similar probe to that used above was fitted on the belly of each of 3 Hunters. These aircraft were undergoing lengthy endurance flying at Idris in N. Africa for the purpose of engine matching, and this provided an unique opportunity of consolidating the information already obtained. Altogether 72 sets of calibrations were obtained and the results which are shown in Reference 2 indicate a very fair consistency from one aircraft to the next. However there was a considerable amount of scatter in the points at any one altitude, but a mean line through all the calibrations showed that the recovery factor decreased with increase in altitude up to about 40,000' above which it began to increase again. As an indication of the scatter which was obtained during these tests, 26 calibrations were carried out at 40,000', and of the recovery factors which were measured, 2 lay between 0.5 and 0.6, 4 between 0.6 and 0.7, 17 between 0.7 and 0.8, 2 between 0.8 and 0.9 and one between 0.9 and 1.0. Thus the recovery factor covered a wide band from 0.541 to 0.962, and this was the general case at all altitudes but to a lesser extent.

From the work which has been done on the measurement of air temperature up to the present time, two conclusions may be drawn. The first is that the recovery factor of a surface temperature thermometer is not independent of altitude but it increases suddenly at about 30,000' to 35,000' and it may then decrease just as suddenly at a higher altitude. The second conclusion is that a ventilated pitot thermometer has a recovery factor which is very much nearer to unity, and which, from the few results so far available, does not appear to have any particular trend but just random scatter.

The purpose of these flight trials was to obtain at as many altitudes as possible, as many values of the recovery factor as time permitted. The reason for this was to confirm the trend of the recovery factor which had been found by Rolls Royce for the surface temperature probe; and also to carry out a more detailed investigation of the recovery factor of a ventilated pitot probe than that which had so far been accomplished. In this earlier work most of the calibrations were carried out between 30,000' and 48,000', in which band there was a random scatter, and it was intended to investigate this region more fully and also to extend it to a much lower altitude. It was originally intended to cover the altitude band from 5,000' to 45,000' six times in increments of 5,000', and this would have involved about 30 flights covering 2 altitudes on each. In this way it was hoped to check the consistency with which a recovery

factor could be measured from one flight to another and also to establish whether there was any particular trend of the recovery factor of a ventilated pitot probe with altitude as there was with the surface temperature probe. However it was apparent from the outset that there was insufficient endurance of the aircraft to enable more than one altitude to be covered on any one flight if the tests were to be carried out in a conscientious manner, and so the programme had to be adjusted accordingly.

Altogether 37 flights were made, of which 31 were wholly or partly successful, and these produced 149 calibrations which were evenly distributed throughout the altitude band. Of the 5 probes mounted on the aircraft, 3 were fitted with thermistors and these were all pitot thermometers. The 4th probe used a nickel wire sensing element while the standard thermometer had a platinum resistance wire coil.

The majority of the sorties consisted of series of stabilised levels at a nominal altitude and over a wide range of airspeeds. This procedure was adopted for the tests at all altitudes and it is described in more detail in the appropriate section.

Some accelerated and decelerated levels were carried out at two altitudes at the commencement of the programme in order to assess the lag of the various probes. These highlighted the tremendous advantage which the thermistor has over a resistance wire coil in the rapid measurement of temperature.

Some calibrations were obtained which included temperatures measured in transonic dives, and although these necessitated high rates of descent, the probes fitted with thermistors proved that they were quite capable of responding quickly to these rapid changes of temperature.

In addition two sets of levels were carried out at 4,000^{ft} in the vicinity of a barrage balloon which had apparatus on board which was measuring the ambient air temperature. This provided a useful check on the measurements which were recorded in the aircraft.

The results were analysed on an I.B.M. computer which calculated the recovery factor and the ambient air temperature, and these have been presented in tabular and graphical form at the end of this report.

2. The Test Equipment.

2.1. Description of the Aircraft

The aircraft which was available for the testing of these probes was a Hawker Hunter F. Mk. II, serial number WN 893. This was in a standard configuration with the exception that it had nylon tufting on the port mainplane, and an extra pitot head mounted on a nose boom. An incidence vane and another pitot head were mounted on booms springing from approximately the mid-span of each tailplane, and these had been used in connection with some previous experimental work involving the measurement of tail loads.

The Hunter F. Mk II is powered by an Armstrong Siddeley Sapphire turbo-jet engine rated at 8,000 lb. s.t. and this particular aircraft was capable of attaining a level speed Mach number of about 0.93. However an account of some stogger in the hinge-blocks in the tailplane, cases of tailplane flutter were reported after flights at high I.A.S. in connection with the tail load measurements, and for this reason the aircraft was limited to a maximum speed of 500 kts E.A.S. There was no Mach number restriction, and so this limitation only affected the speed range covered in this present experiment below 11,500'.

The four 30 mm. cannon had been removed from the gun pack, and it was in this region that four of the probes were mounted and the recorders housed. The probes had to be located on the aircraft where cut-outs in the skin already existed, and the most suitable cut-outs were those through which the expended shell cases were ejected. The probes have been numbered 1 - 5 and nos. 1, 2, 4 and 5 were mounted on panels which fitted flush into these cut-outs, each being held in place by two Dzus fasteners. Probe no.3 was mounted on the radar cooling connection cover plate which is situated about 3' 6" from the nose on the port side, and angularly displaced by about 120° from the upward vertical. Probes no.1 and 2 were located approximately 12' and 13' aft of the nose on the port side and at angular displacements of about 140° and 130° respectively from the upward vertical. Probes No.4 and 5 were located symmetrically opposite to Nos. 1 and 2, the No.4 probe being in the forward position (Plates 8 - 12).

The thermometers which were fitted with thermistors were nos. 1 - 3 and thus all these were located on the same side of the fuselage. This was in order that each would be operating under similar conditions of solar radiation, and a direct comparison could therefore be made between the results of these three.

None of the probes was situated directly in the wake of another one and so any disturbance effect was only slight. However as a precautionary measure, the ventilated pitot on the starboard side was placed forward of the standard surface temperature thermometer, and on the port side, the smaller of the two probes was located in the forward position.

2.2. Design and Construction of the Probes

2.2.1. The No. 1 Probe

This was a modified version of the No. 1 probe which was used for the wind tunnel tests described in Part II. It was a ventilated pitot tube with two concentric stagnation chambers, and a thermistor was mounted at the end of the inner one. Both chambers were independently vented to the atmosphere, and the vent to inlet area ratios were $12\frac{1}{2}\%$ and 50% for the inner and outer chambers respectively. The overall length of this probe was $1\frac{1}{2}$ " and the diameter was $\frac{1}{4}$ ". The inner chamber was the bore of a 3 mm. O/D stainless steel tube, and the outer chamber was the annular space between this and a brass tube having a bore of $\frac{3}{16}$ " and an O/D of $\frac{1}{4}$ ". The two tubes were thermally insulated from each other by tufnol distance pieces, and by this means the temperature of the air in the inner chamber was very nearly independent of the external wall temperature. The increased mass flow through the outer chamber was necessary to compensate for the heat transfer through the outside wall. This arose because the temperature of the outside surface was lower than that of the inner by virtue of the viscous dissipation in bringing the air to rest through the external boundary layer on the probe.

The outer chamber also reduced any effects from solar radiation which might otherwise have affected the temperature which was measured by the thermistor.

A more detailed description of this probe has been included in Section 2.2 in Part II, and modifications to it for this flight work were mostly confined to the support and mounting fixture.

The variable incidence support which was made from 20 swg brass sheet was removed, and it was replaced by one of greater thickness chord ratio which was constructed from 22 swg brass moulded round a streamlined former and soldered at the trailing edge. This support, which was swept back at 35° , maintained the probe at zero incidence to the fuselage, and the length of it was such that the probe was situated outside the boundary layer of the aircraft. At the station at which this thermometer was located, the aircraft boundary layer thickness was just over 1" and so the centre line of the probe was placed at a distance of $1\frac{1}{2}$ " from the fuselage surface.

In the wind tunnel version, the leads from the thermistor were led externally down the trailing edge of the support strut, but this arrangement was modified with the new support, and they were taken through the inside of it and connected to a terminal block secured on the inside of the mounting panel.

A small base plate was soldered to the end of the support, and this was fixed to a paxolin distance piece which was $1\frac{1}{4}$ " square by $\frac{3}{16}$ " thick by means of four 4 BA counter-sunk screws and nuts. This distance piece was in turn bolted onto the mounting panel and it formed a complete thermal insulation between the probe and the aircraft.

Finally the probe was finished off to give a highly polished metallic surface which had a low surface emissivity.

A sectional drawing of this thermometer is shown in Figure 1 and a photograph is included as Plate 1.

2.2.2. The No. 2 Probe

This probe was a scaled up version of the previous one and it was designed with a view to investigating the scale effect on the recovery factor. The scaling factor was 4 but the tube sizes were governed by available stocks. The outer tube was 1" O/D x 16 swg brass and the inner one was $\frac{1}{2}$ " O/D x 18 swg stainless steel. The vent area ratios were maintained at $12\frac{1}{2}\%$ and 50% as before, and the chief differences were in the support design and assembly technique. Also a matched pair of thermistors was mounted in this probe in order to improve the sensitivity.

The thermistors were mounted side by side about 0.080" forward of the vertex of the wedge shaped end of the central plug, and the faces of the wedge lined up exactly with the two vent holes which were inclined rearwards at 30° to the normal.

The elements were connected in series with each other and so the resistance change per degree change of temperature was double that of the No.1 probe. A tag strip was mounted on the rear face of the central plug and the platinum thermistor wires, which were led through this plug in the same manner as for the No. 1 probe, were soldered to it. Two multi strand plastic insulated cables were then soldered to this, and passed from there through a hole drilled in the tail fairing. The tag strip was a safety precaution to ensure that the platinum wires should not be broken by the accidental application of tension when the fairing was removed.

The individual components of this probe were all locked in position by a series of countersunk grub screws, whereas in the No.1 probe they were held in place with an adhesive.

The support strut had a streamlined section made of 16 swg brass sheet which was moulded round a former and soldered at the trailing edge. It was swept back at 45° from the probe to which it was soldered, but a tufnol insulating strip $\frac{1}{2}$ " wide was inserted at mid span. This was to provide a heat insulation between the aircraft and the probe, and the two halves of the support were fixed to it by means of 4 bolts passing through the brass skins and the tufnol insert. The support was soldered to a brass base plate having dimensions $4" \times 3" \times \frac{1}{8}"$ and this was rigidly bolted to the detachable mounting panel.

The cables were led externally from the hole in the fairing through which they emerged into the support through a hole in the trailing edge. From there they were passed down through the tufnol insert and out through the base plate where they were connected to a terminal block mounted on the inside of the detachable panel.

In all other respects this probe was a true scaled up version of the No.1 probe which has been described in more detail in a previous section.

Finally this thermometer was given a highly polished finish, and when liquid polish was used, care was exercised to prevent it from blocking or partially blocking the vent holes.

A sectional drawing and various photographs of this probe have been included as Figure 1 and Plates 2 and 3.

2.2.3. The No. 3 Probe

This probe was manufactured by Rolls Royce from drawings supplied by the A. & A.E.E. at Boscombe Down, and it was modified slightly by the R.A.E. at Bedford to whom it was on loan. It was of the ventilated pitot type having two ventilated chambers and an overall length and diameter of 7.0" and 0.984" respectively. The original probe used a resistance coil as the sensing element, and this was mounted in the centre of the inner chamber allowing the air to flow both through and around it. The R.A.E. at Bedford, however, replaced this coil by two thermistors connected in series.

These thermistors were of the standard M.53 type, and had a nominal resistance of 5000 Ω at 20°C. But whereas in the standard form they were supplied with a copper disc attached to the bead by means of a thin layer of glass, in this installation this had been removed in order to reduce the size and so enable it to fit into the inner chamber.

The thermistors were mounted in the probe by first making a fibreglass tube $2\frac{1}{2}$ " long x $\frac{3}{8}$ " dia., and then glueing the elements to two small struts which were mounted across the tube in planes at right angles to each other. The thermistors were in the centre of the tube, and they were situated about 1.3" apart, with the forward one about 0.6" from the mouth. This fibreglass tube was secured at its rear end by a tufnol collar, and it formed the inner chamber of the probe. This chamber was vented through 4 holes drilled in a brass rig which covered a circumferential groove in the tufnol union block. This groove was connected to the rear of the inner chamber by a passage drilled through the union block and inclined rearwards at 45° to the centreline. The vent area ratio of this chamber was about 25% based on the area of the 4 holes themselves, but was only about 13% when based on the cross sectional area of the passage.

The outer chamber wall was made of chromium plated brass, and this screwed onto the union block to allow easy access to the elements. Then holes were placed symmetrically around the circumference of this wall, and these were the vents of the outer chamber giving an area ratio of approximately 50%.

The forward end of the probe was chamfered to provide a smooth entry for the airstream, and the total included angle of the chamfer was 60°.

The thermistor wires were led back along the wall of the fibreglass tube to which they were affixed with adhesive. From the rear of this tube they were passed through the union block and soldered to studs mounted at the back of it. Multi strand cables were soldered to these, and they passed further down the probe and through the wall into the support strut, from where they were led out through a hole in the base plate.

The section of the support strut, which was made up from 20 swg brass sheet, was a semi-circular leading and trailing edge of different radii with plane upper and lower surfaces fairing into them. The leading and trailing edge radii were 0.3" and 0.1" respectively and the chord of the section was 2.6". The support was swept forward from the probe at 25°, and there was no thermal insulation between it and the aircraft because the forward part of the probe, which was the working section, was completely insulated from the rear part to which the support was attached.

The surface finish of the outer chamber was a chromium plate, and the rear half of the probe, which was machined aluminium alloy, was painted glossy white. The support strut and the mounting plate were both painted glossy silver.

A sectional drawing of this probe is shown in Figure 2 and some photographs have been included as Plates 4 and 7.

2.2.4. The No.4 Probe

This was a total head thermometer designed by the A. & A.E.E. at Boscombe Down who kindly supplied a full set of drawings for its construction for this test work. This was also of the ventilated pitot configuration, but of a more elaborate design than the previous probes. It had two ventilated stagnation chambers, and external to these there was an unventilated annular air space.

The entry to the probe did not have a plain chamfer, but instead had a convex contraction with blunt lips and boundary layer bleeds just forward of the entry to the two stagnation chambers.

The overall length and diameter of the probe was 7½" and 1.0" respectively, and the forward part which housed the working section and the sensing element was thermally insulated from the rear part to which the support was attached.

The sensing element was a Smiths nickel wire resistance coil with a nominal resistance of 99.2Ω at 20°C . A nickel coil was preferred to a platinum wire coil for this work since platinum is rather sensitive to any strains imposed on it. Such strains would arise from internal stresses due to the contraction of the wire at low temperatures. This coil was mounted centrally in the inner chamber, and the air flowed both over and through it to the rear of the chamber whence it passed through 4 passages into a circumferential groove which was vented to the atmosphere through 4 holes in the brass ring covering it.

The vent area ratio of this inner chamber was 39% when based on the total inlet area, but the diameter of the coil was 70% of that of the chamber and although the air could pass through the centre of the coil, this caused quite a restriction and the effective area was considerably reduced.

The outer wall was made from brass tubing which was machined to give a highly polished finish, and it was threaded at one end so that it could be screwed on and off in order to gain access to the element. Four slots were machined through this wall about $\frac{3}{4}$ " from the forward end, and these were the boundary layer bleed exits. The outer chamber also vented through 4 holes which were drilled through the wall near the aft end. The entry to this chamber was the annular gap between the inner tube and the tufnol deflector body which separated the two tubes, and also deflected the boundary layer bleed air out of the slots.

This deflector body also formed the unventilated annular air space which was adjacent to the outer wall. The purpose of this was to provide a further heat sink or source to compensate for any heat transfer through the wall, and so reduce the temperature difference between the two chambers. The vent area ratio of the outer chamber was approximately 20% which was considerably smaller than that of the other probes, but this was compensated for by the extra unventilated air space external to this chamber.

The inner tube was also made from brass but it was lined throughout with $\frac{3}{8}$ " cork sheet which was glued to the wall, and this provided added insulation for the element from external heat transfer.

The afterbody, to which the support was fixed, was machined from aluminium alloy, and this was connected to the working section, or forebody, by a tufnol union block which insulated the two halves from each other.

The support was made from mild steel plate which was bent round a former which had equally radiused ends and plain surfaces, and it was braised along the trailing edge. It had a thickness and chord of 0.45" and 2.48" respectively, and its spanwise length was 3.6". It was rigidly bolted and sealed to the afterbody of the probe at one end, and a mounting plate was braised to the other end.

The electrical leads from the elements were led through the union block and into the afterbody, from where they passed into the support and out through the mounting plate.

The body of the probe was given a highly polished finish and the support was painted glossy black.

A sectional drawing and photographs of this probe may be found in Figure 3 and Plate 5.

2.2.5. The No. 5 Probe

This was a standard resistance thermometer which was used for measuring outside air temperature on aircraft. It was a Sangamo-Weston thermometer bulb of type S 110 and Form 5. This particular form had the resistance coil which was platinum, enclosed in an elbow shaped probe, and the part containing the coil was situated at a distance of 2" from the aircraft skin and was parallel to it. The probe itself was surrounded by a shield of thin gauge alloy, the purpose of which was to reduce the solar radiation directly onto the probe, and also to prevent the flow from impinging on it at an incidence as the measured temperature was rather sensitive to flow direction. The shield was open at both ends allowing an unrestricted flow of air to pass, and it was $1\frac{1}{2}$ " wide and $2\frac{3}{4}$ " high with a semi-cylindrical top and parallel walls.

The nominal resistance of the platinum was 140Ω at 20°C . and the approximate value for the temperature coefficient of resistance was $\frac{1}{2} \Omega/^{\circ}\text{C}$.

This probe was included in the programme for the purpose of comparing this type with the ventilated pitot thermometer, and although a large amount of work has been carried out on the evaluation of the performance of this type of air thermometer, the results have in general shown a wide band of scatter. In one particular series of tests² with an unshielded version of this probe, the value of the recovery factor at 40,000' varied

from 0.541 to 0.962, and although these were extreme values, the standard deviation from the mean line through 26 calibrations at this altitude was about ± 0.09 . Thus it was apparent that this standard thermometer not only gave recovery factors vastly different from unity, but the recovery factor did not remain constant at any particular altitude on two different flights. It also had a comparatively slow response to a change in temperature and thus it was hoped that probes 1 - 4 would compare very favourably with this one during the lag tests.

From the results of the 1st ten flights it was apparent that the recovery factor of this probe was higher than had been expected, and it was decided to remove the shield after about 25 flights in order to assess its effectiveness. However before this was done, the base of the shield fractured on both sides from the leading edge rearwards, and when the aircraft landed at the end of a sortie, it was found to be hanging on by a very short length of material at the rear end. It was, therefore, removed completely and the remainder of the tests were carried out with an unshielded probe.

Further examination of the fracture revealed that it was due to fatigue, and it was probable that the alternating stresses necessary to set up fatigue conditions were caused by engine vibrations. These were particularly severe at certain combinations of engine and forward speed, and, as described elsewhere, they excited the galvanometers in one of the recorders which resulted in an oscillating trace.

A sectional drawing of this probe is shown in Figure 4 and an illustration of it in Plate 6.

2.3. The Recording Apparatus

The temperatures measured by the 5 probes were recorded on two Hussenot A,22 trace recorders which were mounted on the gun pack. The three probes having thermistors as sensing elements (viz. 1,2 and 3) were connected to one recorder, (Blue), and the other two probes were connected to the second one, (Red). The thermistors were energised from a 2v standard cell and, as the current was being measured on galvanometers, it was important to have a record of the true voltage and therefore a voltage galvanometer was included in the Red recorder.

The A.2 2. recorder used a paper which was 60 mms. wide with an available recording width of 58 mms. The running endurance of these recorders was about 4 mins, but this could be extended if required by removing the exposed paper after, say, 2 minutes running, and then relacing the spool. The reason for the increase was that the driving spool rotated at constant r.p.m., and therefore the paper speed varied with the change in diameter of the spool. The recorders were mounted on the gun pack, one above the other, the Blue one being initially in an upright position in the upper fixing bracket while the Red one beneath it was placed on its side.

The thermistors required a very low current to pass through them in order to keep the self heating errors to a minimum, and it was therefore necessary to use extremely sensitive galvanometers which took a low current for full scale deflection. A suitable instrument for this purpose was the SFIM. E. 312 galvanometer which required $31\mu\text{A}$ for a full scale deflection, and this was used with a 250Ω shunt resistance. The circuit was basically a series one and as the internal resistance of the galvanometers was 90Ω , the maximum current which passed through the thermistors was $42.15\mu\text{A}$. The power dissipation was therefore extremely low and any self heating effects were negligible.

In order to utilise the maximum amount of the trace width which was available, the circuit was arranged in the form of potential dividers so that at the maximum anticipated temperature, the thermistors had their minimum resistance and the current flowing through them was $42.15\mu\text{A}$. Similarly at the lower end of the temperature scale the thermistors had their maximum resistance, and the potential dividers were so arranged that the current flowing through them was about $5\mu\text{A}$.

In order to improve further the sensitivity in terms of $^{\circ}\text{C}$ per mm. of trace width, the temperature range was split into two portions which overlapped slightly. The dividing line corresponded to $22,500'$, and thus a double potential divider was built into the circuit for each thermistor with a switch provided for selecting the particular range required.

The two probes with resistance wire elements were energised from the aircraft's 28 v supply, and E 525 ratiometers were used in the Red recorder to measure the change of resistance. As they were ratiometers as opposed to galvanometers, a knowledge of the exact voltage was not important because it was the proportion which was measured, and this was unaffected by quite large variations in the supply voltage.

The entire circuitry for all five probes was built into one junction box which was fixed into the aircraft, and the two recorders and the power supply were connected in through Plessey plugs (Plate 13).

An interrupter box was also wired into the circuit in order to provide some means of indentifying the individual traces. It consisted of an electrically driven rotating contact maker which introduced a resistance of 910Ω into each circuit in turn, with the exception of No.3 probe which was not interrupted. This had the effect of displacing the trace through a small amount and it thus afforded a means of identification. The time for one complete cycle of the interrupter was about 2 secs.

At the forward end of the gun pack was an automatic observer panel which was filmed by a 35 mm. cine camera running at about 8 frames per second. Displayed on this panel were two altimeters and airspeed indicators, a clock, a veeder counter, and various other pressure and temperature gauges. One set of altimeter and airspeed indicator was connected to a pressure head mounted on the standard wing boom, whilst the other set was connected to a head on the nose probe. For this work the wing boom altimeter and A.S.I. were used because the pressure error corrections for this boom were built into the I.B.M. computer on which the results were analysed. The clock was useful during the accelerated and decelerated levels and the transonic dives, and the veeder counter, which changed each time the camera was operated, provided a positive identification of one recording from the next. The other gauges on the panel were remnants from some previous work on the aircraft, and they were not used for this investigation. The camera was run off the 28v supply and it was synchronised to operate when the recorders were started by the pilot.

The entire instrumentation was controlled from the cockpit where the pilot had two master switches which operated the 28v supply and the 2v supply. When both these were switched on, he could record either by pressing a button on the top of the control column, or else, if a long burst was required, he could switch on a "record" switch and thus be relieved of the necessity to keep the button depressed.

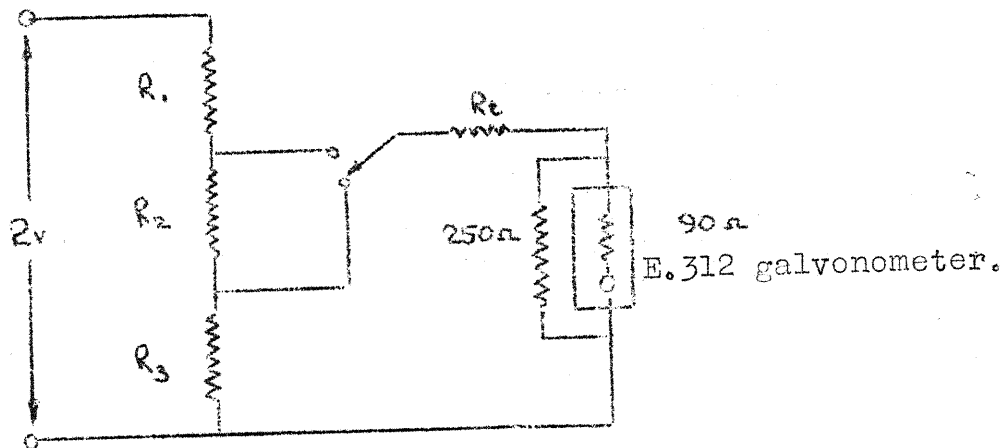
Plates 16 and 17 show specimen trace recordings made in both Hussenots. The first record shows a stabilised level at 35,000' followed by a transonic dive through this altitude, and the second record shows two more transonic dives.

Plate 15 shows a specimen from the A.O.P. films and this particular sample was taken from a transonic dive. The wing boom altimeter and airspeed indicator may be seen side by side at the top left hand corner of the panel.

2.4. The Electrical Circuit.

The circuit for the three thermistors was basically a series combination of an element with a shunted galvanometer and a cell. However the change of resistance of the thermistors over the temperature range was so large that, in a simple series circuit, the consequent variation of the current would have been far greater than the galvanometer could stand. It was therefore necessary to adjust the voltage so that the current change corresponded with the maximum of which the galvanometer was capable. By doing this the maximum sensitivity of the circuit was obtained and for this purpose a potential divider was used.

However as mentioned in the previous section, the sensitivity was further improved by splitting up the resistance band of the thermistors and covering each half separately. This was accomplished with the circuit diagram shown below in which the two potential dividers have been combined and a switch has been provided for the selection of the desired band.



Standard 2v cells were available and they could have been connected up in series if desired, but as the required voltage was so low, a single cell was adequate and it was changed periodically.

It was now necessary to make some calculations for the resistances R_1 , R_2 and R_3 for each probe in turn.

Firstly the temperature range to be covered depended on the speed and altitude ranges, and for this purpose I.C.A.N. temperatures were assumed.

The minimum temperature at which the probes would be operating was that corresponding to about 135 knots at 40,000'. This was 226°K or -47°C.

The maximum temperature was that pertaining to 500 kts E.A.S. at 4,000' which was 318°K or + 45°C.

This temperature range was split at values corresponding to 22,500' which was half way up the altitude band which was covered. Therefore the highest temperature in the upper altitude band was that pertaining to $M = 0.94$ at 22,500' and this was 287°K.

Similarly the lowest temperature in the lower altitude band was that corresponding to 150 kts at 22,500' which was 249°K.

Therefore the two temperature bands were

Below: 22,500'	$249^\circ < T_w < 318^\circ$.
Above: 22,500'	$226^\circ < T_w < 287^\circ$.

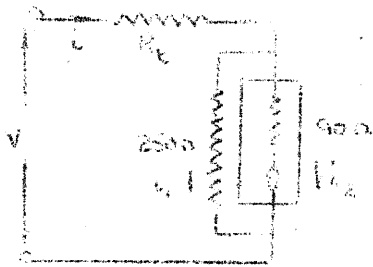
It was now possible to calculate the resistance ranges appropriate to the above temperatures for each of the elements, and this is summarised in the following tables.

Temp °K	Probe No.1		Probe No.2		Probe No.3		Probe No.4	Probe No.5
	R _t lower (Ω)	R _t upper (Ω)	R _t lower (Ω)	R _t upper (Ω)	R _t lower (Ω)	R _t upper (Ω)	R _e (Ω)	R _e (Ω)
225		42,500		85,000		326,000	71	105
235		25,000		50,000		166,000	75	110
245		16,500		33,000		98,000	79	115
255	10,000	10,000	20,000	20,000	55,000	55,000	83	121
265	6,800	6,800	13,600	13,600	34,000	34,000	87	126
275	4,700	4,700	9,400	9,400	20,200	20,200	91	131
285	3,400	3,400	6,800	6,800	13,500	13,500	96	136
295	2,500		5,000		9,600		100	141
305	1,850		3,700		6,600		105	146
315	1,400		2,800		4,500		110	151

Probe No.	Approx. Resistance Ranges	
	Lower Altitude	Upper Altitude
1	1,400 - 10,000	3,400 - 42,500
2	2,800 - 20,000	6,800 - 85,000
3	4,500 - 55,000	13,500 - 326,000

Having fixed the resistance ranges over which it was anticipated that the elements would be operating, it was then possible to evaluate R_1 , R_2 and R_3 .

Firstly it was necessary to calculate the voltage which was required across the thermistor and the galvanometer, and a specimen set of calculations are shown below for the No. 1 probe.



The resistance of the parallel pair:-

$$\frac{1}{R} = \frac{1}{250} + \frac{1}{90} = .0151$$

$$\therefore R = \underline{66 \Omega.}$$

But $i = i_1 + i_2$ and $\frac{i_1}{i_2} = \frac{90}{250.}$

\therefore when $i_2 = 31 \mu\text{A}$ which is its maximum, $i = 42.15 \mu\text{A}.$

Consider the 1st resistance range:- $1400 \Omega - 10,000 \Omega.$

$$\frac{V_1}{(1400 + 66)} = 42.15 \mu\text{A} \quad \therefore \underline{V_1 = 0.062 \text{ volts.}}$$

also $\frac{V_1}{(10,000 + 66)} = i = 6.15 \mu\text{A}$ when V_1 is substituted.

If $i = 6.15 \mu\text{A},$ $\underline{i_2 = 4.52 \mu\text{A.}}$

Therefore when $R_t = 1,400 \Omega,$ $i_2 = 31 \mu\text{A}$ and there is a full deflection on the galvanometer. When R_t has increased to $10,000 \Omega,$ the galvanometer current has become $4.52 \mu\text{A}$ and there is a small deflection.

A similar procedure is followed for the 2nd resistance range. Thus

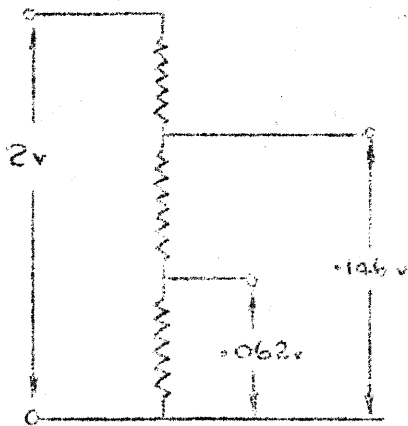
$$\frac{V_2}{(3,400 + 66)} = 42.15 \mu A \quad \text{from which } V_2 = \underline{0.146 \text{ volts.}}$$

Also
$$\frac{V_2}{(42,500 + 66)} = i = \underline{3.44 \mu A.} \quad \text{when } V_2 \text{ is substituted.}$$

From this result, $i_2 = \underline{2.52 \mu A.}$

Thus it is apparent that if voltages of 0.062 and 0.146 are applied to the above circuits, the galvanometer will deflect over very nearly its full range and maximum sensitivity will be obtained.

Knowing these voltages, it is a simple matter to calculate R_1 , R_2 and R_3 in the potential dividers.



Two equations may be written down which will yield the ratios of the resistances. These are:-

$$\frac{R_3}{R_1 + R_2 + R_3} = \frac{.062}{2} ; \quad \frac{R_2 + R_3}{R_1 + R_2 + R_3} = \frac{.146}{2}$$

R_3 was arbitrarily chosen to be 10Ω for every case and solution of the above equations gives:-

$$R_1 = 298.5 \Omega$$

$$R_2 = 13.5 \Omega$$

The method was adopted for each probe in turn and the following table summarises the results.

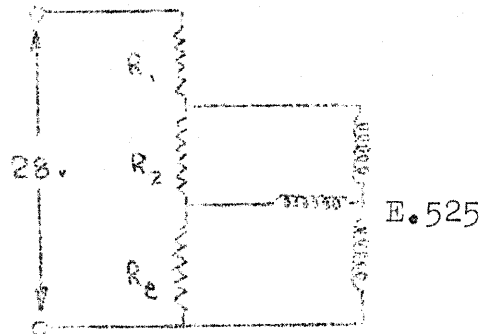
Probe No.	R_1	R_2	R_3
1	298.5	13.5	10
2	141.1	13.9	10
3	74.0	19.5	10

The table below shows the power dissipated in the No.1 probe thermistor throughout the temperature range; and also the variation of galvanometer current, i_2 .

Temp $^{\circ}\text{K}$.	Galvanometer i_2		Power Dissipated	
	Lower Alt.	Upper Alt.	Lower Alt.	Upper Alt.
225		2.52 μA		.503 μW
235		4.28 "		.846 "
245		6.50 "		1.295 "
255	4.52 μA	10.66 "	0.378 μW	2.10 "
265	6.63 "	15.6 "	0.550 "	3.06 "
275	9.55 "	22.5 "	0.793 "	4.40 "
285	13.15 "	31.0 "	1.085 "	6.05 "
295	17.75 "		1.455 "	
305	23.8 "		1.945 "	
315	31.0 "		2.49 "	

From this it is apparent that any self heating was negligible.

The circuit diagram for the wire wound elements was a standard one which is used with the E 525 ratiometer and this type of resistance coil. It is illustrated in the diagram below for a single element having a resistance R_e .



$$R_1 = 90 \Omega$$

$$R_2 = 100 \Omega$$

A wiring diagram of the complete instrumentation is shown in Figure 5.

2.5. Modifications to the Blower Tunnel.

When the tunnel was operated with iced water in the tank, it was noticed that the temperature of the air in the circuit was about 10°C which indicated that an excessive amount of heat transfer was taking place. As the tank was going to be filled with a mixture of acetone and dry ice which would have a temperature of about -70°C , it was readily apparent that many improvements were necessary. However a trial run was made first with a small quantity of dry ice which cooled the acetone to about -60°C , and all doubts were then immediately dispelled. The temperature of the air in the circuit would not fall below about -30°C , and the addition of more dry ice would not have improved this situation by more than a few degrees.

The primary requirement was the need for better insulation, and this was effected by increasing the asbestos covering all round and continuing it over the impeller. The asbestos thickness was increased to about $\frac{3}{8}$ " everywhere, and finally the entire circuit outside the box was covered with plaster of paris to provide added heat insulation and to seal any leaks which might have been missed.

The second modification which was required was the fitting of a thicker cork washer between the motor and the impeller in order to reduce the amount of heat which was transferred to

the working medium from the motor.

The third major modification involved a complete redesign of the window through which the probes were admitted to the working section. The original window was of the sliding type, and this required a large amount of sealing round the edges in order to keep the circuit airtight. More important still was the fact that because it was of the sliding type, a large area behind it had to be left relatively clear of insulation in order that it could be operated. This was definitely undesirable as it was permitting a heat transfer into the circuit which was centred just upstream of the probes which were being calibrated.

In order to overcome these difficulties, a rectangular platform was built up around the cut out in the working section, and it was made of brass which was tangential to the top of the circuit. Sidewalls were soldered onto this and they were raised about $\frac{3}{8}$ " above it. A rectangular cork washer was made which just rested on the platform, and then a $\frac{1}{4}$ " thick perspex window was dropped onto it. Two pieces of wood were sawn to length to fit across the ends of the window and protrude above the sidewalls of the frame. Then two lengths of bungee cord, which passed over them and round the working section, held the window tightly onto its cork seating. Further sealing around the edges was effected with plasticine.

Two windows were made and they had cut-outs in them to allow the supports of the probes to pass through them. The first window had a large cut out to accommodate those of probes no. 2, 3 and 4, while the second had only narrow slots for those of the Nos. 1 and 5 probes. The gaps around these slots were again sealed with plasticine.

The fourth modification concerned the thermometer which was used to measure the temperature of the air in the tunnel. This was of the low temperature pentane filled variety which was calibrated from $+30^{\circ}$ — — -120° C. It was too long to be completely accommodated inside the working section so it was necessary to drill a hole in the sidewall. This was positioned so that the thermometer bulb was located just in front of the mouth of the probes. As the thermometer was now external it was necessary to lag it very carefully, and for this purpose it was placed inside an oversize thermometer case which was packed with felt. This had a perspex window in the side which was $\frac{1}{4}$ " wide and 3" long and exposing the temperature range 0 — — 50° C. Then a still larger case was placed over this

and small chips of dry ice were packed in the annular space between them. In this way the thermometer was kept at very nearly the tunnel air temperature and so any measuring errors were reduced.

This arrangement was found to be not entirely satisfactory because of the difficulty in controlling the temperature of the thermometer external to the circuit. At the very low temperatures this was accomplished satisfactorily with the chips of ice, and similarly at room temperature without them, but at the intermediate values, errors of nearly 2°C . were detected. Thus it was found to be far more satisfactory to drill a hole in the elbow upstream of the probes, and insert the thermometer into the working section between the corner vanes. In this way the position of the thermometer could be adjusted until the bulb was exactly above the mouth of the probe which was being calibrated, and the length protruding outside the tunnel was about 1" - 2" depending on the probe inside. This was very satisfactory as all the pentane in the thermometer was within the circuit at the tunnel temperature, and in order to read the thermometer it was momentarily withdrawn a few inches and then replaced.

A tray with four stub legs was made for this tunnel out of Dexion angle which was bolted together, and a triangular foot was braised onto the bottom of each leg. Adjustable length legs were fitted to the stub ones, and these were for use when calibrating probes 'in situ' on the aircraft so that the tunnel could be raised to the appropriate height.

A tap was provided in the bottom of the tank so that the liquid therein could be drained off after use.

When all these modifications had been effected, some trial runs were carried out in order to perfect a technique for calibrating. $2\frac{1}{2}$ gallons of acetone were introduced into the tank and then 20 lb. of dry ice were broken up into conveniently sized lumps and lowered into the acetone. Initially the dry ice boiled off in a most violent manner, but as the temperature decreased the reaction became less rapid until eventually the temperature of the acetone reached that of the dry ice. Then the ice rested on the bottom of the tank and bubbled gently while maintaining the temperature constant at about -70°C . The tunnel was started and the air in the circuit eventually stabilised at -58°C . which was very satisfactory.

With every successive cycle of cooling and heating the tunnel the insulation became less efficient due to minute cracks and air leaks, and the minimum attainable temperature in the working section rose. At the end of the flight programme it had risen to -46°C .

A photograph of the tunnel is shown in Plate 14 with the thermometer protruding from the side wall.

3. Calibration of the instrumentation.

As a preliminary to the calibrations it was necessary to set up the galvanometers and ratiometers and check that the zeros were near to the edges of the paper. It was also necessary to verify that the temperature ranges to be covered utilised as much of the paper width as possible.

The setting up of the zeros on the galvanometers was performed by opening the recorders, and supplying power to them so that the light source was illuminated. The zero reading of the galvanometer could then be seen projected onto the paper at the end of the recorder, and if it was not in the required position relative to the edge of the paper, the galvanometer could be rotated until it was, after two clamping screws had been slackened off. In this way the three galvanometers in the Blue recorder were set up, and in order to avoid overcrowding of the traces, Nos. 1 and 2 were set with their zeros at the top of the trace, and No.3 with its zero at the bottom and moving in the opposite sense to the other two.

Unlike the galvanometers, the ratiometers did not have a zero setting and when no current was flowing, the mechanism assumed an arbitrary position. The correct orientation of these was set by fixing the two ends of the temperature range to be covered.

This was accomplished with a standard resistance box which was a time saving method of doing it because the extremes of the temperature range to be covered were converted into resistances. The resistance box was connected into the circuit in place of the probe, and the extreme values were then set up on it at the turn of a switch. The ratiometer was then rotated in the same way as the galvanometer in order to position the temperature range most favourably on the paper.

This procedure was also applied to the galvanometers because apart from setting up the zeros, it was necessary to check the other end of the temperature ranges. Once the zeros had been set, and provided that the values for the resistances in the potential dividers had been calculated correctly, the extreme values should automatically have taken up positions near to each edge of the trace. This was in fact the case with all three galvanometers, and there was no need for any further adjustment.

At this juncture it was possible to commence the calibrations, and initially these were carried out in two separate parts. The first part consisted of calibrating the probes alone, and this was done in the blower tunnel in the laboratory. The resistance was measured in a bridge circuit which was balanced with a standard resistance box, and a sensitive Scalamp galvanometer was used as in the previous calibrations of the No.1 probe for the wind tunnel tests (Part II § 5.1).

The procedure was to put $2\frac{1}{2}$ gallons of acetone in the tank, and then to introduce small lumps of solid CO_2 into it until the temperature of the mixture was reduced to about -65°C . At this stage the temperature of the air circulating in the tunnel was about -50°C . which was a convenient starting point.

The first probe was placed inside the working section and sealed round with plasticine, and the tunnel was then set into motion. The thermometer was positioned so that the bulb was just above the mouth of the probe, and was therefore indicating the exact temperature of the air entering it. The tunnel was left for at least 5 minutes for the temperature to stabilise, but this condition could be ascertained by balancing the bridge and noting that the galvanometer did not deflect from the null position over a period of time. When this was so the resistance and temperature were recorded and the next probe was fitted into the working section. This procedure was repeated for each probe in turn, and by the time that the 1st one was back in the working section again, the temperature had risen by 5° or 10° depending on external conditions. The temperature could not be controlled accurately but if it was required to stabilise at a particular value for any length of time, it was necessary to continually add solid CO_2 . Conversely if it was required to increase the temperature more rapidly than the normal rate, cans of hot water were partially immersed in the acetone, taking care to ensure that the water did not spill from the can into the tank. This technique was only necessary when a few spot check calibrations were required over a wide temperature range, but for a complete calibration the normal heating rate was quite sufficient. The temperature during a run did not vary at all, but it would change by $1^\circ - 2^\circ$ between the runs owing to the warm air entering the tunnel when the window was removed.

Thus the calibration was carried out by measuring each probe in turn as the temperature rose, until it reached about $+5^\circ\text{C}$. At this temperature the acetone was removed from the tank and cold tap water was substituted, and a measurement was taken at about $13^\circ - 15^\circ\text{C}$. depending on the temperature of the day.

Hot water was then added until the temperature rose to about + 45°C, and at this value the air in the tunnel would stabilise at about 40°C. The cyclic calibration procedure was then continued as before with the temperature falling between each run, until a complete set of points was obtained for all 5 probes over the range - 50°C. to + 40°C.

These were then plotted logarithmically against $1/T$ °K in the case of the thermistors, and this resulted in 3 straight lines. The two resistance coil elements were plotted on graphs of R against T.

The sensitivity of the bridge circuit was such that it was possible to detect on the Scalamp the current change produced by 1% change in the resistance of the thermistors at the lowest temperature. In general this was equivalent to about $\frac{1}{2}$ °C. However it was not possible to read the thermometer to a greater accuracy than + 0.1°C, as it was calibrated from + 30° — - 120°C. in 1° divisions on a 9 $\frac{1}{2}$ " stem length. The thermometer, which was pentane filled, had been previously calibrated against a standard one, and there was a small error which was allowed for in the results.

The second part of the calibrations was that of the instrumentation on the aircraft, and this was accomplished by replacing each probe in turn by the standard resistance box against which it had been calibrated. The temperature range to be covered was converted into a resistance range by means of the laboratory calibrations, and this was split into a suitable number of test points which gave approximately the same temperature interval between each. These test resistances were set up in turn on the box, and then a burst was taken on the recorders. In this way the aircraft instrumentation was calibrated quickly and accurately, covering both the high and low altitude ranges on probes No.1, 2 and 3 and the single range on Nos. 4 and 5. Additional points could be included at will, and the result was a set of very smooth curves with an extremely small amount of scatter.

Then the two sets of calibrations were combined to produce curves of temperature plotted against the distance of the trace from the datum position, and this was the form in which they were required for analysing the records.

While accepting the fact that by calibrating in this way, errors might be introduced in the intermediate steps, it was

nevertheless most worthwhile as the form of the final curve was correct, and there was very little scatter in the points used to plot it. Also this proved to be a great time-saver because the entire temperature range could be simulated for all 5 probes in less than an hour, whereas the actual cycle of calibrations in the blower tunnel took 8 or 9 hours.

After these preliminary calibrations were completed, the first 'in situ' one was carried out. Firstly the blower tunnel was positioned directly beneath the gun pack, and an extension lead was connected onto the No.3 probe so that it would reach back there from its nose position. In this way all 5 probes could be calibrated without moving the blower tunnel. The 4 probes on the gun pack were all connected up with an extra length of flex, so that they could be lowered from their position and placed in the tunnel without removing any wires.

The tank was filled with a mixture of acetone and dry ice, and the tunnel was started with the first probe in place and with the temperature at about -50°C . Subsequently it was found that this was not a sufficiently low temperature at which to start, and it was therefore necessary to reduce it still further. When the temperature in the working section had stabilised, as indicated by the thermometer placed just above the probe, a burst was taken on the recorders with the switch on the junction box in the appropriate position. At the higher temperatures, at which the ranges overlapped, two records were taken at the same temperature, one being on each range. The calibrations were continued in rotation until the temperature rose to about $+5^{\circ}\text{C}$., when the acetone was drained out of the tank and cold water was substituted. The upper temperature range was then calibrated in an identical manner to that which has been described previously.

The cycle was repeated two or three times on different days, and as a result a final set of calibration curves was obtained which displayed a remarkably small amount of scatter throughout the entire range.

However after the first few flights, it was found that there were some slight discrepancies in the temperatures measured by the 5 probes, and a spot calibration on the aircraft with the blower tunnel revealed that this was due to two causes. The first was a shift of the galvanometer zeros, and the second was a change in the voltage supplied by the 2v cell.

As a result, some ground tests were carried out in order to investigate the cause of the shifting of the galvanometer zeros.

The instruments themselves were quoted by the manufacturers to have a 'g' sensitivity of 0.1 mms/g, but recordings made with them upright and on their side revealed that the zeros shifted by 1.5 mms, 2.0 mm and 1.7 mms per 'g' for the Nos. 1, 2 and 3 galvanometers respectively. Initially the Blue recorder was fixed in the aircraft in an upright position, but the galvanometers were being excited by some stray vibration from the engine at full throttle, and this caused the trace to fluctuate at about 7 c.p.s. As a countermeasure this recorder was fitted on its side, and as this successfully damped out the excitation, it was left in this position from the second flight onwards.

Another cause of galvanometer zero shifting was the method by which the recorders were secured in the aircraft. This was by means of a strip of alloy across the top which was tightened down by wing nuts on two long studs which screwed into the structure. It was found that this distorted the case of the recorders, by an amount depending on the torque applied to the wing nuts, and this in turn caused the galvanometer zero reading to shift. The maximum change which was measured on a ground test was 1.6 mms, but the significant factor was that the position of the zero would change from one flight to another, as there was no conclusive means of ensuring that they were tightened to the same extent each time they were fitted. However this was not a serious defect as provided a record was taken with the 2v master switch off after the recorders were installed, the zero position could be measured and the appropriate shift could be added or subtracted as required.

The second source of error was the change with time of the 2v supply from the cell. Nominally the voltage was 2v but a new cell could yield as much as 2.1v. If the voltage should fall to 2.08v (i.e. approx. 1%), then in a typical case, the error in using the 2.1v calibration would be 0.4°C. Thus a close check was kept on the voltage and the voltage trace and the former was usually measured daily. In fact the current taken by the thermistors was so low that the voltage of the cell only fell as a result of chemical action. However a series of calibration curves were calculated from the measured one for a range of supply voltages between 2.0v and 2.1v.

Towards the conclusion of the test programme, a final calibration was carried out over the entire temperature range, and it was found from this that probes Nos. 1, 2, 3 and 5 had not shifted at all. However the No. 4 probe had diverged from its

original calibration by a constant amount of 5° throughout the range, and this was probably due to an unstable resistance in the circuit. It had been apparent from the records that there was a gradual shift, and in the absence of further evidence, the results were corrected on the assumption of a linear variation from one calibration to the other over the time interval between them. This variation, as it was constant throughout the range, had an extremely small effect on the ultimate recovery factor.

Figures 6 and 7 show the final calibration curves for the Nos. 1, 2 and 3 probes at high altitude, and the curves for the Nos. 4 and 5 probes over the entire range. Figure 6 has been based on galvanometer zero positions of 50 mms, 50 mms and 0 mms above the datum for Nos. 1, 2 and 3 probes respectively. This accounts for the apparent reduction in the utilised trace width, but in fact the zero positions for Nos. 1 and 2 probes were greater than 50 mms. which resulted in an improvement in this respect.

4. The Flight Programme.

The purpose of the flight trials was to obtain at as many altitudes as possible, as many values of the recovery factor as time permitted. For this reason flexibility was all important and a rigid programme was not adhered to. The flights were dependent on stable air conditions in order that any temperature gradients would be small, and therefore a suitable altitude was selected just prior to each sortie.

Flying through cloud was initially avoided whenever it was possible, but as the programme proceeded this limitation was relaxed slightly. However flying through rain, hail or snow was definitely undesirable, and this was avoided on every occasion except in an emergency. These were precautionary measures, which were taken because damage could be sustained by the thermistors from the entry of rain drops or hail stones into the probes at high speed. It was indeed fortunate that these precautions were taken, because at the end of the penultimate day's flying, it was necessary to return to the airfield through a shower of rain, and in so doing the No.2 probe was rendered unserviceable. A rain drop had apparently entered the probe and struck the two thermistors, and this caused a fracture in the platinum wire so making the elements open circuit.

The flight programme was split into 3 parts of which the most important one was that involving the stabilised levels. The techniques which were adopted, and the factors which were taken into consideration, have been described in detail below.

The flights have been numbered from 121 onwards for the purpose of consistency, because this was in keeping with the records maintained by the R.A.E. at Thurleigh.

4.1 Instrument Lag Tests.

These were tests carried out to investigate the lag of the various sensing elements, and to determine in consequence the length of time for which it was necessary to maintain a stabilised airspeed in order that the temperature might become steady. These sorties were made at 5,000' and 45,000' which represented the extremes of the altitude band which was covered, and this was to investigate the effect of altitude on the lag of the instruments.

They took the form of a full power acceleration in level flight starting from, and finishing at, a stabilised condition, and the speed ranges were 150 kts to 500 kts and 189 kts to $M = 0.94$ at 5,000' and 45,000' respectively. A 180° turn was then made, and again starting from a stabilised condition, a rapid deceleration was made with air brakes out to the lower speed. Recordings of the temperature were made throughout the range at the selected speeds which have been given below. The purpose of this was to measure the difference in indicated temperature, at any given Mach number, between the acceleration and deceleration, and to evaluate the lag from this.

In addition to the above tests, a further one was made to determine the time which was required for the lagging temperature to stabilise at the equilibrium condition. This was performed by allowing the temperature probes to stabilise at a low I.A.S. at about 40,000', and then diving so that the airspeed increased rapidly. This was followed by a lengthy stabilised level at a high Mach number, and recordings of the temperature were made every 15 secs. From these records it was possible to fix the length of time required for a stabilised level, in order to ensure that all the probes had attained a steady temperature.

The full results of the lag tests have been discussed later, but the outcome of them was that the three thermistors had a very small lag while the two resistance wire coils had rather more. In view of this, as described in § 4.2, it was decided that the stabilised levels could be kept very short and yet still allow all the probes to reach their equilibrium temperature.

4.2. Stabilised Levels.

This was the major part of the trials, and it consisted of a series of level runs at stabilised airspeeds at each altitude detailed in the table below. It was originally planned to cover two altitudes on each flight in order to accumulate more test data, but, as recorded later under Flight 125, it was found that there was insufficient endurance to carry this out in a conscientious manner. It was therefore decided to concentrate on one altitude per flight, and make the runs as accurate as possible. The pilots were briefed to stabilise the airspeed at or around the specified value, and then to maintain this condition for at least $\frac{1}{4}$ minute before making a 3 second recording

on the instrumentation. In practice this necessitated flying within a knot or two of the stabilised speed for considerably longer than $\frac{1}{2}$ minute while the pilot made the final trimming, so that this gave the slower elements in Probes No.4 and 5 ample time to settle down before the recording was made.

Consecutive runs were all made on reciprocal headings across the sun, so that the radiation did not fall directly upon the thermistors. It would have done so if any of the runs had been made into the sun because at this time of the year it was still low in the sky even at mid-day.

In order to control the airspace in which these tests were carried out, the heading was reversed after each run and the turn was made in the same direction each time. This reduced the possibility of encountering changes in the ambient temperature, which would affect the measured values if a lengthy level or set of levels was carried out on the same heading. However at the higher altitudes, the pilots reported that a great deal of time was spent in making this turn at the end of each run in view of the small amount of excess thrust. This was particularly the case at low Mach numbers, and so in order to conserve fuel, turns were made only at the end of every other level or at the pilot's discretion.

Two sets of levels were flown at 4,300' in the vicinity of a barrage balloon which was hoisted from R.A.F. Cardington. This balloon carried a copper-constantan thermocouple unit for measuring the air temperature, and one junction was exposed to the airstream while the other was sealed in a vacuum flask containing a mixture of ice and water. The thermocouples were made of 26 S.W.G. wire joined together in the usual way, and the electrical circuit was made through leads within the balloon cable. The circuit consisted of a standard potentiometer which was balanced by varying a resistance, and the temperature of the test couple was obtained from a calibration curve by inserting the value of the resistance required to balance the circuit. The accuracy to which the temperature could be measured was $\pm 0.1^{\circ}\text{C}$, and it was taken every 2 or 3 minutes over the period of these sorties. The variation of the temperature over this time is shown in Figure 11.

The aircraft was flown as close to this balloon as was considered practicable, and the sorties covered the full range of airspeeds. The procedure was the same as for all the other levels, and a burst was taken on the recorders as the aircraft passed the balloon. A wide 180° turn was then made, and the pilot lined up again on the balloon on a reciprocal heading.

This was made more difficult by the lack of horizon on the day of these flights, but the results which were obtained were most encouraging.

As the desired altitude parameter was pressure altitude, the pilot's altimeter and those in the A.O.P. were set to 1013.2 mb. During any set of levels the indicated altitude was maintained well within a tolerance of $\pm 50'$, and any small changes were taken into account in the analysis.

On most sorties, 11 stabilised speeds were flown at each altitude although this figure did vary either way according to the pilot's discretion. Usually the 1st six were made at an increasing airspeed, and the remainder at a decreasing airspeed at the intermediate values. On some occasions at the higher altitudes, the lowest speed was left until the end when the weight was reduced, and the aircraft was more easily controlled. This decision was left to the pilot's discretion.

In order to make an allowance for the variation in the galvanometer zeros from one flight to another, the procedure which was adopted was to take a burst on the recorders with the 2v master switch off, either on the climb or just prior to commencing the levels. This gave a record of the zero positions, and so any shift could be taken into account.

4.3. Transonic Flying.

Some attempts were made to measure the temperature of the air whilst flying at transonic speeds. In the Hunter this necessitated diving at a steep angle in order to attain a moderate Mach number, and therefore it was important to select suitable days when the tropopause was fairly low. This was because these dives had to be carried out in the stratosphere where in theory the temperature was constant, and therefore when the tropopause was low it was not necessary to climb so high, or conversely a dive could be maintained for a longer duration. It was not expected that probes No. 4 and 5 would respond sufficiently quickly in these conditions to give an accurate reading, although in fact on one occasion they had become stabilised when the recording was made.

These dives had to be carried out over the sea, and this necessitated flying to the Wash before any tests could be made. On the first occasion on which a transonic dive was included in the sortie, the pilot flew to 35,000' over the Wash and carried out a brief set of 6 stabilised levels at that altitude. He then

climbed to about 47,000' and commenced a dive in which he attempted to maintain a stabilised Mach number. As he approached 35,000', he took a long burst on the recorders and commenced to pull out at about 33,000'. In this way there was sufficient fuel for the return to base but insufficient for a further dive. On the second occasion on which a dive was included, the pilot climbed straight up to 47,000' over the Wash, and commenced a dive in which he attempted to attain and maintain a high stabilised Mach number. A recording was made in the same manner as above on passing through 35,000', and the pilot then pulled-out and climbed back to 45,000' before commencing a 2nd dive in which he tried to hold a Mach number of about unity. At the end of this he returned to 35,000', and carried out a shortened series of 5 stabilised levels on the return flight to Thurleigh.

On both these flights, especially the latter, a considerably larger air mass was used for the levels and dives, and the ambient temperature might have varied accordingly.

4.4. Table of Airspeeds and Altitudes.

The table contains the airspeeds which were specified for the stabilised levels at each altitude. Above 10,000', the maximum I.A.S. in each case corresponds to $M = 0.94$, while at 10,000' and below, the maximum value corresponds to 500 kts E.A.S. which was a limitation on the aircraft, which has been mentioned earlier. The specified speeds in each case represent equal increments in M^2 throughout the range. This was to facilitate graphical representation as the results were plotted in the form of straight lines of T against M^2 .

Altitude	Airspeed Range (I.A.S.)	Specified Airspeeds for Stabilised Levels (I.A.S.) kts.										
5,000'	150 kts- 510 kts.	150	260	340	405	460	510	485	435	370	305	210
10,000'	150 kts- 515 kts.	150	260	340	405	460	515	485	435	370	305	210
15,000'	150 kts- 490 kts.	150	255	330	385	445	490	465	415	360	290	205
20,000'	150 kts- 440 kts.	150	235	295	345	390	440	415	370	320	265	195
25,000'	150 kts- 395 kts.	150	215	275	320	360	395	380	340	295	245	185
30,000'	150 kts- 360 kts.	150	210	255	295	335	360	350	315	280	230	170
35,000'	145 kts- 325 kts.	145	192	231	266	297	325	315	284	252	210	167
40,000'	143 kts- 287 kts.	143	180	210	239	265	287	275	251	225	195	164
45,000'	139 kts- 257 kts.	139	168	192	216	238	257	247	226	204	180	153

4.5. Summary of Test Flights.

The running time of the trace recorders was just over 4 minutes, whilst that of the fully loaded camera was $3\frac{1}{2}$ minutes. There was therefore sufficient film available for 4 sets of levels without reloading, provided that the burst at each speed was kept to about 3 secs. This gave the interrupter time to complete one cycle and thus provide complete identification of the trace, and usually the camera was reloaded at the end of the third or fourth sortie, or at the end of the day's flying depending on the amount which had been exposed.

It was intended in this way to achieve a rapid turn-around between flights, and to fly 4 or more sorties per day, weather conditions and aircraft serviceability permitting. However these two factors combined contrived to prevent this ideal being attained except on one occasion, and the overall utilisation of the aircraft over the test period 6.3.58 - 25.4.58. was just over one sortie per flying day.

A total of 37 sorties were flown during this period, and of these 33 were directly connected with this work and 4 were miscellaneous. Of these 33 sorties, 26 were completely successful from the test point of view, 3 were only partly successful due to a failure of one or other of the probes or recorders and 4 were practically unremunerative owing to aircraft defects after take-off, or weather deterioration.

Each altitude was covered once initially, and then the range was condensed in order to concentrate on a smaller number and so obtain an indication of the consistency of the measurements on different flights. The altitudes which were then left out were 10,000', 20,000' and 45,000', and on an average, 4 flights were carried out at each of the others.

The following table contains a flight by flight record of the weather conditions and any relevant remarks, while at the end of this a further table summarises the number of flights made at each altitude.

Flight No.	Date	Detail.	T/O Time G.M.T.	Tropopause	Met forecast of Temperature
121	6.3.58.	Accelerated/Decelerated Levels at 45,000'	1630 hrs.	37,000'	-56°C.
122	10.3.58.	Acc/Dec. Levels and Stab ^d levels at 45,000'	1600 hrs.	27,000'	-48°C.
123	11.3.58.	Diving Lag test & Stab ^d Levels at 30,000'	1700 hrs.	25,000'	-54°C.
124	12.3.58.	Acc/Dec Levels & Stab ^d Levels at 5000'	1030 hrs.		-9°C.
125	12.3.58.	Stabilised Levels at 10,000'	1140 hrs.		-20°C.
126	12.3.58.	Stabilised Levels at 15,000'	1245 hrs.		-35°C.
127	13.3.58.	Stabilised Levels at 25,000'	1000 hrs.	35,000'	-34°/-52°
128	17.3.58.	Stabilised Levels at 35,000'	1640 hrs.	34,000'	-55°C.
129	20.3.58.	Air Test			
130	20.3.58.	Stabilised Levels at 20,000'	1640 hrs.		-35°C.
131	21.3.58.	Stabilised Levels at 20,000'	1200 hrs.		-36°C.
132	21.3.58.	Pilot Familiarisation			
133	27.3.58.	Stabilised Levels at 20,000'	1415 hrs.		-28°C.
134	27.3.58.	Training Flight			
135	1.4.58.	Stabilised Levels at 25,000'	1130 hrs.	34,000'	-43°C.
136	1.4.58.	Stabilised Levels at 30,000'	1500 hrs.	34,000'	-54°C.
137	1.4.58.	Stabilised Levels at 35,000'	1700 hrs.	34,000'	-54°C.
138	2.4.58.	Stabilised Levels at 5,000'	1030 hrs.	32,000'	-4°C.

Remarks

Not very successful as a test flight owing to lack of acceleration.
Invaluable for pilot familiarisation.

Far more satisfactory, but the acceleration was still poor from $M = 0.72$.

Diving lag tests not very successful because of the time required to stabilise the speed at the bottom.

A rapid acceleration and deceleration and everything very satisfactory.

On this flight it was found to be impracticable to cover more than 1 altitude/sortie.

Satisfactory.

Satisfactory.

Aileron stiffness made trimming more difficult than usual.

Modifications had been made to aileron & fuel system.

Due to the nose U/C warning light failing to go out, the pilot did not exceed 230 kts.

The bulb in the Blue recorder had failed, so records were only obtained from Probes 4 and 5.

Satisfactory.

Slight Turbulence.

Satisfactory.

Satisfactory.

Very Slight Turbulence.

Tables (Contd.)

Flight No.	Date	Detail	T/O Time G.M.T.	Tropopause	Met forecast of Temperature
139	2.4.58.	Levels at 15,000'	1140 hrs.	32,000'	-20°C.
140	2.4.58.	Levels at 40,000'	1445 hrs.	32,000'	-52°C.
141	10.4.58.	Levels at 35,000' & Transonic Dive.	1445 hrs.	34,000'	-54°/-57°
142	10.4.58.	Stab ^d Levels at 25,000'	1615 hrs.	34,000'	-33°/-54°
143	15.4.58.	Stab ^d Levels at 15,000'	0920 hrs.		-16°C.
144	15.4.58.	Stab ^d Levels at 15,000'	1315 hrs.		-16°C.
145	15.4.58.	Stab ^d Levels at 15,000'	1440 hrs.		-16°C.
146	16.4.58.	Stab ^d Levels at 25,000'	1315 hrs.	31,000'	-30°/-51°
147	16.4.58.	Stab ^d Levels at 35,000'	1515 hrs.		-51°/-56°
148	22.4.58.	Air Test			
149	22.4.58.	Stab ^d Levels at 40,000'	1545 hrs.	40,000'	-65°C.
150	23.4.58.	Stab ^d Levels at 4,300' past a balloon	0955 hrs.		4°C.
151	23.4.58.	Stab ^d Levels at 4,300' past a balloon	1100 hrs.		
152	23.4.58.	Stab ^d Levels at 30,000'	1350 hrs.	39,000'	-45°C.
153	23.4.58.	Stab ^d Levels at 30,000'	1505 hrs.	39,000'	-45°C.
154	24.4.58.	Stab ^d Levels at 40,000'	0850 hrs.	39,000'	-60°C.
155	24.4.58.	Stab ^d Levels at 40,000'	1015 hrs.	39,000'	-60°C.
156	25.4.58.	Stab ^d Levels at 15,000'	0845 hrs.		
157	25.4.58.	Levels at 35,000' and Transonic Dives (2)	1015 hrs.	35,000	-50°C.

Remarks

Satisfactory.

Satisfactory.

This was the 1st attempt at a transonic dive and everything went as planned. Only one dive was possible.

Owing to the nose U/C warning light failing to go out, only 4 levels were completed.
The weather was found to be unsuitable on arrival at the test altitude.

As for Flight 143 above.

Satisfactory.

At the end of this flight, the shield was removed from the No.5 Probe.

Towards the end of this sortie there was a total hydraulic failure in the aircraft.

Subsequent to the repair of the hydraulic system.

Satisfactory.

The pilot reported that it was difficult to line up on the balloon owing to the lack of horizon.

Very much better this time.

Satisfactory.

Satisfactory.

The met. office reported a temperature gradient of $6^{\circ}/1000'$ between 39/41,000'.

Satisfactory.

Satisfactory.

The two dives were made at the beginning of the sortie followed by the stabilised levels on the return.

Table of Flights at each Altitude.

Altitude								
5,000'	10,000'	15,000'	20,000'	25,000'	30,000'	35,000'	40,000'	45,000'
124	125	126	130	127	123	128	140	121
138		139	131	135	136	137	149	122
150		145	133	142	152	141	154	
151		156		146	153	147	155	
						157		

5. Analysis of the Results

5.1 Interpretation of the Records.

The film from the A.O.P. camera was read in a film-reader, and the quantities which were required were the airspeed and altitude from the wing boom pitot head, and the time in the cases of the accelerated and decelerated levels and the transonic dives.

The traces from the recorders were first annotated in conjunction with the film, and then they were measured up with a scale to an accuracy of ± 0.1 mm. The temperatures of the probes were determined by using a graticule on the calibration curves, and in this way all the flight records were interpreted and tabulated.

5.2 Evaluation of the Instrument Lag.

The I.A.S. from the film record was corrected for instrument error, scale altitude error and pressure error, and the altimeter reading was treated in the same manner. Then the Mach number was evaluated, and this was plotted against time for the periods of the acceleration and deceleration (see Figure 9).

The measured temperatures for each probe were plotted against M^2 , and this yielded a series of loops similar to hysteresis loops in an electrical inductance. The probes with the slowest response had the largest loop, and two sets of these have been shown in Figures 8 and 10. The abrupt change of slope in some of the curves when the air brakes were extended was due to the increased deceleration at that point. The ordinate, δ max, represented the maximum difference between the temperatures measured on the acceleration and the deceleration at any Mach number. Corresponding to this Mach no., the values of the acceleration and the deceleration were evaluated from the plotted history, and the sum total was converted into a rate of change of temperature. The lag of each probe was then obtained by dividing δ max by this rate of change of temperature.

A specimen example is shown below, and this was worked for the runs at 5,000' on Flight 124.

The Mach no. corresponding to δ max was $M = 0.63$, and at this speed the values of the acceleration and deceleration were 8.9 ft/sec^2 and 11.25 ft/sec^2 respectively.

At this speed and altitude, these values were equivalent to rates of change of temperature of $0.600^\circ/\text{sec}$. and $0.662^\circ/\text{sec}$. respectively, and the sum total is $1.262^\circ/\text{sec}$.

Considering No.1 probe, for example,

$$\delta_{\text{max}} = 0.25^\circ$$

and therefore the lag of this probe is $\frac{0.25^\circ}{1.262^\circ/\text{sec}} = \underline{0.2^\circ/\text{sec}}$

The dive, in which it was hoped to transform from one stabilised condition to another of higher temperature, was not altogether successful. This was because the time taken to stabilise the speed at the end of the dive was more than sufficient to allow the temperatures of all the probes to become steady. However this test did indicate that lengthy stabilised levels were not necessary, and that in the normal course of a gradual change from one airspeed to another, the probes would have ample time to reach their equilibrium temperature.

5.3 Evaluation of the Recovery Factor.

As shown in Part I, the measured air temperature may be expressed in an equation of the form:-

$$T_m = T_\infty \left(1 + r \cdot \frac{\gamma - 1}{2} M^2 \right). \quad (1)$$

where r is the recovery factor.

Thus in order to obtain T_∞ from a measured temperature, both r and M must be known.

However when r is unknown, it must be evaluated by measuring T_m at different Mach nos., and then plotting the results on a graph. This is exactly what was done, and the stabilised levels were the means by which an accurate set of measurements of T_m was obtained.

If a graph is plotted of T_m against M^2 , the result will be a straight line if it is assumed that r is independent of Mach number. The slope of this line is proportional to $r.T_\infty$, and T_∞ is the intercept of the line with the temperature axis corresponding to $M = 0$. Therefore both r and T_∞ may be evaluated by this process. Having once obtained a value of r for the probe at any particular altitude, T_∞ may then be determined from a single measurement of T_m at this altitude by substituting into eqn.(1).

5.3.1. The I.B.M. 650 Computer.

This computer was programmed to calculate the best straight line through a set of points, and by applying it to temperature measurements, it produced accurate values of r and T_∞ .

The information was supplied on input sheets (Figure 19), and this was transferred onto punch-cards by a double-checking system before being fed into the computer. The input data which was required was the indicated values of altitude, airspeed and measured temperature after each had been corrected for instrument error only.

In the analysing process, the scale altitude and pressure error corrections were applied to the airspeed and altitude, and a correction, based on the standard lapse rate of the atmosphere, was made to the measured temperature to allow for any errors in the altitude (Reference 3).

After the input data had been corrected in this manner, the computer evaluated (M^2) corresponding to each temperature, and then calculated the best straight line which could be drawn through a graph of T_m against M^2 . The best straight line is defined as that about which the points have the minimum moment of inertia, assuming that each has the same weight. However initially two lines were calculated by regressing first on the (M^2) axis and then on the temperature axis, and these imply that all the error is in the temperature and Mach number respectively.

Since the temperature was being measured by a number of different instruments and the measurement of airspeed and altitude was quite a standard process, it was assumed that any errors would be attributable to inaccuracies in the temperature measurement. Therefore the best straight line through the points would be that resulting from a regression on the speed parameter, and the slope of this was taken to be proportional to the recovery factor.

The difference between the two slopes obtained by regressing on each axis in turn has been regarded as a measure of the consistency of the points. In order to give some scale to this, values of the consistency have been obtained for a given scatter of $\pm 0.5^{\circ}\text{C}$. and $\pm 1.0^{\circ}\text{C}$ evenly distributed about a straight line. It has been shown in Reference 2 that quite large values of the consistency factor, Δr , can be tolerated before the effect on an aircraft or engine performance parameter is noticeable.

In addition to the above processes, the computer also evaluated the standard deviation, and all the results were printed onto an output sheet of which a specimen is shown in Figure 20.

The results from the I.B.M. computer for each flight have been plotted on graphs of $T \sim M^2$, which are included in the appropriate section, and a summary of them has been drawn up in tabular form in § 5.4.

In the case of those sorties in which transonic dives were carried out, two sets of results were computed. The first was based only on the measurements from the stabilised levels, and these results have been plotted in pencil (Flights 141 and 157). The second set included the transonic measurements with those from the levels, and these results have been plotted in red pencil on the same sheets. This was to investigate the effect of the transonic points on the subsonic recovery factors.

In the analysis of the transonic dives, an allowance was made for the lag in the A.S.I. and altimeter readings before including them on the input sheets. This was carried out in accordance with the results quoted in Reference 4.

Table of Results of Instrument Lag Tests.

Probe Altitude	1	2	3	4	5
5,000'	0.2°/°/sec. ‡	0.6°/°/sec. ‡	1.8°/°/sec.	6.0°/°/sec.	5.75°/°/sec.
45,000'	5.5°/°/sec.	-	3.13°/°/sec.	15.6°/°/sec.	15.6°/°/sec.

‡ The reason for this high value of the lag was that the vent holes to the inner stagnation chamber had become partially blocked, and the flow of air was seriously restricted.

‡ The reason for zero lag in this case was because the acceleration was so slow, that for all probes, especially those with thermistors, δ_{max} was very small and was indeterminate for Probe No.2.

6. Discussion of the Results

6.1 The Lag Tests

These showed the tremendous advantage which the thermistor had over the resistance wire coil in the measurement of a fluctuating air temperature. The modified thermistors in Probes No. 1 and 2 were particularly quick in response, and were very nearly capable of giving an instantaneous value of temperature in the most rapid acceleration of which the Hunter was capable. In general the lag of all the probes was greater at the higher altitude, and this was in accordance with expectations. It has been shown in Part I that the rate of convective heat transfer is proportional to the density, and therefore it would be less at 45,000' than at 5,000'.

The response of the No. 1 probe at 45,000' was seriously affected by a blocked set of vent holes, and the measured value of the lag was considerably larger than it would otherwise have been.

The lag of the No. 2 probe at 45,000' was indeterminate because of the very small difference of temperature between the acceleration and the deceleration. This was because the acceleration was so slow that the response of the probe was such that the two sets of points could not be separated.

The knowledge that probes No. 1, 2 and 3 had such a small lag was very useful in the analysis of the transonic dives. With a test of this nature in an aircraft of this type, it was inevitable that the Mach number could not be perfectly stabilised. In addition the dives were probably not in isothermal conditions even though they were made above the tropopause. Therefore the measured temperature was varying (Plates 16 and 17) but it was permissible to assume, in view of the lag test results, that the thermistors at least would be following this variation very closely. The results from Flights 141 and 157 bear this out, and indicate that the assumption was justified.

6.2. The No. 4 Probe

At the beginning of the test programme, this probe was yielding values of the ambient temperature which were the same as those from Probes 1, 2 and 3. However as the programme continued, it was apparent that the temperatures measured by this probe were becoming steadily less than those of Probes 1, 2 and 3, and this is illustrated in the results up to Flight 140.

Towards the conclusion of this programme a final calibration of all the probes was carried out, and this confirmed that the calibration of this probe had shifted by 5° over a period of about 5 weeks. Fortunately the shift was a constant one over the entire temperature range, and this implied that the recovery factor would only be in error because of the false ambient temperature. It is probable that this shift occurred because of the instability of one of the resistors in the junction box, although wire wound ones had been used because of their superior stability. In the absence of further evidence, the results of Flights 141 onwards were corrected on the assumption of a linear variation from one calibration to the other over the time interval between them.

6.3. The No. 5 Probe

The first point of interest which was immediately apparent from the early results, was that the temperatures which were being measured by the No. 5 probe were considerably lower than those measured by the others. The difference between the ambient temperature evaluated from the results of probes 1 - 4 and probe 5 did not remain constant but it was of the order of 4° .

At first the calibration of this instrument was suspected, and it was recalibrated very carefully in the blower tunnel. The final calibration curve for this probe was compiled from measurements made over a period of 2 - 3 weeks, and these showed very little scatter about the mean line. The temperature difference persisted and, in view of the careful calibration, the only possible deduction which could be made was that the measured temperature was in fact lower than that pertaining to the other probes.

This deduction was confirmed later on Flights 150 and 151, on which sorties the stabilised levels were flown in the vicinity

of a barrage balloon. The measured ambient temperature at the test altitude at the time of the runs (Figure 11) has been plotted onto the graphs of these two flights, and it was established beyond any doubt that this probe was undermeasuring the other four which agreed very closely with the observed temperature.

A theoretical investigation was then carried out into the behaviour of a probe such as this, and an account of it has been given in Part I. In this section radiation effects were taken into account, and a heat balance was drawn up in which the convective heating was equated to the radiative heat transfer. The result of this was that the equilibrium temperature of the surface was lower than the zero heat transfer value, and this was been illustrated in Figure 1 Part I. These results therefore showed a marked similarity to those obtained from the flight tests, although it should be stressed that the theoretical results were based on a surface emissivity of 1.0 and the assumption that the radiation was to a surface at absolute zero temperature. These assumptions are not grossly overexaggerated because for a steel probe of this nature, the surface emissivity would lie somewhere between 0.60 and 0.80. In addition there is a large difference of opinion about the temperature to which radiation takes place, but in view of the low absorbtivity of gases it would not be unreasonable to assume that a proportion of the heat is radiated to infinity.

After Flight 146, the shield which protected the probe from solar radiation was removed because of a fatigue failure in the air. The effect of this was immediately apparent and was illustrated best on Flights 150 and 151. On these flights it was noticed that the equilibrium temperature of the probe was considerably greater in the levels when the airspeed was being reduced than when it was being increased. This was due to solar radiation on the body of the thermometer which was preventing it from cooling from one stabilised condition to the next at a lower temperature. There was no noticeable effect of this tending to increase the equilibrium temperature when the airspeed was being increased, but there is no theoretical reason why it should not do this. However it is probable that the time during which the temperature remained stabilised was insufficient to allow the probe to reach its equilibrium condition.

The magnitude of this effect was a maximum at the lower Mach numbers, and this was in agreement with the theoretical considerations. In Part I it was shown that the convective heat transfer to the body was proportional to the forward speed, and therefore at these lower Mach numbers the radiation effects would be more pronounced.

On the graphs of Flights 150 and 151, a differentiation has been made between the temperatures measured by the probe when the airspeed was increasing and decreasing. In the latter case a modified symbol \ominus has been used, whilst for the former case the symbol remains unchanged.

It was not readily apparent from the results which of the runs were made with the sun shining directly onto the probe, but as no record was kept of this, nothing further can be deduced.

As a result of the above effect, the removal of the shield caused a reduction in the recovery factor of the probe, and a substantial increase in the consistency, Δr , and the standard deviation, σ . The increase in Δr and σ was due to the scatter of the measurements at low Mach numbers, and this in turn caused a reduction in r because it tended to raise the extrapolated ambient temperature.

The final, and very important, outcome of removing this shield was that the response time of the probe was considerably increased.

6.4. The Inhomogeneity of the Atmosphere.

The inhomogeneity of the atmosphere is an indeterminate quantity but in reference 2 it has been suggested that it is not likely to be better than $\pm 0.5^{\circ}\text{C}$.

It was for this reason that 180° turns were made the end of each stabilised level, for it was hoped, by conducting the tests in this manner, to fly in an isothermal air mass and hence obtain more accurate results.

On many sorties the atmosphere was particularly homogeneous, and this was apparent from the values of Δr in the results. However it did vary from day to day, and on some sorties Δr was quite appreciable and the inhomogeneity is easily discernible on the graphs.

As mentioned previously, in order to give some scale to the consistency, Δr , values have been calculated for a scatter of $\pm 0.5^{\circ}\text{C}$. and $\pm 1.0^{\circ}\text{C}$. evenly spaced about a straight line. These have been presented in graphical form

in reference 2 in which Δr has been plotted against the number of levels in the calibration for different values of r and the temperature error. The average number of levels in each calibration in these tests was 11, and making use of this graph, it was deduced that a value of Δr greater than 0.012 represented an even scatter of more than $\pm 1^\circ\text{C}$ for a probe having a unit recovery factor. From the table of results it may be seen that Δr exceeded this value in very few cases, and for probes 1 - 4, disregarding the transonic results, only $11\frac{1}{2}\%$ of all the levels resulted in values of Δr in this region. For the No. 5 probe which had a lower recovery factor, the permissible Δr for the same scatter was 0.014, and as a result of the increase in Δr with the shield removed, 24% of the levels were outside this limit.

In a similar manner it was deduced that values of Δr less than 0.003 and 0.004 represented an even scatter smaller than $\pm 0.5^\circ\text{C}$. for probes having recovery factors of 1.0 and 0.7 respectively. From an analysis of the results it was apparent that no less than 45% of all the levels which were flown yielded values of Δr smaller than this.

During Flights 150 and 151, the ambient air temperature was measured from a balloon at 4,300', and the temperature history has been plotted in Figure 11. From these results it may be seen that the temperature fluctuated within a band width of 1.1°F over a period of 100 minutes.

However on Flight 155, the homogeneity of the atmosphere had reached the other extreme as shown by Figure 13. Before this sortie was flown, the meteorological office forecast a temperature gradient of $6^\circ/1000'$ at 40,000', and the flight was intentionally planned for that altitude. The analysis of the results showed that the recovery factor of each probe had increased out of all proportions, and the consistency and standard deviation had reacted similarly. In view of this a recovery factor was assumed for each probe, and it was based on the recovery factor obtained at this altitude from other flights. Using this value, the ambient temperature was evaluated for each point in the set of levels, and these results have been plotted in Figure 13. Probes 1, 2 and 3 showed a very close agreement with one another, and probe No.4 displayed the same form but at a reduced temperature. This, as explained earlier, was due to an unfortunate shift in the calibration of the probe, but unfortunately it was constant over the temperature range and did not affect the recovery factor. Probe No.5 was still measuring a reduced temperature, but the variation of the ambient

value followed the same form as the others up to the maximum Mach number. Thereafter, due to the radiation effect described earlier, the measured temperature was higher than the equilibrium value and this was reflected in a corresponding increase in the effective ambient temperature. This is clearly illustrated in Figure 13.

The magnitude of the temperature fluctuation on this sortie was 5° , and it was unfortunate that the highest ambient value should correspond with the maximum speed, because this caused the very large increase in the recovery factors.

Flights 137 and 149 provided further good examples of the inhomogeneity of the atmosphere. It may be seen from the graphs of these sorties that the temperatures measured by all 5 probes have shifted in unison relative to a neighbouring set, and that this was not an erroneous measurement by any particular probe. Using an aircraft fitted with a number of different probes such as these, it would be possible to investigate the inhomogeneity of the atmosphere by flying over a wide area at a constant airspeed and taking a continuous recording of the air temperature throughout.

6.5. The Transonic Dives.

When the records of these dives were analysed, the A.O.P. film was studied in the film reader and the mean rate of descent was evaluated over a band of about 1500'. Then the lag in the altimeter and A.S.I. was estimated by making use of the results of some pitot-static lag tests on a Hunter F MK I (reference 4).

Having evaluated this, a frame was selected such that the altitude would be 35,000' when corrected for instrument error and static lag. The scale altitude and pressure errors were applied in the I.B.M. computer. The indicated airspeed was read off this frame and both this and the altimeter reading were taken from the instruments which were connected to the wing boom pitot head as this was the one for which the I.B.M. was programmed. The I.A.S. was corrected in a similar manner to the altitude for instrument error and pitot-static lag, and the temperature of each probe was measured from the trace records at a time corresponding to this frame.

These readings were then analysed on the I.B.M. computer in the usual manner, and the results have been plotted on the graphs for Flights 141 and 157. The black lines were the results

from the subsonic stabilised levels only, and these appeared to be quite normal. The points which were analysed from the transonic dives have been encircled in red, and the red lines are the results which include the transonic points.

From these results it was immediately apparent that the effect of including the transonic points was to increase the value of the recovery factor from that of the subsonic levels. Also in every instance, the new recovery factor was greater than unity.

As the probes were heating up from a lower temperature as the Mach number was increased in the dive, any temperature lag in the instruments would indicate that the true value was greater than the measured one. The effect of this, although the lag was quite small for probes 1, 2 and 3, was to increase the transonic recovery factor even further.

It has been shown in Part I that there is no fundamental reason why a ventilated pitot probe should not give satisfactory results in a supersonic airstream. In fact, theory predicts that any errors in the measurement of the recovery factor will have a progressively smaller effect on the temperature as the Mach number is increased.

In view of these test results, an investigation was made into the accuracy with which the Mach number had been measured. It was decided to use the readings on the A.O.P. film from the A.S.I. and altimeter which were connected up to the nose boom. This was because the nose boom has a zero pressure error in a supersonic airstream once the shock wave in front of the aircraft has passed over the static holes in the pitot head.

The first difference which was noticed was that between the two indicated altitudes. These differed by 1500' - 2000' depending on the dive Mach number, and this immediately revealed that the transonic points had been evaluated at an altitude in the region of 37,000' instead of 35,000' when pressure errors had been taken into account. This implied that the temperatures would be lower because, as shown on the trace records (Plates 16 and 17), they were all increasing throughout. This was probably due in part to an increase in the ambient temperature (although it was above the tropopause) and in part to an increase in the Mach number.

The Mach numbers were recalculated for a true pressure altitude of 35,000' assuming no pressure error, and these results have been plotted on Flights 141 and 157 and encircled in blue. These show a large increase in M^2 (which is a much smaller increase in M) and a subsonic Mach number actually became greater than $M = 1.0$. It would appear that the transonic pressure errors for the wing boom which were programmed into the I.B.M. computer might have been incorrect, and this would account in part for these differences. However the corrected points fell very closely onto the original subsonic lines, within the limits of experimental accuracy when it was considered that these dives were not made in the same air mass as the levels.

Therefore the conclusion to be drawn from these transonic dives is that the recovery factor is not increased, and from these limited tests which were carried out, it would appear to follow the subsonic value fairly closely. However it is important that the Mach number should be determined accurately because, at supersonic speeds, a small error in M is considerably magnified in M^2 .

Undoubtedly there is scope for further investigation into the supersonic regime; and in view of the restrictions and limitations on supersonic flying in this country, a ventilated pitot fitted with a rapid-response thermistor is probably the most suitable probe to use as an accelerated/decelerated technique can be adopted.

6.6. Variation of the Recovery Factor.

6.6.1. The No. 5 Probe.

From figure 18, it is apparent that the recovery factor of this probe varied quite considerably with altitude, and reached a peak value at about 35,000'. Above this altitude the recovery factor fell off sharply and it appeared to be levelling off at about 0.85. The value at low altitude was about 0.90 and the peak value was 1.06.

When the radiation shield was removed, the recovery factor was generally reduced, but it again showed this tendency to increase with altitude. However, insufficient calibrations were obtained to draw any conclusions about the form of this curve above 40,000'.

The results for this probe with the shield showed very similar characteristics to some curves obtained by Rolls Royce in reference 5, for an identical probe on a variety of aircraft. In particular it compared very favourably with some results for a probe such as this mounted on a Canberra, and in this installation, the recovery factor again started from 0.93 at sea level and reached a maximum value of 1.05 at 35,000' before falling rapidly.

A suggestion is now put forward in an attempt to explain this variation, and indicate the correct values of the recovery factor which should be used.

It was apparent from figure 18 that the recovery factor attained a value in excess of unity. This implied one of the following two statements:-

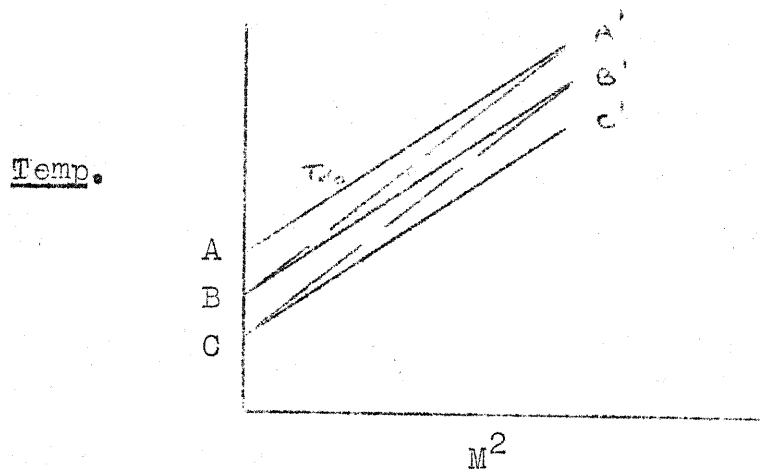
1. The probe was measuring a temperature in excess of the true total temperature of the airstream.
2. The probe was measuring a temperature between the true total and ambient values of the airstream, but the method of analysis was such that it was leading to false values of the recovery factor.

The first statement has no theoretical backing whatsoever, and this was disregarded as being an unlikely cause of the variation. It was therefore the second statement on which the investigation was concentrated in order to find a solution to this problem.

It has been shown earlier that for a surface temperature probe of this type, radiation can have an appreciable effect and can cause a reduction in the measured temperature owing to the heat transfer which is taking place.

It was also pointed out that this effect was noticed from the test results, and it was conclusively confirmed on Flights 150 and 151 when the true air temperature was measured.

A sketch is shown below which illustrates this effect, and which may be useful in the following reasoning.



The line AA^1 represents the zero heat transfer temperature for a surface temperature probe in laminar flow which theory predicts will have a recovery factor of 0.848. This is the temperature which will be measured at any M^2 if radiation does not take place. However when radiation does occur, the equilibrium temperature T_w will be less than T_w^0 and this will shift the characteristic line from AA^1 to BB^1 . The recovery factor of this line was shown in Part I to be greater than that of AA^1 by virtue of the reduced effective ambient temperature, and the variation of this was also investigated and found to be apparent but insignificant.

However the slope of this line could be appreciably increased by adopting one of the following two courses:-

1. The difference between T_w^0 and T_w becomes negligible at the higher M^2 but still remains significant at the lower values. The new line therefore joins the points BA^1 .
2. The difference between T_w^0 and T_w remains significant at the higher Mach numbers, but it increases at the lower values. The line now joins the points CB^1 .

The difference ($T_{w_0} - T_w$) is dependent only on the respective rates of radiative and convective heat transfer, and at a given altitude and Mach number the radiative heat transfer is constant. However the rate of convective heat transfer can be increased by introducing a turbulent boundary layer around the surface, and the two above statements can be rewritten in the following form:-

1. The boundary layer is laminar the lower Mach numbers but becomes turbulent at the higher values (BA^1).
2. The boundary layer is initially wholly turbulent (BB^1) but it then becomes laminar at the lower Mach numbers (CB^1).

The first statement will be disregarded temporarily, and the second one will be expanded to cover the variation of altitude. If it is assumed that at sea level the flow around the probe is turbulent, then as shown in Appendix I in Part I, turbulent flow will exist at any Reynolds number greater than, say, 2×10^5 based on the length of the probe.

At 36,000' it may be seen that the flow has become laminar at Mach numbers up to nearly 0.6, and therefore the heat transfer rate will be reduced and ($T_{w_0} - T_w$) will increase in this region. At higher Mach numbers than this, turbulent flow exists, and so the conditions of statement 2 are satisfied.

At 45,000' it is apparent that the flow is completely laminar and there will therefore be an even difference ($T_{w_0} - T_w$) throughout the Mach number range. This line has now been displaced from CB^1 to CC^1 and the recovery factor will be very nearly that for a laminar boundary layer - viz. 0.848.

The recovery factor at sea level owing to the wholly turbulent boundary layer will be 0.90, and as the altitude is increased the transition point will move aft along the body. The measuring element inside the probe has a finite length, and this will measure a mean skin temperature over it. Therefore as the transition point moves aft, there will be a smooth

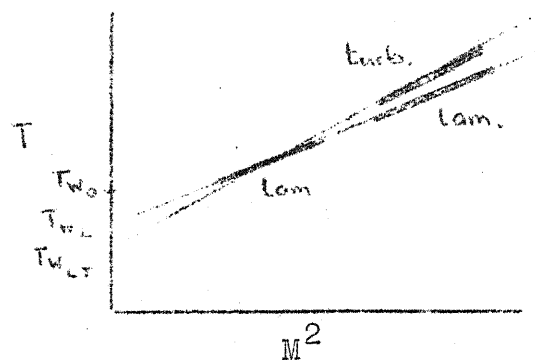
decrease in the temperature and this results in the smooth increase of the recovery factor.

Similarly above 36,000' the change will be smooth but more abrupt because so much of the probe already has laminar flow.

The validity of the above hypothesis was further enhanced when the results from the flight tests were analysed more fully.

The first point which was investigated was the variation of $(T_{W_0} - T_w)$ with altitude. It was not possible to obtain this accurately but T_{W_0} was assumed to lie somewhere within the scatter of the ambient temperatures of probes 1, 2 and 3. Working on this assumption it was immediately apparent that $(T_{W_0} - T_w)$ was a maximum on the flights at 35,000' (viz. Flights 128, 137, 141), and the results showed that the magnitude of this was about 7°C. Only flights 121 - 146 inclusive were analysed in this respect because the configuration of the probe was altered subsequently.

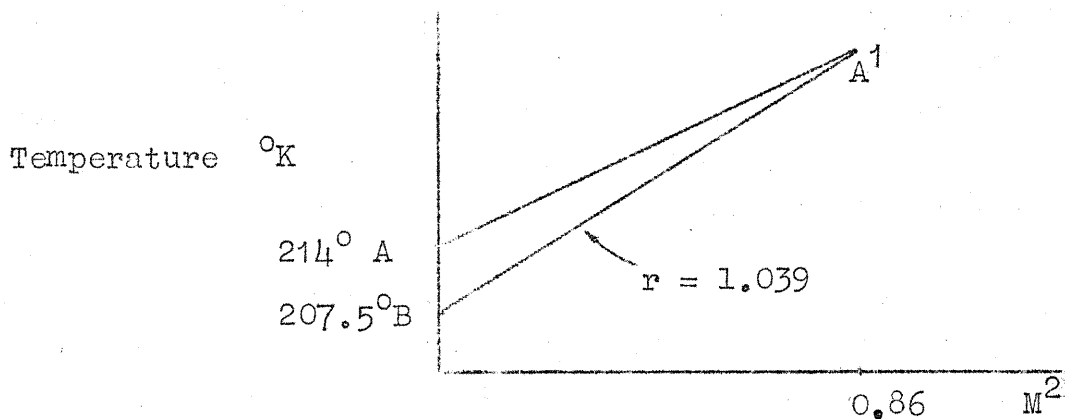
Above 36,000' the flow progressively became laminar, and it might be expected that $(T_{W_0} - T_w)$ should remain higher than at the lower altitudes. This was in fact the case although it does not attain the same value that it had at 35,000' by virtue of the following reason.



In the above sketch, the measured points have been split up into two short lengths of line which represent laminar flow

at the lower Mach numbers with a slope of 0.848, and both laminar and turbulent flow at the higher Mach numbers with slopes of 0.848 and 0.90 respectively. The recovery factor of these two cases is obtained in the usual way by constructing the best straight line through each set of points, and it is apparent from these that $(T_{w_0} - T_w)_{45000} < (T_{w_0} - T_w)_{36000}$ on account of the high minimum Mach number at which the aircraft could be flown.

In order to investigate the magnitude of the effect which this difference $(T_{w_0} - T_w)$ had on the recovery factor at 35,000', Flight 137 was analysed in a little more detail.



In the above sketch, the line BA^1 represents the No.5 probe which had a recovery factor of 1.039 and an extrapolated ambient temperature of 207.5°K. Point A is the zero heat transfer temperature which is based on the ambient values of Probes 1, 2 and 3. The true recovery factor is given by the slope of the line AA^1 which is

$$r = \frac{(207.5 \times \frac{\gamma-1}{2} \times 0.86 \times 1.039) - 214}{\frac{\gamma-1}{2} \times 0.86 \times 214} = 0.83.$$

Thus it is apparent that there is a substantial difference in the recovery factor. A similar result to this was obtained for the other two sorties at 35,000'.

The final aspect of this hypothesis which was investigated was to determine whether it was possible to detect a change of slope of adjacent points. On Flight 128 this was definitely discernible, but on Flight 137 the inhomogeneity of the atmosphere swamped any such changes. The variation was again apparent on Flight 141 but was not so pronounced because only 6 stabilised levels were flown. However on Flight 147, the results showed a perfect example of this gradual change of slope. A very smooth curve could have been drawn through these plotted points and a straight line clearly did not do justice to these measurements. Although on Flight 147 the radiation shield had been removed, and this must have had some effect on the measurements, there is no justification for supposing that the unshielded probe would not have displayed similar changes of slope. Therefore this example remains valid in the enhancement of the hypothesis.

The conclusion which may be drawn from this result is that an erroneous ambient temperature will be evaluated if the recovery factor is assumed to vary as shown in figure 18. The correct variation for this factor is from 0.90 at low altitude to 0.85 at high altitude, and in between it will assume some intermediate value.

However an ambient temperature evaluated on this assumption will still be in error because it will be based on an equilibrium temperature instead of a zero heat transfer value. The difference between this evaluated ambient temperature and the true value will depend on whether the equilibrium temperature has been measured through a turbulent or a laminar boundary layer. This in turn is dependent on both Mach number and altitude.

As a good approximation to the true ambient temperature, the following rule might be applied:-

For altitudes below 20,000', add about 4° to the measured equilibrium temperature and assume that $r = 0.90$.

For altitudes above 40,000', add about 2° to the equilibrium temperature and assume that $r = 0.85$.

For altitudes between 20,000' and 40,000', adopt an intermediate value.

Although this is rather laborious, it will be more accurate at all M than ignoring the difference ($T_{w0} - T_w$) and compensating for it by using a lower recovery factor.

6.6.2. Probes No. 1 - 4.

Figures 14 - 17 show the results of the flight tests plotted in the form of recovery factor against altitude. The first and very important conclusion which was drawn from these results was that the recovery factor lay very much closer to unity at all altitudes than for the No. 5 probe. In general all these probes had recovery factors which varied only within a band of ± 6 or 7% of unity, and in particular No.2 probe was within $\pm 4\frac{1}{2}\%$ at all altitudes up to 45,000'.

The second striking feature about these results was that at certain altitudes each probe appeared to have a recovery factor greater than unity. The altitude at which this occurred varied from probe to probe, but for the larger ones it was about 25,000' - 35,000' whilst for the No.1 probe which was a $\frac{1}{4}$ scale version of No.2, the critical altitude was a band around 15,000'.

In the case of the three larger probes, there did appear to be a systematic variation in the recovery factor which gradually increased to its peak value and then fell off rather rapidly. There was a larger amount of scatter in the results from the No.1 probe, but this again showed a trend which reached a peak value at about 15,000' and then fell off gradually.

These variations appear to be very similar to those found for the No.5 probe, but an explanation of this nature is very difficult to justify. The reason for this is that all these probes were of the ventilated pitot configuration, and each had double stagnation chambers in order to prevent radiation from the inner chamber. However the results showed that the recovery factor was in excess of unity at certain altitudes and this can only be obtained by virtue of one of the following reasons:

1. The probe was actually measuring a temperature greater than the true total temperature of the airstream,
2. The probe was measuring some fraction of the adiabatic temperature increase in the normal manner, but the method of evaluating the recovery factor gave rise to false results.

Once again it was this latter course which was pursued in order to determine whether there was any possibility of radiation, or a heat transfer similar to radiation, causing an error in the recovery factor.

It was noticed from the results for probe no. 1, and to a very much lesser extent no. 2, that the recovery factor at low altitude was greater than unity. It was fortunate that on two flights at these low altitudes (Flights 150 and 151), the true ambient air temperature was measured from a balloon, and the recovery factor of each individual point in the set of calibrations for Nos. 1 and 2 probes were evaluated from this. This gave a most interesting result because although in three of the cases the overall recovery factor of the levels was greater than unity, none of the individual values which were calculated exceeded this limit. Indeed at the higher Mach numbers, the recovery factor tended to unity and decreased appreciably at the lower values. The overall recovery factors for Flights 150 and 151 based on the measured ambient temperature were 1.008 and 1.000, instead of the computed values of 1.052 and 1.034 for Nos. 1 and 2 probes respectively. The computed values were of course obtained from the best straight line through the measured points. A graph showing the variation of the recovery factor of the No. 1 probe with Mach number is included as figure 12.

This effect seemed to indicate that once again heat transfer was definitely taking place at the lower Mach numbers, and it could be due to a combination of laminar flow giving rise to a lower rate of convective heat transfer, and a lower mass flow of air through the outer chamber. Both these factors would allow the effects of radiation to become more pronounced at the lower Mach numbers, although the overall effect would be much smaller than for the No. 5 probe.

If this was the reason for the No. 1 probe having recovery factors consistently greater than unity at the lower altitudes, it was to be expected that the larger probes would experience the same effect at a similar Reynolds number which implied a greater altitude. This was in fact the case with these results and it further supports this reasoning.

At sub or supercritical altitudes at which the flow was entirely turbulent or laminar respectively, this effect would not occur by virtue of the reasoning given in the previous section and the recovery factor would once again assume a value near unity.

Thus it would appear that for these probes the recovery factor does not vary in the manner suggested by the results but that it assumes some value in the neighbourhood of unity. This value would naturally depend on the geometry of the individual probe, but one parameter which would influence it would be the mass flow of air through the outer chamber. Of all the probes which were tested, No.2 had the largest inlet area to this chamber and the results indicated that this probe had the smallest variation of the recovery factor. No. 1 probe had the smallest inlet area and this was the least consistent of the four.

From the above reasoning it is suggested that the variation of the recovery factor is caused by the method of analysing the measured temperatures, which themselves are affected slightly at the lower Mach numbers by radiation despite the shielding. The overall effect is similar to that for the No. 5 probe but to a much smaller extent, and Reynolds number plays an important part in the determination of the critical altitude at which the apparent recovery factor is a maximum.

However in spite of these apparent variations, it should be remembered that the recovery factor is only a by product - albeit an important one - and that the end product is the ambient temperature. If the recovery factor of any probe is known to within $\pm 5\%$ of unity, the maximum possible error in the ambient temperature will be only $2\frac{1}{2}^{\circ}$, and this will occur at $M = 1.0$ at sea level. This represents a maximum percentage error of less than 1% and probes no. 1 - 4 were certainly capable of achieving this accuracy.

Conclusions.

The first conclusion to be drawn from the results of this work is that a thermistor in a ventilated pitot tube makes an ideal instrument for the measurement of outside air temperatures. It has an extremely rapid response to temperature fluctuations, and its large temperature coefficient of resistance is conducive to accurate measurements.

This implies that it is particularly suitable for use on high performance aircraft which are capable of rapid accelerations, and that a probe of this kind could be calibrated by an accelerated/decelerated level technique, thus saving a large amount of flying time.

The recovery factor of such a probe is very close to unity, and the results showed that this was so for a variety of shapes and sizes. In particular the small No. 1 probe gave very good results, and even if they were not quite so consistent as those of its larger counterparts, the error in an ambient temperature evaluated from them would only be about 1%. This implies that probes such as this one could be used with confidence in measuring temperatures in an air intake or on the outside of an aircraft, and that its larger and more cumbersome counterparts could be dispensed with.

From the limited tests carried out in this programme it appeared that ventilated pitot probes behaved quite normally in a transonic airstream, and there is no reason to suppose that they would do otherwise at supersonic speeds. However it is imperative that the Mach number should be evaluated accurately as the results are plotted against M^2 .

The most important conclusion drawn from this work concerns the variation of the recovery factor with altitude. This was most pronounced for the surface temperature thermometer although the ventilated pitot probes all showed similar but lesser variations. A suggestion has been put forward that this is entirely due to the method of analysing the results, and that the calculated values are misleading. The apparent variation arises from the combined effects of radiation and Reynolds number, and it occurs at altitudes at which the boundary layer changes from laminar at the lower end of the Mach number to turbulent at the higher end.

This suggestion is fully supported by theoretical considerations, and it is further backed up by many of the flight test results.

When this large apparent variation of the recovery factor is disregarded, there still remains a smaller one which is fully justified from the theoretical aspect and is again borne out by the flight results. This concerns the surface temperature thermometer, and it is again a Reynolds number effect. At the lower altitudes where the boundary layer on the probe is likely to be turbulent throughout the Mach number range, the recovery factor should be about 0.90 as compared with 0.85 at high altitudes where the boundary layer is entirely laminar. At intermediate altitudes the recovery factor will lie somewhere between these two.

Finally if the recovery factor of a ventilated pitot probe lies within $\pm 5\%$ of unity, the maximum possible error in the calculation of the ambient temperature from a measured value will be only 1%, and each of the four tested probes was quite capable of achieving this accuracy.

List of References.

<u>No.</u>	<u>No.</u>	<u>Author</u>	<u>Title</u>	<u>Date</u>
1	Rolls Royce Technical Report PB/JRF I/AM.		Flight Calibration of a ventilated pitot outside air thermometer.	Oct. 1956.
2	Rolls Royce Technical Report PB/JRF I/AD.		The calibration of an O.A.T. head by flight test levels.	Sept. 1956.
3	Rolls Royce Technical Report PB/JRF I/MS.		Calibration of an O.A.T. by flying at a constant pressure altitude over a range of airspeeds.	Nov. 1957.
4	R.A.E. T.N. Aero 2354.	D.R.Andrews J.E.Ne thaway	Pressure Errors of a nose and a wing boom airspeed system on a swept wing aircraft.	Jan. 1955.
5	Rolls Royce Technical Report Gtx/IDS I/FEB		The measurement of free air temperature from aircraft.	Feb. 1955.

FLIGHT No.	ALTITUDE FT.	No. 1 PROBE				No. 2 PROBE				No. 3 PROBE				No. 4 PROBE				No. 5 PROBE			
		r	Δr	T _∞ °C	σ	r	Δr	T _∞ °C	σ	r	Δr	T _∞ °C	σ	r	Δr	T _∞ °C	σ	r	Δr	T _∞ °C	σ
121	45,000	ACCELERATED/DECELERATED LEVELS																			
122	45,000	.91049	.00123	226.015	.17607	.92020	.00047	228.48	.14142	.96988	.00310	225.689	.27386	.86922	.00153	227.188	.21679	.86287	.00408	224.558	.30496
123	30,000	.91357	.00337	223.326	.53198	.98317	.00286	222.488	.51284	.97391	.00263	221.686	.48580	.96463	.00439	221.081	.62209	.100766	.00432	216.415	.61644
124	5,000	1.0493	.00197	263.103	.49900	.99641	.00106	264.474	.36469	.94628	.00119	264.612	.37014	.97182	.00179	262.758	.46260	.91435	.00525	258.914	.75299
125	10,000	1.05841	.00432	253.92	.82098	.95900	.00247	255.943	.60083	.96185	.00165	255.229	.48374	.99169	.00371	253.215	.74364	.89851	.00218	251.376	.53666
126	15,000	1.05876	.00226	245.918	.55946	.96493	.00070	247.895	.29833	.98831	.00159	246.674	.44833	.97776	.00256	245.471	.57706	.92652	.00133	243.138	.40375
127	25,000	1.00761	.00937	230.862	.96177	.98687	.00299	232.685	.53572	1.00304	.00567	231.511	.74297	.97421	.00228	230.522	.45717	.93802	.00196	227.368	.41352
128	35,000	.97785	.00775	211.651	.71764	1.04344	.00489	210.224	.57793	.93649	.00546	211.685	.58737	1.04183	.00276	208.445	.43589	1.06282	.00972	203.845	.78867
129	AIR TEST																				
130	20,000																				
131	20,000																				
132	FAMILN.																				
133	20,000	1.04169	.00144	243.894	.41473	.97223	.00085	246.799	.31780	.98318	.00124	245.665	.37148	.95197	.00152	244.213	.41110	.92756	.00246	241.355	.51186
134	TRAINING																				
135	25,000	.99793	.01312	232.452	1.14673	.97908	.00714	234.398	.84794	.95499	.00909	233.463	.95499	.98254	.00699	231.500	.83247	.93457	.00727	229.073	.82096
136	30,000	.96794	.00242	222.537	.47011	.99177	.00156	223.479	.38341	.98650	.00191	222.894	.43012	1.01884	.00109	220.362	.31305	.98046	.00233	217.643	.45935
137	35,000	.99116	.01156	213.846	.97673	1.01388	.01123	214.034	.97108	.99626	.01603	213.616	1.15715	1.04525	.01408	210.701	1.08766	1.03875	.01722	207.453	1.18364
138	5,000	1.07256	.00263	268.341	.53009	1.01723	.00173	268.879	.41952	.95253	.00116	269.516	.31937	.99150	.00190	265.097	.42661	.92070	.00239	263.003	.46904
139	15,000	1.07993	.00149	248.982	.49295	.95866	.00100	251.991	.37815	.97753	.00134	251.624	.44497	.98240	.00337	247.816	.68264	.91885	.00296	248.771	.62290
140	40,000	.88518	.00209	225.547	.38987	.97200	.00104	225.147	.28284	.94836	.00135	224.916	.32558	.94198	.00028	222.368	.16125	.89866	.00114	220.826	.28810
141A	35,000	.99908	.00863	213.410	.85732	1.00485	.01683	214.915	1.21614	.98755	.01702	214.523	1.21491	1.03689	.00446	213.126	.60992	.97089	.01330	208.711	1.02713
141B	35,000	1.05995	.00746	212.325	1.07564	1.06241	.01160	213.883	1.34944	1.07438	.01504	212.959	1.53851	1.03789	.00211	213.108	.57271	1.06576	.01419	207.045	1.06576
142	25,000																				
143	15,000																				
144	15,000																				
145	15,000	1.09841	.00338	249.294	.71694	.97875	.00225	252.348	.56125	.95939	.00301	252.936	.64730	.96969	.00394	252.221	.73959	.86396	.04475	249.863	2.44366
146	25,000	1.04851	.00729	232.152	.88318	1.01897	.00240	234.102	.50794	1.04580	.00519	232.982	.74431	.98119	.00184	234.711	.42308	.88317	.00562	230.740	.71063
147	35,000	.97097	.00410	213.949	.44497	1.01612	.00414	213.862	.46797	.90157	.00812	215.971	.63246	.93308	.00320	216.208	.40866	.77994	.02418	213.470	1.02421

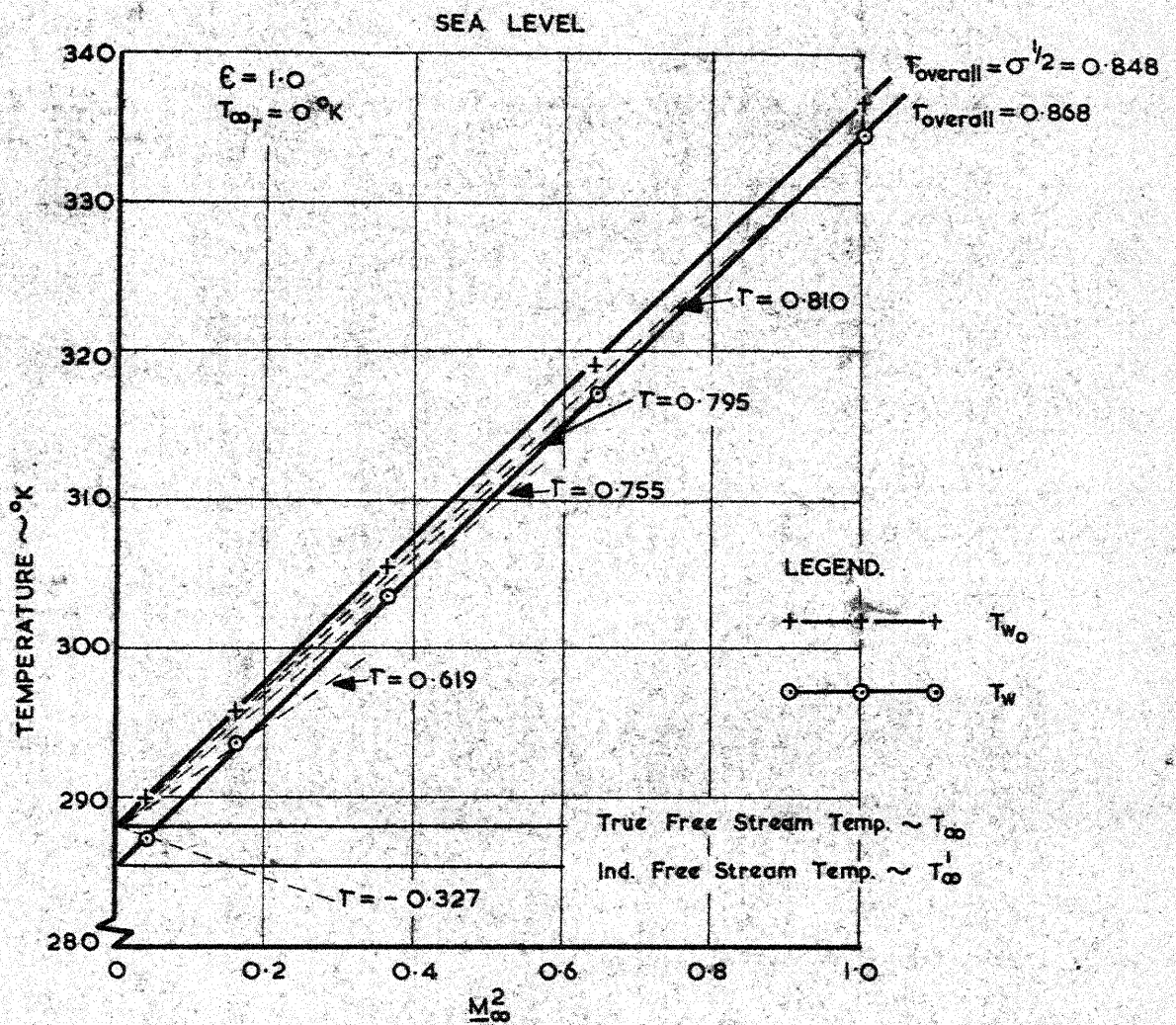


FIG. 1. GRAPH SHOWING THE EFFECT WHICH THE VARIATION OF RECOVERY FACTOR HAS ON THE FREE STREAM TEMPERATURE AND OVERALL RECOVERY FACTOR.

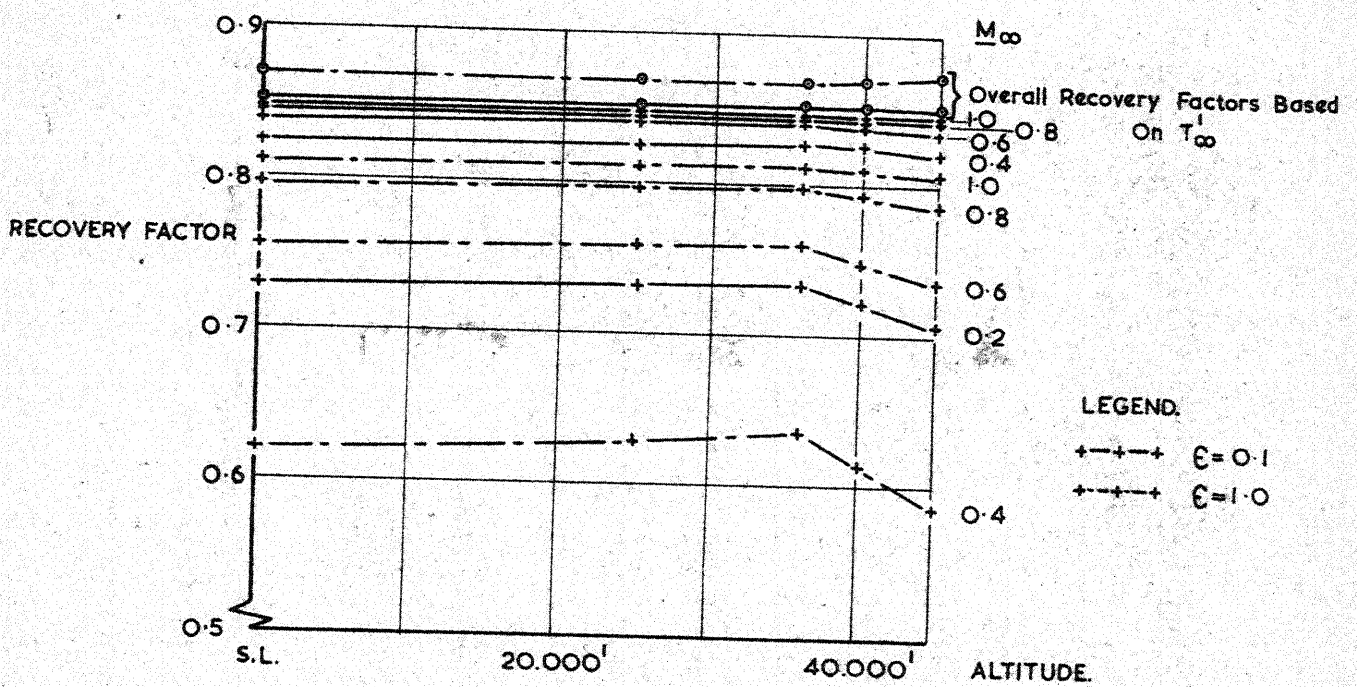
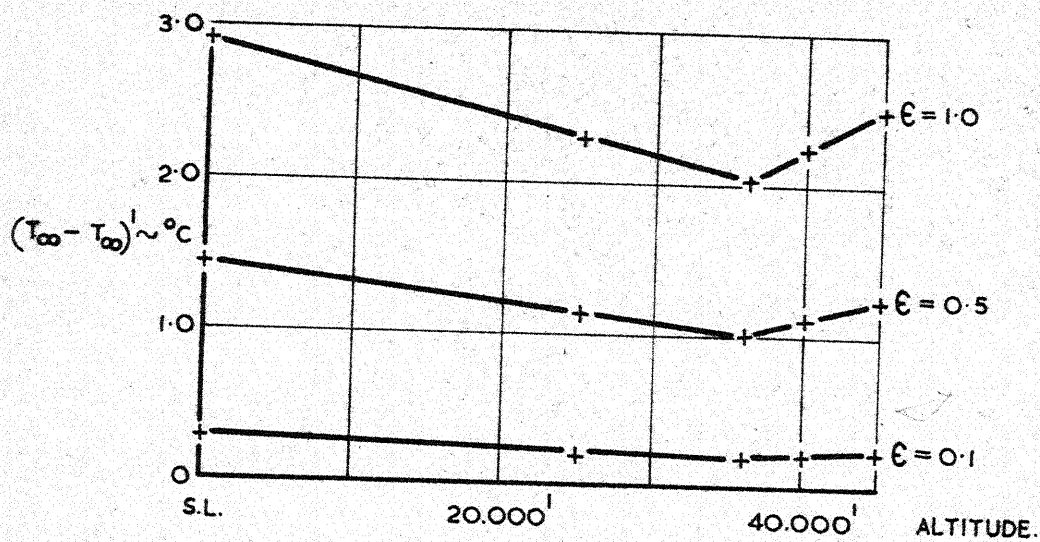


FIG. 2. GRAPHS SHOWING THE EFFECT OF SURFACE EMISSIVITY ON $(T_{\infty} - T_{\infty})^1$ AND RECOVERY FACTOR.

SECTIONAL VIEWS OF No. 1 PROBE

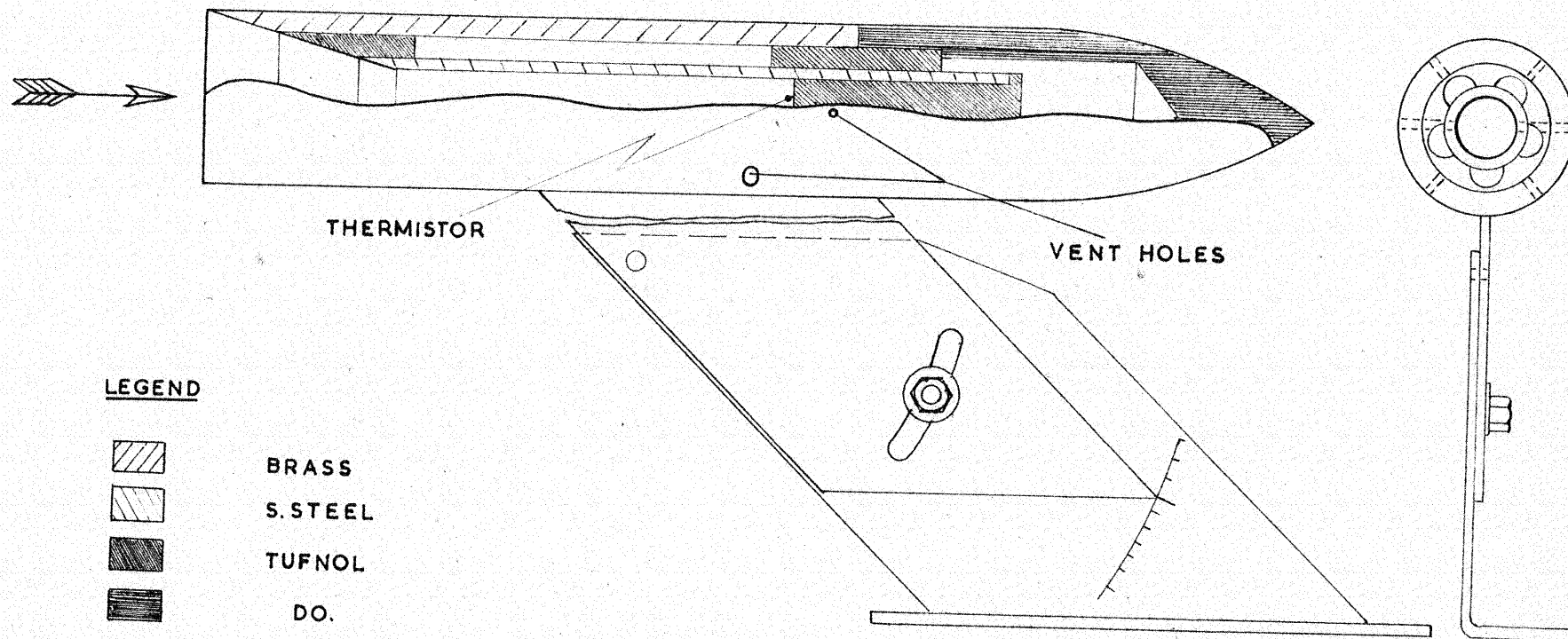
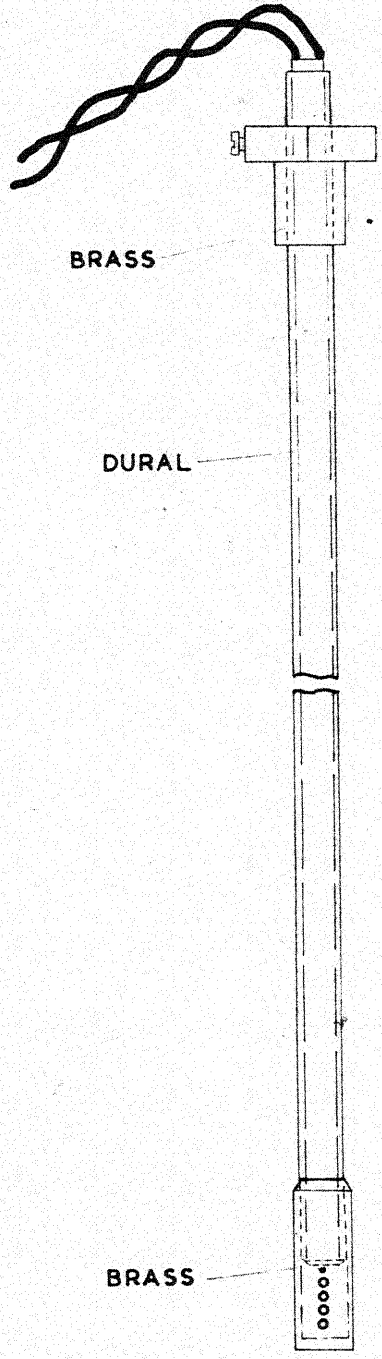


FIG 1

THE THERMISTOR THERMOMETER



SCALE 1:1

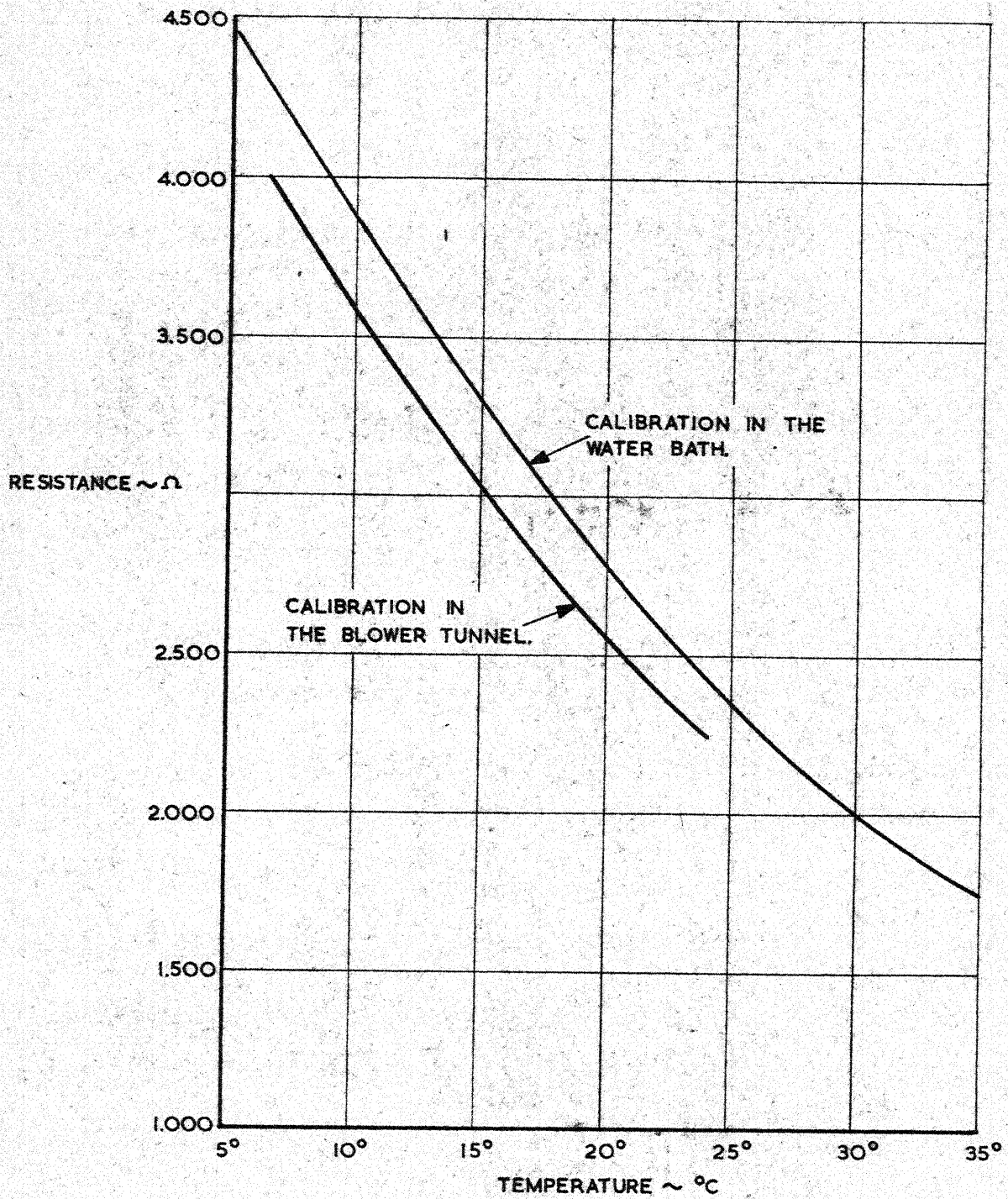


FIG. 4. CALIBRATION OF THE PROTOTYPE PROBE.
 COMPARISON BETWEEN THE WATER BATH AND THE BLOWER TUNNEL.

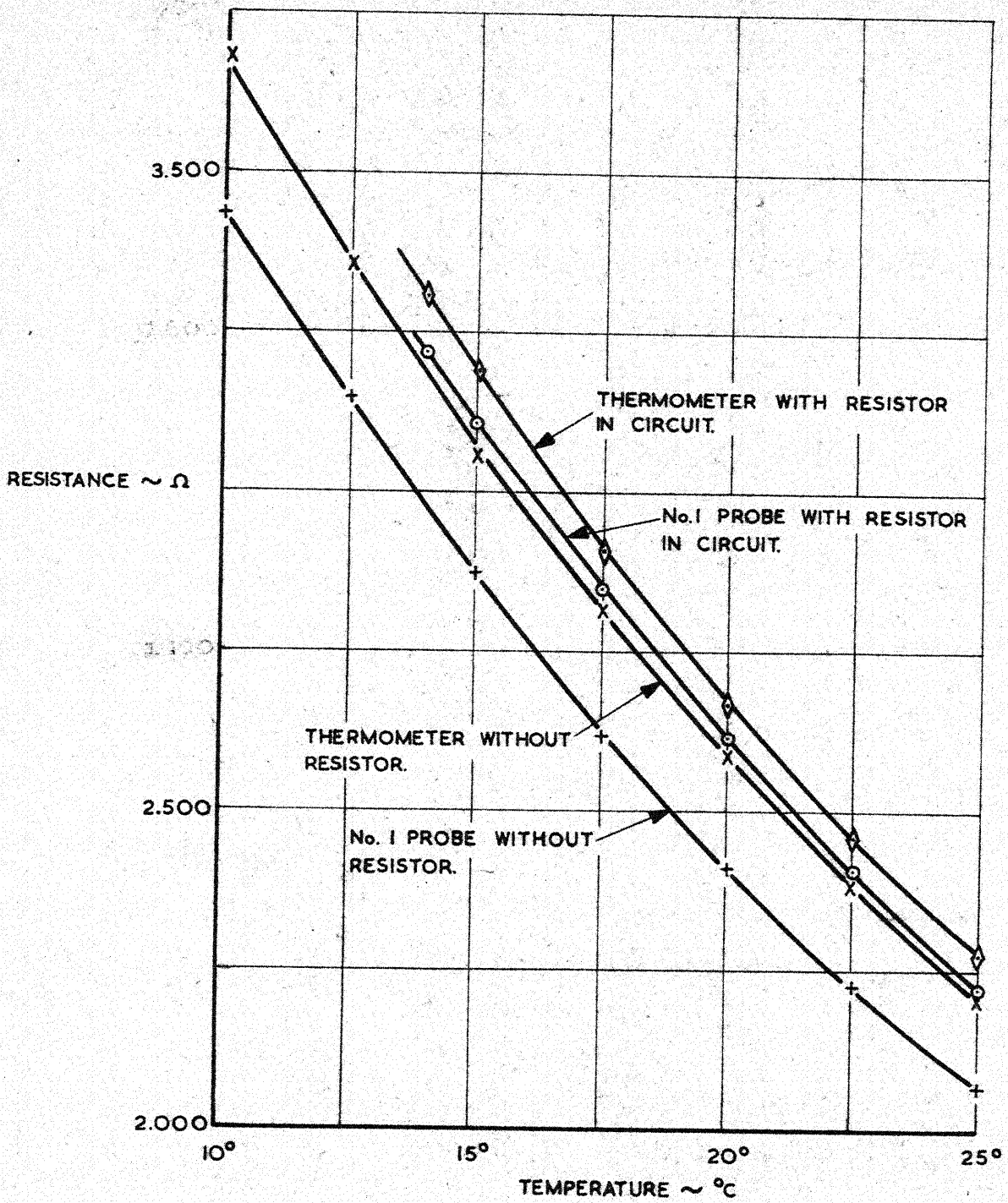


FIG. 5. CALIBRATIONS OF THE No. 1 PROBE AND THERMISTOR THERMOMETER.

CALIBRATIONS IN THE BLOWER TUNNEL WITH AND WITHOUT THE 10 k Ω RESISTOR IN CIRCUIT.

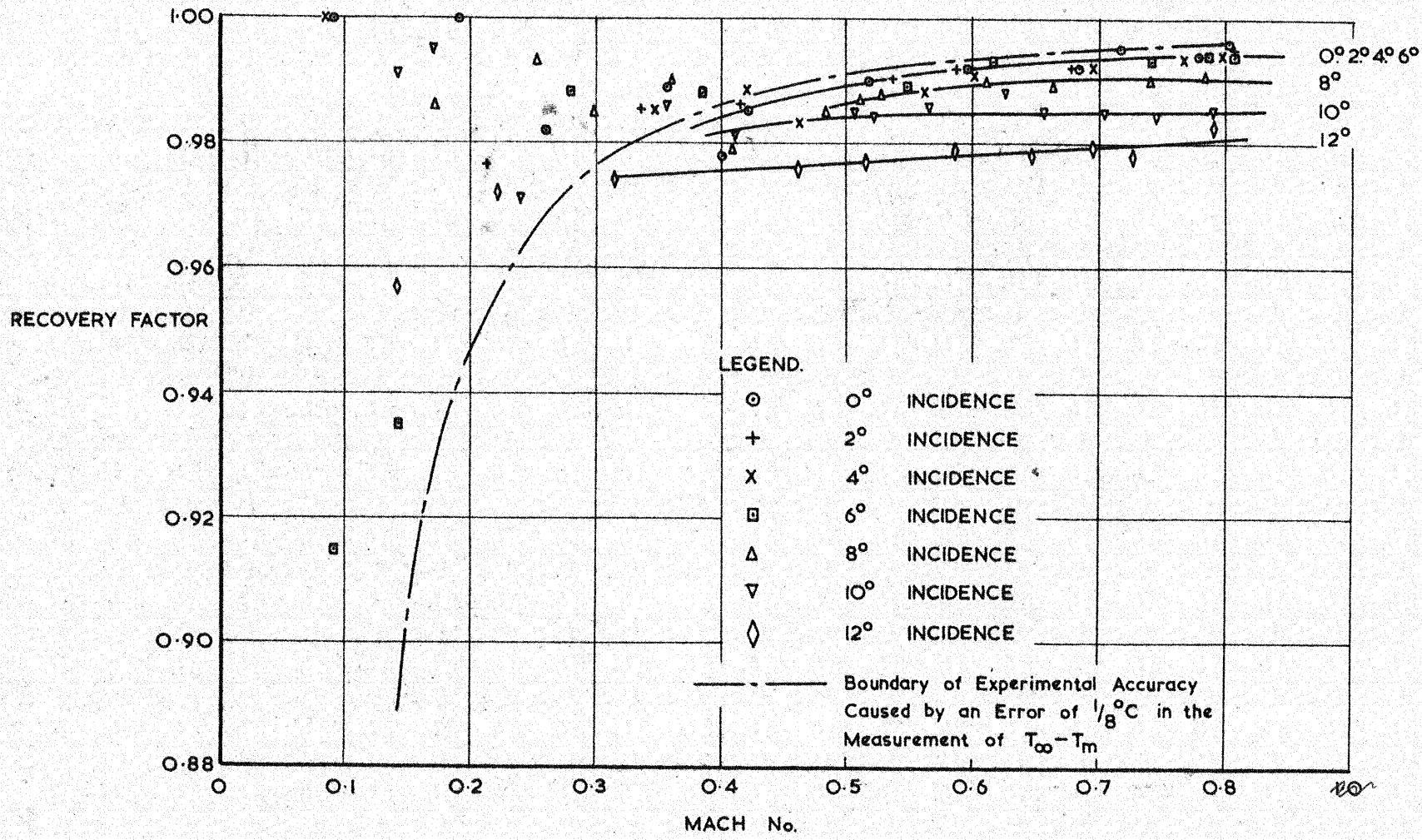


FIG. 6. RESULTS OF THE WIND TUNNEL TESTS. RECOVERY FACTOR OF THE No.1 PROBE.

PLATE 1

THE No.1 & PROTOTYPE PROBES

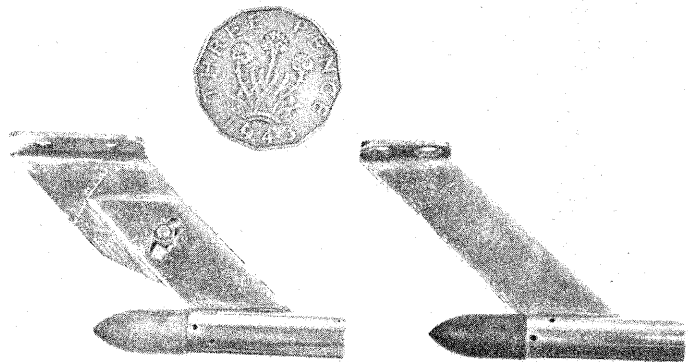
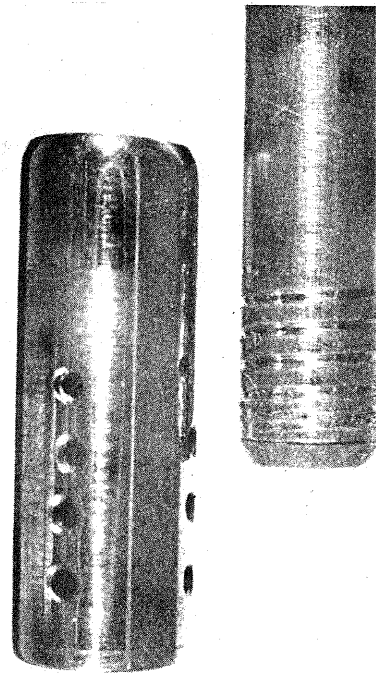


PLATE 2

THE THERMISTOR THERMOMETER



MAGNIFIED 5 TIMES

PLATE 3

THE WIND TUNNEL

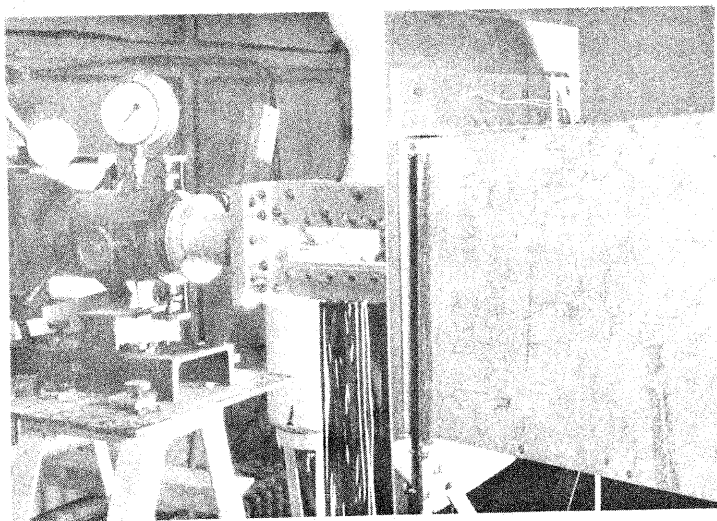
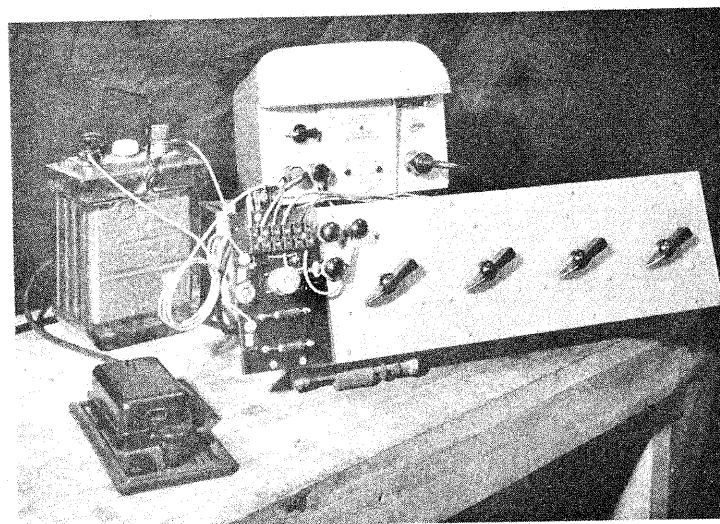


PLATE 4

THE BRIDGE CIRCUIT



SECTIONAL VIEWS OF Nos. 1 & 2 PROBES.

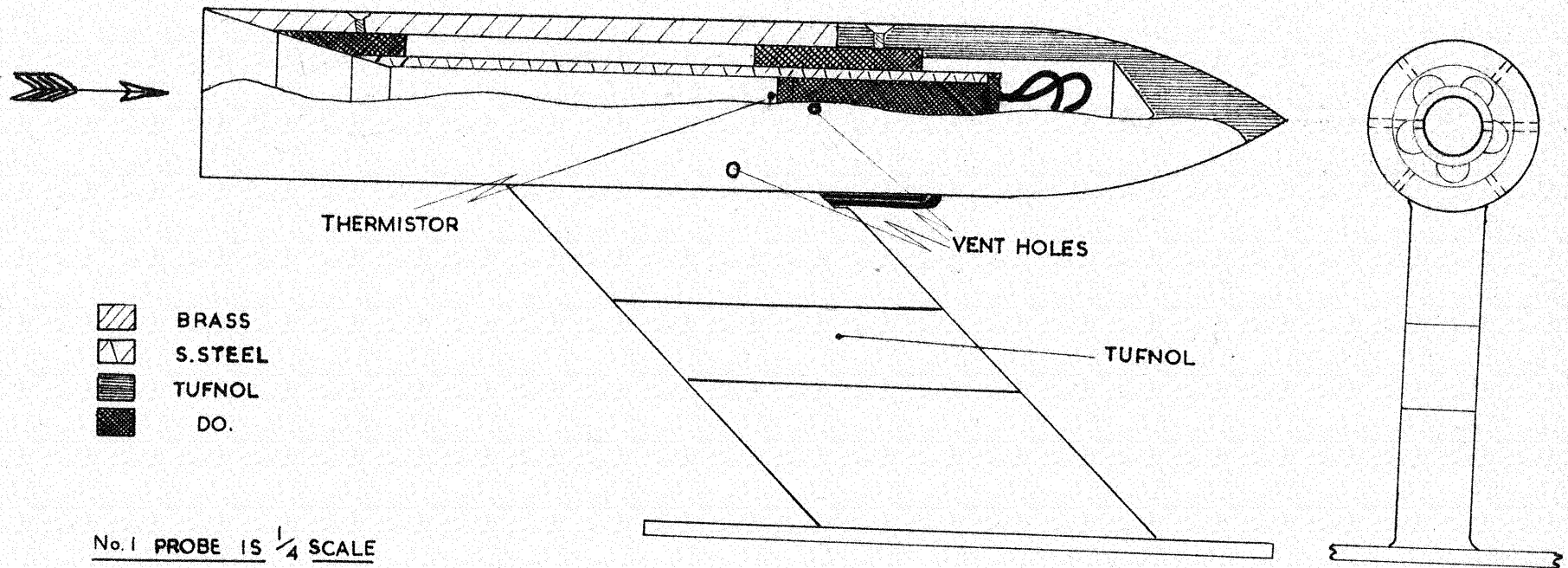


FIG 1

SECTIONAL VIEWS OF N.3 PROBE

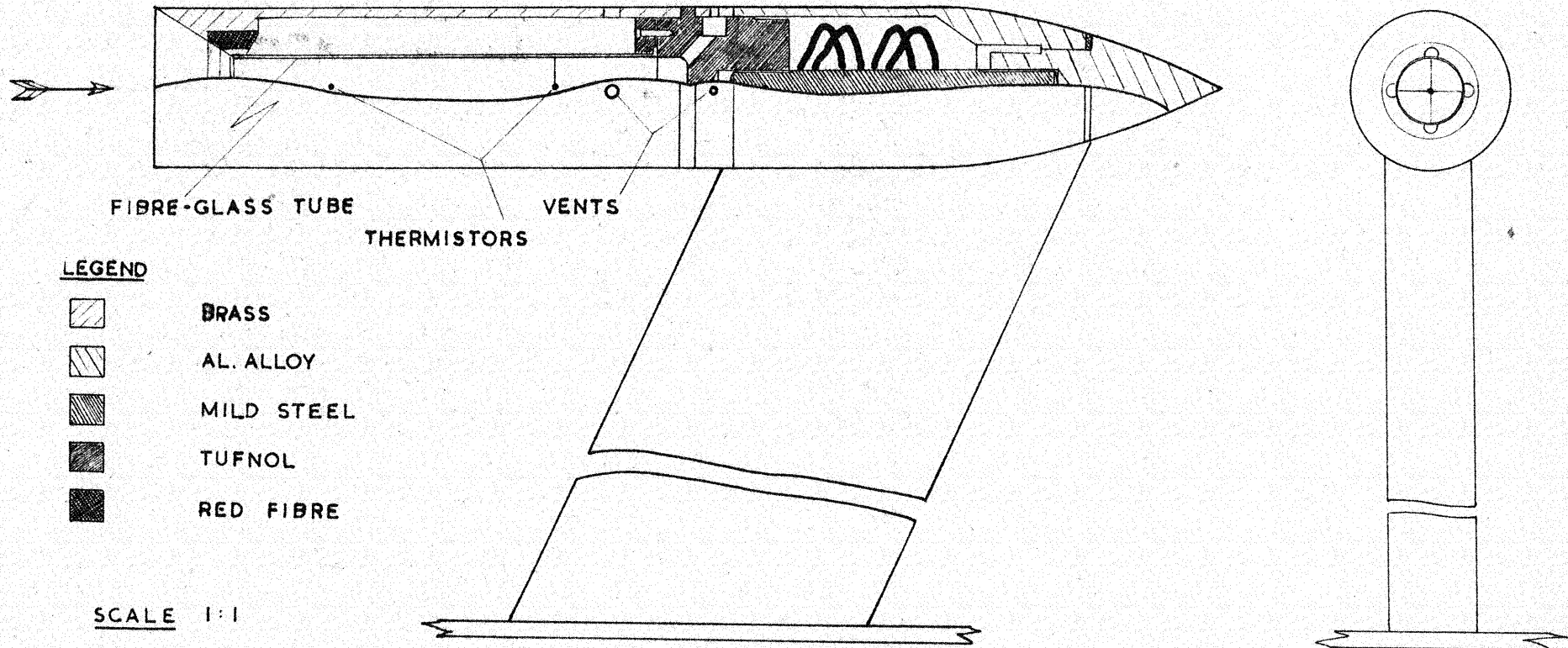


FIG 2

SECTIONAL VIEWS OF No. 4 PROBE

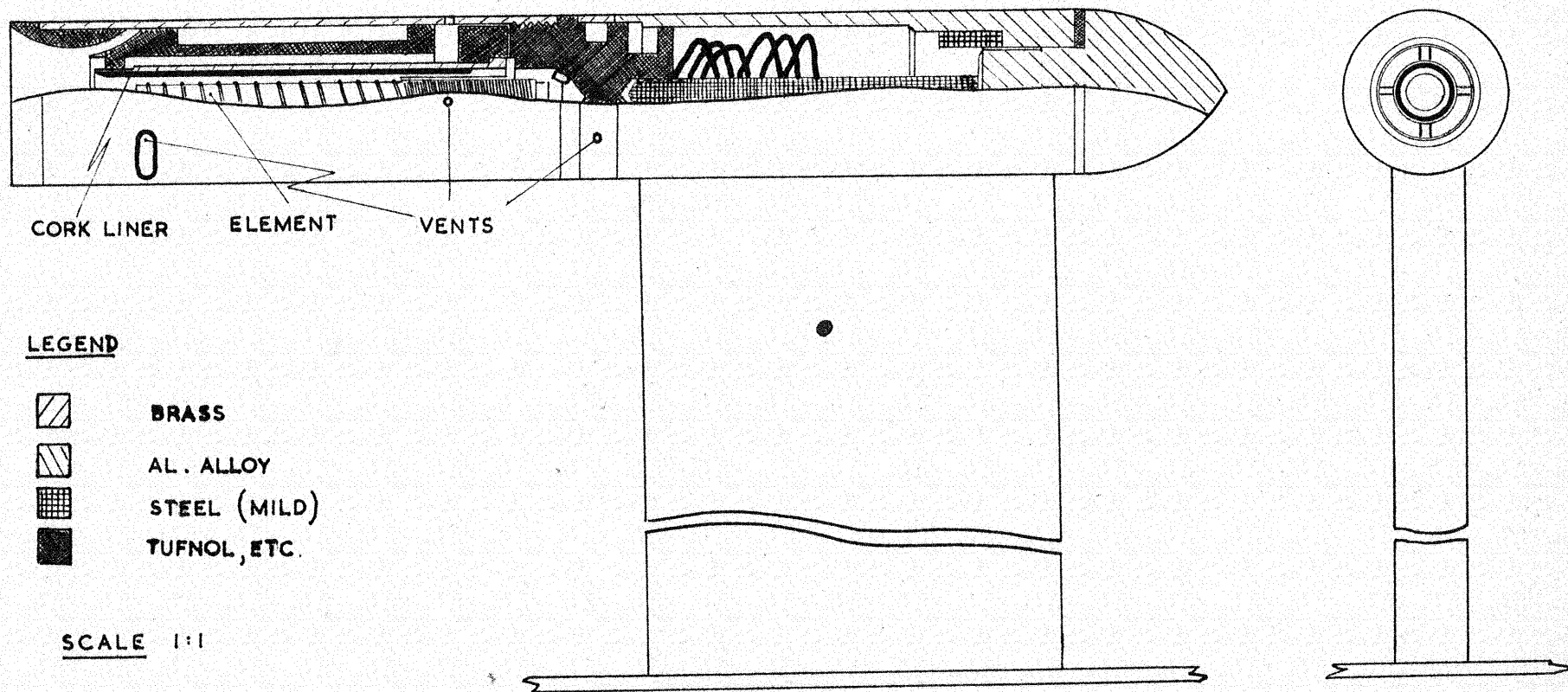
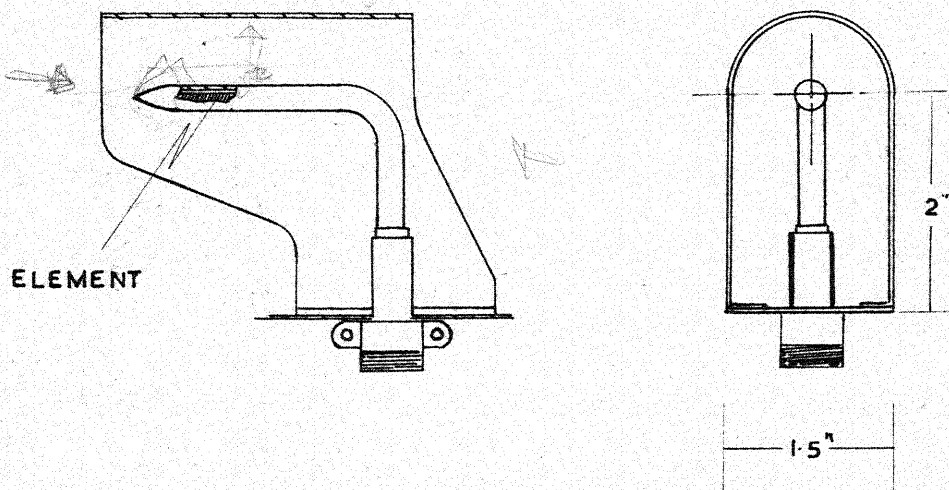


FIG 3.

SECTIONAL VIEWS OF No.5 PROBE



SANGAMO WESTON THERMOMETER HEAD

S. 110 FORM 5

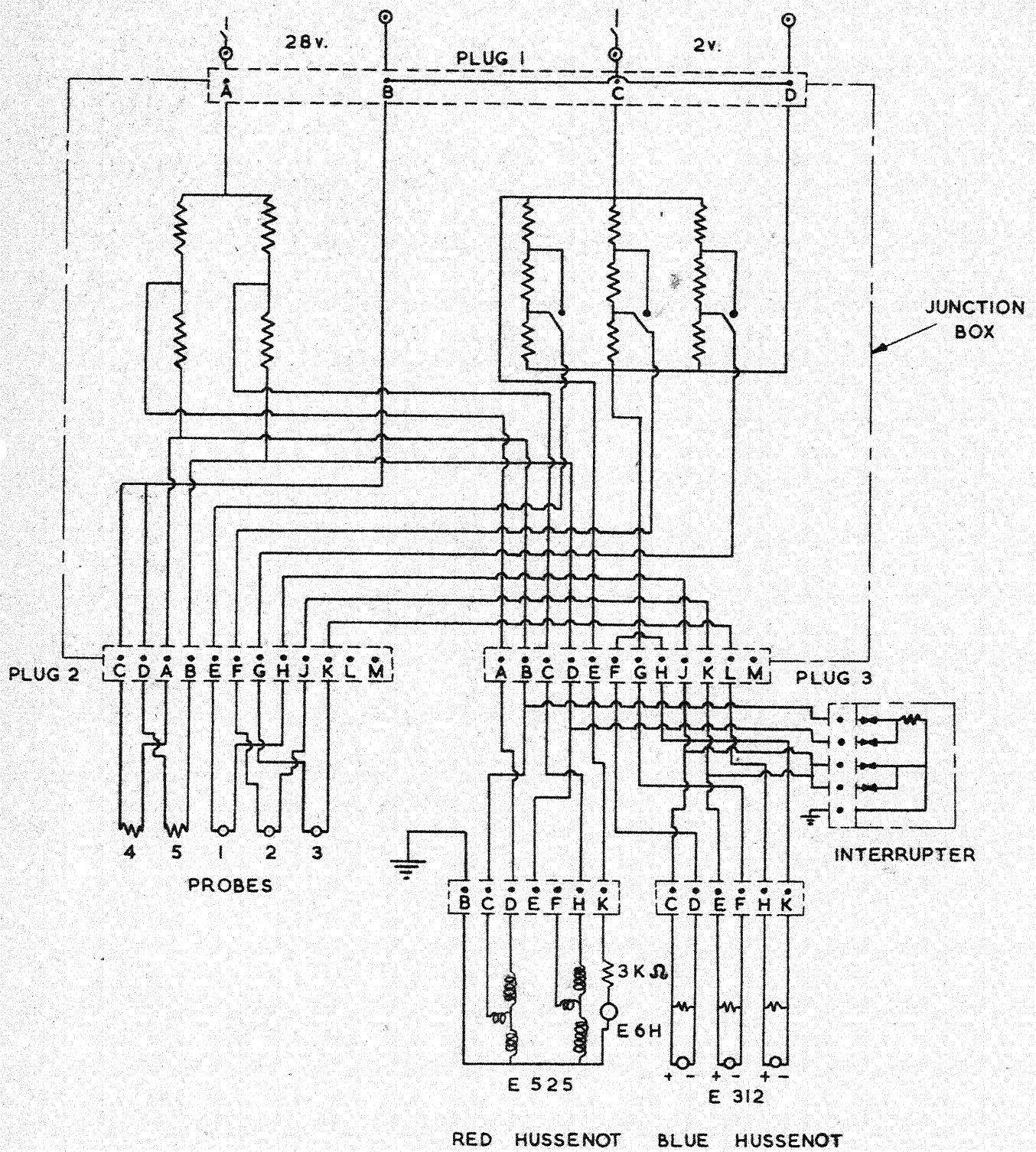


FIG. 5 WIRING DIAGRAM FOR WN 893

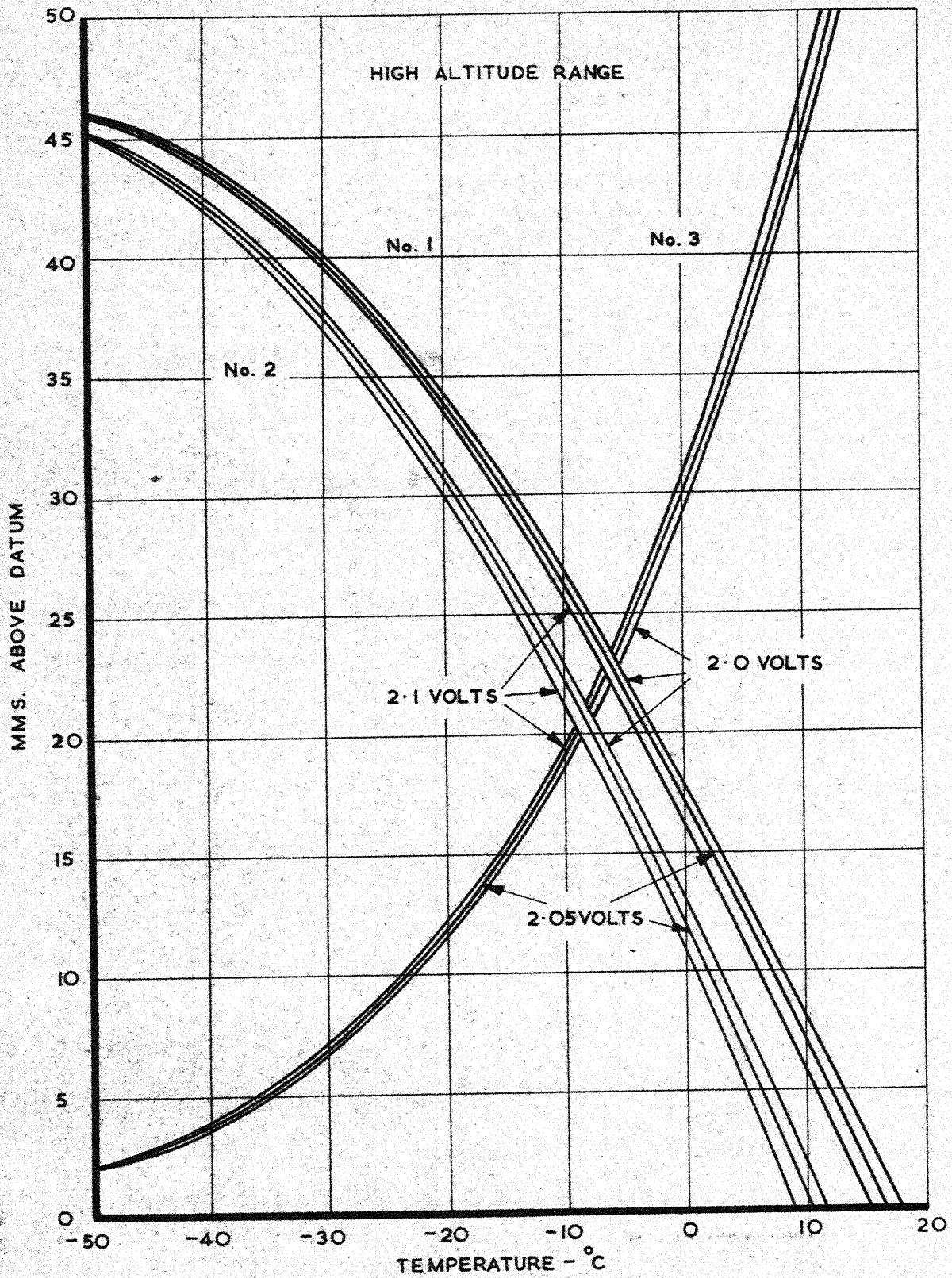


FIG. 6 CALIBRATION CURVES OF PROBES 1 2 & 3

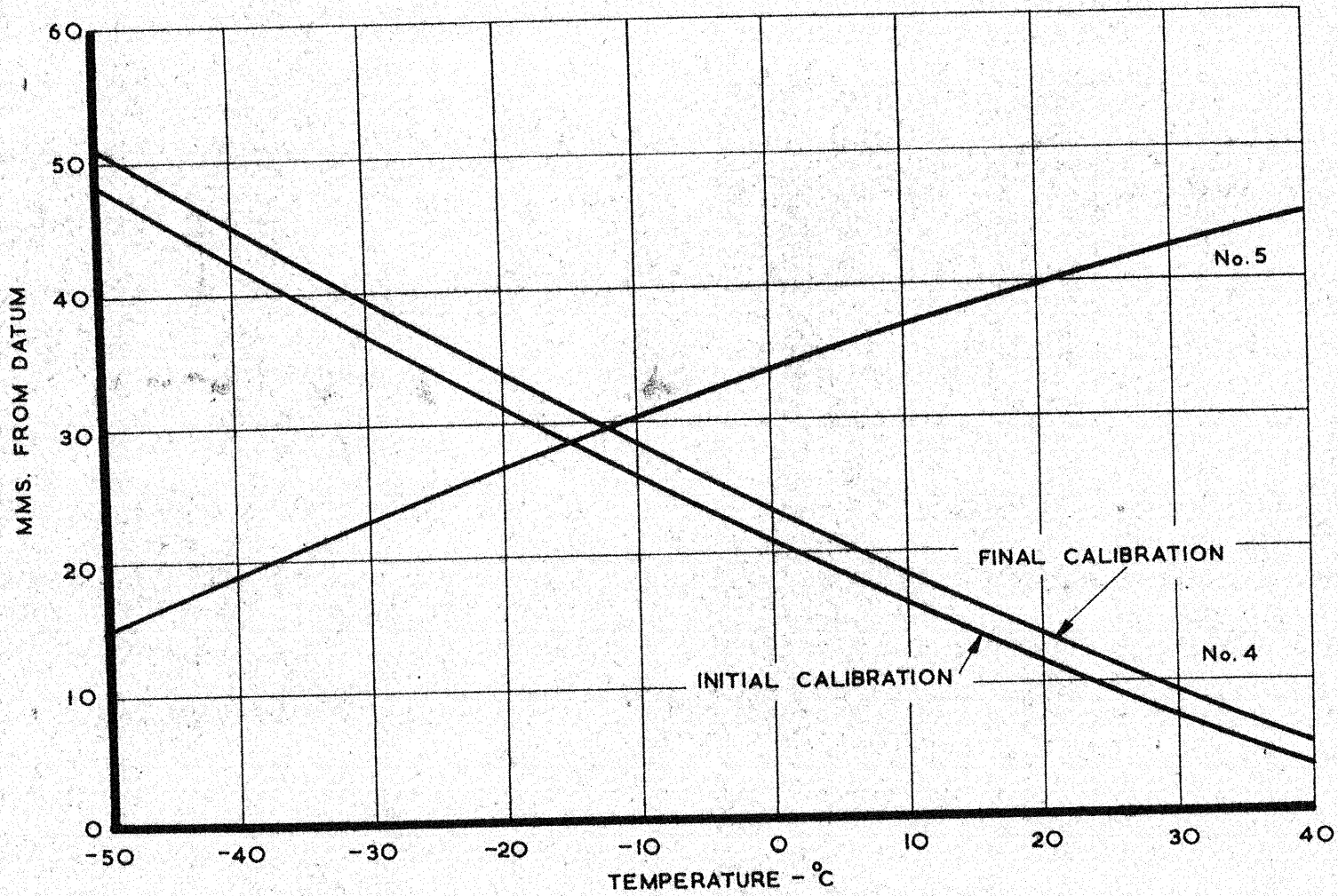


FIG. 7 CALIBRATION CURVES OF PROBES 4 & 5

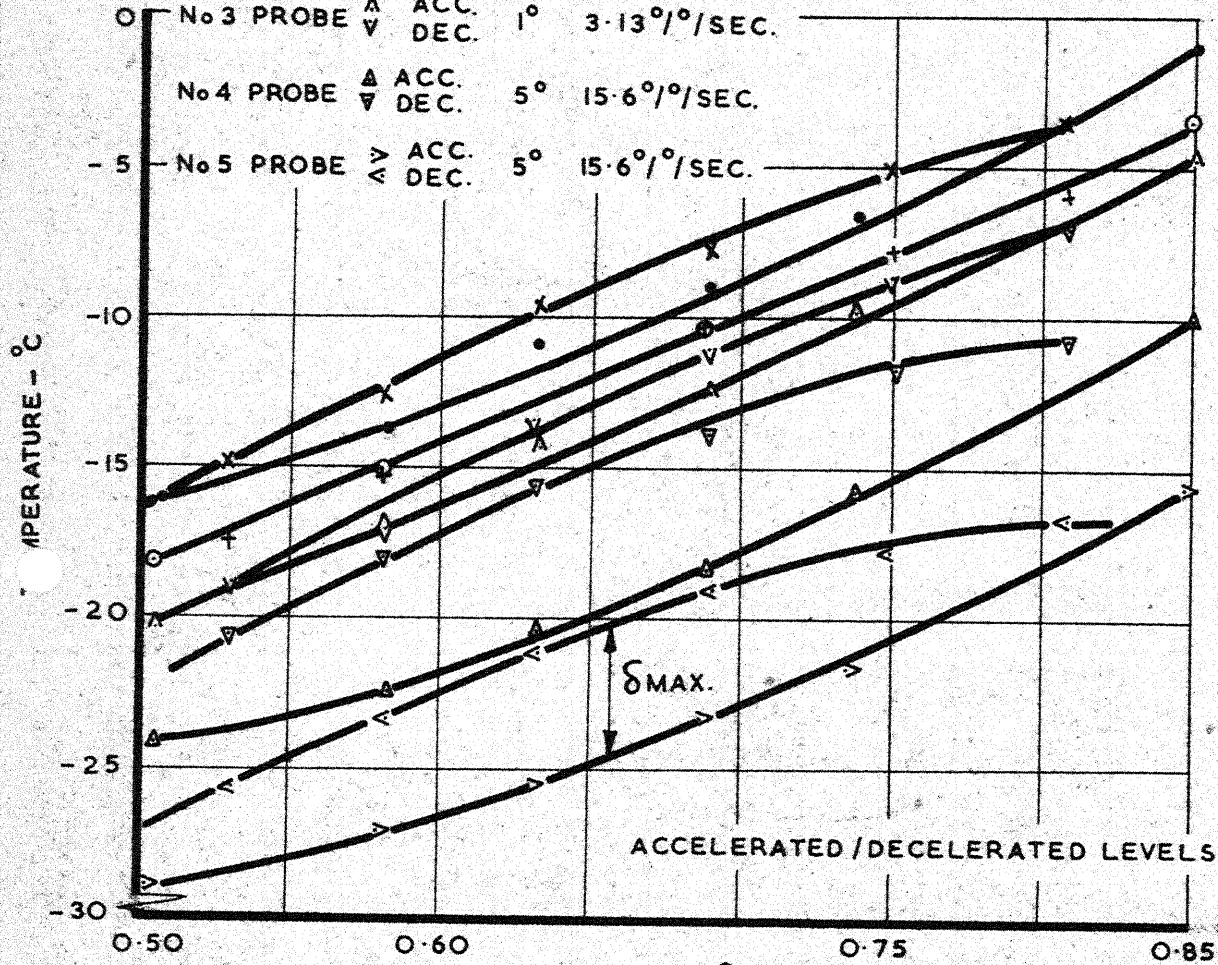
No 1 PROBE ● ACC. $1\frac{3}{4} \cdot 5 \cdot 5^\circ/\text{SEC.}^*$
X DEC.

No 2 PROBE ○ ACC. — — — — —
+ DEC.

No 3 PROBE ▲ ACC. $1^\circ \cdot 3 \cdot 13^\circ/\text{SEC.}$
▼ DEC.

No 4 PROBE ▲ ACC. $5^\circ \cdot 15 \cdot 6^\circ/\text{SEC.}$
▼ DEC.

No 5 PROBE > ACC. $5^\circ \cdot 15 \cdot 6^\circ/\text{SEC.}$
< DEC.



* THIS HIGH LAG WAS DUE TO A PARTIALLY BLOCKED SET OF VENT HOLES TO THE INNER CHAMBER (CF. FLIGHT 124)

(MACH No.)²

N.B THESE CURVES HAVE BEEN DISPLACED VERTICALLY FOR THE SAKE OF CLARITY

FIG. 8 INSTRUMENT LAG TESTS AT 45,000 FT. FLIGHT 122

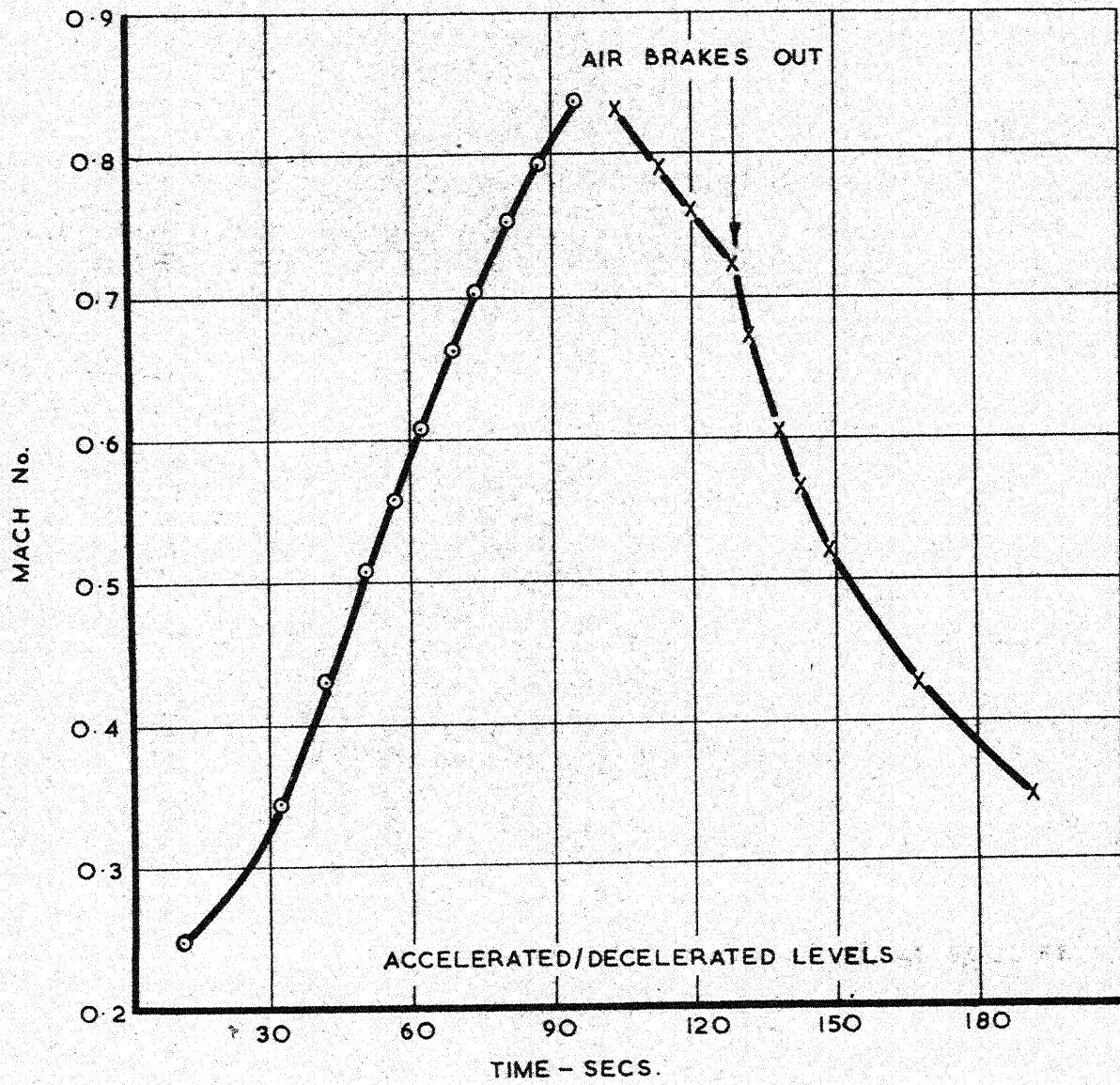
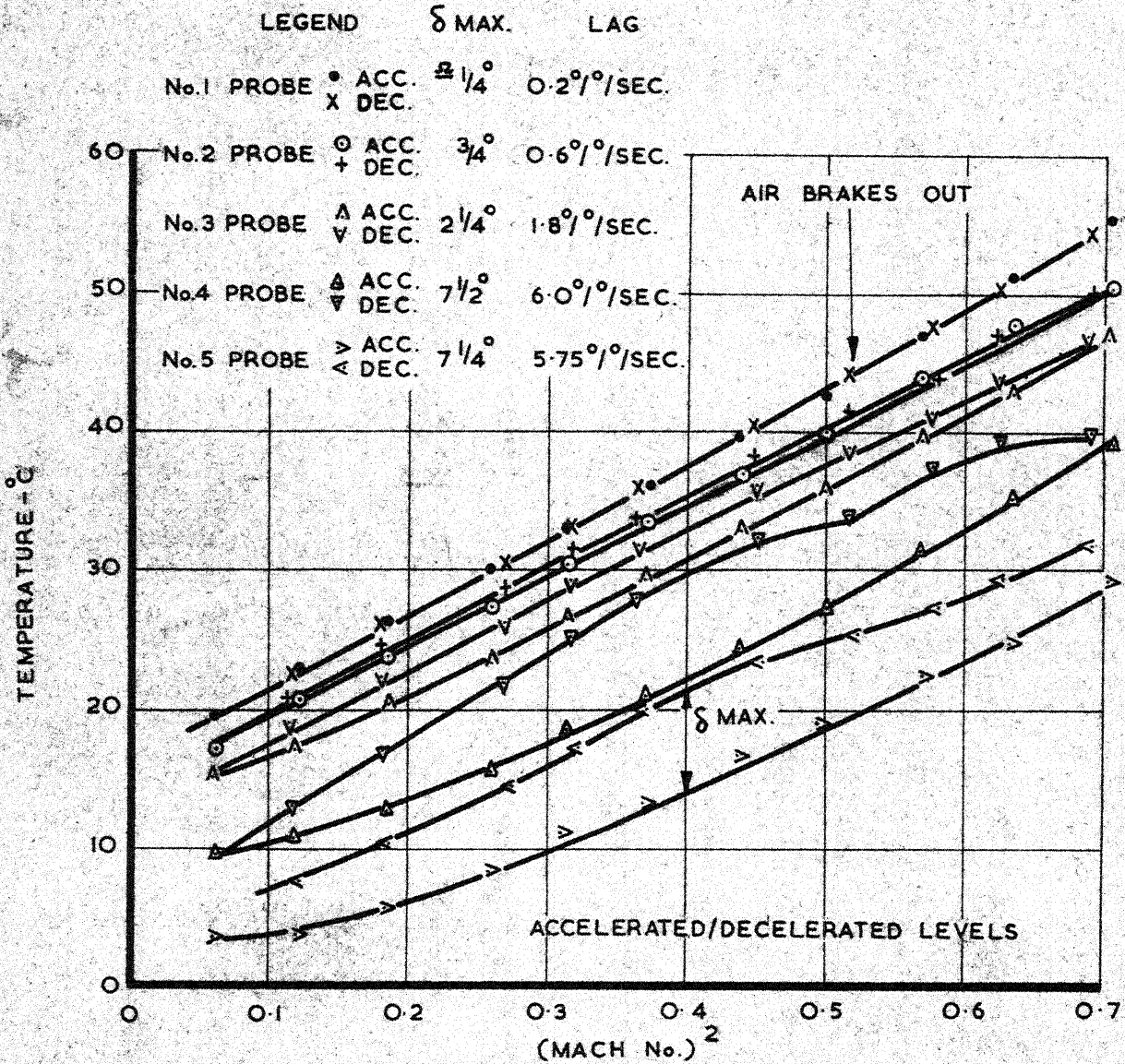


FIG. 9 INSTRUMENT LAG TESTS AT 5,000 FT.
FLIGHT 124



N.B. THESE CURVES HAVE BEEN DISPLACED VERTICALLY FOR THE SAKE OF CLARITY.

FIG. 10 INSTRUMENT LAG TESTS AT 5000 FT.
FLIGHT 124

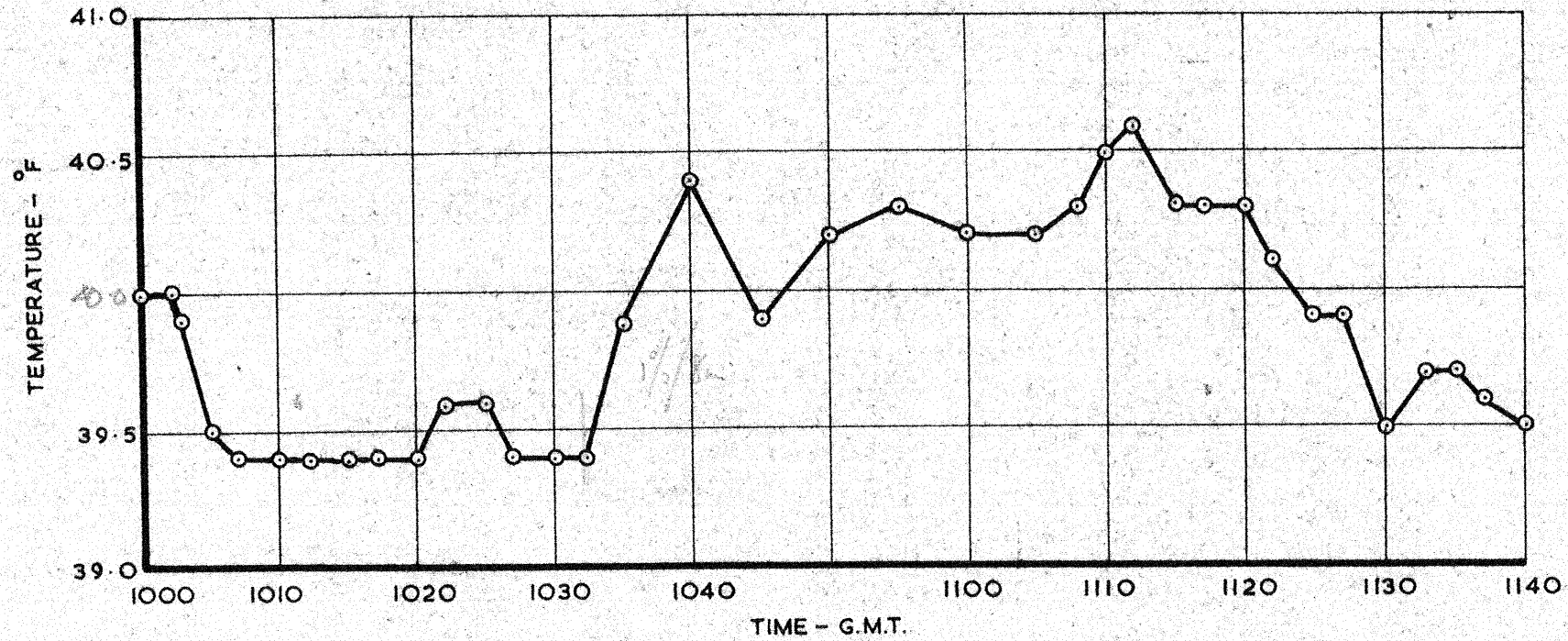


FIG. II OBSERVED VARIATION OF THE AMBIENT AIR TEMPERATURE AT 4300FT.
 (APPROX.) ABOVE R.A.F. CARDINGTON. IN CONNECTION WITH
 FLIGHTS 150 & 151. 23 - 4 - 58

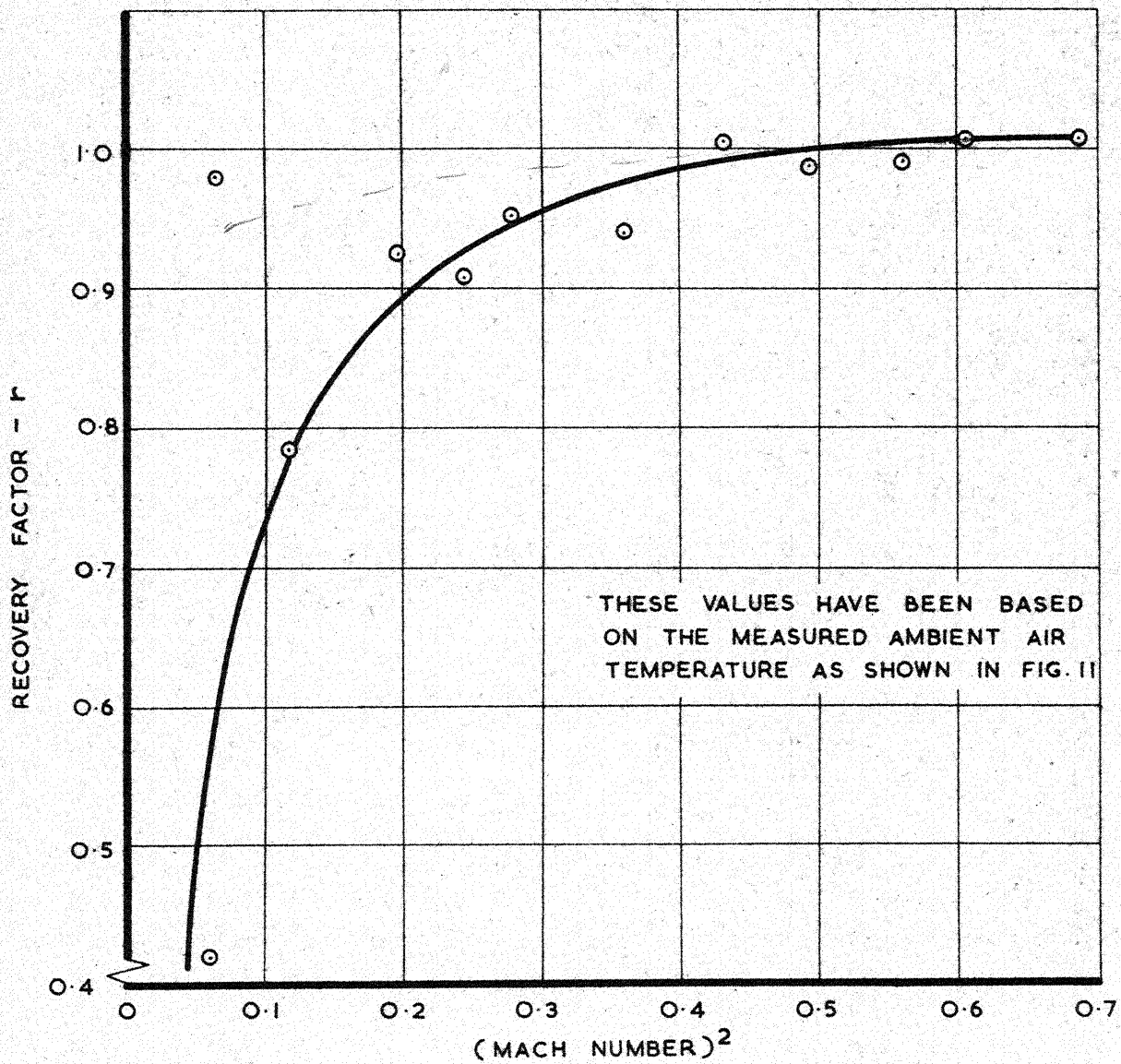


FIG. 12 GRAPH SHOWING THE VARIATION OF THE RECOVERY FACTOR OF THE No.1 PROBE. FLIGHT 150

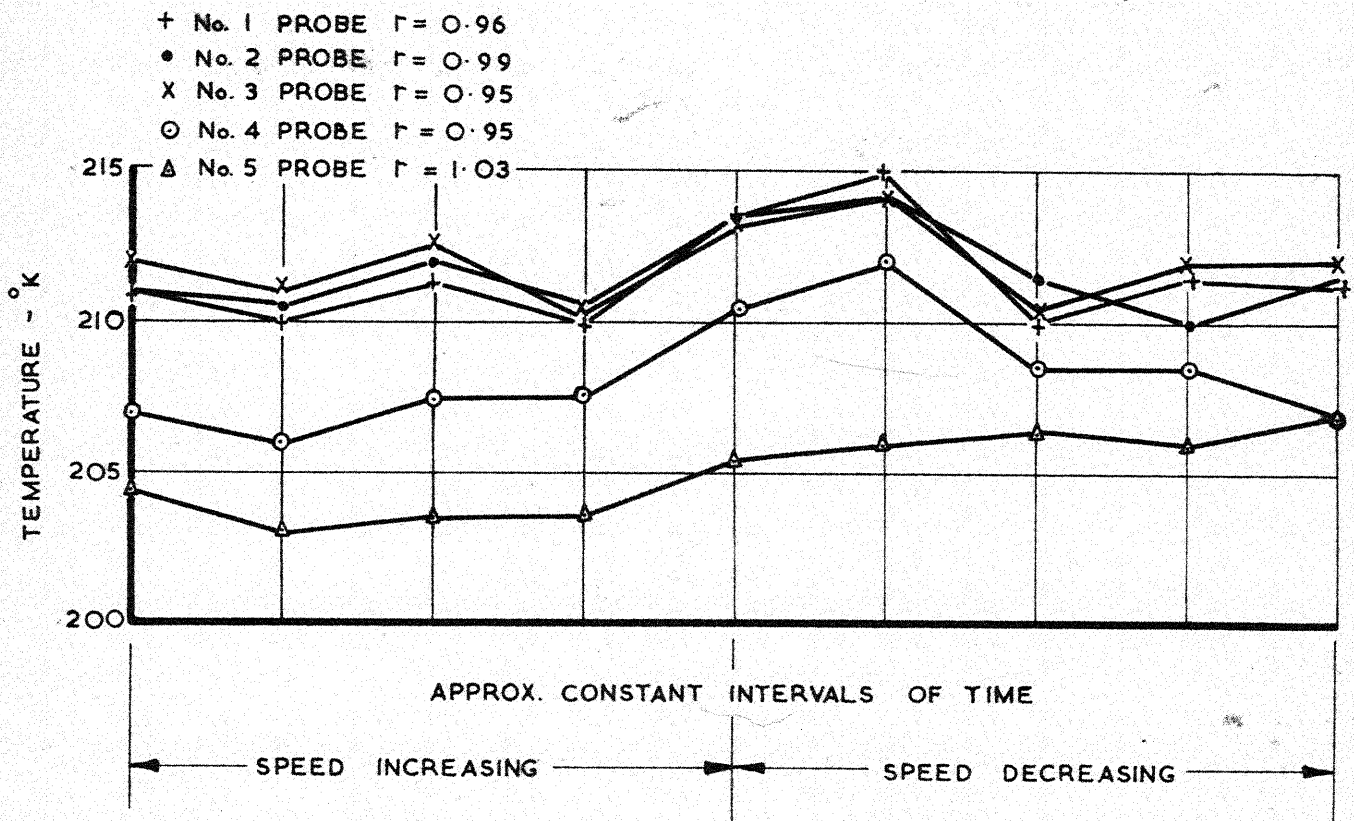


FIG. 13 A GRAPH OF THE AMBIENT TEMPERATURE OF EACH INDIVIDUAL POINT BASED ON THE RECOVERY FACTORS OBTAINED FROM THE OTHER CALIBRATIONS. FLIGHT 155.

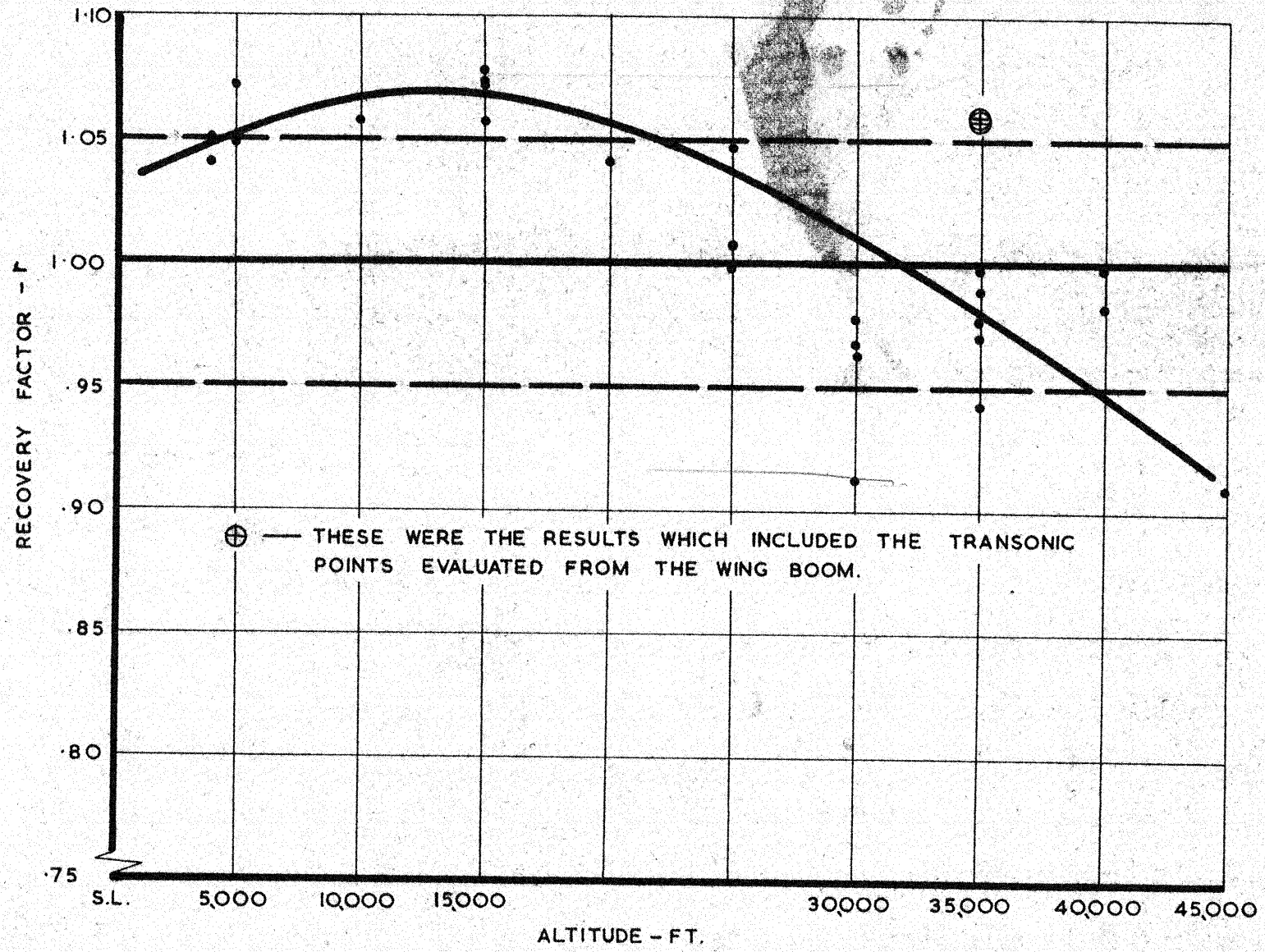


FIG. 14 VARIATION OF THE RECOVERY FACTOR OF THE No. 1 PROBE

(Thermistor)

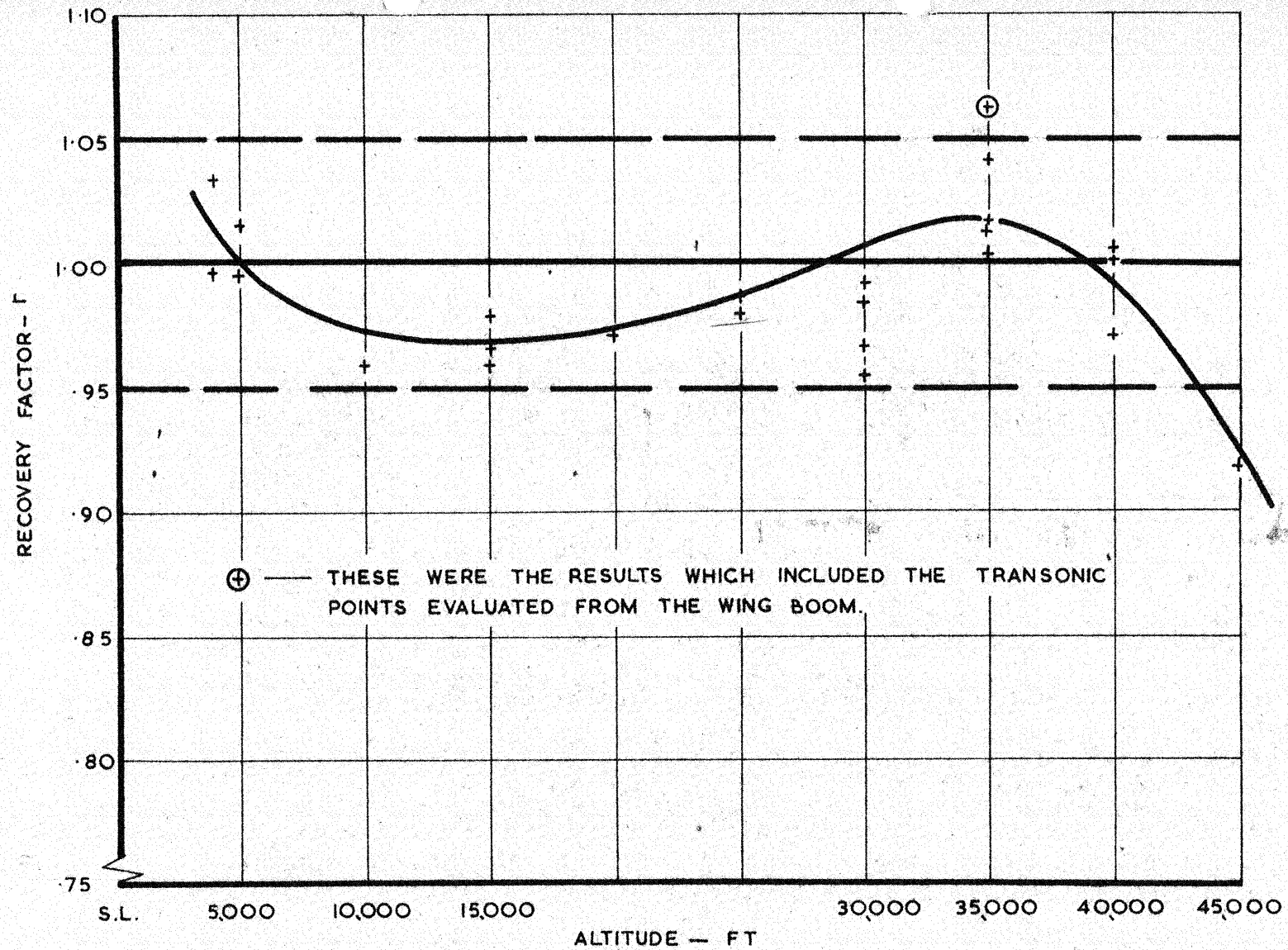


FIG. 15 VARIATION OF THE RECOVERY FACTOR OF THE No. 2 PROBE

(Thermistor)

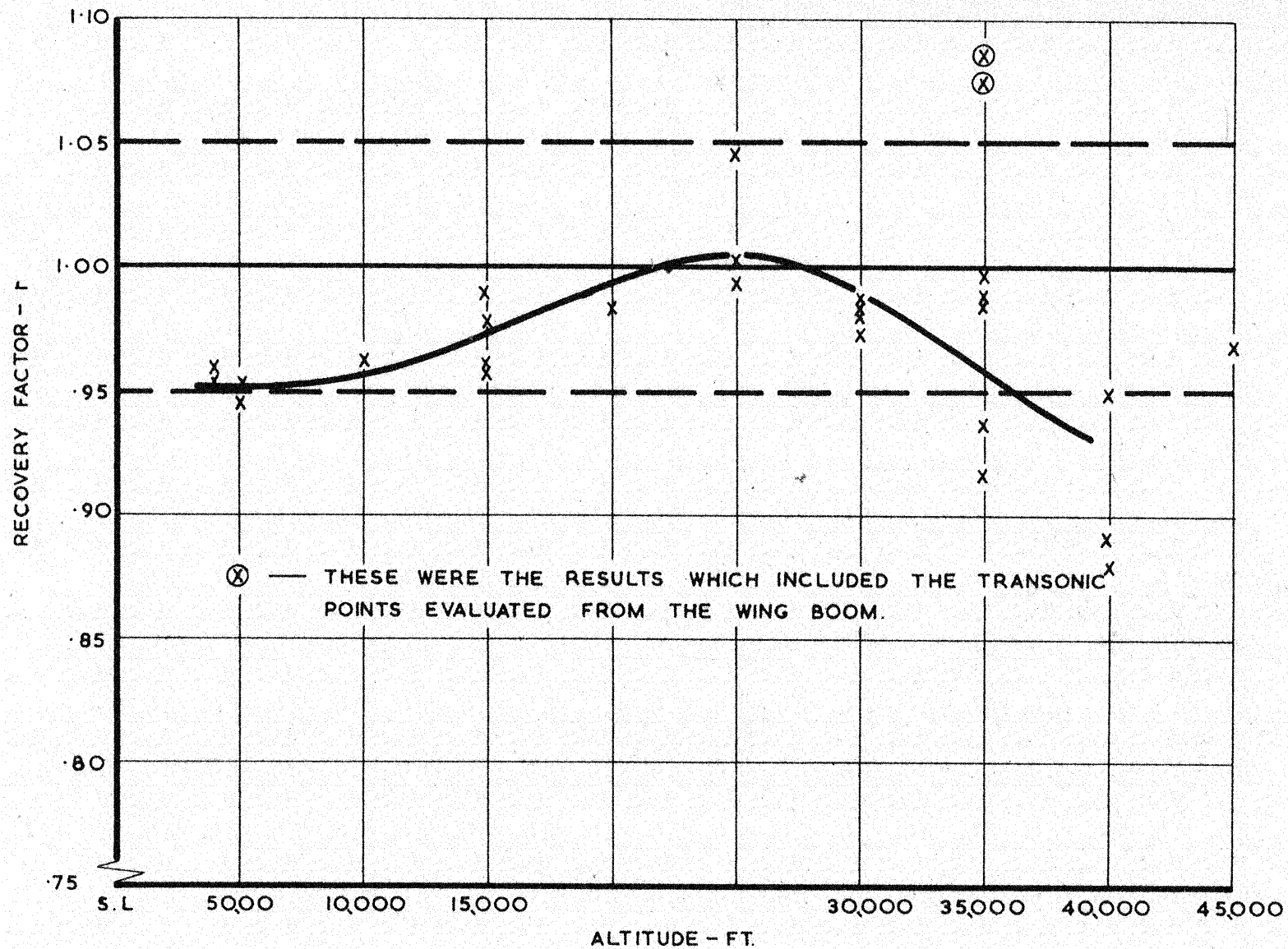


FIG. 16 VARIATION OF THE RECOVERY FACTOR OF THE No. 3 PROBE

Thermistor

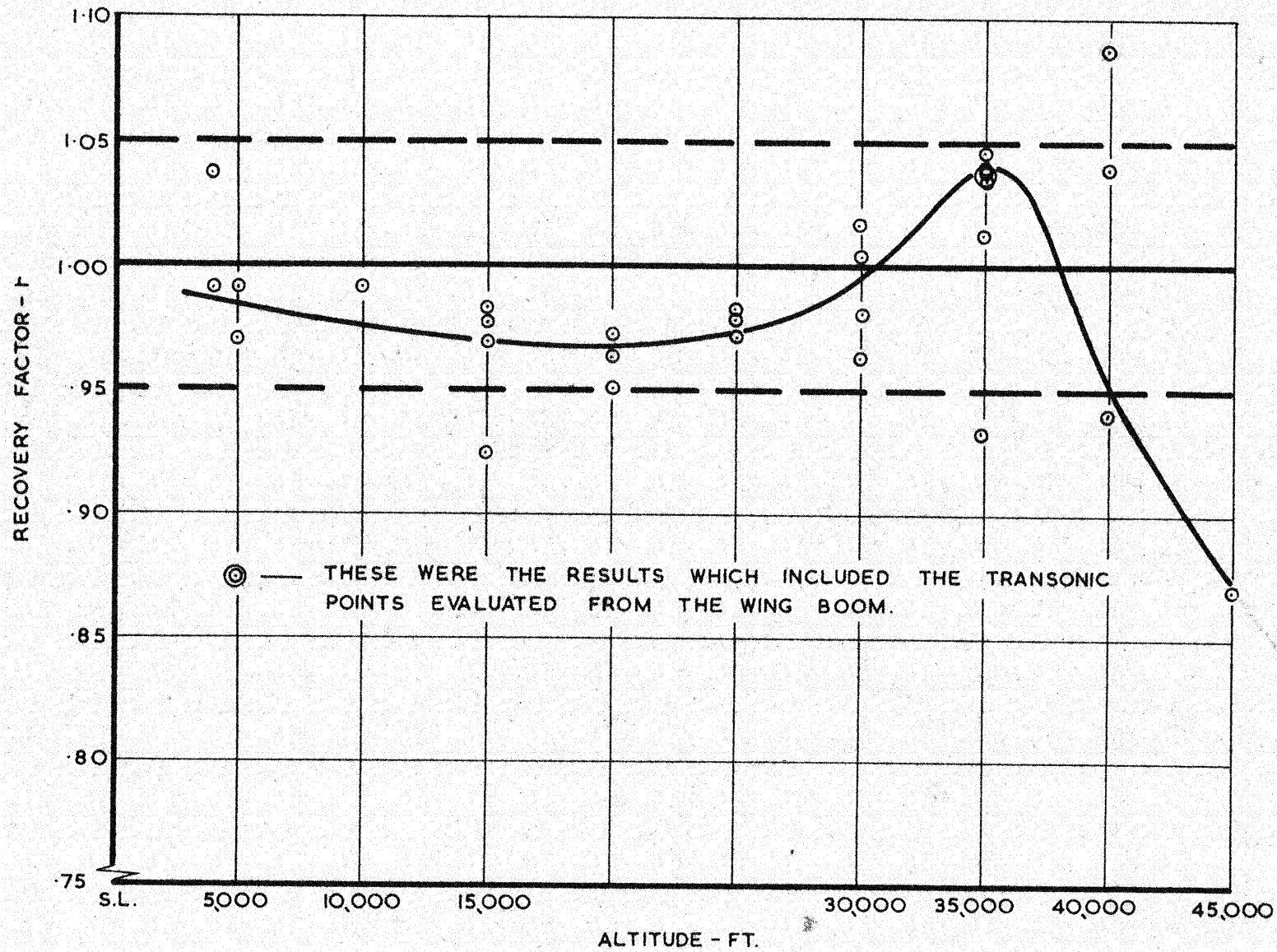


FIG. 17 VARIATION OF THE RECOVERY FACTOR OF THE No. 4 PROBE

(reference)

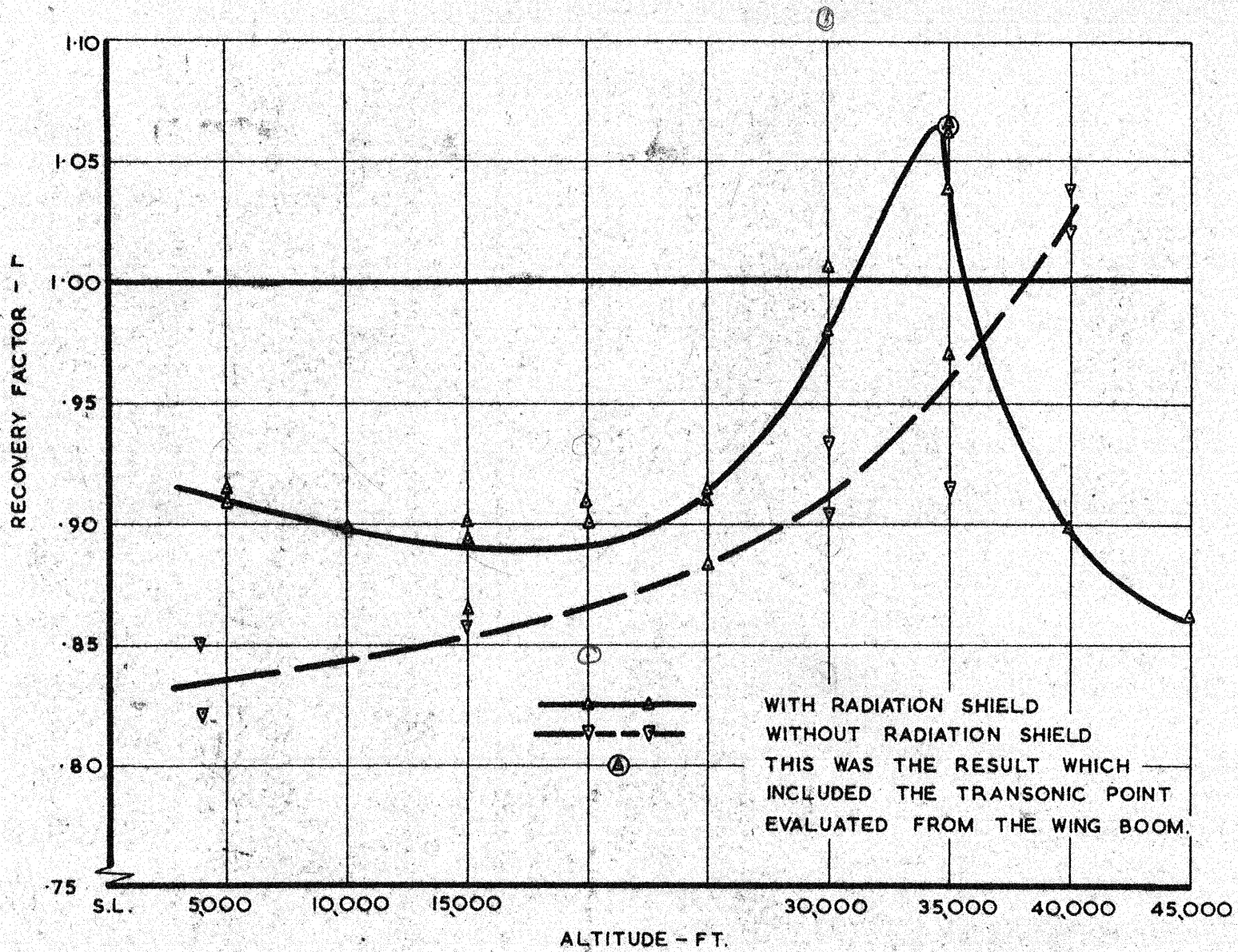


FIG. 18 VARIATION OF THE RECOVERY FACTOR OF THE No. 5 PROBE

(resistance)

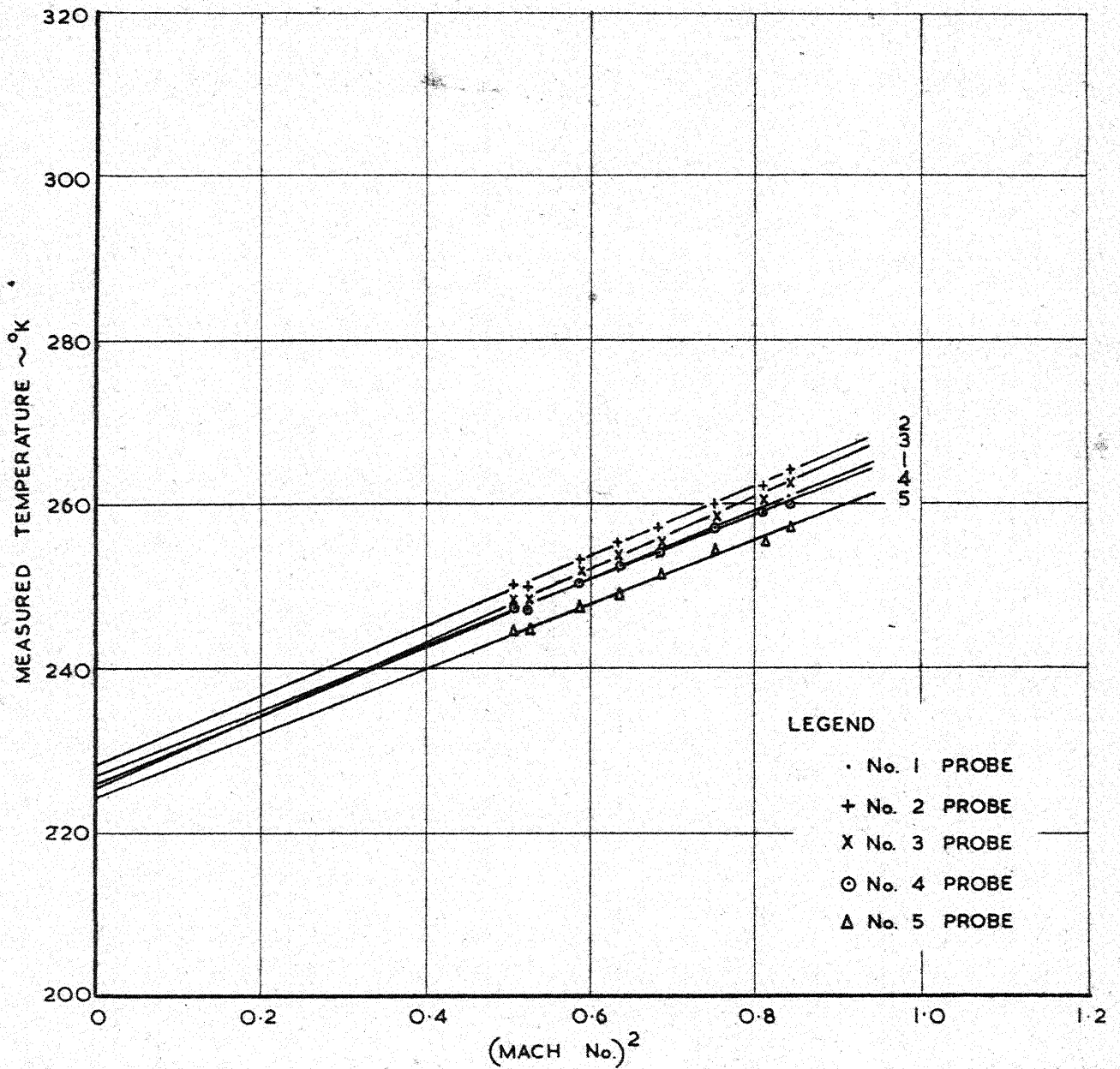
MEASUREMENT OF FREE AIR TEMPERATURE.

THERMOMETER CALIBRATION LEVELS.

HUNTER WN 893

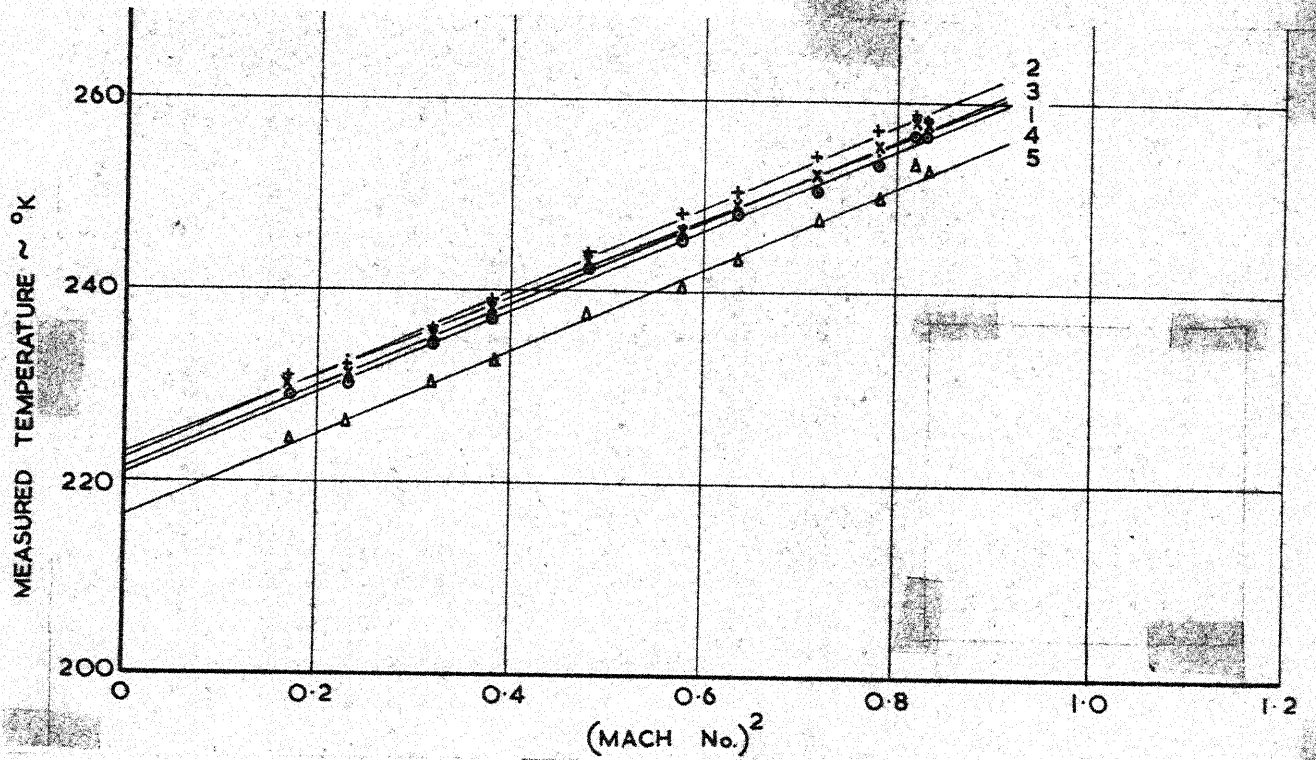
FLIGHT No. 122.

PRESSURE ALTITUDE 45,000'



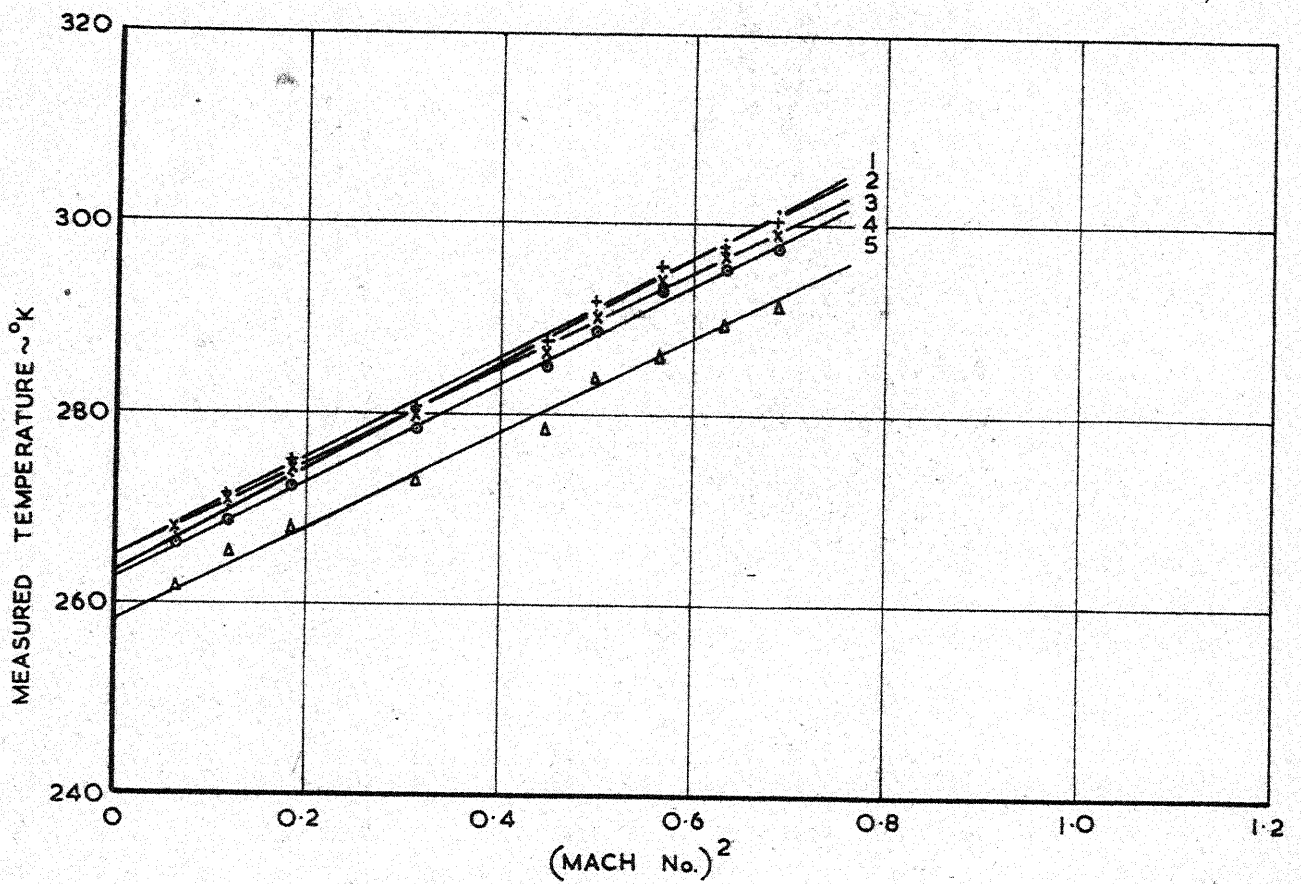
FLIGHT No. 123

PRESSURE ALTITUDE 30,000'



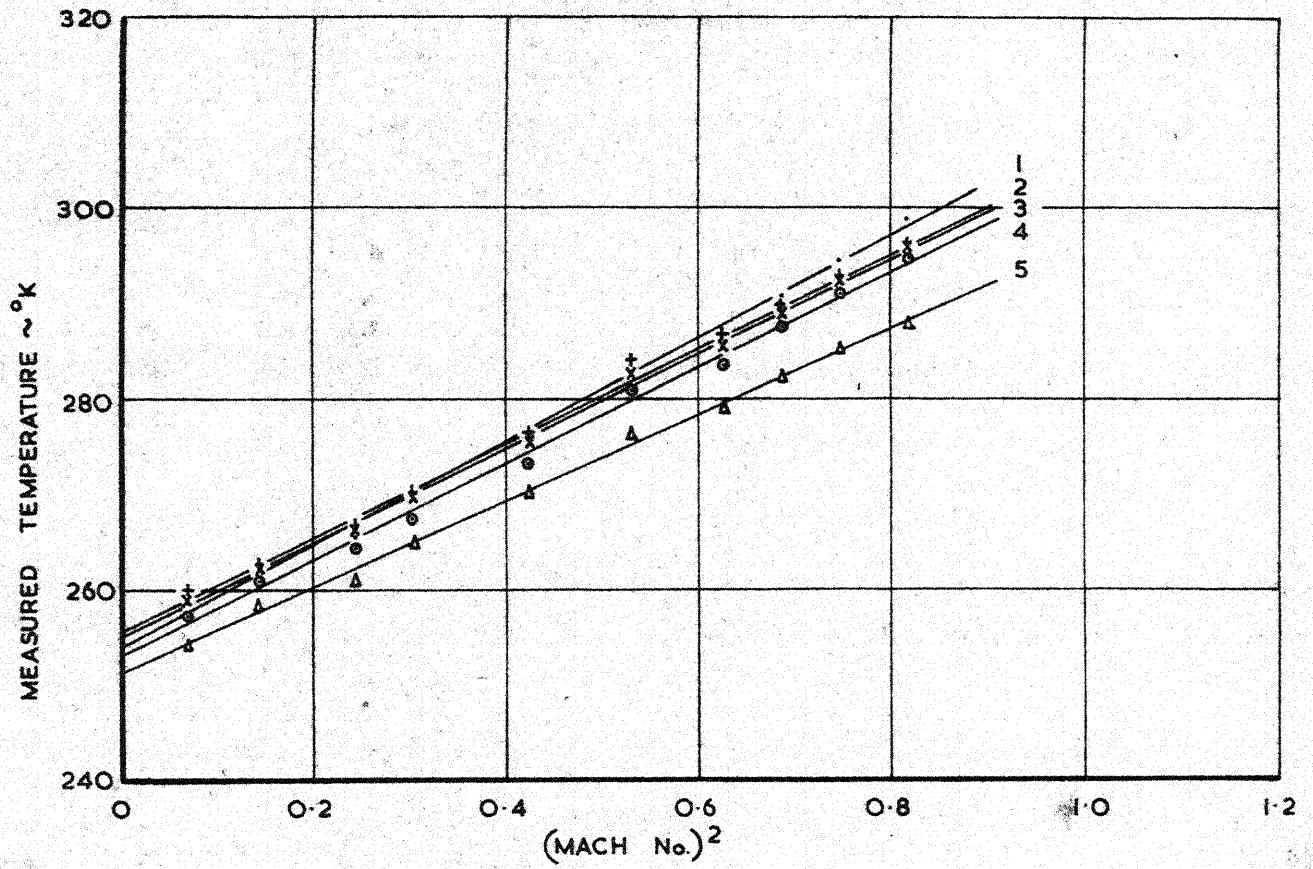
FLIGHT No. 124

PRESSURE ALTITUDE 5,000'



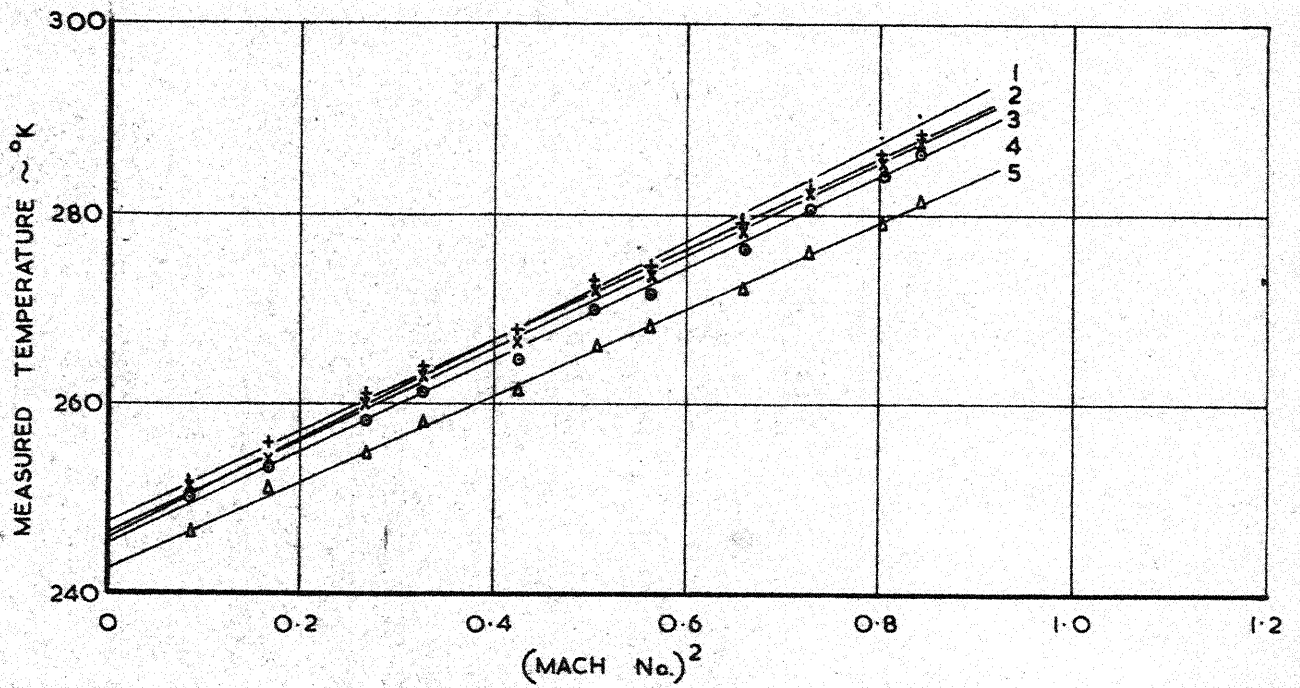
FLIGHT No. 125

PRESSURE ALTITUDE 10,000'



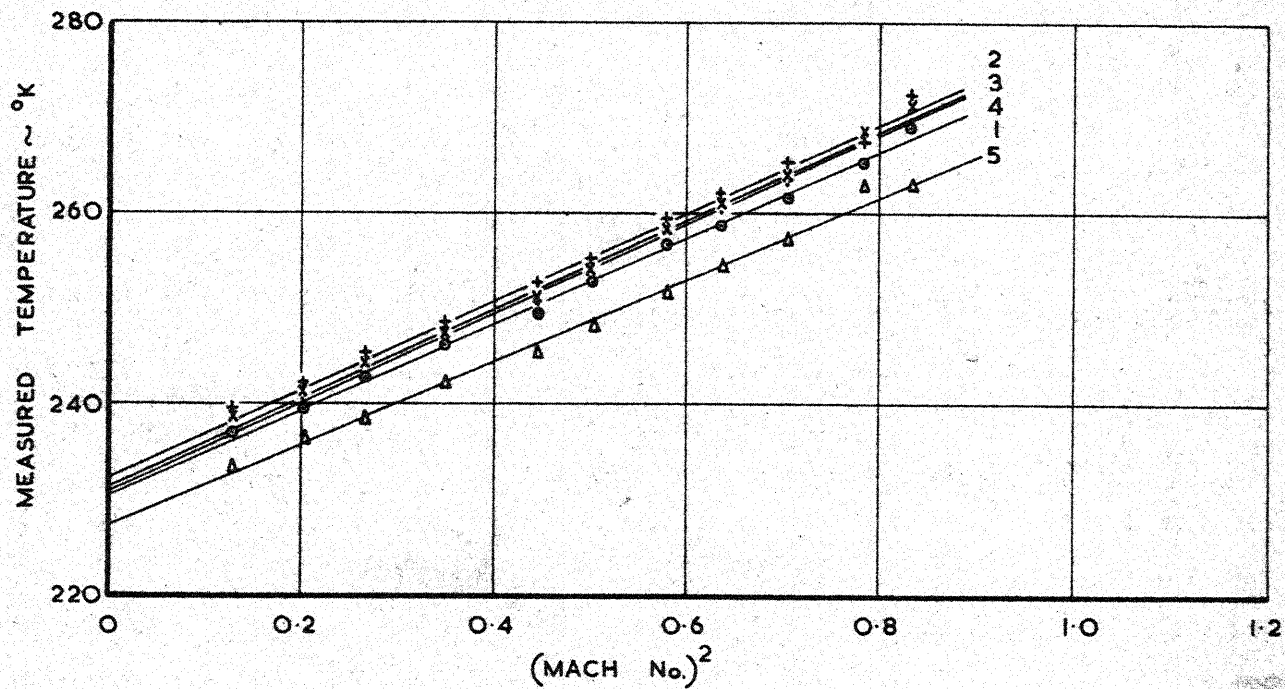
FLIGHT No. 126

PRESSURE ALTITUDE 15,000'



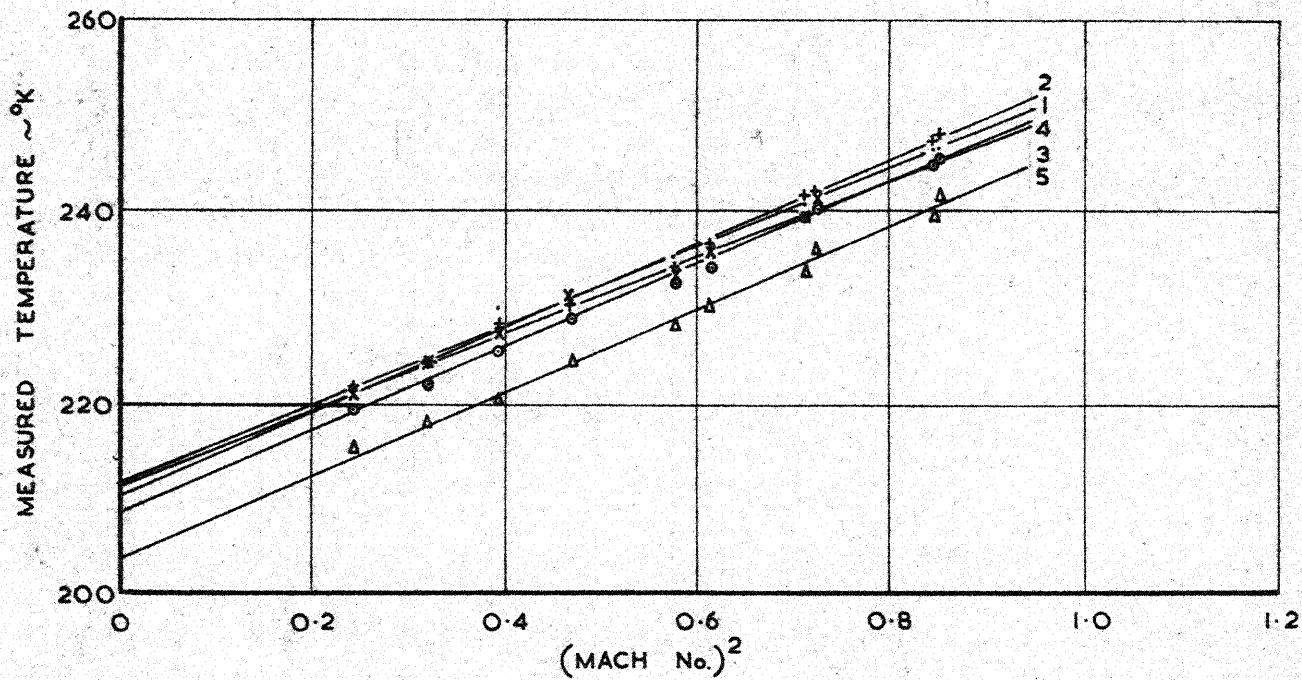
FLIGHT No. 127

PRESSURE ALTITUDE 25,000'



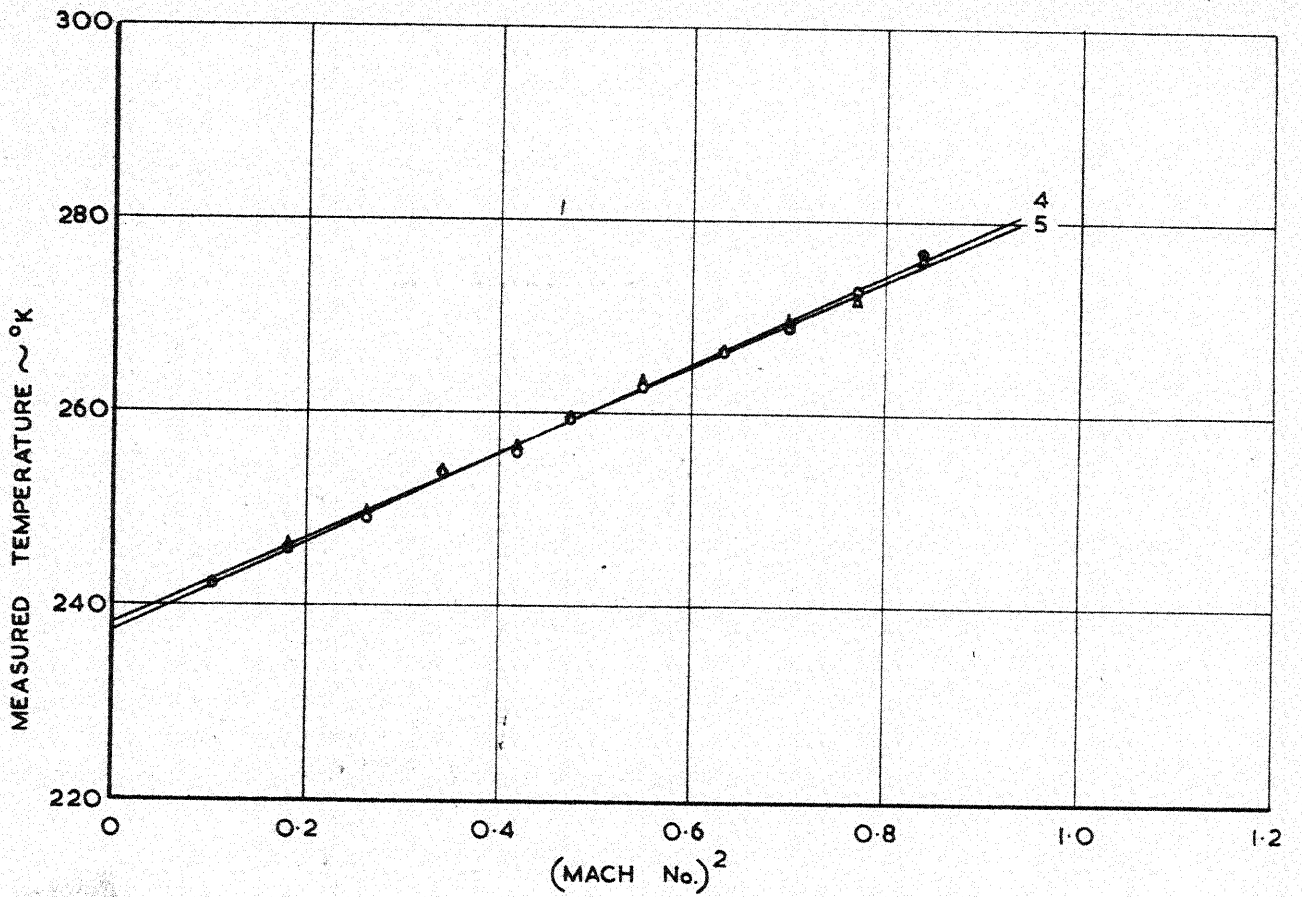
FLIGHT No. 128

PRESSURE ALTITUDE 35,000'



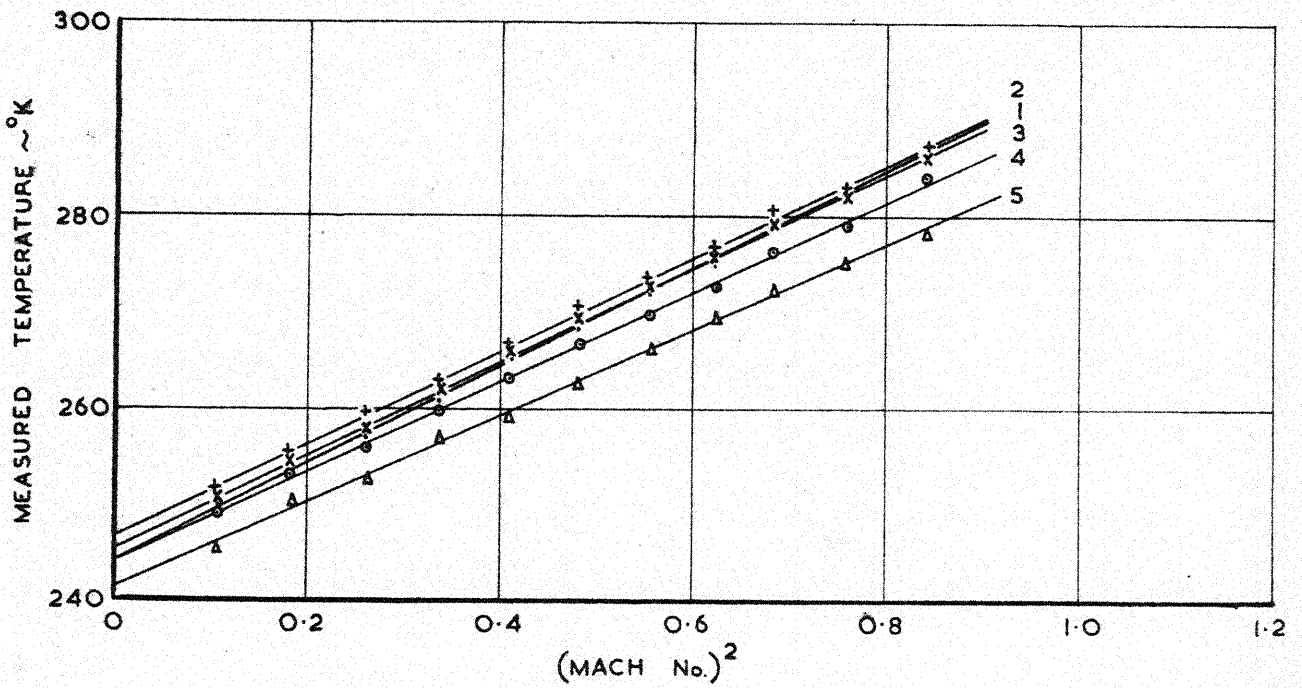
FLIGHT No. 131

PRESSURE ALTITUDE 20,000'



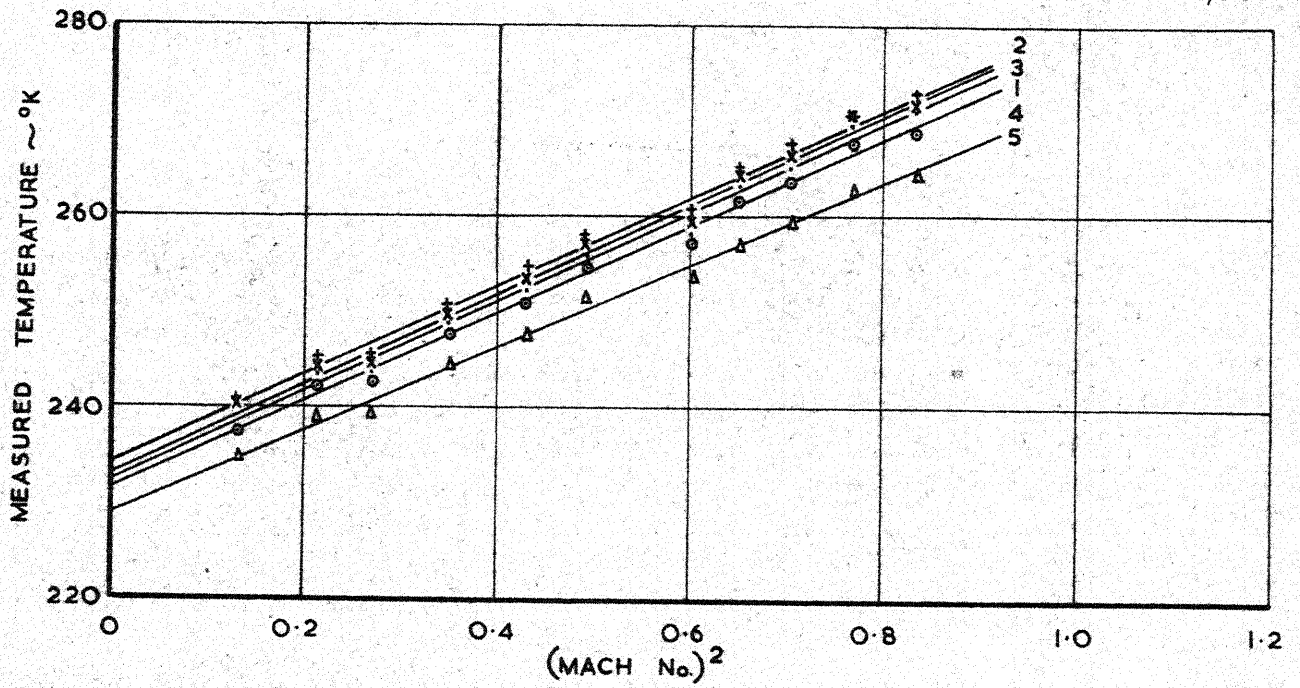
FLIGHT No. 133.

PRESSURE ALTITUDE 20,000'



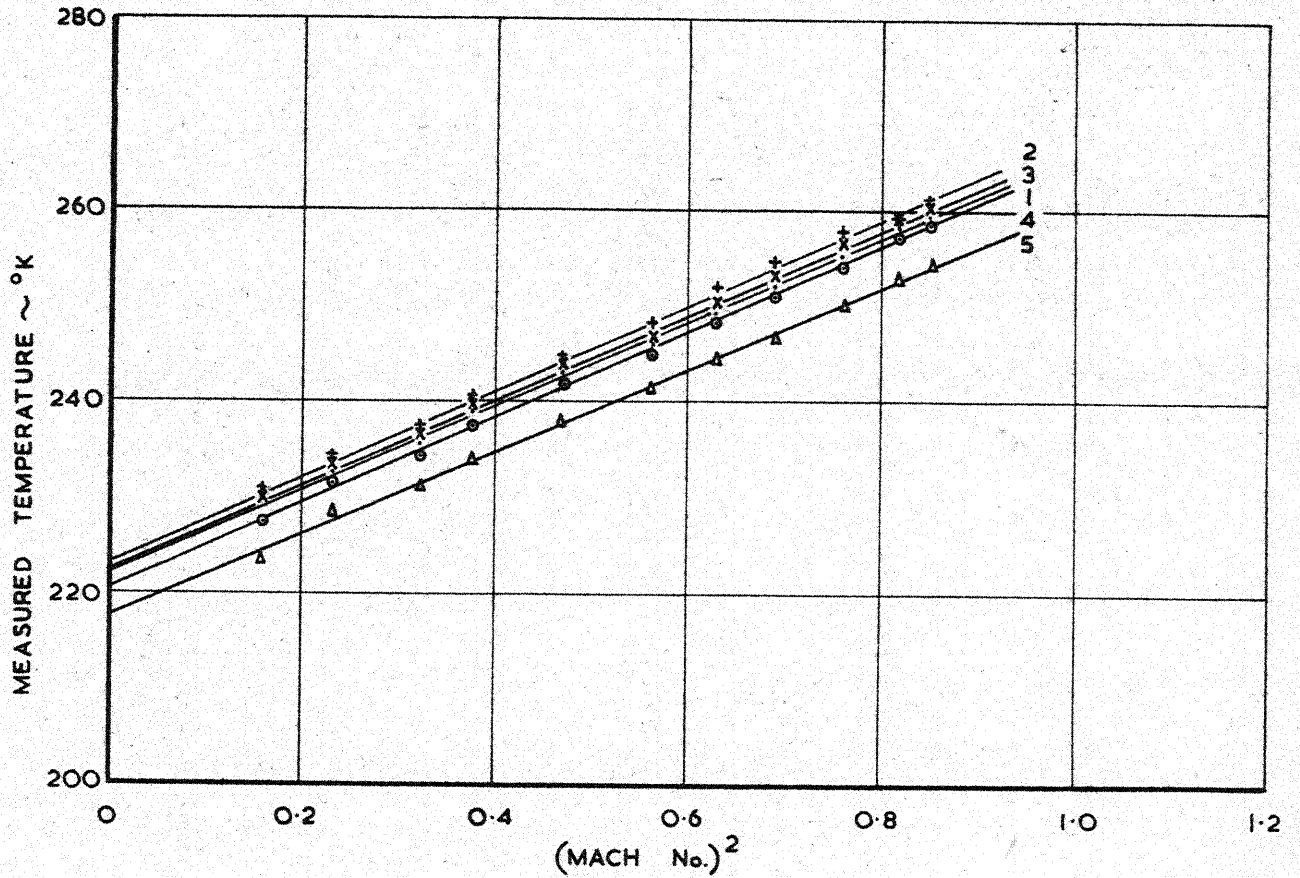
FLIGHT No. 135

PRESSURE ALTITUDE 25,000'



FLIGHT No. 136

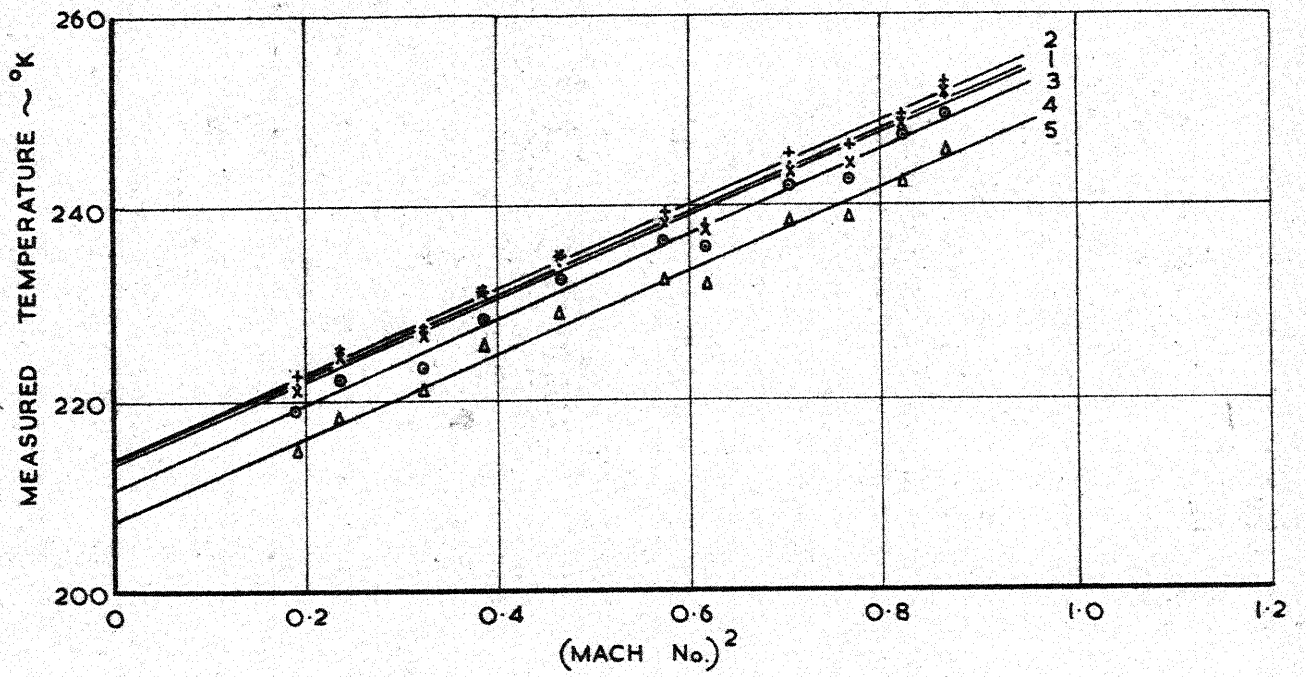
PRESSURE ALTITUDE 30,000'



9

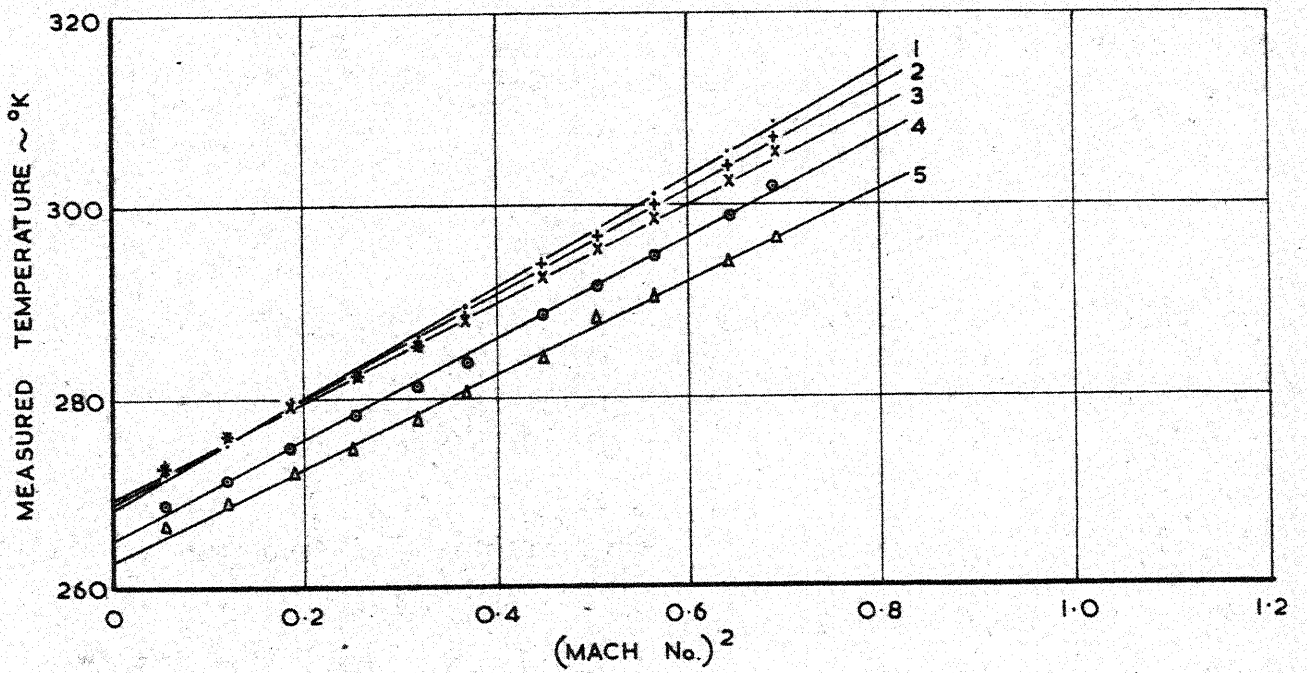
FLIGHT No. 137

PRESSURE ALTITUDE 35,000'

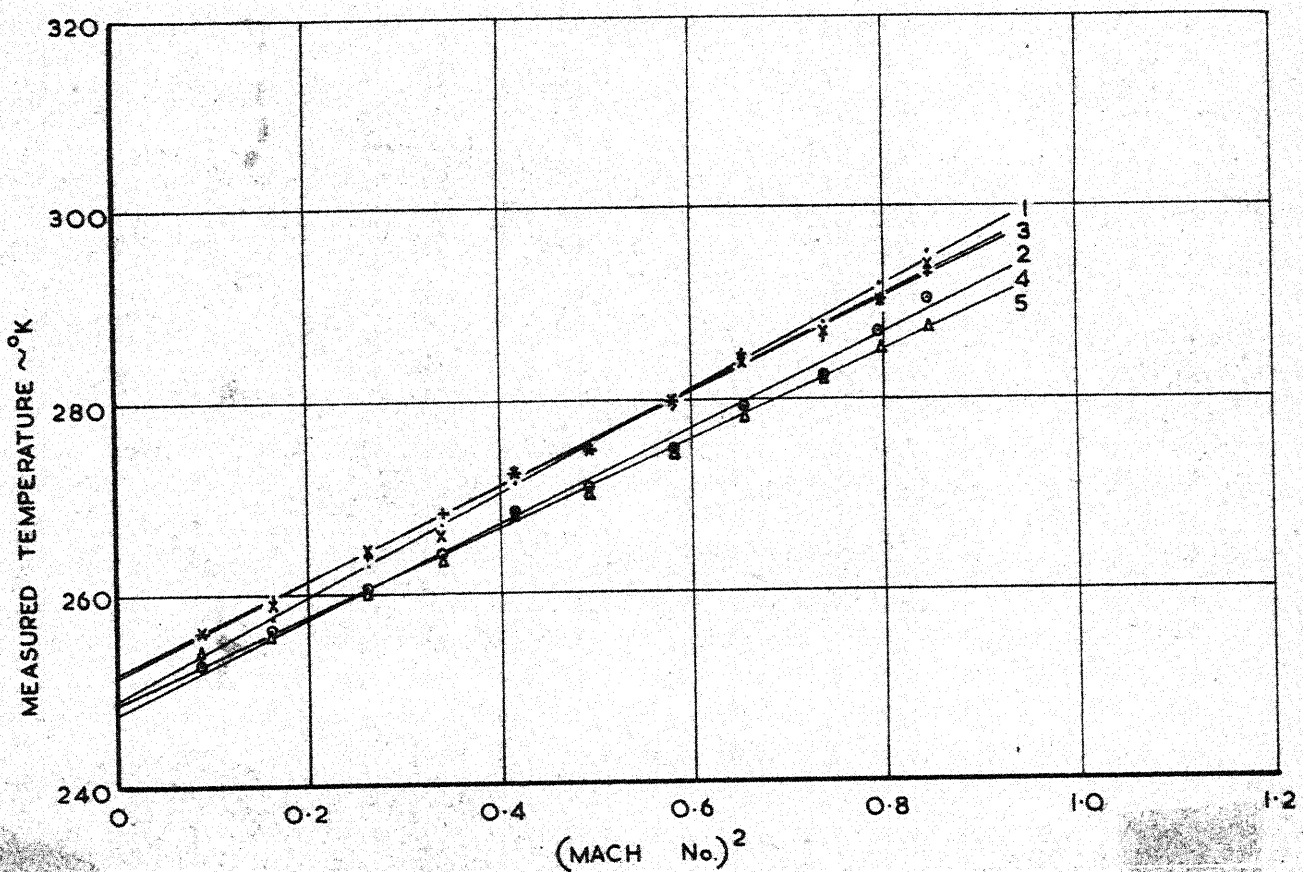


FLIGHT No. 138

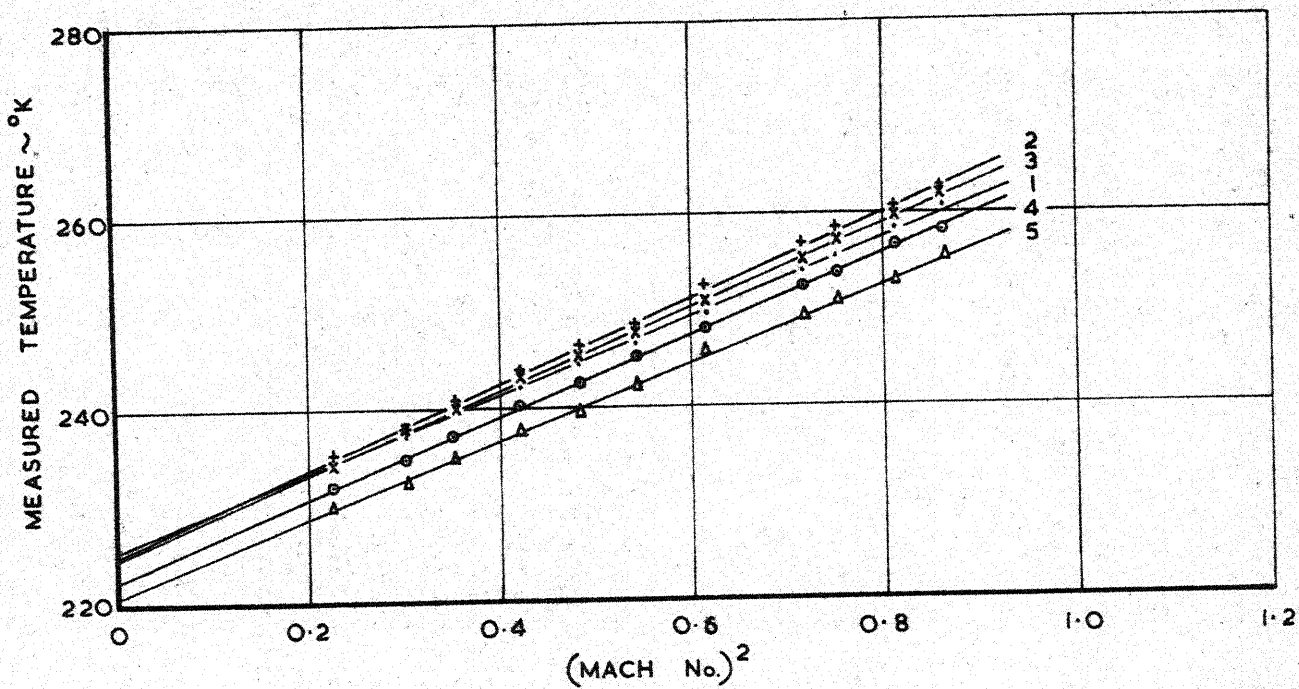
PRESSURE ALTITUDE 5,000'



FLIGHT No. 139
PRESSURE ALTITUDE 15,000'

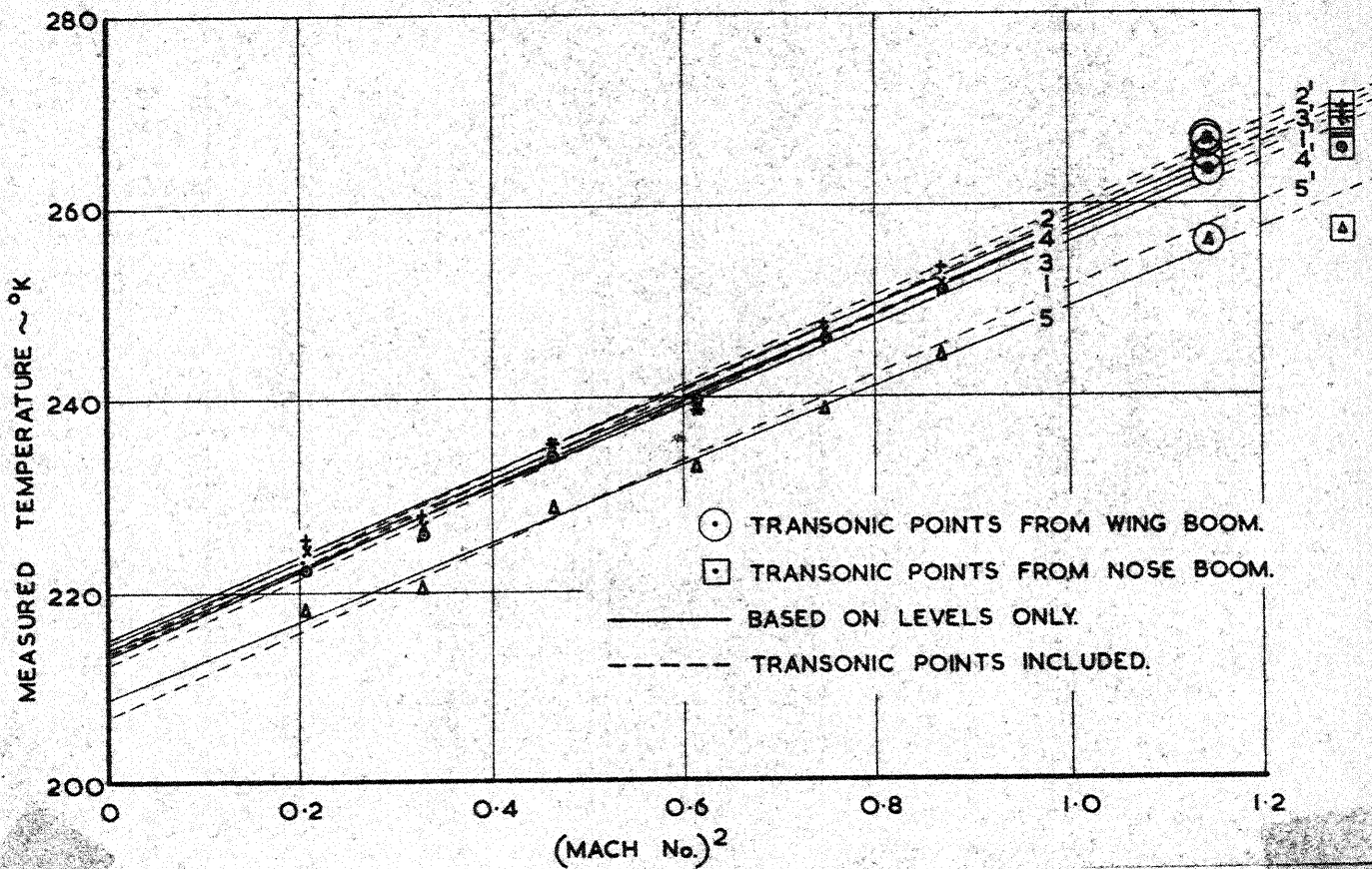


FLIGHT No. 140
PRESSURE ALTITUDE 40,000'



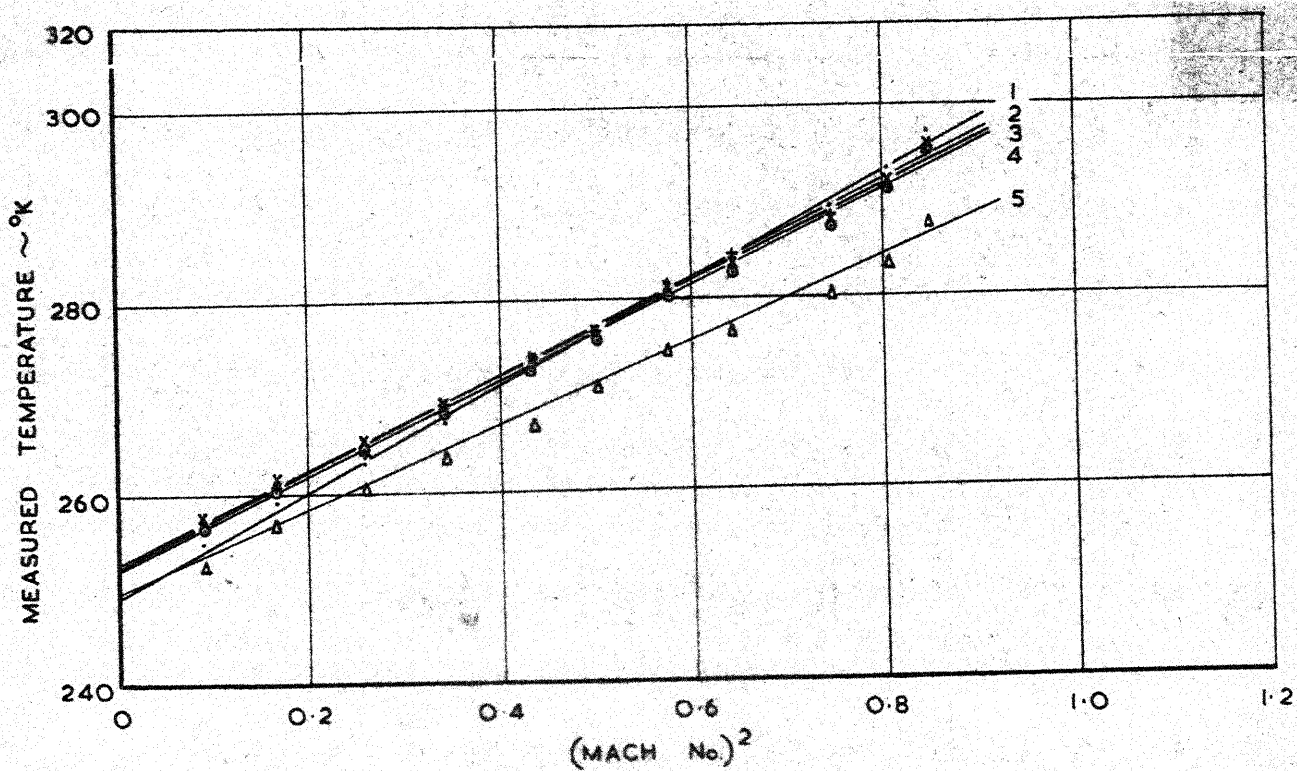
FLIGHT No. 141

PRESSURE ALTITUDE 35,000'



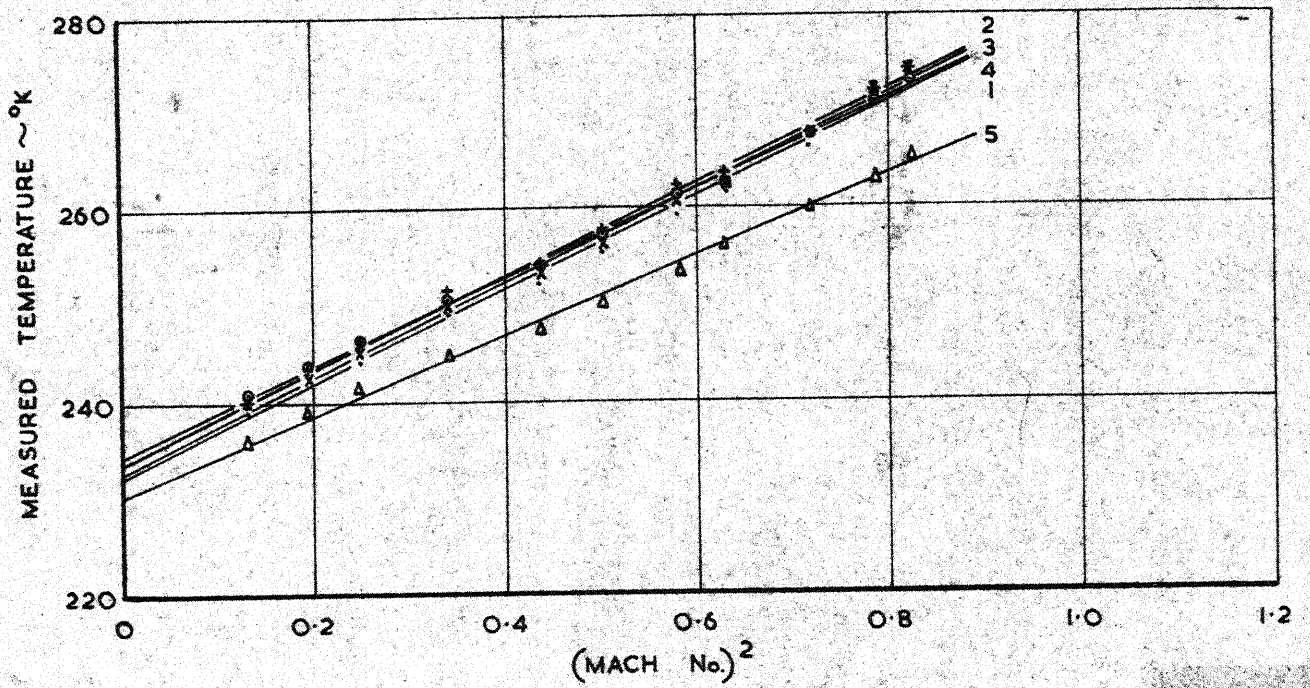
FLIGHT No. 145

PRESSURE ALTITUDE 15,000'



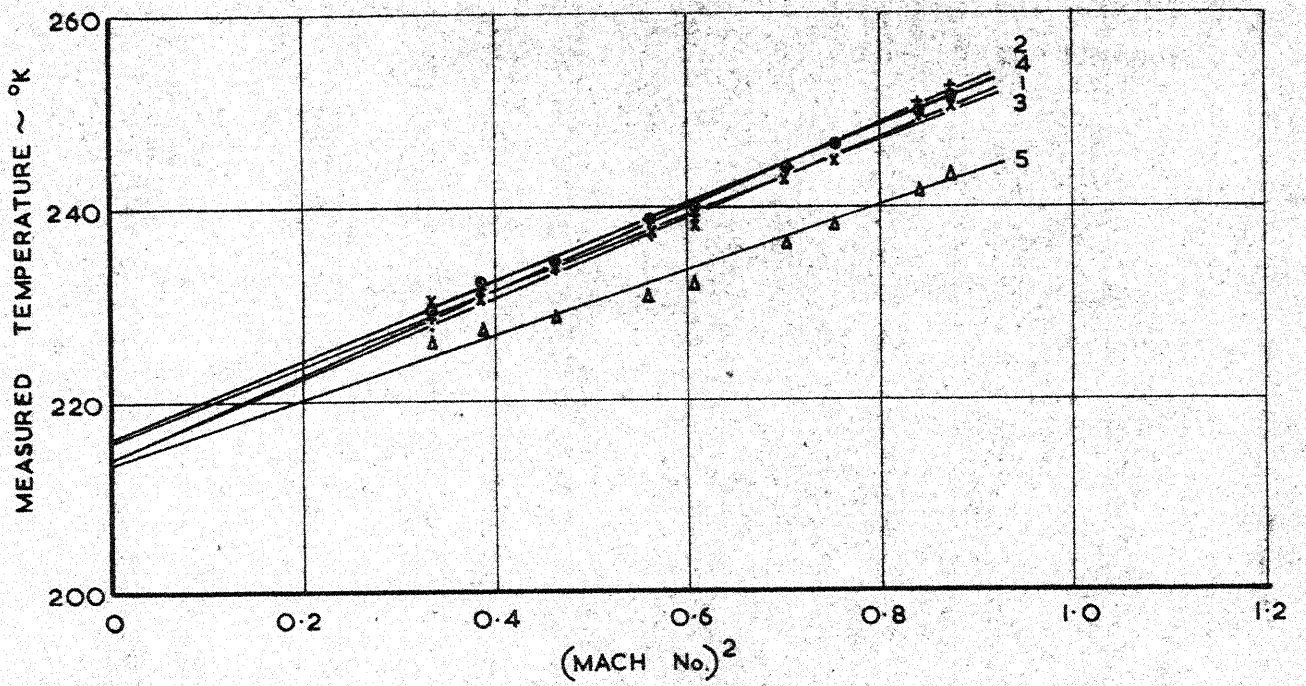
FLIGHT No. 146

PRESSURE ALTITUDE 25,000



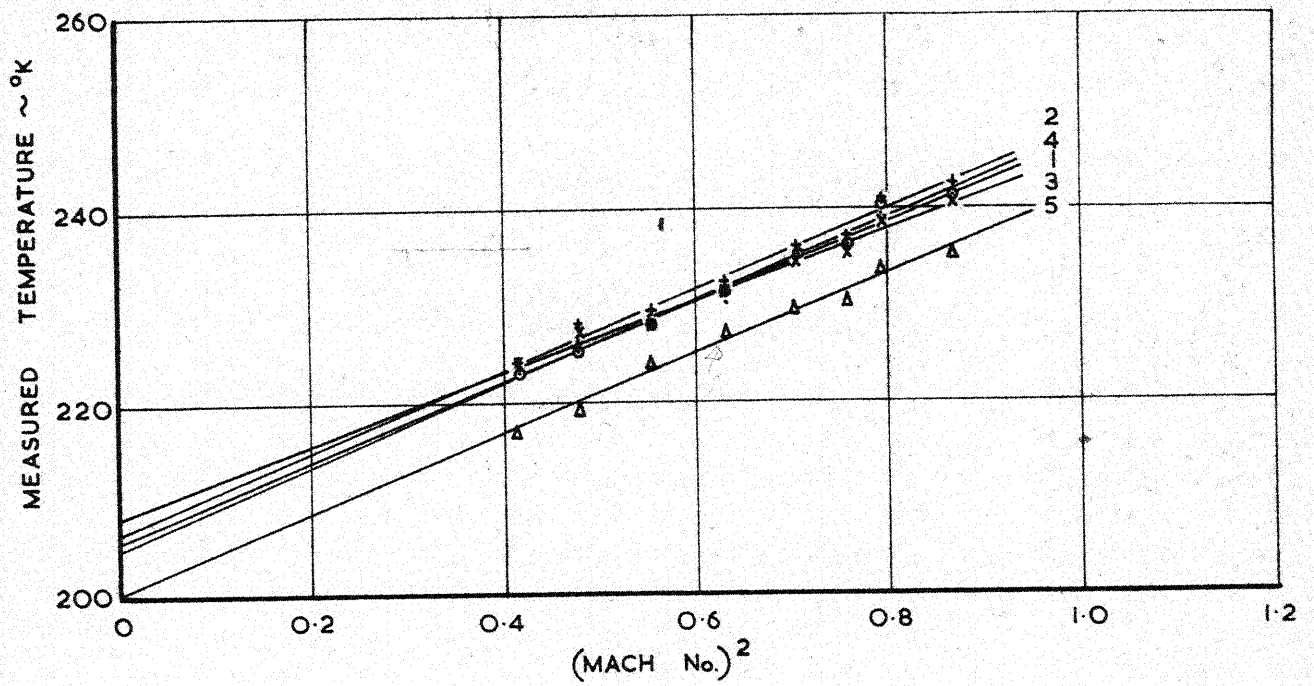
FLIGHT No. 147

PRESSURE ALTITUDE 35,000



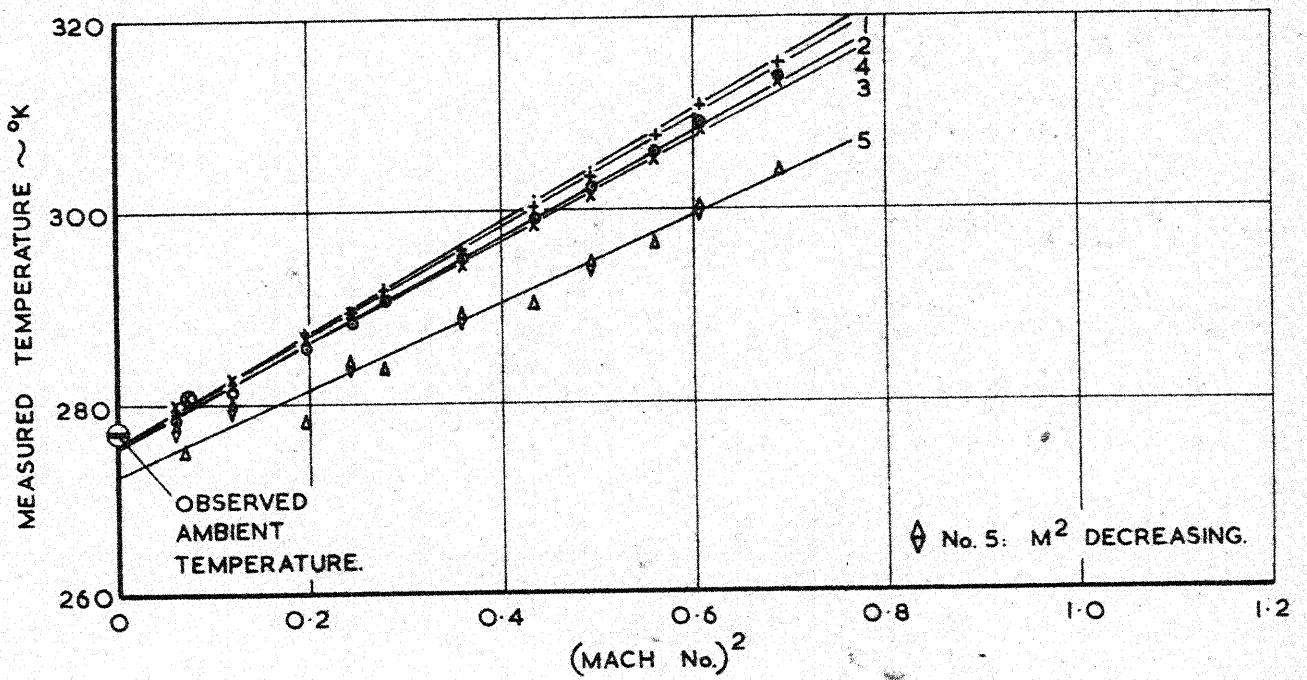
FLIGHT No. 149

PRESSURE ALTITUDE 40,000'



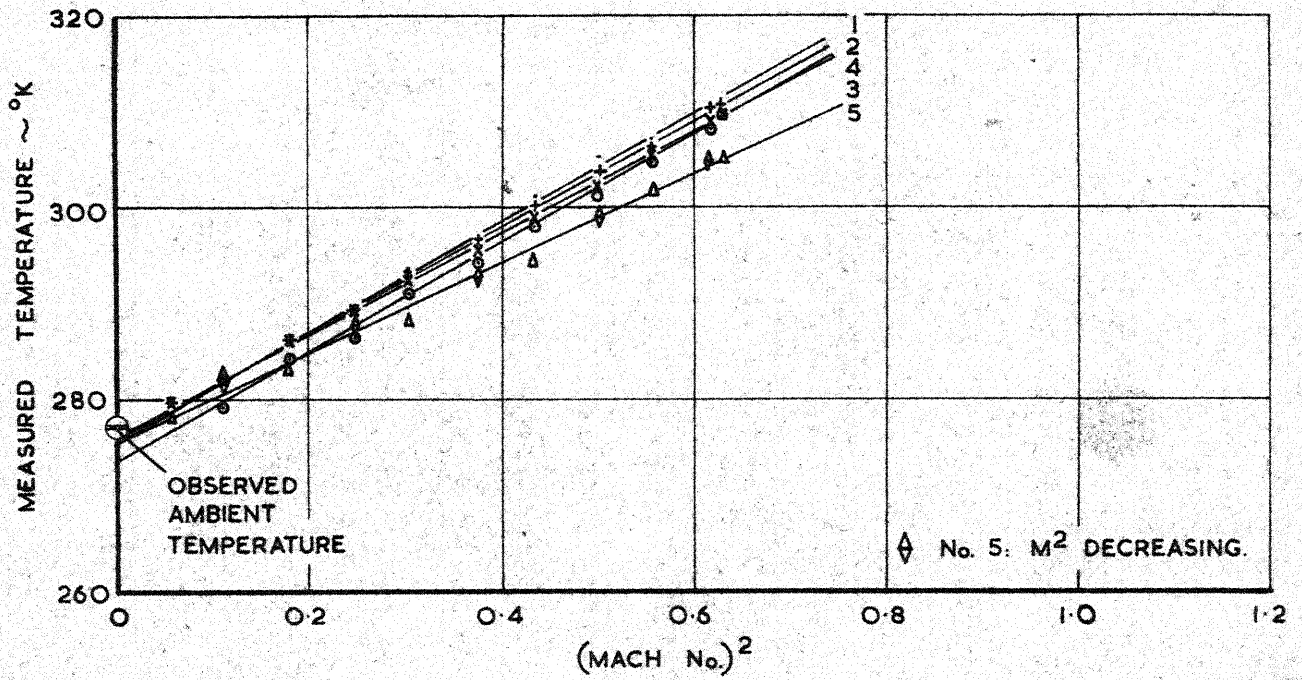
FLIGHT No. 150

PRESSURE ALTITUDE 4,000'



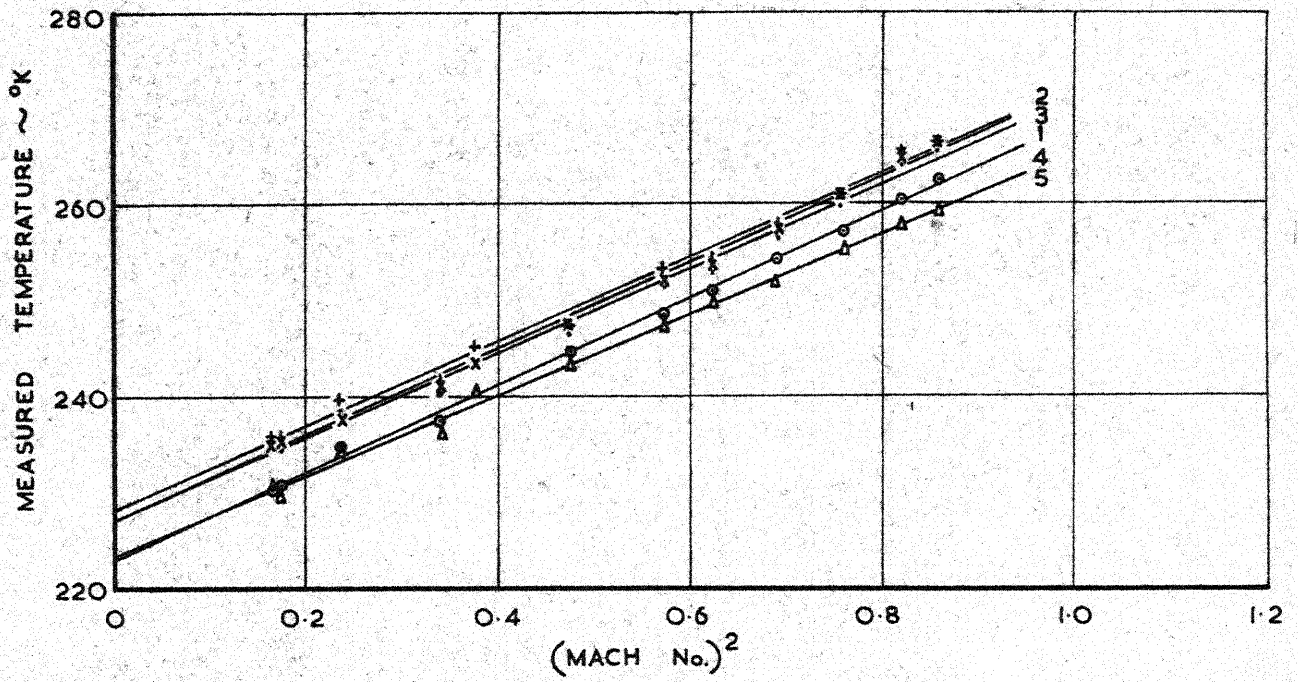
FLIGHT No. 151

PRESSURE ALTITUDE 4,000'



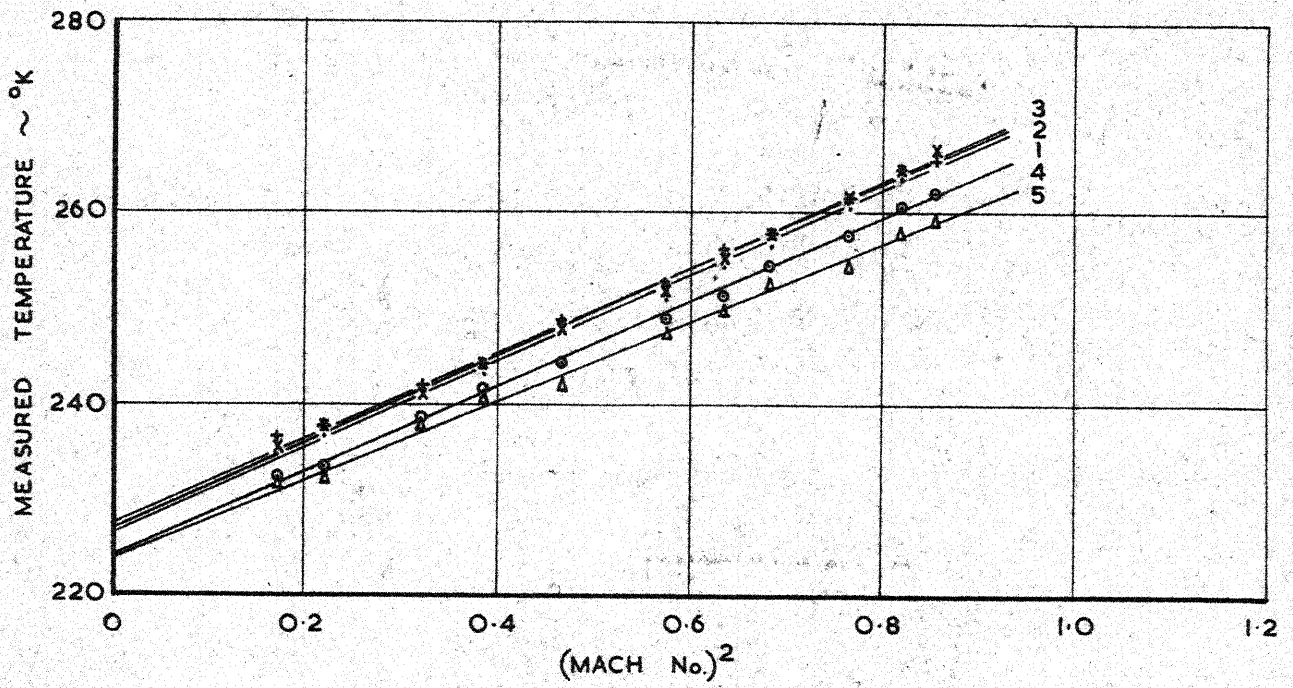
FLIGHT No. 152

PRESSURE ALTITUDE 30,000'



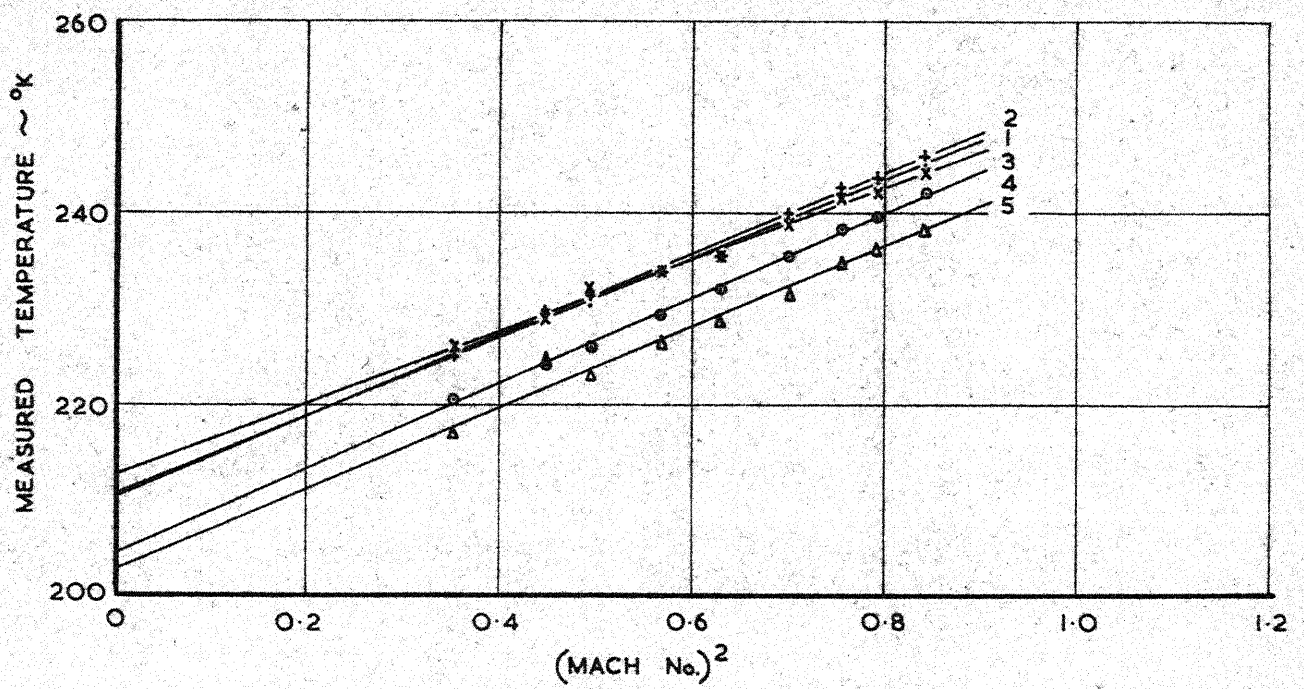
FLIGHT No. 153

PRESSURE ALTITUDE 30,000'



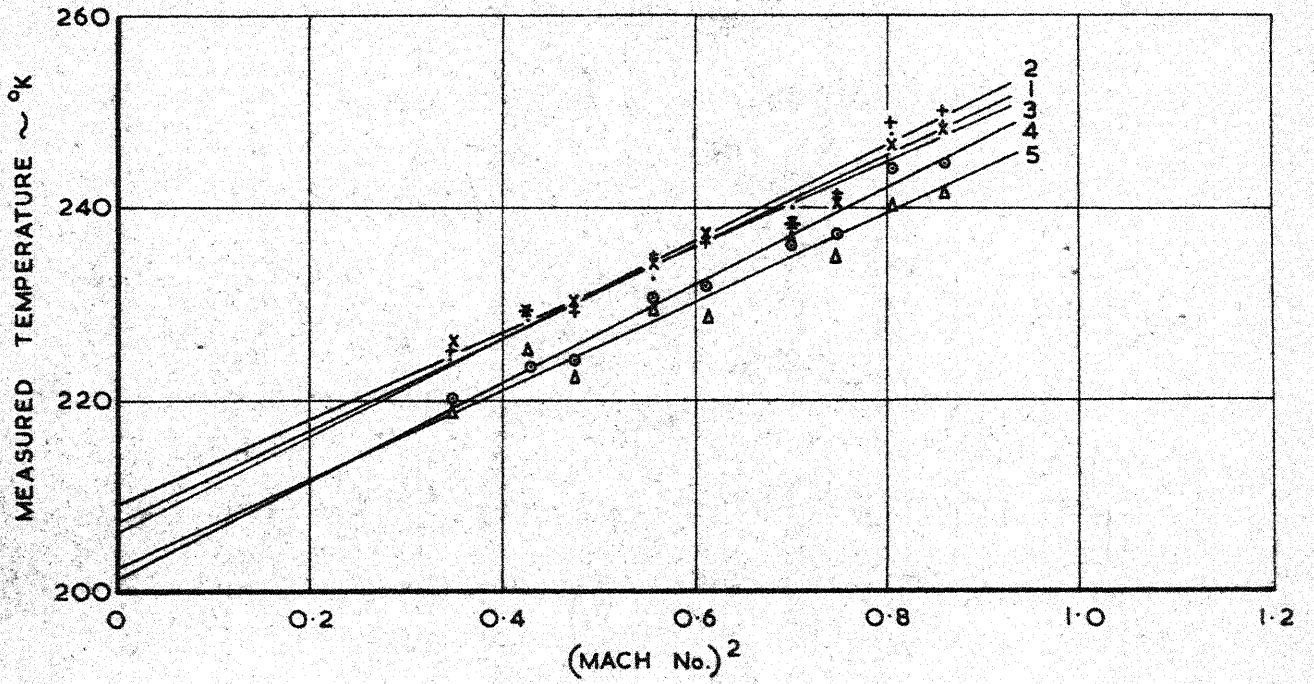
FLIGHT No. 154

PRESSURE ALTITUDE 40,000'



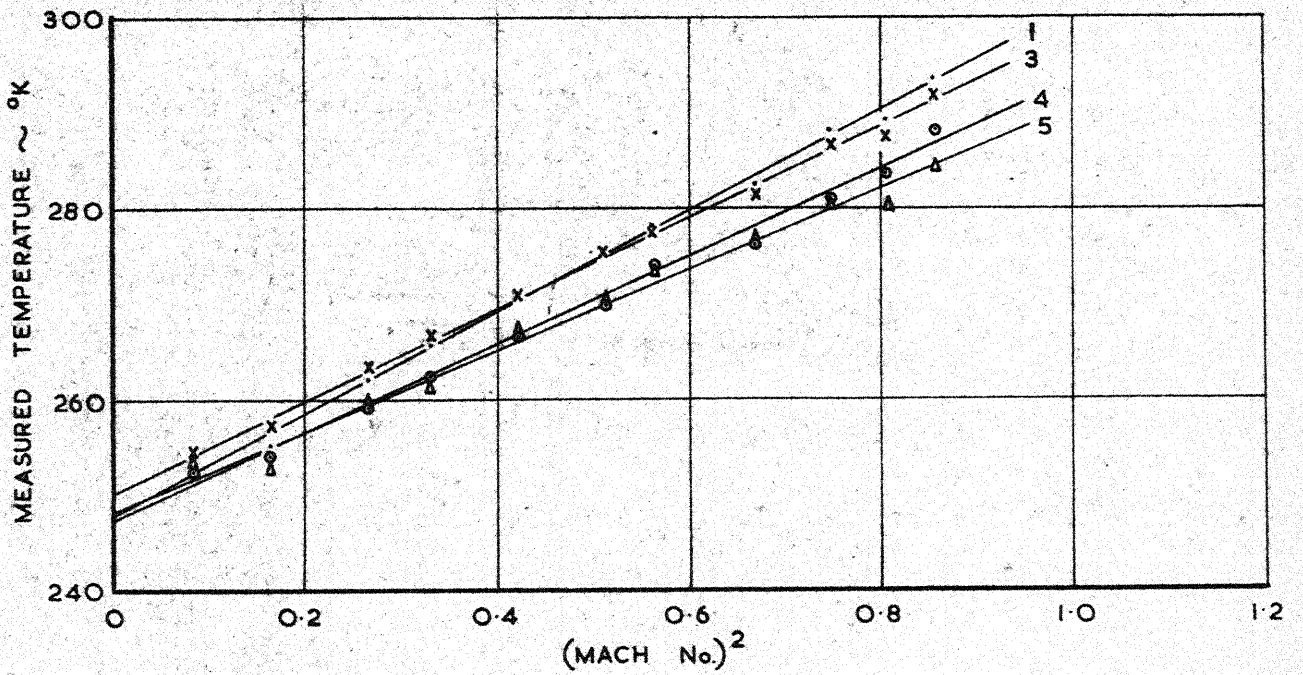
FLIGHT No. 155

PRESSURE ALTITUDE 40,000'



FLIGHT No. 156

PRESSURE ALTITUDE 15,000'



FLIGHT No. 157

PRESSURE ALTITUDE 35,000'

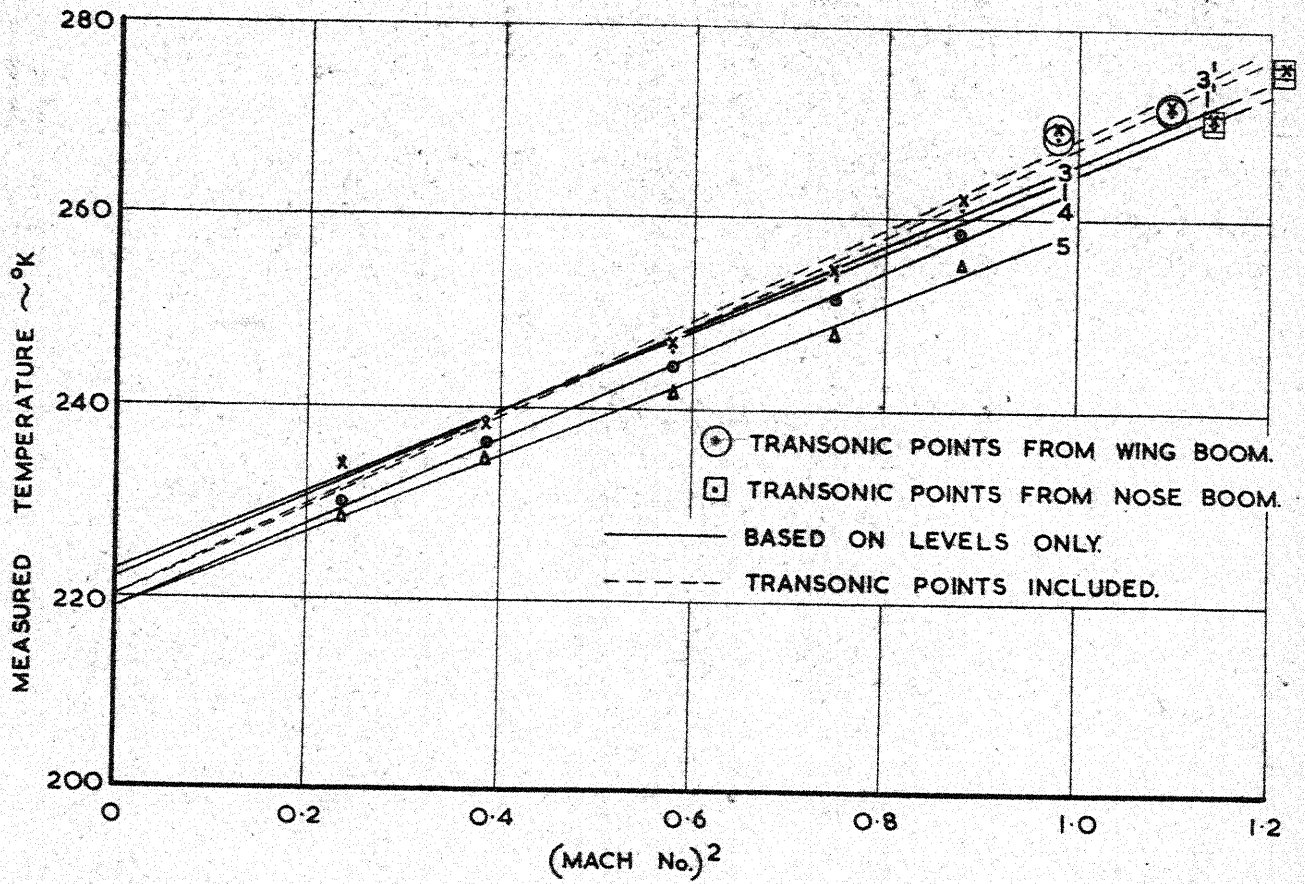


PLATE 1

No. 1 PROBE

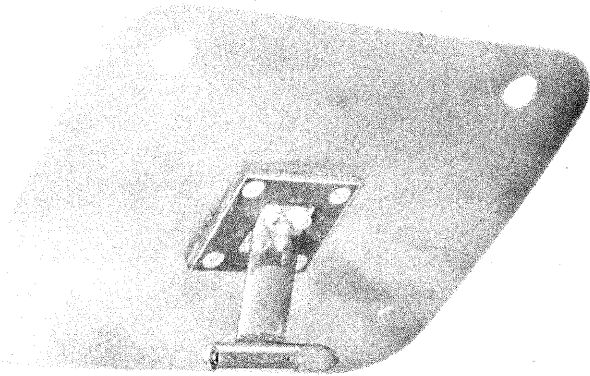


PLATE 2

No. 2 PROBE

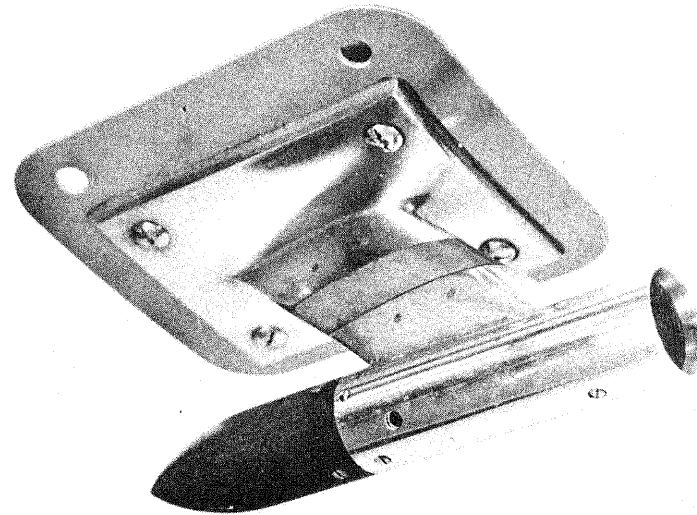


PLATE 3

No. 2 PROBE

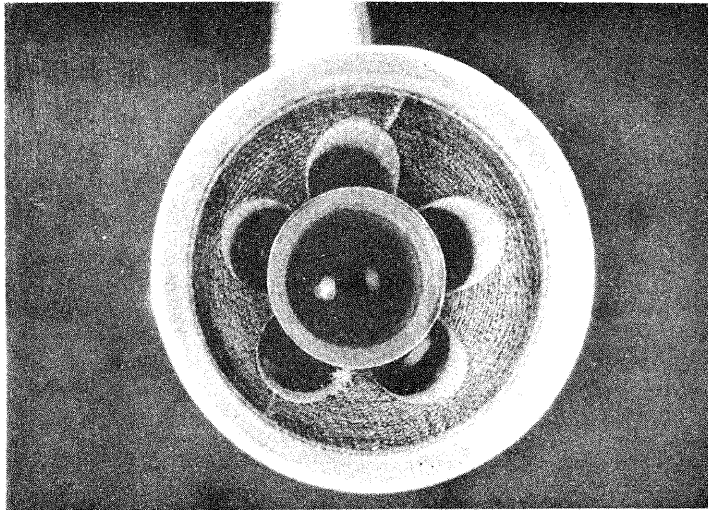


PLATE 4

No. 3 PROBE

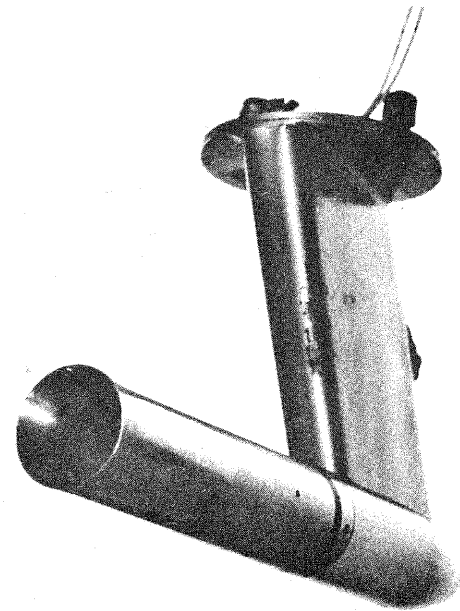


PLATE 5

No. 4 PROBE

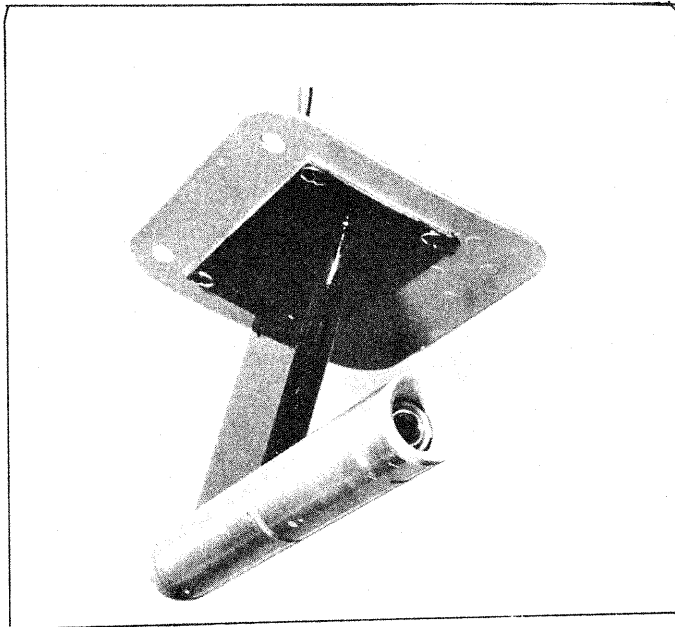


PLATE 6

No. 5 PROBE

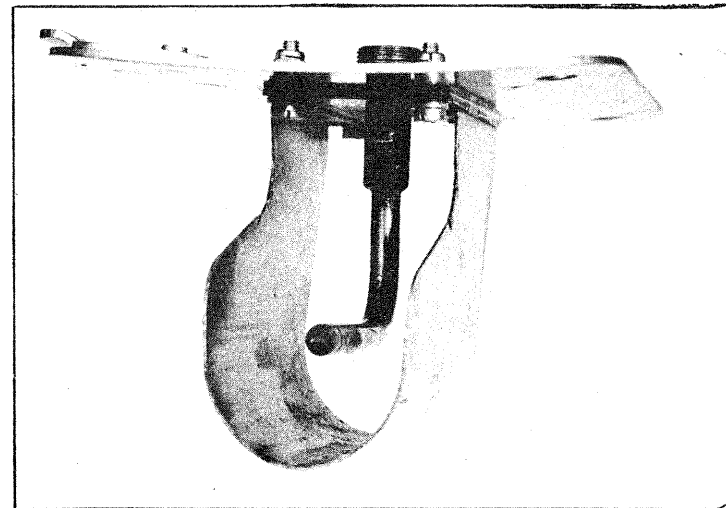
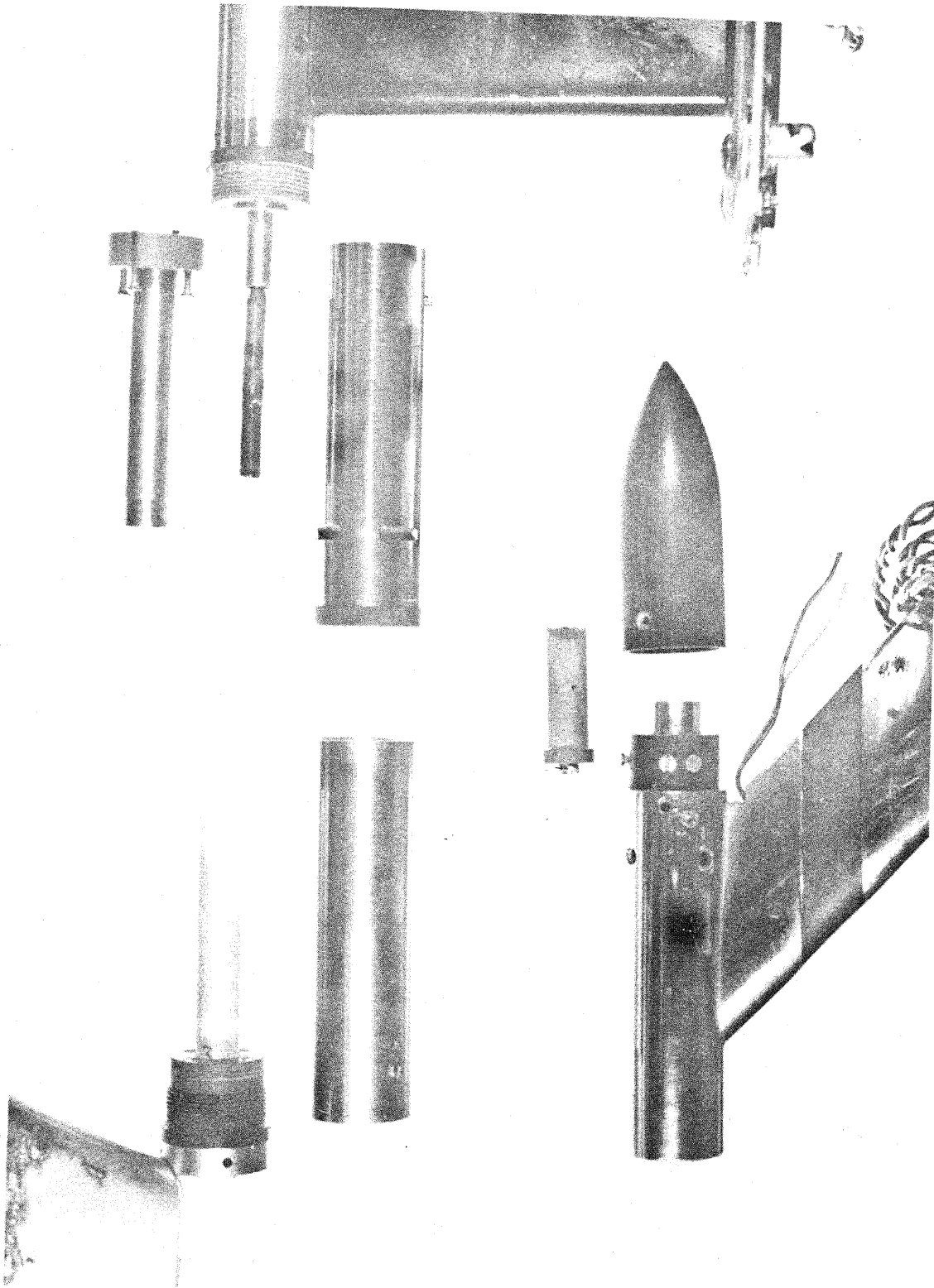


PLATE 7



No. 4

No. 2

No. 3

WN 893

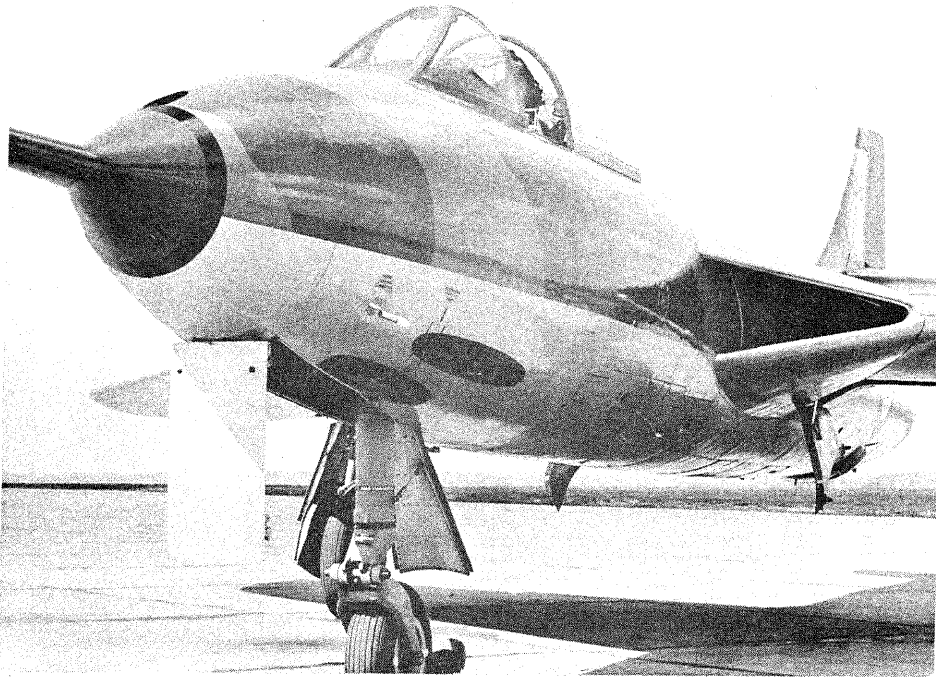


PLATE 8

WN 893

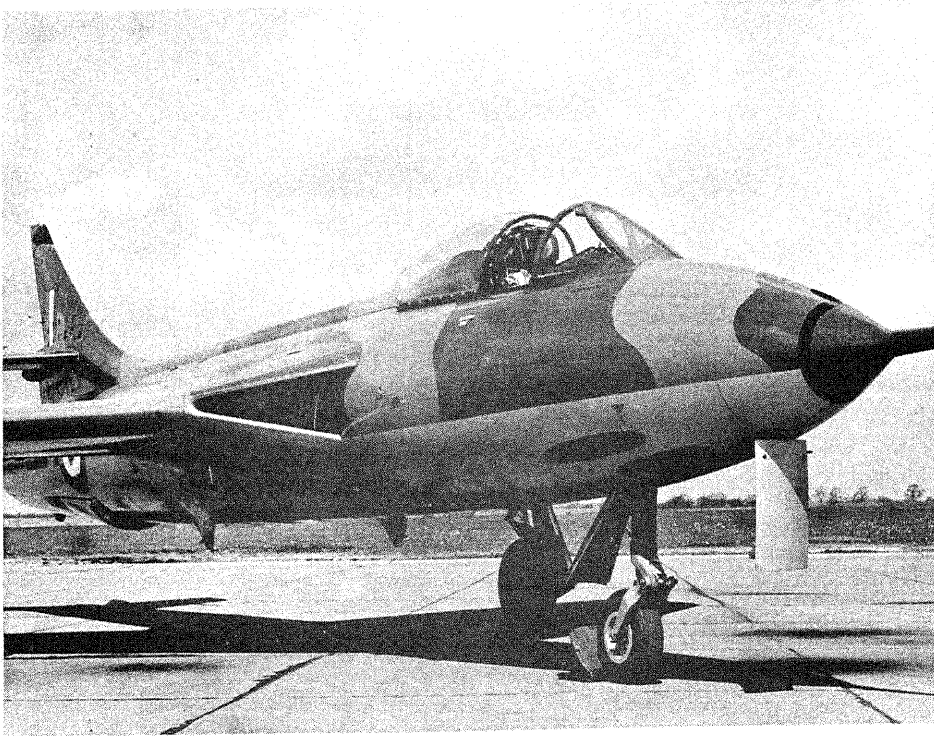


PLATE 9

Nos. 1 & 2 PROBES (PORT)

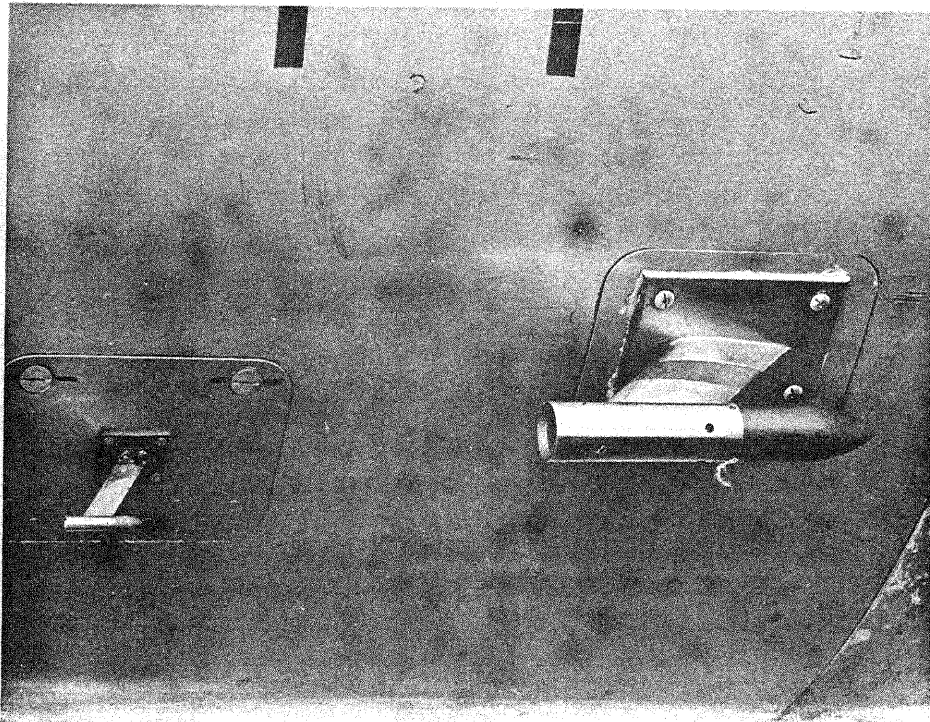


PLATE 10

No. 3 PROBE (PORT)



PLATE 11

Nos. 4 & 5 PROBES (STBD.)

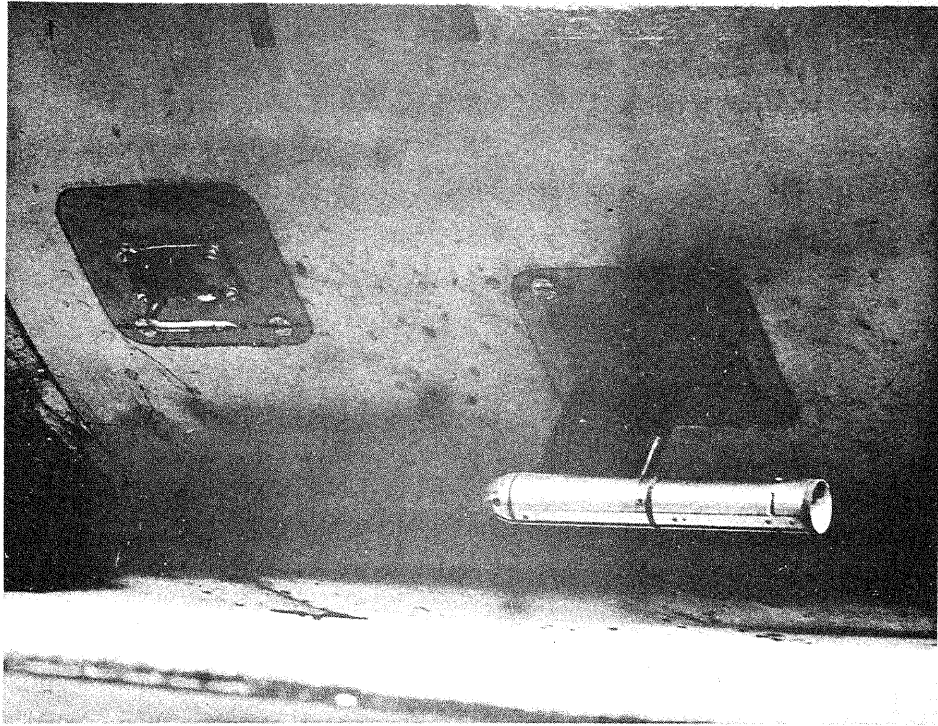
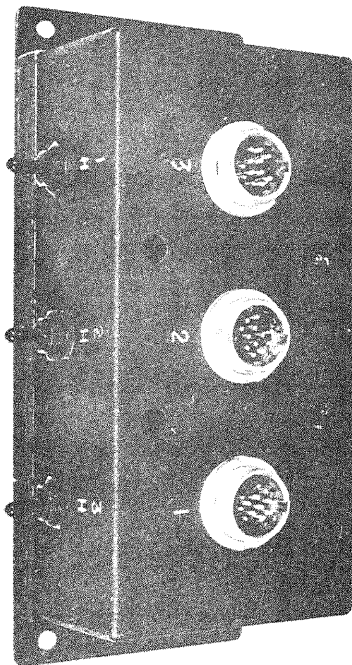


PLATE 12



THE JUNCTION BOX

PLATE 13

PLATE 14

THE BLOWER TUNNEL

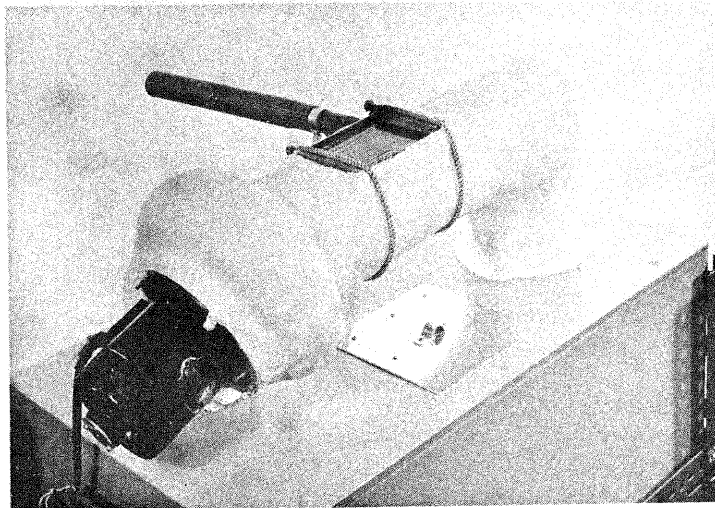
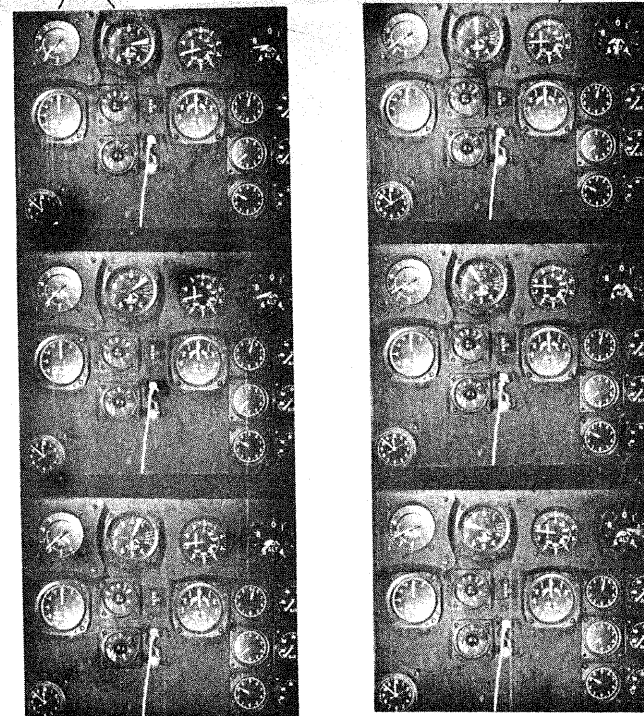


PLATE 15

THE AUTOMATIC OBSERVER PANEL

WING BOOM

NOSE BOOM



TRANSONIC DIVE FLT. 157

M = 1.045 AT 35,000'

